UNIVERSITY OF LEICESTER

Effects of Myopathy-causing Mutations on Tropomyosin Structure and Function

Thesis submitted for the degree of Doctor of Philosophy at the University of Leicester

By

Saeed Ahmed Asiri

Department of Molecular and cell Biology

College of Medicine, Biological sciences and Psychology

September 2016

Abstract

Tropomyosin determinants for actin binding have not been identified completely and the nature and position of residues involved in thin filament dynamics has not been established. To date a number of Tropomyosin mutations have been linked to several muscle diseases including cardiomyopathies and skeletal muscle myopathies. In this thesis, we aimed to investigate the following tropomyosin mutations R90G, E163K, R167G, E240K, R244G and M281I which have been shown to cause several severe skeletal muscle myopathies. We used various structural, biochemical and kinetic methods to assess the impact of these mutations on tropomyosin structure and biochemical properties. Fluorescence emission spectroscopy, and transient kinetics were used to assess the effect of these mutations on the equilibrium distribution and kinetics of transitions between different thin filament regulatory states. Overall the data demonstrated that: 1) all tropomyosin mutations except (E163K, E240K, M281I and R90GR167G) affected the thermal stability of tropomyosin but not the α-helical coiled coil structure. 2) The size of the cooperative unit *n* was reduced by all tropomyosin mutations. 3) Tropomyosin mutations did not affect the proportion of thin filaments in the blocked state (at low Ca^{2+}). 4) Tropomyosin mutations did affect the maximum observed rate constant of thin filament transition between the ON and OFF states. 5) Several tropomyosin mutations have affected tropomyosin-troponin binding affinity but none of the mutations had any effect on the actin binding affinity.

Overall these results provide insight into the mechanism by which tropomyosin bind actin and troponin, tropomyosin related thin filament cooperativity and allosteric transitions.

Acknowledgement

I would like first to thank and praise Allah the Almighty for enabling me to finish this work and for the endless favours he gracefully bestowed on me.

I am deeply indebted to my supervisor Dr. Mohammed El-Mezgueldi for his motivating suggestions and encouragement throughout the research and writing of this thesis.

I would like to express my gratitude to my PhD committee members Prof Mark Carr and Prof Russell Wallis for their great guidance and support. I would like to thank Prof Charles Redwood for providing cDNA. Also, I would like to thank Prof Kristen Nowak (University of Western Australia) for all the *baculovirus* constructs.

I would like to thank all lab 2/11 members and all my friends and colleagues for helping me through all this work.

Special thanks for my father and my wife Amal and my daughters Wteen and Sirin and my son Ahmed for their support and priceless smiles every day. Their support and prayers have driven me out of all obstacles.

Abbreviation

ADP	Adenosine diphosphate
ATP	Adenosine Triphosphate
CD	Circular Dichroism
CFTD	Congenital Fibre Type Disproportion
cTnC	cardiac Troponin C
cTnI	cardiac Troponin I
cTnT	cardiac Troponin T
DCM	Dilated Cardiomyopathy
DNA	Deoxyribonucleic Acid
DTT	Dithiothreitol
EDTA	Ethylene diamine tetra-acetic acid
EGTA	Ethylene glycol tetra acetic acid
F-actin	filamentous actin
G-actin	Globular actin
HCM	Hypertrophic Cardiomyopathy
IPTG	IsoPropyl-beta-d-ThioGalactopyranoside
K_B	equilibrium constant between blocked and closed states
K_T	equilibrium constant between closed and open states
LB	Luria-Bertani

LVNC	Left Ventricular Non-Compaction
MOPS	3-(n-Morpholino) Propanesulfonic Acid
n	size of the cooperative unit
n_H	Hill's coefficient
NM	Nemalin Myopathy
NMR	Nuclear Magnetic Resonance
PCR	Polymerase Chain Reaction
PIA	N-(1-pyrenyl)-iodoacetamide
Pi	inorganic phosphate
PIPES	Piperazine-1,4-Bis-2-Ethanesulfonic Acid
PMSF	Phenylmethanesulfonyl Fluoride
S1	Myosin subfragment 1
SDS	Sodium Dodecyl Sulfate
SR	Sarcoplasmic Reticulum
TCA	Trichloroacetic acid
Tpm	Tropomyosin
Tn	Troponin

Units/Symbols

A	Absorption

Å	Angström (1 Å = $1x10^{-10}$ m)
bp	base pairs
g	gram
h	hour
kb	kilobase
kDa	kilo Dalton
l	litre
M	molar
min	minute
mV	milli Volt
°C	degrees Celsius
OD	optical density
rpm	revolutions per minute
s	second
v/v	volume to volume
w/v	weight per volume
ε	Absorption coefficient
λ	wavelength

Table of content

List of figures

List of tables

Chapter 1

Introduction

1.1 Introduction

Muscle contraction drives a wide range of physiological functions including locomotion, all types of body or body parts movement, respiration, blood circulation, blood pressure, digestion, urination and childbirth. These functions are achieved by various types of muscles including skeletal muscle, cardiac muscle and smooth muscle. The importance of muscle contraction is clearly illustrated by a vast number of diseases that are triggered by malfunction of various components of muscles. The human body contains different types of muscles which are expressed in different organs. Skeletal muscles are attached to the human skeleton by tendons and are responsible for powerful and rapid contractions. There are different types of skeletal muscle depending on the speed of their contractions (fast and slow skeletal muscles). Cardiac muscle forms the wall of the chambers of the heart and its contraction is responsible for the pumping of oxygenated blood into the circulation. Smooth muscle is found in the walls of various hollow tubes and organs such as the stomach and blood vessels. Its contraction is responsible for pushing around the material inside these tubes. In addition to the processes described above, various biological processes inside the cell are driven by cellular components similar to those that drive muscle contraction. These cellular processes are responsible for whole cell motility and contribute to various motile functions inside cells.

1.1.1 The structure and components of striated muscle

In the human body, skeletal muscle represents the largest tissue accounting for almost 40% of the body weight. Under the microscope, the skeletal muscle exhibits a distinctive pattern of banding due to the arrangements in the cytoplasm of subcellular structures that are displayed regularly and give skeletal muscle a striated pattern (Huxley, 1953). The basic unit of the skeletal muscle is a muscle fibre or myofibril which has a diameter of 1-2 μm. each muscle fibre is a single multinucleated cell and contains thousands of contractile structures called: myofibrils arranged side by side. The myofibril that makes up a muscle cell, contains repeating units responsible for the striations observed under light microscope called sarcomeres. Sarcomeres are units repeated every 2.3 μm (Berg

et al., 2007, Alberts *et al*., 2015). In addition to the large number of contractile fibres (directly responsible for muscle contraction) muscle fibres contains several other cellular structures needed for triggering contraction and providing the required energy. Mitochondria, glycogen and fats are providing the energy needed to power the contractions while a network of sacs, tubules and channels called the sarcoplasmic reticulum and transverse tubules stores the calcium ions. The calcium is released to initiates the muscle contraction when is required.

1.1.2 The sarcoplasmic reticulum: The calcium store

The activation of muscle is driven by electrical and or hormonal signals depending on the type of muscle. These signals lead to muscle excitation. The excitation process is coupled to contraction by a process called excitation-contraction coupling that converts the excitation signal to a chemical stimulus (calcium) which diffuses between the contractile elements and activates them.

The cellular structures responsible of excitation-contraction coupling, are the sarcoplasmic reticulum (SR) and transverse tubules (T-tubules). The T-tubules are a network of rings that runs across the muscle fibres and connects the myofibrils to the exterior of muscle fibres. The sarcoplasmic reticulum is a complex network of chambers limited by membranes that surrounds the myofibrils. The main functions of sarcoplasmic reticulum are calcium storage, calcium release following excitation and calcium reuptake once the excitation has completed. The calcium is stored at the ends of the sarcoplasmic reticulum precisely in the terminal cisternae which are in contact with T-tubules. In many vertebrates, two cisternae are connected to each T tubule on opposite sides and form a complex involved in excitation-contraction coupling called: the triad (Ayasinghe and Launikonis, 2013; Lamboley *et al*., 2014). The T-tubule system is responsible for the conduction of the action potential that arrives to the muscle fibre membrane. The T tubule is adjacent with the terminal cisternae of the sarcoplasmic reticulum. The conduction of the action potential and the subsequent depolarisation of the sarcolemma and transverse tubules leads to the release of calcium by a voltage sensor subunit of the dihydropyridine receptors and/or further release large amounts

of calcium into the cytoplasmic medium (Rebbeck *et al*., 2014). The released calcium then binds a specialised protein which then initiates a series of molecular changes that leads to the activation of muscle contraction (Lamboley et al., 2014).

1.1.3 The contractile unit: the sarcomere

The muscle fibres are made of bundles of myofibrils considered to be the building blocks of the muscles. Each myofibril is 1-2 µm in diameter and extends all over the whole length of the muscle fibre. Longitudinal sections of muscle observed under light microscope revealed alternating bands of low and high density that were named I bands and A bands respectively. In the centre of the I band there is a prominent dense line named the Z line while in the centre of the A band there is a prominent line named the M line. The A band contain one group of myofilaments named thick filaments. They are about 14-16 nm in diameter. The I band contains another type of filaments named thin filaments. They are about 6-8 nm in diameter (Geoffrey, 2013). The area between two Z lines has been named a sarcomere. In skeletal and cardiac muscles, the sarcomere represents the basic contractile unit (Clark *et al*., 2002). The sarcomere is about 2.3 µm long and exists in every myofibril which is organised as a chain of contractile units. The highly-organised structure of the sarcomere is responsible for the striated appearance of striated muscle and plays an important role in the proper generation and transmission of force from the microscopic force generators (contractile proteins) to the macroscopic level (contraction at the level of whole muscle). The Z line is the area where the thin filaments are attached while the M line is the area where the thick filaments are anchored at (Geoffrey, 2013). Vast arrays of proteins are involved in the very well defined architecture of the sarcomeres. For instance, the giant protein Titin extends from the Z line to the M line (half a sarcomere and is believed to play a fundamental role in muscle biology from the sarcomeric organisation to muscle elasticity and possibly linking force generation to gene expression). Various actin binding proteins form the Z line and crosslinking in anti-parallel with actin filaments from two adjacent sarcomeres. Another interesting protein is Nebulin which, thought to be the key protein regulating the length of myofilaments in the I band (Lange *et al*., 2006). Early microscopic studies showed that the myofibril is made of an array of

protein filaments or myofilaments arranged in a well organised manner. There are two types of myofilaments: Thick filaments which are 14-16 nm in diameter and extend from the M line to the centre of the A band. Thin filaments are 6-8 nm in diameter and extend from the Z line toward the M line covering the A band (figure 1.1).

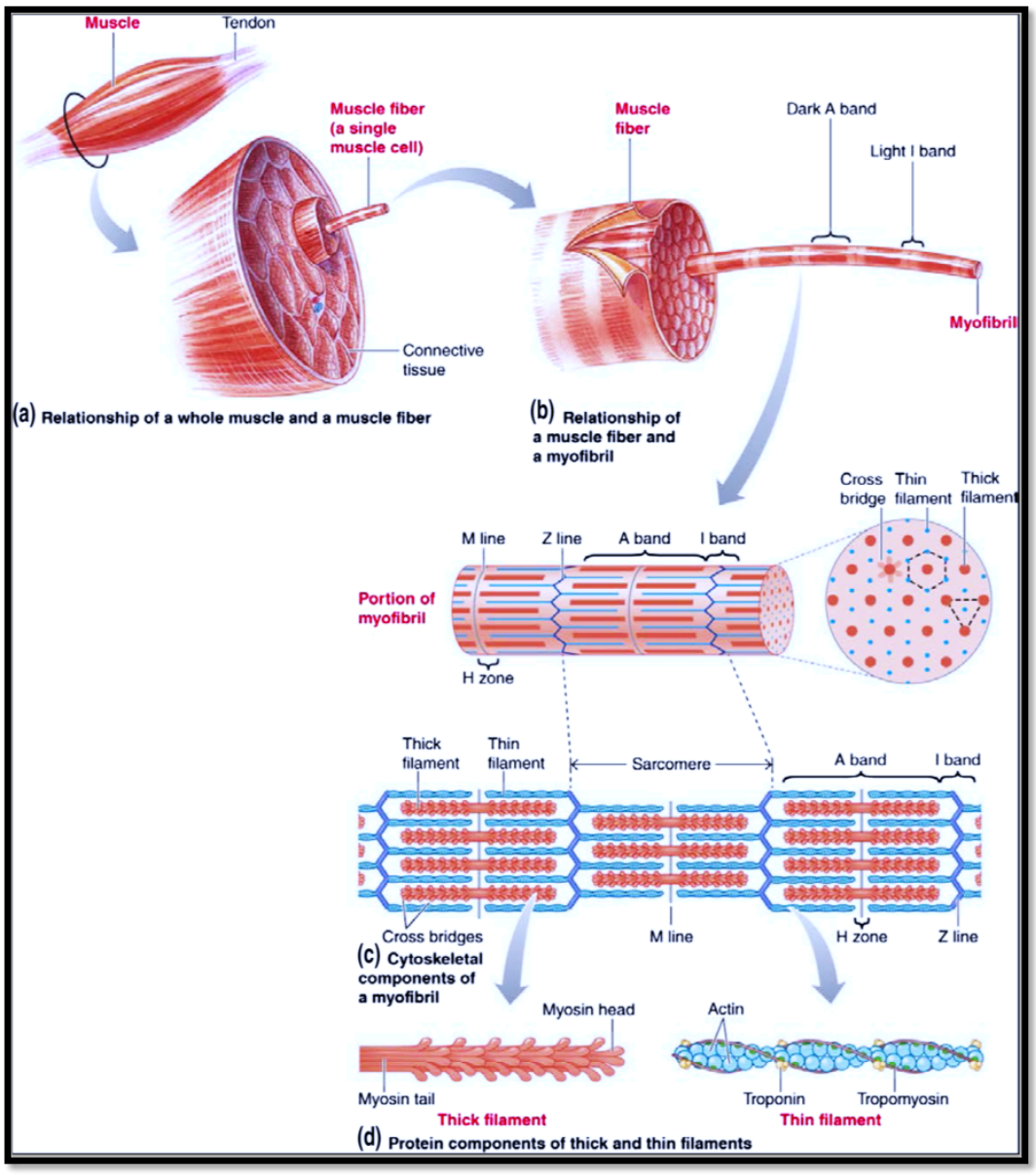

Figure 1.1: skeletal muscle structure

The figure illustrates a cross section of the muscle components. (A) The muscle consists of a large number of muscle fibres surrounded by connective tissue. (B) The muscle fires are also consisting of myofibril. (C) Each myofibril is divided into Dark A band and Light I band. These bands are consisting of thick and thin filaments. (D) The main component of thick filament is myosin and Actin is the component of thin filament. Thin filament is also composed of tropomyosin and troponin adopted from (Raven, 2013).

1.1.4 Myosin is the thick filaments motor protein

Thick filaments are fundamental components of the contractile machinery in the muscle. They are primarily made from a protein named myosin (Craig and Padrón, 2004). Thick filaments in striated muscle are bipolar structure with a rod in the middle made from their tails in an antiparallel fashion and parallel heads at the two ends. The thick filaments are attached to each other by cytoskeletal bridges connected to the M line (Huxley, 1963; Craig and Woodhead, 2006).

Myosin is the major component of thick filament and is composed of two identical heavy chains (about 220 kDa each) and two essential light chains (about 17 kDa) and two regulatory light chains (about 20 kDa) (lowey *et al*., 1993; Trybus, 1994; Szczesna, 2003; Kazmierczak *et al*., 2009). The heavy chain can be further subdivided into three parts: subfragment 1 (S1), subfragment 2 (S2) and light meromyosin (LMM). The LMM is located at the C-terminal of the heavy chain and is 100% made of an α-helical coiled coil (the same structure is found in the tropomyosin molecule and explained in the corresponding section). The N-terminal part of myosin is made of a globular domain called the myosin head and represents the motor domain of the myosin molecule containing the ATP binding site, the actin binding site and the region responsible for the power stroke. The globular head can be further subdivided into three domains: The N-terminal domain (25 kDa), the C-terminal domain (20 kDa) and the central domain (50 kDa) (Rayment *et al*., 1993; Geeves and Holmes, 2005; Sellers and Knight, 2007).

A crystal structure of the myosin head was obtained be Rayment and co-workers in 1993 (Rayment *et al*., 1993). The crystal structure revealed several features that allowed a deep understanding of the mechanism of muscle contraction. It showed that the myosin head is an asymmetric molecule that consists of a globular motor domain and a long tail (Raymant *et al*., 1993). The globular motor domain contains the actin binding site and the catalytic site where ATP binds and hydrolysed. The actin and ATP binding sites are on opposite sides of the myosin head. The tail is made of a long alpha-helix where both the essential and the regulatory light chains are bound. This region was later named as the lever arm which is linked to the actin and nucleotide binding sites by a region named the converter domain (figure 1.2) (Tyska and Warshaw, 2002).

Several crystallographic studies had been made using myosin from different tissues and with different nucleotide bound at the catalytic sites. Models of these structures are: truncated Dictyostelium myosin II (Smith and Rayment, 1996), truncated chicken smooth muscle myosin II (two forms) (Dominguez *et al*., 1998) and scallop adductor myosin (Houdusse *et al*., 2000). These studies demonstrated that myosin head from these species have a similar structure and that the nature of the nucleotide that occupies the catalytic site induced a substantial change in the position of the lever arm in relation to the globular part. The observed rotation of the lever arm is led by a 60º rotation of the converter domain. Other important structures such as the relay helix, switch 1 and 2 were also slightly different (Smith and Rayment, 1996; Geeves and Holmes, 1999).

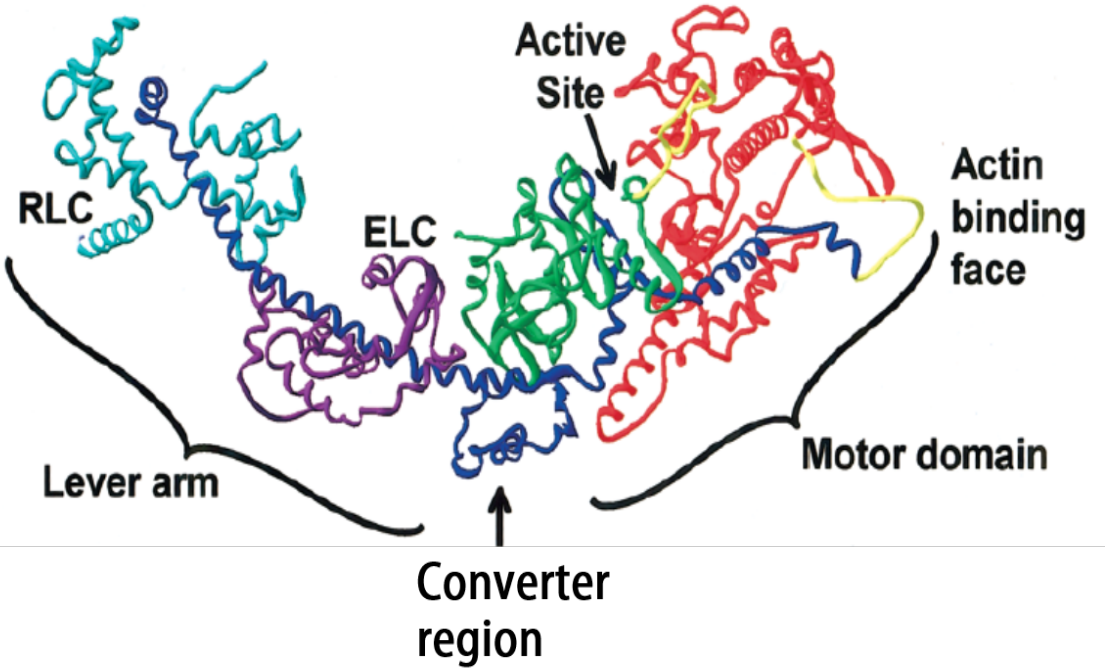

Figure 1.2: A ribbon representation of the myosin II sub-fragment 1

The figure shows the N-terminal in Green and in Red the upper and lower domains. In Blue the C-terminal. The Cyan colour represents the regulatory light chain. In Purple the essential light chain. The lever arm and the motor domain is separated by the converter region (Tyska and Warshaw, 2002).

1.1.5 Thin filaments are primarily made of actin

Thin filaments are the second important component of muscles. Thin filaments are around 6-8 nm diameter and are formed by several polymerized actin monomers. Thin filaments also consist of two important proteins: tropomyosin and troponin (Devine and Somlyo, 1971; Hooper *et al*., 2008). Actin is ubiquitous and an essential protein for so many cellular functions. Actin isoforms are derived from six different genes and is one of the most conserved amongst all proteins (Kabsch and Vandekerckhove, 1992). Four genes code for muscle actin isoforms including: Alpha skeletal muscle actin present in skeletal muscle (100%) and in cardiac muscle (about 20% of cardiac actin), alpha cardiac muscle actin present in cardiac muscle (80%), alpha smooth and gamma smooth muscle actin present exclusively in smooth muscles. The other two genes (beta and gamma cytoskeletal) code for non-muscle actins (Perrin and Ervasti, 2010).
Actin can exist in two forms monomeric or Globular G-actin and Filamentous or F-actin. Monomeric actin is a 42 kDa protein made of 375 amino acids. Upon polymerization actin monomers form a helical polymer (Holmes *et al*., 1990).

Since actin is playing a fundamental role in muscle and in the cytoskeleton, a huge effort was dedicated to determine its three-dimensional structure. This was very challenging since obtaining the crystals required for crystallographic studies involves the addition of salt, and actin in the presence of salt polymerises to form long unequal filaments of actin (which cannot be crystallised). Therefore, it was necessary to induce the formation of actin crystals in the presence of other proteins, small molecules or modified actin that does not polymerise. Kabsch and his collaborators were the first to determine the crystal structure of G-actin with bovine pancreatic DNase I in the presence of ATP at a resolution of 2.8 Å (Kabsch *et al*., 1990). This study showed that actin has a small domain (also called the outer domain) divided into subdomains 1 and 2 and a large domain (also called the inner domain) divided into subdomains 3 and 4 (Figure 1.3). The inner and outer domains are separated with a cleft that contains nucleotide and divalent cation binding sites. The movement of the cleft with its bound nucleotide is limited due to the hinge joins the two domains. Between these two domains there is a region that works as a hinge between them (residue Lys336 located in a loop and Gln137-Ser145 in the

linker helix). Between the two domains 1 and 3, the lower cleft is predominantly lined up with hydrophobic residues (Oda *et al*., 2009; Fujii *et al*., 2010). Subdomain one contains the N and C-terminals of the actin that have been predicted to be close to each other; it also contains the myosin head binding sites (Holmes *et al*., 1990). The crystal structure of G-actin complexed with fragments of gelsolin, profilin or modified G-actin showed all similar structures to the G-actin-DNase I structure.

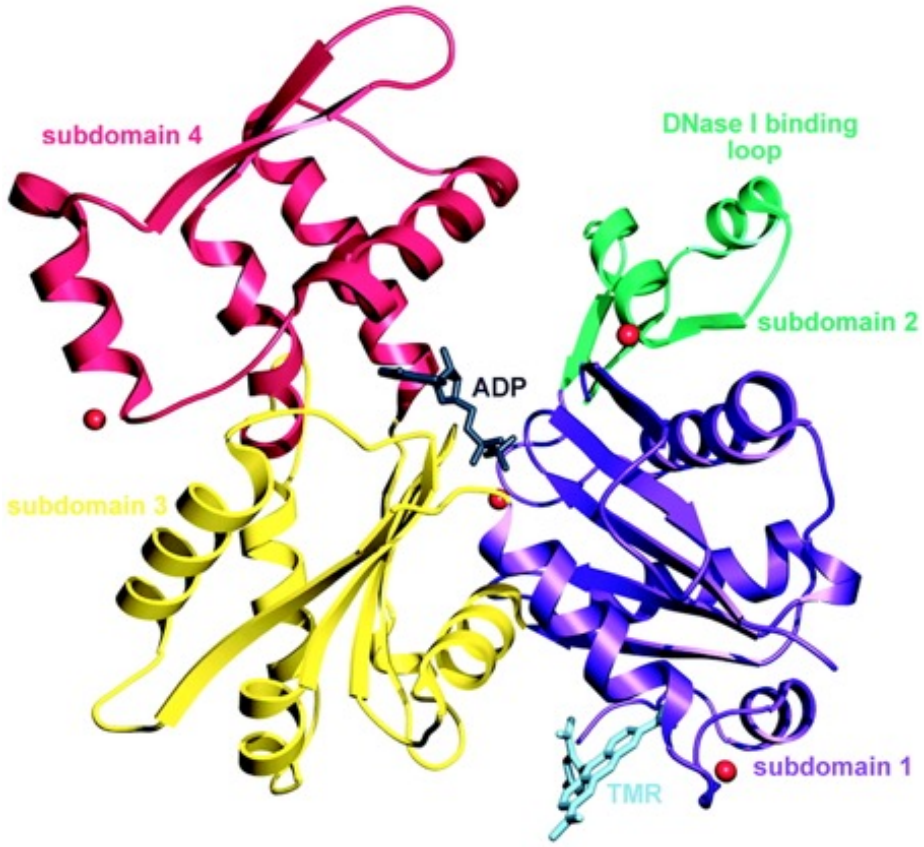

Figure 1.3: Structure of G-actin

The diagram illustrates the four subdomains of actin monomer. In purple subdomain 1, in Green subdomain 2, in Green which include the DNase I binding, subdomain 3 in Yellow and the Red is subdomain 4. TMR is Tetramethylrhodamine-5-maleimide. (Kabsch *et al*., 1990).

Under physiological salt concentrations, globular G-actin can spontaneously polymerise into the filamentous form (F-actin) that forms the backbone of the muscle thin filaments (figure 1.4). Both myosin heads (the molecular motor) and tropomyosin-troponin (the regulatory proteins) are interacting with this form of actin, and consequently determining the structure of the actin filaments is required for a full understanding of the mechanism of muscle contraction and its regulation. F-actin cannot be crystallised but its structure can be studied by electron microscopic studies and three-dimensional reconstructions. A model for the actin filament (F-actin) was derived from the atomic structure of the actin monomers (Holmes *et al*., 1990). More recently, Fujii and his colleagues have visualised the secondary structure of the F-actin filament using cryo-electron microscopy at 6.6 Å resolution. The model showed that the actin filaments are made of a double strand of actin monomers where each monomer contacts three monomers (one above, one below, and 2 on the opposite strand). Actin monomers are organised as a right-handed helix with a pitch of 72 nm. In the direction of the filament axis along the two-start long-pitch helix, a stronger bonding between molecules takes place between neighbouring actin molecules (Fujii *et al*., 2010).

Figure 1.4: Cartoon Structure of F-actin geometry formation

The cartoon structure shows the arrangement of actin monomers to form F-actin. The structure is formed by monomers spaced by 5.5 nm adopted from (Holmes *et al*., 1990; Lorenz *et al*., 1993).

1.2 Thin Filament associated proteins

The actin filament is decorated with a number of actin binding proteins that plays a fundamental role in the calcium dependent regulation of muscle contraction. I will focus on two protein complexes, the tropomyosin dimer and the troponin complex that are bound to actin filament every seven actin monomers and represents the macromolecular complex that regulate the interaction between the key contractile proteins actin and myosin. Troponin and tropomyosin together with actin monomers are considered as the major components of thin filaments. However, there are two other proteins that interacting with the thin filaments: Tropomodulin and Nebulin but are less abundant and are not required for the regulatory process (at least *in vitro*). Since this thesis is dedicated to tropomyosin, we will briefly introduce tropomodulin because it binds both tropomyosin and actin and caps the thin filaments (Engel and Franzini-Armstrong, 2004).

1.2.1 The Troponin complex

Troponin has been recognised as a key regulatory protein that mediates calcium dependent regulation in striated muscle in the late 1960s (Gergely, 1968). Troponin binds actin with a high affinity and a stoichiometry of 1 troponin per 7 actin monomers. It was demonstrated that troponin is a complex made of 3 different proteins that are coded by different genes and display completely different biochemical properties. The three subunits are: troponin C, troponin I and troponin T. The main role of the troponin complex (CIT) is to regulate the motor function of the actomyosin complex following a change in intracellular calcium concentration. At low calcium, troponin inhibits the actomyosin ability to hydrolyse ATP and the subsequent power stroke while at high calcium it activates the actomyosin chemomechanical function.

1.2.1.1 Troponin C

TnC is the Ca^{2+} binding subunit of the troponin complex. Troponin C is expressed as two isoforms in vertebrates, the fast-skeletal muscle isoform and the slow skeletal muscle (and cardiac muscle) isoform. All isoforms are 18 kDa acidic proteins of around 161 residues. The structure of TnC has been intensively studied by various structural methods including crystallography and nuclear magnetic spectroscopy. These studies established that all examined troponin isoforms have overall similar shapes. Troponin C is dumbbell shaped and is about 76 Å long. It is composed of two domains: The N-terminal domain and the C-terminal domain which are attached by a central helix (figure 1.5). TnC has four metal binding sites that can be occupied by calcium or magnesium. The N-terminal domain has 2 calcium binding sites (designated sites I and II) and is the domain responsible for calcium dependent regulation of muscle contractions. The metal binding sites in this domain have high calcium selectivity but lower binding affinity and the structure of this domain is different between the cardiac and skeletal muscle. The cardiac variant (cTnC) has only one calcium binding site (site II) while the skeletal variant (skTnC) has two calcium binding sites (site I and II) (van Eerd and Takahashi, 1975). The C-terminal domain also contains two metal binding sites. These sites comprise two high affinity binding sites for both Ca^{2+} and Mg^{2+} and are believed to play a structural role. The first X-ray crystal structure of the TnC was determined for skeletal TnC (Herzberg, 1985; Herzberg, 1986). These studies showed that troponin C is made of 9 helices: helix N spans residues 5-11, helix A spans residues 14-27, helix B spans residues 41-46, helix C spans residues 54-63, helix D spans residues 75-86, helix E spans residues 95-105, helix F span residues 116-124, helix G span residues 131-141, helix H span residues 151-158. These helices are grouped in pairs connected by a loop that form the well-known motif: helix-loop-helix which is a characteristic form of many calcium binding proteins. These studies established the mechanism of calcium binding and the subsequent conformational change. They showed that calcium binding to the regulatory domain induces an opening in the N-terminal domain (‘closed’ to ‘open’ transition model) (Gagne, 1995; Slupsky,1995). This model suggests that the B and C helices are folded down in parallel to the central helix in the (close) calcium free state while in the presence of calcium this configuration is

altered and the B and C helices become perpendicular. The binding of calcium also induces an opening of a hydrophobic site or pocket where TnI binds. The main difference between the NMR and crystal structure is in the linker connecting the N-lobe to the C-lobe which appeared to be unstructured and flexible in the NMR derived structure but α-helical in the crystal structure (Putkey, 1989; Spyracopoulos, 1997). The role of calcium binding to troponin C is to trigger a cascade of conformational changes in the other subunits TnI and TnT which are communicating with tropomyosin which lead to actin–myosin binding, actin activation of the myosin head ATPase and the power stroke (Slupsky and Sykes, 1995).

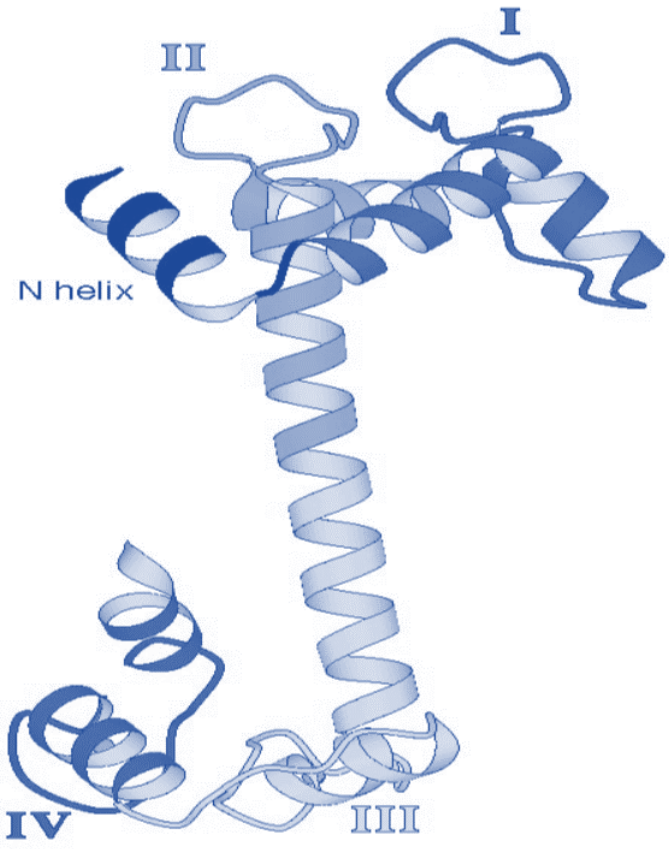

Figure 1.5: A ribbon diagram of the TnC structure

The TnC composed of two helix loops (EF hand) connected by a linker. The domains are labelled from I-IV (Houdusse *et al*., 1997).

1.2.1.2 Troponin I

TnI is the subunit of the troponin complex responsible for inhibiting the activity of the actomyosin ATPase and holds the troponin complex bound to the actin. TnI is expressed as three different isoforms that are muscle specific: cardiac, fast skeletal and slow skeletal muscle isoforms (Sadayappan *et al*., 2008). In skeletal muscle TnI is about 24 kDa and is made of 195 residues while cardiac TnI is made of 210 residues. The N-terminus, depending on the species, has a unique extension ranging from 30-33 amino acids. The N-terminal part of cardiac TnI has two Protein Kinase A (PKA) phosphorylation sites. Earlier proteolytic studies of the skeletal muscle isoform showed that the protein can be divided into four regions. The IT arm named so due its importance in troponin T binding. The inhibitory peptide spanning residues 96-117 which is essential for acto-myosin inhibition (Syska, 1976). The switch peptide (cardiac 150-160) which lies upstream of the inhibitory peptide, is believed to play an important role in the activation of muscle contraction. The C terminal part of TnI is unstructured and very mobile. The interaction of TnI with other subunits of troponin (TnC and TnT) and with actin is ruled by several well-defined peptides of TnI and these regions plays a major role in the biochemical function of TnI. There is a substantial interest in determining the structure of TnI. However isolated TnI has tendency to aggregate and this makes the crystallisation of this protein very difficult. Partial crystal structures of a fragment of both skeletal muscle and cardiac TnI reconstituted with TnC and TnT have been determined (Takeda *et al.,* 2003). The study showed several helices including TnI H1, H2, H3 and H4. An NMR study has shown that in the presence and absence of calcium the “mobile domain” which comprises of α-helices and two antiparallel β-strands adopts a solid structure and flips independently of the rest of the complex (Murakami, 2005). A later study confirmed the presence of this structure in the C-domain but disputed the effect of calcium (Blumenschein, 2006). Overall the main function of TnI is driven by its binding to actin in the absence of calcium (responsible for actomyosin inhibition) and the dissociation from actin leading to bind troponin C after calcium binds troponin C.

1.2.1.3 Troponin T

TnT is the third subunit of the troponin complex. Troponin T is expressed from three genes in vertebrates which are also muscle specific: slow skeletal muscle, fast skeletal muscle and cardiac muscle genes. In addition, TnT is subjected to substantial alternative splicing which leads to the expression of several TnT isoforms. For instance, TnT expressed in the heart has four isoforms, one is expressed in adult while the other three isoforms are expressed in the foetus (Anderso *et al.,* 1995). Fast skeletal muscle TnT is composed of 259 residues with a large number of charged residues. The N-terminus is composed of residues 1-59 and is enriched with negatively charged amino acids while the C-terminus contains mainly positively charged residues. The consequence of these differences in the charge of the two TnT regions is leading to the tendency of TnT to aggregate at physiological salt concentration. Electron microscopy studies showed that TnT form a rod with a length of 17 nm and located in the groove of the actin helix together with tropomyosin (Perry, 1998). Biochemical studies have shown that TnT binds TnC, TnI and tropomyosin (Perry, 1998). The N-terminal of TnT binds at the overlap area of the tropomyosin (Gordon *et al*., 2000). The binding of calcium strengthens the interaction of C-terminal part of TnT and TnC and weakens the binding to tropomyosin. Under proteolytic conditions the TnT produces two fragments: TnT1 and TnT2. TnT1 is located at the N-terminal region which composed of residues 1-158 and is responsible for strong binding with tropomyosin. The rest of TnT corresponds to the TnT2 which is believed to bind TnC and TnI (Ohtsuki and Nagano, 1982).

The TnT interaction with TnI involves several segments including residues 152-175, residues 176-230 and residues 202-259 (Jha *et al*., 1996). This interaction is thought to be at residues 41-96 of TnI (Chong and Hodges, 1982). A partial structure of TnT complexed with TnC and parts of TnI showed that the TnT region of the IT arm has two α-helices at residues 155-205 and 205-255. These segments were proposed to form a triple coiled-coil structure with TnI and tropomyosin (Stefancsik *et al*., 1998). The segments of TnT responsible for TnC binding are corresponding to residues 159-259 or 176-230 (Leszyk *et al*., 1988). These interactions include TnC N-terminal globular domain and central helix (Farah and Reinach, 1995). TnT plays two major roles; the first

role is a scaffolding role in which TnT connects the other subunits of the troponin complex (TnC and TnI). The second major role is in the mediation of the calcium induced effect on TnC and TnI to tropomyosin and the thin filament.

1.2.1.4 Troponin complex

Calcium regulation of muscle contraction depends on the presence of all three subunits folded in a complex that senses the presence of calcium in the cytoplasm and communicates with that through a set of elegant allosteric transitions to the rest of the actin filament (actin and tropomyosin). A functional troponin complex has to be folded in an intertwined trimer made of TnC, TnI and TnT in a 1:1:1 stoichiometry (figure 1.6). The three subunits need to be refolded together from an unfolded state to provide the native form of troponin.

X-ray crystallography allowed the determination of the crystal structure of the core domain of human cardiac troponin saturated with calcium at a 2.61 A° resolution (Takeda *et al.,* 2003). The crystallised protein complex included only parts of the Tn complex including TnC residues 1-161, TnI residues 31–163 and a short segment of TnT (residues 183–288). This structure has shown that the troponin complex is composed of various domains. The regulatory head contains primarily TnC bound to the regulatory elements of TnI in an anti-parallel manner. TnI binds through the N-terminal part of H1 helix (residues 29-65) to the C-lobe of TnC through hydrophobic interactions and through residues 147-163 (also known as the switch peptide) to a hydrophobic patch of NcTnC and assumes more compact shape. The IT arm is made of 2 helices from TnI (the C- terminal part of the H1 α-helix (residue 66-79) and H2 α-helix (residue 90-135) connected by a short linker and two helices from TnT H1 (residue 204-220) and H2 (residue 226-271) that come together. All these domains are connected by flexible linkers which make the troponin molecule very flexible. One such region of TnI is the inhibitory domain which span residues 95-105 in the skeletal muscle isoform (137 to 148 in the cardiac isoform). It is a key region of cTnI because it binds strongly with actin in the absence of calcium ion and inhibits the actomyosin ATPase. This inhibitory peptide has not been visualised in the core crystal structure of cTn complex and is assumed to be unstructured (Takeda *et al.,* 2003). Overall troponin flexibility is

considered essential for the allosteric transitions that take place during activation and inhibition of thin filaments. A crystal structure of skeletal muscle troponin was also determined in the presence and absence of calcium by Vinogradova (Vinogradova *et al*., 2005). The structure of skeletal muscle troponin is comparable to the cardiac isoform structure although there are few differences. The skeletal muscle isoform showed that in the presence of calcium the inhibitory peptide (TnI 104-115) bound to TnC had exhibited a well-ordered loop unlike in the cardiac isoform. The central linker (D/E) shows a rigid helix in the skeletal muscle isoform while it is melted in the cardiac isoform.

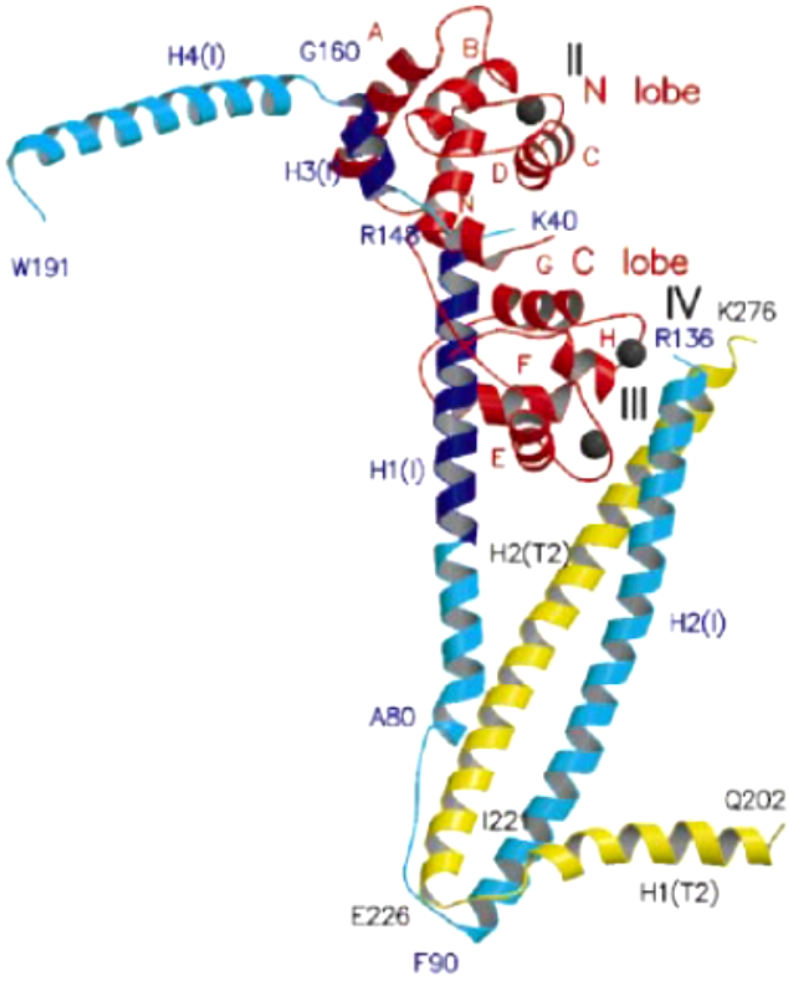

Figure 1.6: Troponin complex structure of Tn52KB molecule

The figure illustrates troponin core domains in the crystal structure. The Red colour is TnC, Yellow colour is TnT and TnI is in Cyan colour. The dark blue is the two stretches of TnC-binding sites. The black spheres are calcium ions. The helices of TnI and TnT are indicated in numbers while letters indicate the TnC helices. Adopted from (Takeda *et al*., 2003).

1.2.2 Tropomodulin

Tropomodulin was firstly detected as a Tpm-binding protein with a molecular mass of 40 kDa in the erythrocyte membrane (Fowler 1987; Sung *et al*., 1992). The Tpmod has four isoforms (Tpmod 1 or E-Tpmod, Tpmod2 or N-Tpmod, Tpmod3 or U-Tpmod and Tpmod4 or Sk-Tpmod). Tropomodulin is a crucial protein in the actin filament macromolecular complex. The key function of tropomodulin is to inhibit polymerisation and depolymerisation of actin filaments, caps the pointed end of these filaments and consequently optimizes the length of thin filaments (figure 1.7). Tpmod 1 consists of two distinct structural domains, the globular C-terminal domain and an unstructured, highly disordered N-terminal domain (Kostyukova *et al*., 2000, 2001; Fujisawa *et al*., 2001; Krieger *et al*., 2002). The N-terminal has one Tpm-dependent actin capping site and two Tpm binding sites (Fowler *et al*., 2003; Greenfield *et al*., 2005; Kostyukova *et al*., 2005, 2006). The C-terminal consists of a Tpm-independent actin-binding site. During capping, the tropomodulin binds two Tpm molecules and one actin monomer. The importance of tropomodulin is based on its interaction with Tpm (Colpan et al., 2013).

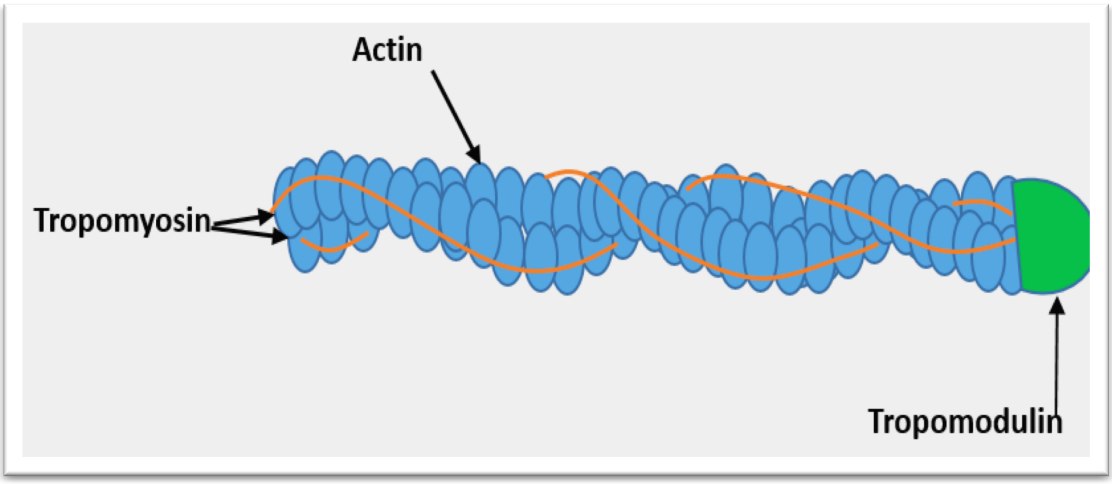

Figure 1.7: A cartoon of thin filaments displaying Tropomodulin position.

The structure shows a representation of Tropomodulin (green) position on thin filament which binds two tropomyosin molecules (Orange) and one actin (Blue). The diagram was edited from Mudry *et al*., 2003.

1.3 The mechanism of striated muscle contraction

Myosin heads projecting from the thick filaments represent the motor elements of muscle. Their interaction with actin monomers in the backbone of thin filaments releases the energy stored during ATP hydrolysis and lead to muscle contraction. The mechanism of this process has been intensively studied over more than five decades. Huxley proposed the sliding filament model to explain muscle contraction. In the 1950s, the study by Huxley found that the (A) band containing the thick filament remained constant during contraction while the (I) band which is mainly made with actin became shorter (Huxley, 1953). The model suggests that actin and myosin filaments slide past each other during muscle contraction. It was later shown that filament sliding was due to an ATP dependent cyclic interaction between the myosin head projecting from myosin filament and actin filament (Lymn and Taylor, 1971; Eisenberg and Hill, 1985). When ATP is made available to an existing actin–myosin (cross-bridge) a series of events occur which result into the force generation. The myosin hydrolyses ATP and produces ADP and Pi and the energy liberated from this reaction is stored in the myosin head as a conformational change. Cross-bridge binding to actin results in swinging of myosin head and liberation of the stored energy during the so-called power stroke. This is initiated by the release of Pi and lead to myosin pulling actin filament resulting in thin filaments sliding past the thick filaments. ADP is released at the end of the power stroke and myosin remains bound to actin in rigor ready for another crossbridge cycle (Lymn and Taylor, 1971; Eisenberg and Hill, 1985). Subsequently several studies found that during the cross-bridge cycle an intramolecular conformational change cause's relative displacement within the myosin head (Cooke *et al*., 1984). The structural studies of the myosin head by crystallography suggested that the change in conformation of the myosin head is primarily due to a change in the position of the long helix in the tail of the myosin head. This part acts as a lever arm amplifying small conformational change driven by ATP hydrolysis or actin binding in their respective sites into a large displacement at the distal end of the neck region by 3-4 nm (Whittaker *et al*., 1995; Spudich *et al*., 1995). The swinging motion of the tail of myosin head is due to a set of structural changes communicated between the nucleotide site and the lever arm as shown from crystallographic studies of myosin complexed with ATP and ADP-Pi

(Houdusse *et al*., 2000). Several structural elements including the relay helix, the switch-1 element (SW1), the switch-2 element (SW2) and the converter region change position by a small amount depending on the presence or absence of the γ-Pi in the nucleotide binding pocket. This small movement leads to a large translation of the myosin tail due to amplification by the lever arm (Geeves and Holmes, 1999).

1.3.1 The role of actin in thin filament in the power stroke

Actin represents the second filament involved in force generation and muscle shortening by the sarcomere. Actin plays several roles in this process. The first role is a scaffolding role that allows the myosin crossbridge to attach and pull the actin filament following the conformational change described above. The second role is the activation of ADP and Pi release from the myosin catalytic site. In the absence of actin, ATP hydrolysis products are stuck in the myosin catalytic site and their release is very slow (around 0.1 S^{-1}). Upon binding to actin, the release of ADP and Pi is accelerated by several order of magnitudes (Trentham *et al*., 1976; Geeves, 1991; Bagshaw and Trentham, 1974).

The actomyosin ATPase cycle can be started from the actin-myosin rigor complex (A.M). In this stage, the actin binding cleft is closed and both sides of this cleft make connection with actin. ATP binding induces the dissociation of actin from myosin. The binding of ATP occurs at the nucleotide binding pocket (catalytic site). The dissociation of actin occurs due to the opening of the major cleft (the actin binding cleft). The ATP is hydrolysed to form the stable M-ADP-Pi complex. Binding of the M-ADP-Pi complex to actin triggers a structural change in the actin binding cleft that destabilises the nucleotide site. This leads to the opening of the nucleotide binding pocket and the release of Pi first and ADP. Consequently, ADP and Pi are released much faster from the actin-M-ADP-Pi complex than from M-ADP-Pi. This activation of the myosin ATPase is crucial for the generation of rapid contraction by muscle (figure 1.8) (Geeves, 1991).

For all muscles, contraction is a regulated process. Regulation is achieved by a change in the concentration of a universal secondary messenger, Ca^{2+}. However, regulation can take place either at the level of myosin (smooth muscle and non-muscle actomyosin

based systems) or actin (Striated muscles). In striated muscles, actin represents the site of regulation of contraction by calcium.

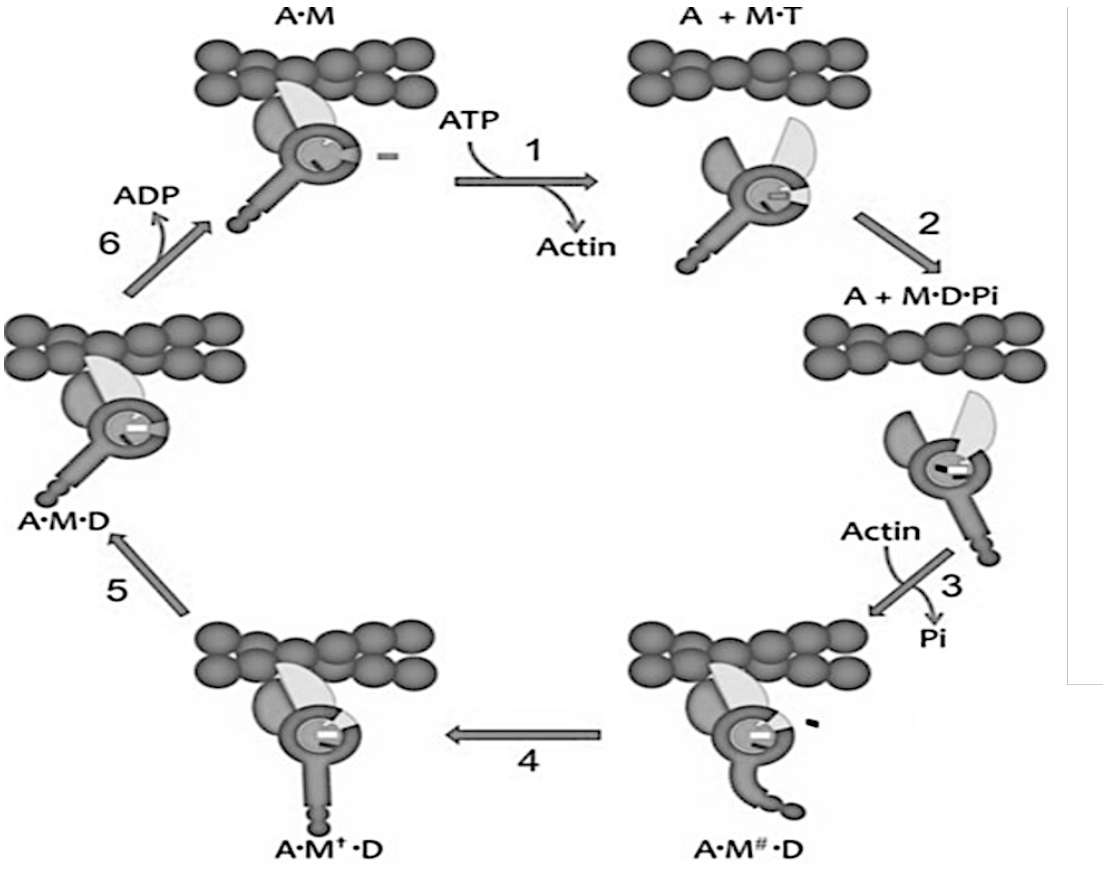

Figure 1.8: A schematic diagram of the ATP binding to myosin head and force generation

The ATP-driven actin-myosin mechanical cycle. Step 1: myosin dissociates from actin once ATP bound. Step2: ATP hydrolysis and recovery stroke. Step 3: actin rebinding. Step 4: force generation and the sliding movement. Step 5 and 6: the nucleotide opens lead to ADP release. Adopted from (Geeves, 2016).

1.4 The molecular basis of regulation of striated muscle contraction

1.4.1 Regulation of muscle contraction

1.4.1.1 Role of Ca^{2+}

In striated muscles, contraction is controlled by calcium release/uptake by the sarcoplasmic reticulum in response to changes in membrane action potential. Calcium concentration changes are relatively modest from around 0.1 micromolar at rest to few micro molars upon calcium release from the sarcoplasmic reticulum. The relationship between calcium concentration and muscle activation is sigmoidal allowing full activation to take place over this narrow change in calcium concentration. When calcium is liberated, it diffuses in the cytoplasm and binds to its receptors (for example calcium binding sites on TnC). Calcium binds to TnC triggers a set of conformational changes on thin filament that ultimately lead to the activation of muscle (as measured by change in actomyosin ATPase or force) (Gordon *et al*., 2000). The sigmoidal shape that characterises the calcium sensitivity curve is a signature of cooperative allosteric behaviour. This behaviour implies cooperation between subunits of a multimeric macromolecular complex following initial activation. This has been explained by the existence of two conformations. An OFF conformation that has a low biological activity and an ON conformation that has a high biological activity.

1.4.1.2 Thin filament switches between ON and OFF state

Early biochemical studies showed that Ca^{2+} regulation of thin filament is allosteric since Ca^{2+} binds to troponin C and controls myosin head binding to actin monomer (the regulation taking place is a long distance from the substrate binding site) (Lehrer and Morris, 1982). Furthermore, myosin binding experiments showed cooperative behaviour suggesting that actin containing thin filaments can exist in two states with different biochemical properties (Hill, 1980). An OFF state that prevails in low calcium concentration, has a low affinity for myosin heads (binds only weakly to myosin heads, K_1), a low actomyosin ATPase, a low force generation and motility properties. The ON state exists in the presence of calcium, has a high affinity for myosin heads (binds initially weakly to myosin heads (K_1) which then isomerise to the strong binding state

(K_2), a high actomyosin ATPase and high force and motility (figure 1.9). It was suggested that thin filaments can be divided into cooperative units that can switch between the ON and the OFF states. The ON-OFF transition is characterised by an equilibrium constant K_T. Each cooperative unit is made of seven actin monomers, one tropomyosin molecule and one troponin complex (with the three subunits I, T and C). The transition between the ON and OFF state is controlled by allosteric effectors that favours one state over the other. The cooperative-allosteric behaviour displayed by muscle thin filaments is comparable to various cooperative-allosteric systems found in biology such as haemoglobin.

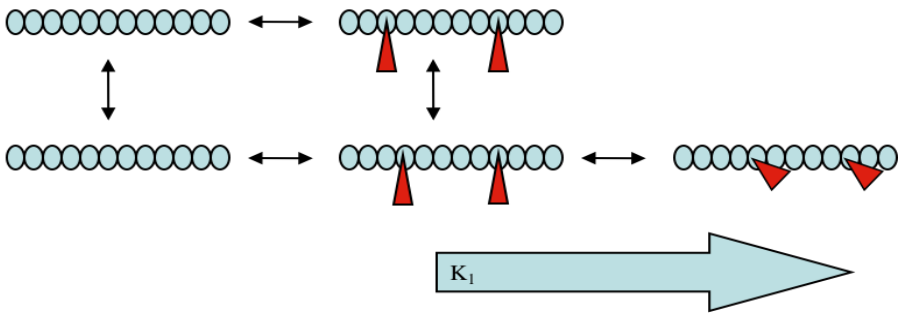

Figure 1.9: Schematic diagram of the thin filament switching between two states (OFF and ON).

The Circles show several actin monomers from an actin filament. The red triangle show myosin heads. K1 is the equilibrium constant of the isomerisation reaction from myosin weak binding to myosin strong binding to actin filaments.

Structural studies were performed to determine the structural basis for the ON-OFF transition. X-ray diffraction pattern from muscle under an activation and relaxation conditions suggested a shift in the position of tropomyosin when the muscle is activated (Kraft *et al.,* 1999). Three-dimensional reconstruction of electron micrographs showed that Ca^{2+} dependent shifts in position of Tpm on thin filaments isolated from vertebrate muscle or actin filaments reconstituted with actin and tropomyosin and the tropomyosin occupies two positions on the surface of actin. In the OFF state, tropomyosin is located towards the outer region of the actin filament in a position that obstructs the interactions between actin and myosin. Upon Ca^{2+} binding to troponin,

tropomyosin moves towards the grove of the actin filament uncovering the myosin binding sites on the surface of actin filaments (figure 1.10) (Lehman *et al*., 1994, 1995).

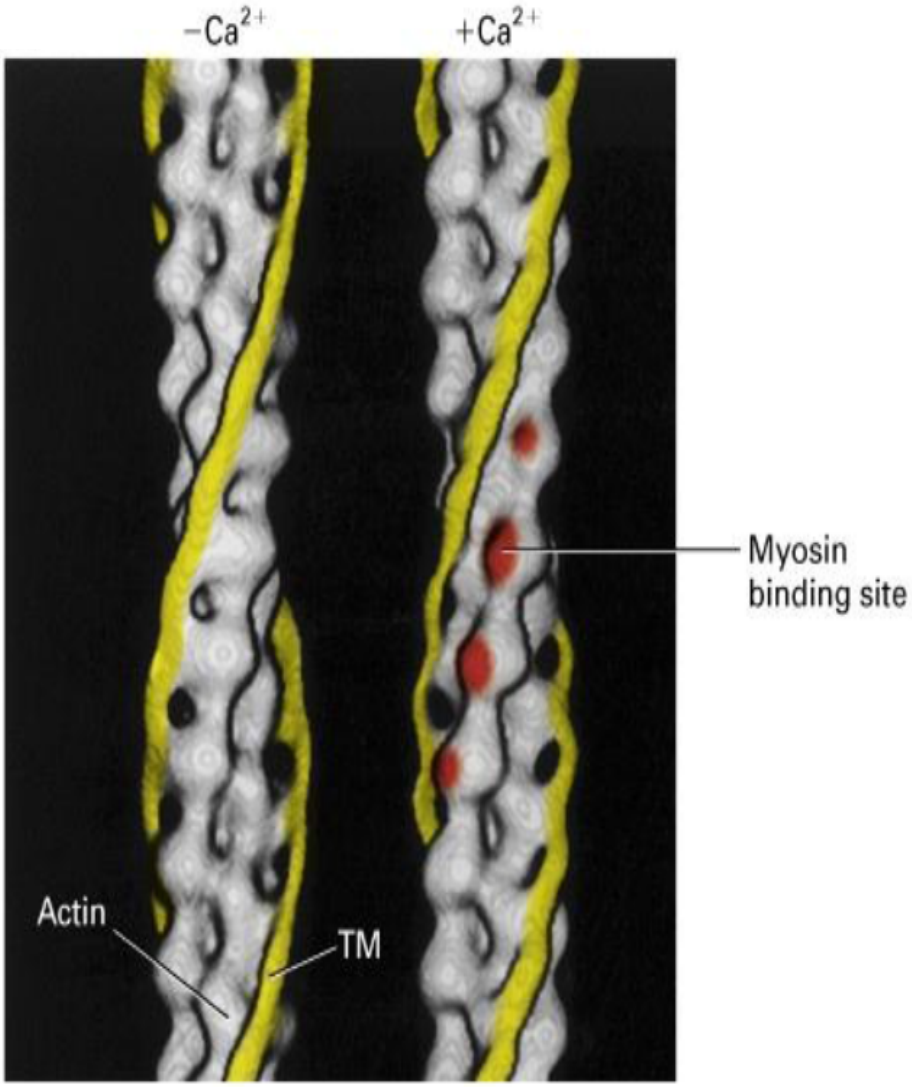

Figure 1.10: Schematic diagram of the Tropomyosin switching between the two states (OFF and ON).

The diagram illustrates the position of Tpm on actin filament. In the absence of calcium, the Tpm blocks the myosin binding sites on actin. In the presence of calcium Tpm moves from the groove of actin and the myosin binding sites on actin are exposed (Red). (The figure adopted from Lodish and Harvey, 2003).

1.4.1.3 Thin filament switching between three states

The two states model described above is able to account for several properties of muscle; however, it was not possible to explain the obtained data for the binding kinetics of myosin heads to the thin filaments in the presence and absence of calcium. A three state model was proposed by Geeves and his colleagues to explain the kinetic data (McKillop and Geeves, 1993). In this model, the thin filament acts as a cooperative allosteric system that switches between three states. A) Blocked state where myosin heads binding is prevented, B) Closed state in which myosin heads can attach to the thin filaments but only in a weakly bound conformation and C) Open state, which allows the isomerisation of myosin heads to the strong binding state. The transition to the open state is the event associated with the activation of the myosin ATPase and generation of force. In this model, the equilibrium between the Blocked and the Closed state (defined by K_B) is under the sole control of Ca^{2+} while the equilibrium between the closed and open (defined by K_T) is controlled by myosin strong binding and Ca^{2+}. A study from the same laboratory showed that the Blocked state is about 66% in skeletal muscle and 50% in cardiac muscle (Maytum *et al*., 2003). A study had refined the three-dimensional reconstructions of thin filaments in the Blocked, Closed and Open states have shown that the OFF state can be separated into two structural states (Blocked and Closed states) in which tropomyosin position is different. In the Blocked state tropomyosin covers the majority of myosin binding sites while in the Closed state tropomyosin is located closer to the thin filament axis covering actin residues involved in myosin strong binding but uncovering actin residues involved in myosin weak binding (Lehman *et al*., 2000; Lehman and Craig, 2008).

1.5 Tropomyosin

1.5.1 History and discovery

Tropomyosin is widely distributed protein in all cells and muscles. Tropomyosin is always co-localised with actin filaments where it regulates their function (Gunning *et al*., 2008). Tropomyosin is one of the first muscle proteins discovered (after actin and myosin). In 1946, Baily treated myofibrils with organic solvents that caused selective denaturation of myosin, and identified tropomyosin as an important muscle protein (Bailey, 1946). The protein was named *Tropomyosin* since its amino acid composition and physical properties appeared to be similar to myosin. In particular, the change in the ionic strength affects the viscosity of tropomyosin solution similarly to myosin. At low ionic strength, Tpm is highly viscous, and this was shown by electron microscopy to be due to the formation of long fibrils of 20-30 nm diameter. Increasing the ionic strength of the solution leads to the dissolution of these fibrils. The fibrils formed at low ionic strength are due to the polymerisation of tropomyosin molecules while high ionic strength induces their depolymerisation. The usage of hydrodynamic studies of tropomyosin in the absence and presence of denaturing agents did help Bailey to conclude to describe the tropomyosin as a dimeric protein. The tropomyosin interactions with actin was also established in the late 1950s (Corsi and Perry, 1958). Overall, the main properties of tropomyosin were quickly established soon after its discovery; however, 60 years later the mechanism of action and cellular function of tropomyosin are not yet fully understood.

1.5.2 Gene structure

In mammalians, tropomyosin proteins are the products of four genes: Tpm1, Tpm2, Tpm3 and Tpm4. Furthermore, each gene can be expressed by alternative promoters and is subject to alternative splicing, which gives rise to over 20 isoforms of tropomyosin in humans (Figure 1.11). Most of these isoforms are expressed in various cells and various stages of development and only few are expressed in muscle.

1.5.2.1 Tpm1 gene

The most complexed mammalian tropomyosin gene is the α-tropomyosin (α-Tpm) gene, which was first studied in a rat genomic clones' analysis (Ruizopazo and Nadalginard, 1987., Miller *et al*., 1990). The α-Tpm gene in humans is similar in structure to that in mice, spanning 27 kb and 29 kb, respectively. Tpm1 gene uses one of two promoters and contains 15 exons and is 29 kb in size. Five exons (exons 3, 4, 5, 7 and 8) are expressed in all isoforms while the other exons (1a, 1b, 2a, 2b, 6a, 6b, 9a, 9b, 9c and 9d) are alternatively spliced exons resulting in different N-terminal and C-terminals parts. In addition, there are two mutually exclusive exons (2a/2b and 6a/6b). The α-Tpm is present in the skeletal muscle (Tpm skα), the smooth muscle (Tpm smα) and the non-muscle (Tpm2, Tpm3, Tpm5α and Tpm5β), including three brain-specific isoforms (TpmBr1, TpmBr2 and TpmBr3) (Lees-Miller *et al*., 1990a; Lin *et al*., 2008; Vrhovski *et al*., 2008).

1.5.2.2 Tpm2 gene

The β-tropomyosin (β-Tpm) gene contains a single promoter, spans 11 exons and depending on the source, is between 8 and 10 kb. Tpm2 has a unique internal mutually exclusive exon (6a:6b) and two different C-terminal exons (9a/9d). The skeletal β-Tpm isoform and the smooth muscle β-Tpm isoforms each of which have two 284 amino acids Tpm proteins produced by the β-Tpm gene (MacLeod *et al*., 1985; Helfman *et al*., 1986). Tpm2 codes for tropomyosin isoform presents in skeletal and smooth muscles and a cytoskeletal isoform Tpm1 (Lin *et al*., 2008).

1.5.2.3 Tpm3 gene

The ϒ-Tropomyosin (ϒ-Tpm) gene was named 'Tpm 30 nm' after first being described in humans, which spans 42 kb. It has two promoters and contains 14 exons and is subject to substantial alternative splicing, it has four C-termini and a single mutually exclusive internal exon (6a:6b) (Clayton *et al*., 1988). The tropomyosin expressed in the slow twitch of skeletal muscle and several low molecular weights cytoskeletal tropomyosins is the ϒ-Tpm gene which encodes 284 amino acids residues. The case is different in rats and mice, whereas the former produces at least ten cytoskeletal isoforms that range from 177 to 248 amino acids, while the latter produces at least 11 cytoskeletal isoforms (Dufour *et al*., 1998). Tpm3 codes for several cytoskeletal tropomyosin isoforms and for the slow twitch skeletal muscle isoform.

1.5.2.4 Tpm4 gene

Tpm4 is unlike the other Tpm genes in which it is not alternatively spliced in rats and mice. Tpm4 spans between 16 and 18 kb of DNA and contains 8 exons and codes for a non-muscle isoforms (Lees-Miller *et al*., 1990b).

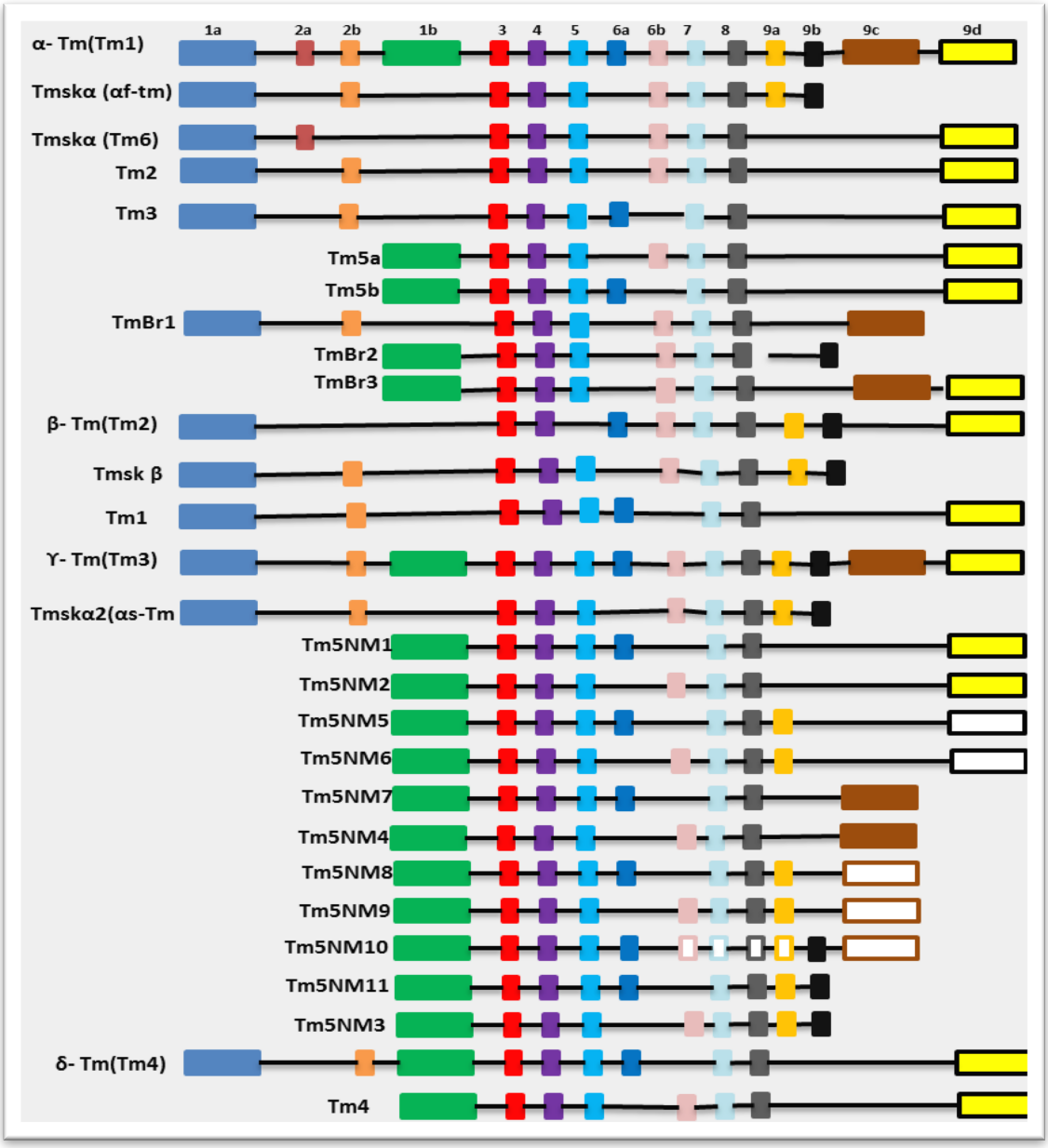

Figure 1.11: Tpm gene map

The gene structure of mammalian Tpm genes. Every isoform where exons are represented by boxes and introns are represented by lines (graph was modified based on Guuning *et al*., 2008; Lin *et al*., 2008; Vrhovski *et al*., 2008).

1.5.3 Tropomyosin protein structure

Tpm can be divided into two groups depending on its number of residues: 1) Tpm containing around 284 residues, called high molecular weight (HMW), and 2) Tpm containing around 240 residues called low molecular weight (LMW). All muscles Tpm are HMW, whereas non-muscles Tpm are both HMW and LMW (Gunning *et al*., 2008). Tropomyosin forms crystals easily; however, they have a high content of water and cannot generate a diffraction pattern of sufficient quality for a high-resolution structure. Nevertheless, the diffraction pattern obtained from these crystalline structures allowed the determination of the structure of tropomyosin as a left handed coiled coil made from two right handed alpha-helices. This structure could be achieved by Crick's structure prediction for coiled coil protein that a repetition of a heptad motif in which the first and fourth amino acids are hydrophobic and located on one side of the alpha-helix which allow the two helices to dimerise. Crick (1953) called the interactions between residues (*a*) and (d) the "*knobs into holes"* due to the interface of the two helices and each residue was localised in a cavity formed by three residues from the other helix.

The determination of the amino acid sequence of Tpm from a rabbit skeletal muscle was achieved by Johnson and Smillie (1975). The sequence of tropomyosin showed periodic arrangements of hydrophobic amino acids within the polypeptide chain and largely agreed with the prediction made by Crick (1953). Tropomyosin consists of 284 residues extended to α-helix that assemble into a dimeric coiled coil (figure 1.12). The sequence shows a repeating heptad motif (residues in a seven amino acid repeats are labelled *abcdefg*, figure 1.12) with an amphipathic character. For each repeat residues *a* and *d* are polar and packed together to form the hydrophobic core of the coiled coil. The coiled coil is further stabilized by electrostatic interactions between the charged residues in position *e* and *g*. The amino acids in position *b*, *c* and *f* are exposed and are likely involved in the interactions with actin and possibly troponin. Crick's model did not exclude the prospect of a chain shift relative to helices for the number of residues multiplied by seven; consequently, it remained unclear whether the Tpm chains were in register or not. A study showed that disulphide bonds formed between cysteine 190

from each chain (Lehrer, 1975). This study confirmed that Tpm chains are parallel and in 'register'.

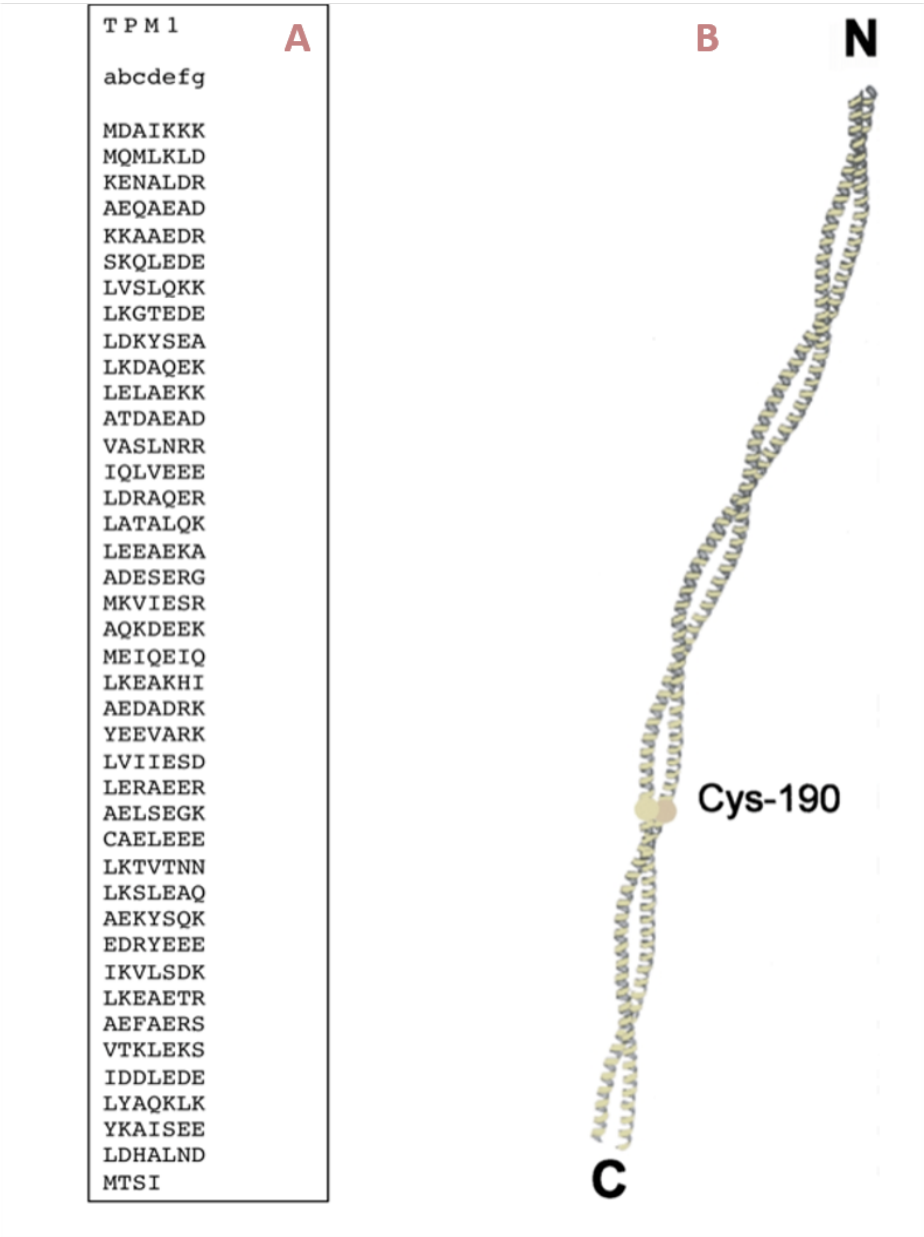

Figure 1.12: Tpm1 sequence displayed to visualise the position of residues in the heptad motif and tropomyosin tertiary coiled coil structure.

(A) Shows Tpm1 amino acids sequence and the seven heptad repeats. (B) Shows the coiled coil of Tpm and the N-terminus and C-terminus (Whitby and Phillips, 2000).

.

1.5.4 Characteristic features of tropomyosin structure

A high resolution structure of Tpm (1-2A) has not yet been determined due to the difficulty to obtain high quality crystals. However, several research groups have determined the atomic structure of several fragments of skeletal muscle α-Tpm at gigh resolution (Whitby and Phillips, 2000). In solution, Tpm forms high quality crystals and para-crystals, also called Bailey crystals. These para-crystals have a high solvent content (> 90 %) and are characterized by a blurred X-ray diffraction pattern. Crystals at 7 Å resolution were used to determine information about the general form and package of individual molecules (Whitby and Phillips, 2000). Since Tpm produces a variety of crystalline and paracrystalline forms, it is thought to be that Tpm molecule exhibits high conformational mobility and is not a pure coiled-coil α-helix. A high resolution structure for the N-terminal fragment of chicken skeletal muscle α-Tpm has been obtained and had shown that the hydrophobic core contained two Alanine clusters. In the region of residues 15–36 of the N-terminal fragment, a characteristic feature was noted in which the distance between the two Tpm chains was shortened to 8 Å, while the inter-chain distance was 9.5–10 Å. Moreover, within the region coinciding with the Ala cluster, there was an axial shift of about 1 Å in the Tpm chains relatively to each other. The chains shift showed that the Tpm molecule is bending in the place of the Ala clusters (on average by 6°) (Brown *et al*., 2001). In 2005, a high resolution structure was obtained for the central part (89-208) of the rat α-Tpm. This redion is of interest because of its significant instability (Brown *et al*., 2005). The results were in agreement with previous findings (Brown *et al*., 2001). In the tropomyosin stretch residues 150-160, is present another set of Ala clusters which allows for the bending of the molecule due to local shortening of the double helix radius. It was also noted that the alternating of canonical residues with a large hydrophobic residue (e.g. Met127 and Met141) with Ala clusters in position *d* (Ala102, Ala109, and Ala116) and in position *a* (Ala134). The alternation of these residues resulted into the formation of cavities in the hydrophobic core of the central part of the Tpm molecule. The presence of these cavities is correlated to the bending. Maeda's group has also analysed the C-terminal fragment of rabbit skeletal muscle α-Tpm and confirmed the earlier findings (Nitanai *et al*., 2007; Minakata *et al*., 2008). Overall, their studies demonstrated the presence of occasional breaks in

the canonical heptad, which cause a bend in the otherwise straight helix. This enables tropomyosin to wrap around the actin double helix. There are also two global bend at two points in the sequence (D137 and E218). Moore *et al*., studied the bend at the conserved D137 and found that it destabilises the α-helical structure and increases the flexibility in this region (Moore *et al*., 2001). Further deviations from the canonical hydrophobic core motif (presence of Ser, Thr, Cys, Gln and Lys in positions *a* or *d*) caused an increase segmental flexibility which is necessary for the change in the actin-tropomyosin conformation during the activation and relaxation of muscle (Kwok *et al*., 2004).

In thin filaments, tropomyosin forms a continuous strand due to nine amino acids overlap of the N and C termini of adjacent proteins. In this region, the four chains form a quadruple helix that maintains the rigidity of the coiled-coil region. A study of the overlap complex of Tpm showed that there was an insertion of 11 residues of the N-terminal of one coiled coil into the resulting cleft of the chains of the C-terminal of the adjacent coiled coil (Greenfield *et al*., 2006). Moreover, this study showed a rotation of the plane N-terminal coiled coil with 90° relative to the plane of the C-terminal (Greenfield *et al*., 2006).

1.5.5 Tropomyosin acetylation

The most important post-translational modifications that takes place on tropomyosin is the N-terminal acetylation. Initially, several studies have shown that in skeletal and smooth muscles the Tpm high affinity binding with actin requires an N-terminal acetylation (Hitchcock-DeGregori and Heald, 1987; Monteiro *et al*., 1994). In the absence of troponin and lack of acetylation of skeletal muscle Tpm, actin binding is inhibited (Urbancikova and Hitchcock-DeGregori, 1994). Skeletal muscle tropomyosin acetylation occurs at the N-terminal Methionine which was shown to be critical for end-to-end interaction and cooperativity of tropomyosin binding to actin (Hitchcock-DeGregori and Heald, 1987; Heald and Hitchcock- DeGregori, 1988). The N-terminal and C-terminal parts of tropomyosin are crucial for tropomyosin polymerisation and binding to actin. It has been reported that the reduction in actin affinity induced by the absence

of acetylation was caused by the disruption of the structure of the N-terminal and C-terminal (Cho et al., 1990; Urbancikova and Hitchcock-DeGregori, 1994). It was suggested that acetylation stabilizes the formation of the coiled-coil structure in the junction between two adjacent tropomyosin molecules (Greenfield *et al*., 1994). A study compared the actin binding of tropomyosin molecules expressed as a fusion and non-fusion proteins. The fusion Tpm proteins with addition of 80 amino acids showed normal binding to the actin (Hitchcock-DeGregori and Heald, 1987). It has been shown that for bacterially expressed tropomyosin (lacking the acetylation), the addition of di or tri peptides at the N-terminal did mimic the acetylation of Methionine and produced a protein able to bind actin and polymerised easily (Monteiro *et al*., 1994). However, this effect is altered in different isoforms of tropomyosin. For instance, the actin binding affinity showed an eight-fold reduction for non-acetylated β Tpm and a forty-fold reduction for non-acetylated α Tpm (Coulton *et al*., 2006). Bacterially systems expressing Tpms are lacking the N-terminal acetylation. Therefore, addition of a di- or tripeptide at the N-terminus mimics the N-acetyl group of muscles Tpm and enhances the actin Tpm binding (Monteiro *et al*., 1994).

1.5.6 Tropomyosin dynamics

The interaction of Tpm with other thin filaments proteins is dependent on Tpm dynamics (Li *et al*., 2009). Tpm dynamics can be classified as internal dynamic motions and global dynamics as reviewed by El-mezgueldi (2014). Several research groups have studied tropomyosin dynamics using a wide range of experiments, including fluorescence spectroscopy, NMR spectroscopy, mutagenesis, atomic force spectroscopy and molecular dynamics simulations (Barua *et al*., 2013; Brown *et al*., 2001; Greenfield *et al.,* 2001, 2006; Ischii and Lehrer, 1991; Lehrer and Qian, 1990; Li *et al*., 2009, 2010; Sousa *et al*., 2010).

Studies using hydrogen exchange have confirmed that 20 % of Tpm was immobile which means that the tropomyosin is a highly dynamic molecule (Sanders *et al*., 1988). The presences of multiple transitions in the unfolding domains of the Tpm molecule were found during the denaturation of Tpm by heat or by chemotropic agents (Ishii *et al*., 1992). The excimer fluorescence in pyrene-Tpm at the interface of the two chains around Cys 190 was suggested to be caused by local unfolding of the coiled coil (Graceffa and Lehrer, 1980). The ability of Tpm to bend in opposite directions in the axis of the coiled coil is believed to be due to the Ala clusters, which increases flexibility. The Tpm molecule can have as many as 128 bent conformations of equal energy due to the presence of Ala clusters (Brown *et al*., 2001). In the middle part of the tropomyosin molecule precisely at position *d* in the heptad repeat, a polar and negatively charged amino acid (Asp-137) is found. This induces instability of Tpm at this residue as shown by tryptic cleavage at Arg-133 and Ala-134 (Sumida *et al*., 2008). A slight increase in local flexibility was seen in a molecular dynamics simulation where Asp-137 mutated to a canonical Leu (Nirody *et al*., 2010). A decrease in the end-to-end angle of the Tpm rod resulted from this single amino acid mutation, which indicated that the Tpm rod straightened or there was a decrease of the Tpm curvature (Moore *et al*., 2011). The consequences of Asp-137 presence is to destabilize the middle region of Tpm and to induce the flexibility of Tpm to move over actin. Also, the presence of non-canonical amino acid Gly-126 increases the tryptic digestion at Arg-133 and decreases the temperature required to induce the unfolding of Tpm (Nevzorov *et al*., 2011). Glu-218 in position (*a)* in the heptad repeat increases the flexibility of the coiled coil and introduced a bend that was non-canonical (Nitanai *et al*., 2007)

1.5.7 Tropomyosin interactions with actin

Tropomyosin binds actin and this interaction plays a key role in the cooperative allosteric activation and inhibition of muscle contraction also plays a cellular role in the cytoskeleton. The details of this cooperative allosteric mechanism of regulation dictate the physiological behaviour of striated muscle and its alteration is likely to compromise muscle performance. The key binding of tropomyosin interactions is with actin. Early studies have shown that tropomyosin is not a typical actin binding protein. Individual

tropomyosin molecules have a very low affinity for actin (10^4 M^{-1}) (Wegner, 1980). This binding affinity only becomes higher when tropomyosin molecules are joined (Wegner, 1979, 1980). This highlights the critical role played by the N-terminal acetylation and the head to tail interactions between adjacent tropomyosin molecules in binding to actin. Tropomyosin-actin binding curves are sigmoidal pointing to the cooperative nature of this interaction. The cooperativity of tropomyosin binding to actin is thought to be due at least in part to the end-end interactions between adjacent tropomyosin molecules.

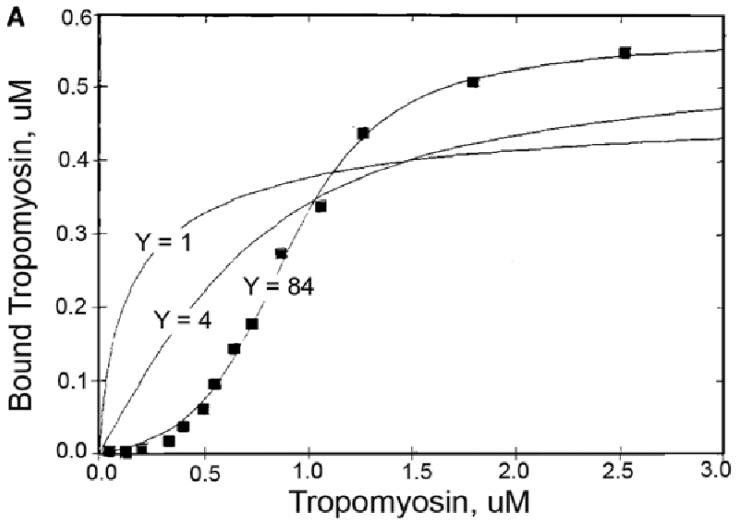

Figure 1.13: the cooperativity of tropomyosin to actin filament

Best fit curves for different parameter of cooperativity (Y=1 no cooperativity, Y=4: low level cooperativity and best fit curve is obtained with Y=84. y is the fold increase in affinity. Figure obtained from Hill *et al*.,1992.

Binding of tropomyosin to actin is also very salt dependent being very weak at low ionic strength (less than 20 mM KCl and 1 mM $MgCl_2$) and tight at (100 mM KCl and 4 mM $MgCl_2$) (Eaton *et al*., 1975). Due to the stoichiometry of tropomyosin-actin interaction, the Tpm can occupies two positions on the surface of actin filaments. McLachan and stewart (1975) proposed the existence of 14 actin binding motifs of 19-20 residues in tropomyosin which are divided into alternating α and β bands. The α and β-bands were proposed to represent actin binding sites for two different thin filament states (ON and OFF states). The α-bands form an interface with actin in the absence of Ca^{2+} (OFF state)

whilst in the presence of Ca^{2+} (ON state), tropomyosin rolls 90° so that the β-bands form an interface with actin. An additional peculiarity in tropomyosin binding to actin is that the radius of Tpm binding to actin was consistently found to be about 38–42 Å from the actin filament axis (Xu *et al*., 1999; Narita *et al*., 2001). This is much bigger than traditional protein-protein interaction distances (few 1-5 Å). Tropomyosin appears to make only a few contacts with actin monomers and both the super-helical pre-shaping of the tropomyosin polymer and electrostatic interactions play a huge role in its binding to actin and that has been termed 'Gestalt binding' by (Holmes and Lehman, 2008).

```
       Alpha bands          Beta bands

MDAIKKK
abcdefg

MQMLKLDKENALDRAEQAEA DKKAAEDRSKQLEDELVSL
abcdefgabcdefgabcdef gabcdefgabcdefgabcd

QKKLKGTEDELDKYSEALKD AQEKLELAEKKATDAEADV
efgabcdefgabcdefgabc defgabcdefgabcdefga

ASLNRRIQLVEEELDRAQER LATALQKLEEAEKAADESER
bcdefgabcdefgabcdefg abcdefgabcdefgabcdef

GMKVIESRAQKDEEKMEIQE IQLKEAKHIAEDADRKYEE
gabcdefgabcdefgabcde fgabcdefgabcdefgabc

VARKLVIIESDLERAEERAE LSEGKCAELEEELKTVTNNL
defgabcdefgabcdefgab cdefgabcdefgabcdefga

KSLEAQAEKYSQKEDRYEEE IKVLSDKLKEAETRAEFAE
bcdefgabcdefgabcdefg abcdefgabcdefgabcde

RSVTKLEKSIDDLEDELYAQ KLKYKAISEELDHALNDMTSI
fgabcdefgabcdefgabcd efgabcdefgabcdefgabcd
```

Figure 1.14: Sequence of skeletal muscle α-tropomyosin

The figure is showing the location of alpha and beta bands in Tpm sequence corresponding to tropomyosin binding in ON and OFF state.

Furthermore, Tpm position on the surface of actin is affected by several allosteric effectors such Ca^{2+}, troponin, myosin head (Greenfield *et al*., 2002; Singh and Hitchcock-DeGregori, 2003, 2006). X-ray diffraction patterns obtained from muscle fibres and early electron microscopy and image reconstruction achieved with reconstituted thin filaments, suggested that tropomyosin only occupies two distinct positions (ON and OFF). However, it is now believed that these studies had several limitations. The fibres

used in the X-ray studies contain both troponin and nebulin and the position of tropomyosin is not unambiguous. The early electron microscopic studies had only a 20 -30 Å resolution. More recent higher resolution cryo-electron-microscopic studies were able to visualise three positions of tropomyosin on the surface of the actin filament. These positions correspond to the Blocked, Closed and Open state identified by kinetic and binding studies (Lehman *et al*., 2013). All structural investigations have indicated that tropomyosin changes position from the outer domain of actin (over subdomain1) covering most of actin residues involved in myosin binding to a position on the inner domain of actin where it does not cover myosin binding sites (Over subdomain 4) (Brown *et al*., 2005; Li *et al*., 2011).

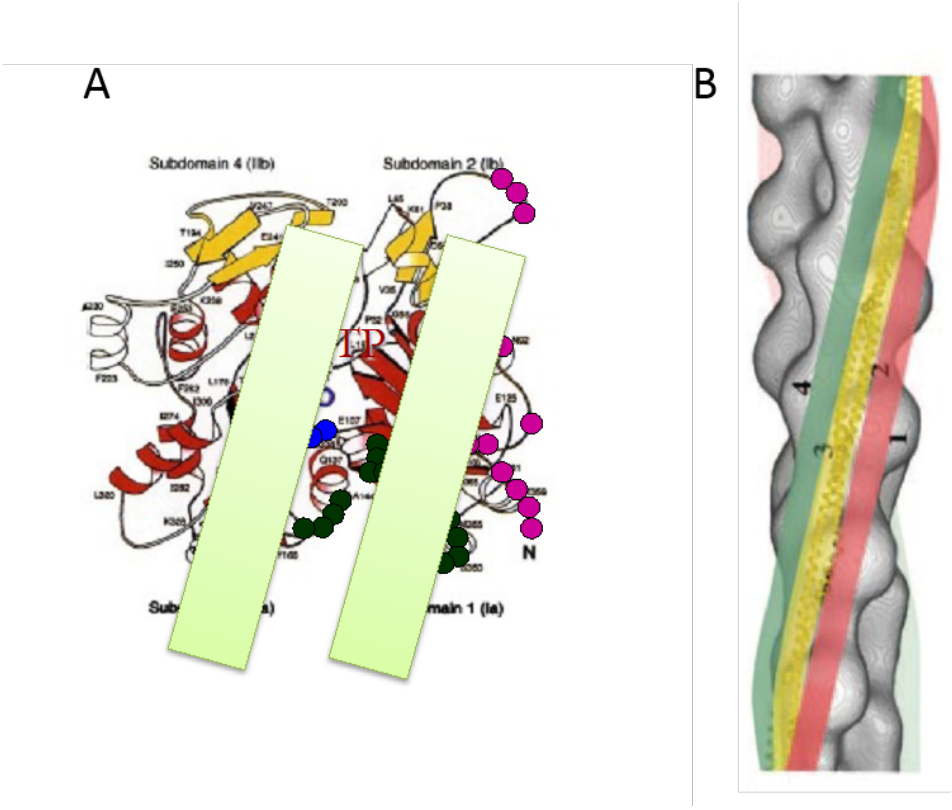

Figure 1.15: Tropomyosin models binding with actin and movements on actin filament.

In A) a representation of the Tpm (green strips) is interacting with subdomains 1 and 2 in the OFF state while it moves to subdomain 3 and 4 in the ON state. Pink, green and blue dots represent actin residues involved in myosin head binding. (B) Shows the movement of Tpm on actin filament from Blocked to Closed to Open and the exposition of myosin binding sites on actin. Original structures adopted from (Kabsch *et al*., 1990; Brown *et al*., 2005).

The mechanism of Tpm movement over actin is still intensely debated. Several research groups proposed that Tpm simply slides over the actin surface with no major changes in its configuration (Behrmann *et al*., 2012; Lehman *et al*., 2013). Other have proposed a rolling mechanism, in which there is an axial rotation of the Tpm chain about its axis (Bacchiocchi and Lehrer 2002; Holthauzen *et al*., 2004). Studies have showed two energy minima between single tropomyosin molecules and the F-actin filament after map calculation. The calculations of these two minima showed that each of which is positioned over a distinct but relatively shallow energy basin. The study illustrates two atomic models of the thin filament and the tropomyosin position is in parallel to the filament axis and is translated longitudinally by 24 Å up and down F-actin (Rynkiewicz *et al*., 2015). The findings came in agreement with EM-reconstructions of actin-tropomyosin (Li *et al*., 2011; von der Ecken *et al*., 2014; and Rynkiewicz *et al*., 2015).

1.5.8 Tropomyosin interactions with troponin

The second most important partner of tropomyosin in muscle is the troponin complex. While tropomyosin is ubiquitous, the troponin complex is only expressed in striated muscle (with isoforms specific to the different types of striated muscle). This imply that the interaction of tropomyosin with troponin is particularly important in the Ca^{2+} dependent regulation of muscle contraction. The interaction of tropomyosin with troponin has two main roles. The first one is to link the site of Ca^{2+} dependent allosteric regulation to the actin filament while the second is to keep the distribution of these Ca^{2+} sites regular along the entire actin filament. On the other hand, troponin increases the affinity of tropomyosin to actin filaments. The interaction of troponin with tropomyosin is mediated primarily by the TnT subunit. As discussed above troponin T has two regions T1 and T2. Two troponin T regions have been postulated as tropomyosin binding sites: the first is at troponin residues 1-158 (T1 segment) while the second is at residues 159-259 located close to the C-terminal end (T2 segment) (Figure 1.16). It has been found that after removing residues 70-150 the interaction of troponin T with tropomyosin is significantly reduced implying that this region of troponin T is an important tropomyosin binding site (Fisher *et al*., 1995). The site within residues 70-150 is possibly the main Ca^{2+} independent site of the TnT-tropomyosin interaction and is

therefore not involved in the Ca^{2+} dependent allosteric transition. The interaction at this site helps keep the troponin complex always attached to the thin filament. It has been proposed that a triple coiled coil is formed between this region of TnT and tropomyosin which is stabilized by hydrophobic interactions (Perry, 1998). This TnT segment is thought to bind at the C-terminus of the tropomyosin dimer (258-284) and possibly extends over the junction with the adjacent tropomyosin molecule (Mak and smillie, 1981). The interaction of the second site (TnT residues 159-259) is Ca^{2+} dependent and involves in the tropomyosin region around Cys-190 of tropomyosin possibly 189-213. (Pearlstone and Smillie, 1983; Filatov *et al*., 1999).

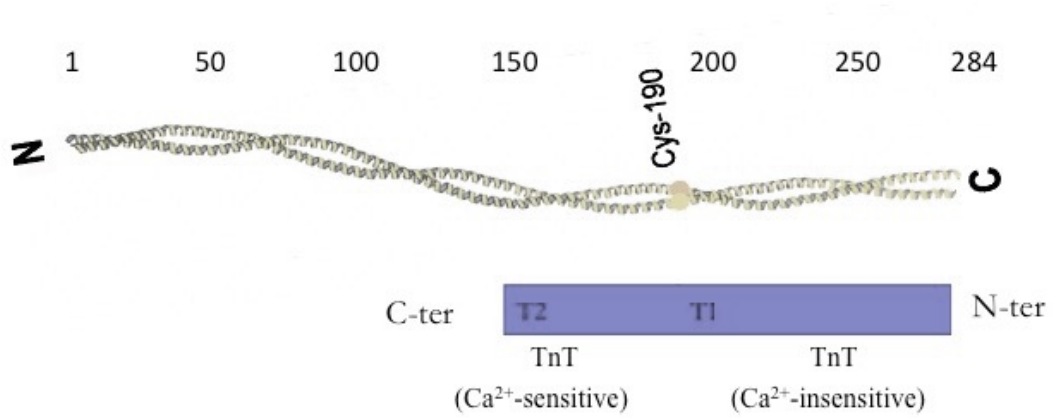

Figure 1.16: A schematic representation of tropomyosin interaction with Troponin T

The figure shows tropomyosin coiled coil and numbers of amino acids. The blue box represents the TnT segments binding T1 and T2 with tropomyosin. The interaction of the two segments with Tpm is from 150-284. (Whitby and Phillips, 2000).

1.5.9 Tropomyosin function

Early Studies of the function of thin filaments components showed that in the absence of tropomyosin, the thin filament activation of myosin head ATPase was hyperbolic and follows simple Michaels Menten kinetics. In the presence of tropomyosin, the effects of thin filaments became cooperative with or without the troponin. These experiments demonstrated that the first function of tropomyosin in thin filament is to introduce cooperativity (Lehrer and Morries, 1982; Lehrer and Geeves, 1998) (figure 1.17).

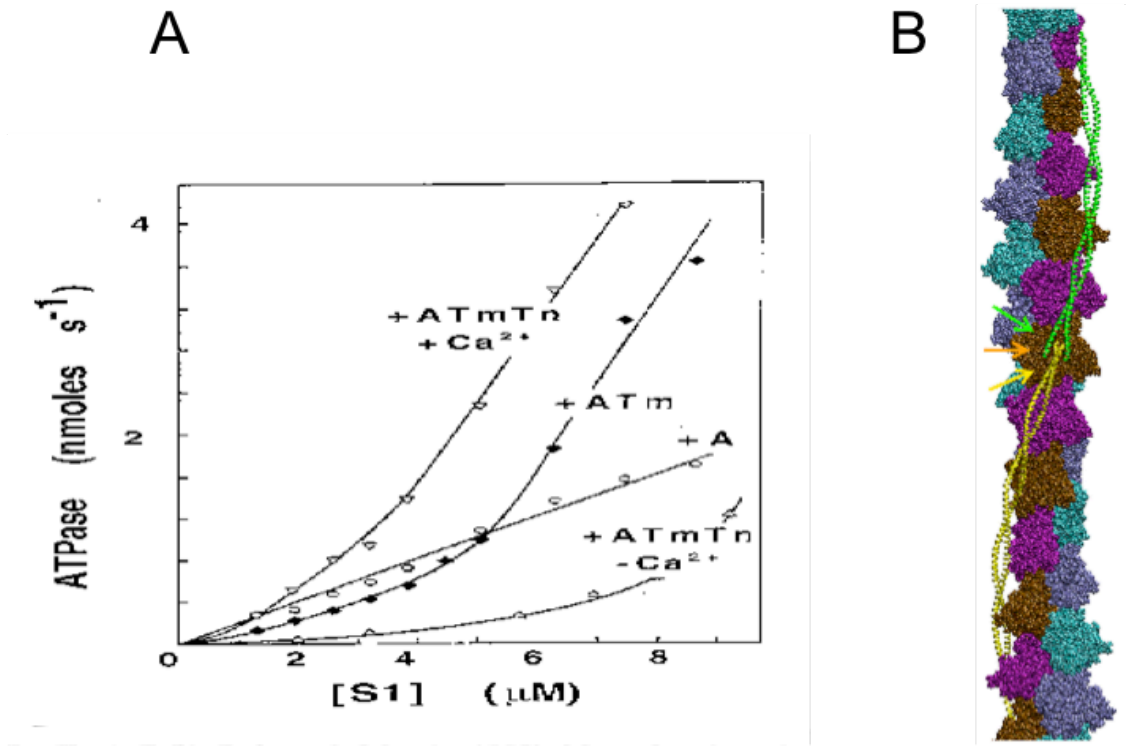

Figure 1.17: The tropomyosin cooperativity on thin filament.

A) Shows the effect of presence and absence of tropomyosin on thin filament cooperativity. B) Shows the importance of tropomyosin polymerisation to introduce cooperativity to thin filament and that is based on the interaction and acetylation of the tropomyosin molecules. Figures adopted from (Lehrer and Morries, 1982; Orzechowski *et al*., 2014).

Cooperativity is defined as an increase in the affinity of a ligand in a multimeric complex as the occupancy of the different sites increases. Traditionally, cooperativity was studied in oxygen binding to haemoglobin, haemoglobin is however a simple system where each isolated independent tetramer acts as a unit. Thin filaments are a more complex system since it is a continuous system with hundreds of monomers in a single filament (Boussouf and Geeves, 2007). Furthermore, in thin filament each Tpm only interacts with one strand of the actin filament (out of the 2 strands). The head to tail interaction is thought to remain even when the local position of Tpm on the surface of actin changes. The determinants of thin filament cooperativity are not well understood. Hill (1980) proposed that the nearest neighbour Tpm-Tn interactions are the origin of thin filament cooperativity (Hill *et al.*, 1980). Others have separated short range and long-range cooperativity. The 3-state model proposed by McKillop and Geeves (1993) did not require longer-range cooperativity and the cooperativity was discussed in the context of a single isolated structural unit of (7 actin: 1 Tpm:1 Tn) (McKillop and Geeves, 1993). The cooperativity in these cases were attributed to tropomyosin global repositioning over the myosin binding sites on actin (Poole *et al*., 2006). The tropomyosin stiffness allows the translocation of the Ca^{2+} binding to troponin and/or myosin binding to actin signals up and down the thin filament. Tropomyosin is trapped in one or another regulatory position on thin filaments when Ca^{2+} frees Tn and myosin head binds actin. Therefore, the propagated repositioning of semi-rigid tropomyosin on actin under the influence of troponin and myosin will defines the simple cooperative on-off switching mechanism (Holmes and Lehman, 2008). The cooperative unit *n* is defined by the average number of actin sites activated by the binding of a single myosin head to an actin filament. The continuous Tpm-Tpm strand along the surface of actin and actin-actin contacts are likely the determinants of long-range cooperativity. Overall, tropomyosin is considered as fundamental protein for the cooperativity allosteric regulator of muscle contraction (Lehrer, 2011).

Other determinants of cooperativity are Ca^{2+} binding to troponin and myosin binding to actin. Skeletal muscle TnC has 4 Ca^{2+} binding sites and the cooperativity of Ca^{2+} binding to thin filaments may contribute to thin filament cooperativity (Moore *et al*., 2011).

1.5.10 Tropomyosin in disease

Mutations in three tropomyosin genes (Tpm1, Tpm2 and Tpm3) (fast skeletal α-tropomyosin, skeletal muscle β-tropomyosin and skeletal muscle γ-tropomyosin isoforms) have been implicated in several cardiac and skeletal muscle genetic diseases. Mutations in α-tropomyosin have been described in genetic hypertrophic (HCM) and dilated (DCM) cardiomyopathies. HCM is a disease characterised by increased thickness of the wall of the ventricles (Fig 1.18) and is associated with a high risk of sudden death. DCM is a cardiac disease characterised by an increase of the volume of the ventricle DCM leads to heart failure and is life threatening.

Several mutations in α-tropomyosin were described in genetic hypertrophic cardiomyopathies including A22S, D58H, E62Q, A63V, K70T, V95A, A107T, I172T, D175N; E180G, E180V, L185R, S215L, M281T and I284V (Thierfelder at al., 1994, Wernicke *at al*., 1999). The impact of these mutations on tropomyosin structure, interactions with actin and troponin, and functional properties such as cooperative allosteric regulation of actomyosin ATPase activity and in vitro motility have been intensively studied. The results showed that, in general, these mutations led to an increase in thin filament calcium sensitivity compared to wild type tropomyosin (Bottellini *at al*., 1998). Some but not all mutations displayed a slight impact on tropomyosin structure as measured by thermal stability assays. For instance, mutation Asp175Asn showed no significant effect on the thermal denaturation with F-actin bound Tpm while E180G has decreased the thermal denaturation with F-actin bound Tpm (Kremneva *et al*., 2004). A pathophysiological interpretation of this effect was put forward. It was suggested that in the case of the common cold or intensive muscular activity when temperature in the heart increases by only a few degrees the E180G mutation begins to dissociate from the actin filament surface and denature (Nevzorov *et al*., 2008). Another study on cardiomyopathy associated mutations in tropomyosin (E180G, E180V, L185R and I172T) showed several differences in tropomyosin structure and function (Matyushenko et al., 2016). The C-terminal thermal stability has been reduced by all these mutations. The in vitro motility assay revealed an increase in thin

filament calcium sensitivity and the velocity of thin filament movement over myosin by tropomyosin mutations E180G, E180V, L185R (Matyushenko et al., 2016). A study on both DCM (E40K and E54K) and HCM mutations (D175N and E180G) showed that these mutations affected the sliding velocity of actin filament movement in the in vitro motility assay (Kopylova et al., 2016). This study showed that tropomyosin mutations D175N and E180G increased both thin filament calcium sensitivity and their sliding velocity. For Tpm E54K, the sliding velocity increased but the calcium sensitivity was not affected. Tpm E40K showed a reduction in calcium sensitivity and thin filament sliding velocity (Kopylova et al., 2016). Overall these studies demonstrate that tropomyosin aminoacid mutations affect tropomyosin function.

Figure 1.18: cross-sections of hearts obtained from normal people and patients suffering from HCM or DCM.

The figure displays changes in the heart chambers morphology between Normal heart (B) HCM hearts (A) and DCM hearts (C) (Seidman and Seidman, 2001).

Congenital skeletal muscle myopathies are neuromuscular disorders characterized by hypotonia and non-progressive or slowly progressive skeletal muscle weakness. These myopathies have clinical features including floppiness at birth, slender body habitus, and high-arched palate and respiratory impairment. Recently, it has been shown that there are more than 140 mutations associated with various congenital skeletal myopathies in actin, myosin, Tpm and Tn. Examples of congenital skeletal myopathies associated with these mutations, are Congenital Fibre-Type Disproportion (CFTD), rod-core myopathy, intranuclear rod myopathy, distal myopathy, distal arthrogryposis, cap disease, actin myopathy, nemaline myopathy (Ochala, 2008). The first mutation identified in Tpm3 (slow skeletal α-tropomyosin) was a case of nemaline myopathy, however recently many more mutations have been identified both in Tpm2 (β-tropomyosin, nemaline and cap myopathy) and in Tpm3 where there is a strong association with (CFTD). Cap disease and distal arthrogryposis are caused by mutation in Tpm2 while CFTD is caused by mutation in Tpm3. Moreover, NM myopathy is caused by mutations in both Tpm2 and Tpm3. Some of these mutations are shown in figure 1.20 and include mutations (E41K, E117K and Q147P) in β-tropomyosin and mutations (A4V, R91P, R167G, R167C, R167H, L100M and R245G) in ɣ-tropomyosin. (Lehtokari et al., 2008; Nowak et al., 1999; Tajsharghi et al., 2007).

Recent studies on tropomyosin mutations have investigated the effect of these mutations on tropomyosin function and structure. A study has found that the calcium dependent actomyosin ATPase was affected by R167H and K168E on Tpm1.1. R167H mutation increased the fraction of actin monomers in the ON state in the presence of troponin and calcium. This effect led to a decrease in the myosin head binding to actin. In contrast K168E decreased the number of actin monomers switched ON while the fraction of myosin head bound to actin was increased (Borovikov *et al.,* 2017). A study using fluorescence polarisation has investigated the effect of R167H, R167G and K168E on the azimuthal movement of Tpm on actin during the actomyosin crossbridge cycle. This study showed an increase in the proportion of actin monomers in the ON state and an increase in the amount of myosin heads strongly bound to actin by R167G and K168E. In contrast R167H reduced thin filament switching to the ON state and myosin head strong binding (Borovikov *et al.,* 2016). In is interesting to note that mutation of R167

to two different aminoacids, G or H, gave opposite effects. Another study has found that seven substitutions (L99M, A155T, R167G, R167C, R167H, K168E 1nd R244G) have decreased the calcium dependent ATPase and thermal stability and the troponin binding affinity (Robaszkiewicz *et al*., 2015).

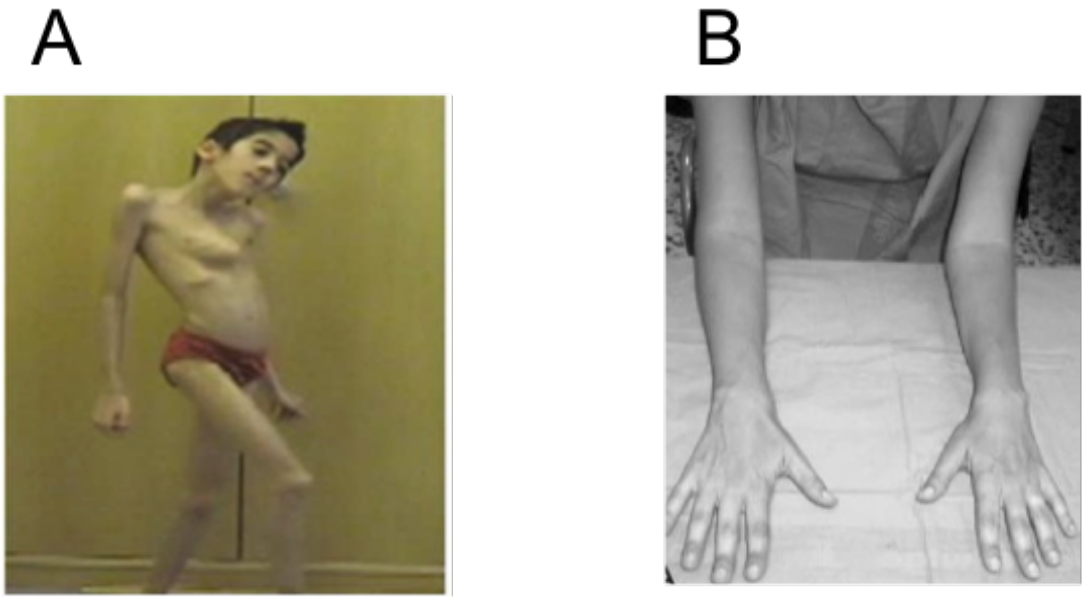

Figure 1.19: Patients with muscle myopathies.

A. 11 years old boy with unusual chest deformity and weakness of neck muscles and also facial weakness (from Lehtokari et al. (2008) European Journal of Human Genetics (2008) 16, 1055–1061). B Upper limb hypotrophy in a patient with nemaline myopathy (from Olive et al. (2010) muscle Nerve, 42, 901-907).

Table 1.1: A list of diseases causing mutations in Tropomyosin (modified form Redwood and Robinson, 2013)

Mutation	phenotype	Position in heptad	References
Met8Arg	DCM	*a*	Lakdawala et al. (2012)
Lys15Asn	DCM	*a*	Hershberger et al. (2010)
Arg21His	HCM	*g*	Fokstuen et al. (2011)
Ala22Ser	HCM	*a*	Otsuka et al. (2012)
Glu23Gln	DCM	*b*	Hershberger et al. (2010)
Lys37Glu	LVNC	*b*	Chang et al. (2011)
Glu40Lys	DCM	*e*	Olson et al. (2001)
Glu54Lys	DCM	*e*	Olson et al. (2001)
Asp58His	HCM	*b*	Frisso et al. (2009)
Glu62Gln	HCM	*f*	Jongbloed et al. (2003)
Ala63Val	HCM	*g*	Nakajima-Taniguchi et al. (1995)
Lys70Thr	HCM	*g*	Yamauchi-Takihara et al. (1996)
Asp84Asn	DCM/LVNC	*g*	van de Meerakker et al. (2013)
Ile92Thr	DCM	*a*	Hershberger et al. (2010)
Val95Ala	HCM	*d*	Karibe et al. (2001)
Leu100M	CFTD	*a*	Clarke et al. 2008
Ala107Thr	HCM	*b*	Otsuka et al. (2012)
Arg160His	LVNC	*f*	Hoedemaekers et al. (2010)
Arg167Cys	CFTD	*f*	Clarke et al. 2008
Arg167Gly	CFTD	*f*	Clarke et al. 2008
Arg167His	CFTD	*f*	Clarke et al. 2008
Ile172Thr	HCM	*d*	Van Driest et al. (2003)
Asp175Asn	HCM	*g*	Thierfelder et al. (1994)
Glu180Gly	HCM	*e*	Thierfelder et al. (1994)
Glu180Val	HCM	*e*	Regitz-Zagrosek et al. (2000)
Leu185Arg	HCM	*c*	Van Driest et al. (2002)
Glu192Lys	HCM/LVNC	*c*	Probst et al. (2011),
Thr201Met	DCM	*e*	van Spaendonck-Zwarts et al. (2013)
Ser215Leu	HCM	*e*	Morita et al. (2008)
Asp230Asn	DCM	*f*	Lakdawala et al. (2010)
Ala239Thr	DCM	*a*	Hershberger et al. (2010)
Lys248Glu	LVNC	*c*	Probst et al. (2011)
Ala277Val	DCM	*d*	Hershberger et al. (2010)
Met281Thr	HCM	*a*	Van Driest et al. (2003)
Ile284Val	HCM	*d*	Olivotto et al. (2008)

1.6 Research project

Tropomyosin plays a fundamental role in the regulation of actin filaments in both the actin cytoskeleton and muscle contraction. Tropomyosin interaction with actin is at the heart of its function. Although, it has been subject of intensive investigations but it is still not well understood. The main reason is inherent to the way tropomyosin binds to actin. The Tpm molecule covers 7 actin monomers and is thought have seven equivalent sites. If tropomyosin binds at three different positions on the surface of actin, then it means that there may be 21 state specific actin binding sites on the tropomyosin molecule. Characterisation of these sites and their implication in the activation/inhibition of muscle contraction is highly desirable.

The aim of this project was to analyse the effect of several tropomyosin mutations on tropomyosin structure, binding to actin and troponin, cooperative behaviour, and allosteric transitions. The mutations investigated are: R90G, E163K, R167G, E240K, R244G and M281I.

1.6.1 Tropomyosin mutations: rational for their design and impact on tropomyosin coiled coil structure.

A sequence comparison was performed to assess the conservation of these amino acids in various tropomyosin isoforms in various species. 4 out of the 6 mutated amino acids (R90, R167, E240 and R244) were fully conserved in all isoforms and species analysed (figure 1.21). The E163 and M281 were not as well conserved although they showed conservative substitution (substitution to an amino acid with the same chemical property negatively charged E to D or hydrophobic M to I). The conservation of these amino acids emphasizes their importance in the Tpm function. In addition, it has been previously suggested that R90, R167 and R244 on Tpm are interacting with actin (Barua *et al*., 2011; Li *et al*., 2011). Consequently, mutating these amino acids to an amino acid with different chemical properties (R to G or E to K) is likely to affect tropomyosin biochemical properties.

Figure 1.20 A sequence logo of tropomyosin.

The figure shows the conservative amino acids (Red boxes) among the three Tpms genes (Tpm1, tpm2 and Tpm3). The figure was obtained by Weblogo3 program. The choice of different isoforms was considered and based on different species to insure validity of comparison between the sequences.

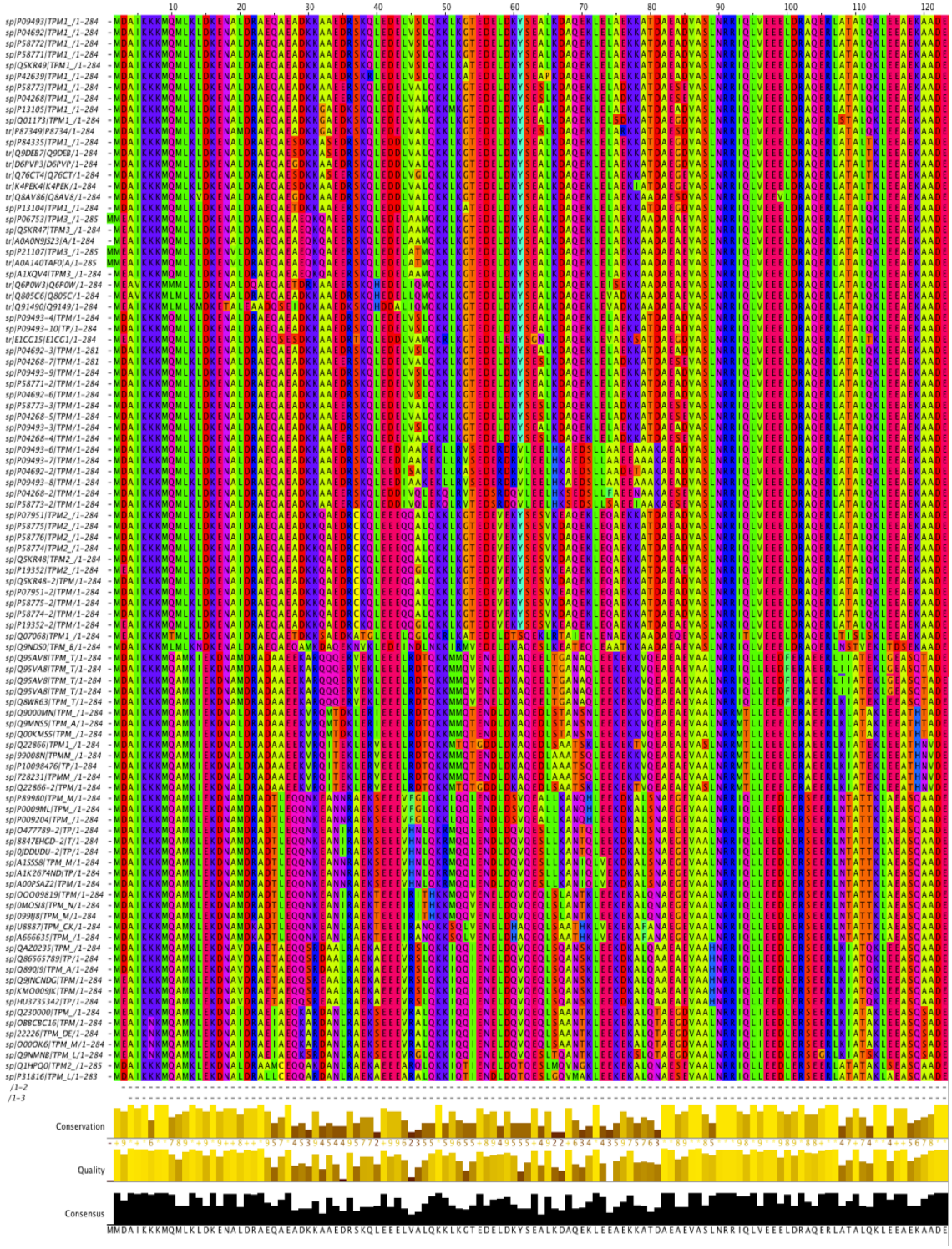

Figure: 1.21 Sequence comparison of different tropomyosin isoforms (Tpm sequence 1-123)

The figure shows the conservative amino acids among the three Tpms genes (Tpm1, tpm2 and Tpm3). The figure was obtained by Jalview program. The choice of different isoforms was considered and based on different species to insure validity of comparison between the sequences.

Figure: 1.22 Sequence comparison of different tropomyosin isoforms (Tpm sequence 124-252)

The figure shows the conservative amino acids among the three Tpms (Tpm1, tpm2 and Tpm3). The figure was obtained by Jalview program. The choice of different isoforms was considered and based on different species to insure validity of comparison between the sequences.

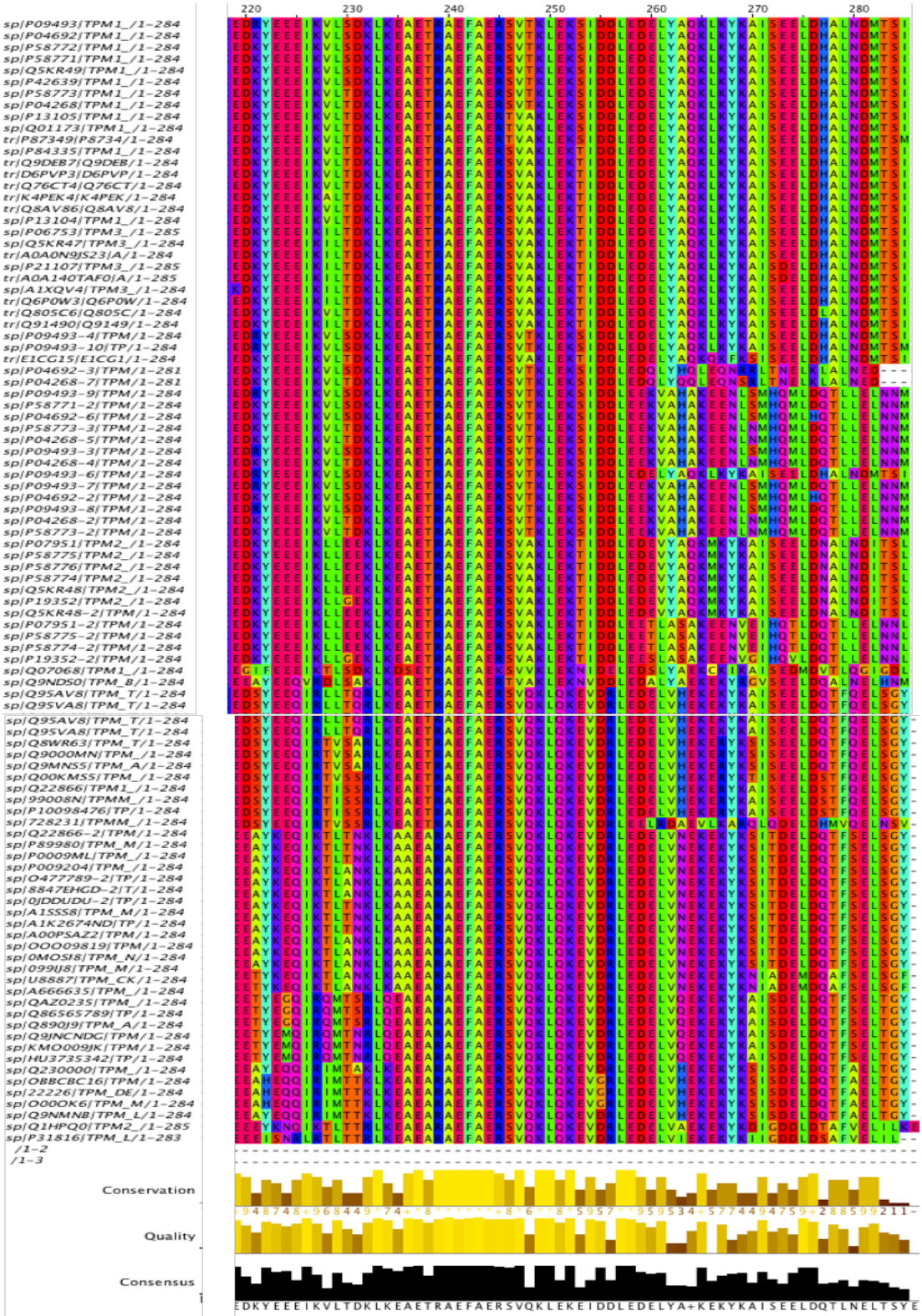

Figure: 1.23 Sequence comparison of different tropomyosin isoforms (Tpm sequence 219-284)

The figure shows the conservative amino acids among the three Tpms (Tpm1, tpm2 and Tpm3). The figure was obtained by Jalview program. The choice of different isoforms was considered and based on different species to insure validity of comparison between the sequences.

1.6.2 Aims and hypothesis.

At the start of this work several reports pinpointed actin binding determinants within tropomyosin in the absence of troponin-Ca^{2+}. However, these studies failed to define precisely tropomyosin amino acids involved in actin binding in the different regulatory states and also used tropomyosin expressed using *E.coli* (characterized by reduced cooperativity). They suggested a critical ionic interaction of tropomyosin R90, R167 and R244 with actin. Interestingly, R167 is a mutational hot spot in several skeletal muscle myopathies with 3 charge neutralizing mutations.

The aim of this project was to analyse the effect of several tropomyosin mutations on tropomyosin structure, binding to actin and troponin, cooperative behaviour, and allosteric transitions. The mutations investigated are: R90G, E163K, R167G, E240K, R244G and M281I. These mutations were selected for two reasons: i) they were found to be highly conserved between different tropomyosin isoforms. ii) they are implicated in several skeletal muscle myopathies. Both of these points suggest that these residues play a great role in tropomyosin function. In addition, we generated double and triple amino acid mutations (R90GR167G, R167GR244G, R90GR244G, E163KE240K, R90GR167GR244G). Although the mutations used in this project were found in Tpm3 gene, the construct used were based on Tpm1 because it has been intensively studied and it was available in the lab.

R90, R167 and R244 are located in tropomyosin α-bands thought to interact with actin in the OFF state. It was hypothesized that mutations R90G, R167G and R244G are likely to disrupt tropomyosin binding to actin in the blocked state (OFF state). Tpm E163 and E240 are in the β-band and we hypothesize that these residues are critical for tropomyosin binding in the open state. Residue M281 is located at the end Tpm sequence and might affect the end-to-end polymerisation of Tpm molecules. We hypothesised that M281I mutation may affect actin binding by compromising tropomyosin end-end interaction.

The importance of end-to-end interactions involved in cooperativity depends upon N-terminal acetylation. There are reports suggested that the Ala-Ser N-terminal extension which has been widely used as a substitute for N-terminal acetylation with E.coli expression, produces reduction in cooperativity and perhaps other abnormalities. Therefore, we initially planned to express tropomyosin using the baculovirus-Sf9 system and study several tropomyosin mutants expressed in this system. However, as our first result chapter (chapter 3) indicates, obtaining tropomyosin fully acetylated using this expression system was challenging. We decided to revert to the bacterial expression with an alanine-serine di-peptide N-terminal extension to all the tropomysin mutants. The biophysical characterisation of these mutant tropomyosin produced in E.coli is described in Chapters 4 and 5.

Chapter 2

Materials and methods

2.1 Preparation of tissue purified proteins

Myosin subfragment-1 (S1), skeletal troponin and F-actin were prepared from rabbit skeletal muscle. Human skeletal tropomyosin was expressed in *Escherichia coli* system.

2.1.1 Preparation and expression of skeletal tropomyosin

Wild-type human tropomyosin cDNAs were obtained as a gift from Dr C. Redwood (University of Oxford, UK). The PCR overlapping technique was used using the cDNA to produce the human skeletal tropomyosin mutants (R90G, E163K, R167G, E240K, R244G, M281I, R90G/R167G, R90G/R244G, R17G/R244G, E163K/E240K and R90G/R167G/R244G). The vector (PLEICS-05) was used to clone the products and the overlap extension PCR was carried out by Dr Xiaowen Yang at the University of Leicester. All tropomyosin in this project were recombinant proteins with Als-Ser extensions (Monteiro *et al*., 1994). The *Escherichia coli* strain BL21 (DE3) plys was used for the overexpression of Tpm constructs. The Tpm proteins were verified by sequencing prior to expression and reconstitution (PNACL, University of Leicester).

The transfected cells were grown at 37°C in LB broth medium and at the late exponential phase when the OD reached 0.6-0.9 at 600 nm the cells were induced using the IPTG (isopropyl-1-thio-ß-D-galactopyranoside) and the expression level was checked using SDS gel (Figure 2.1).

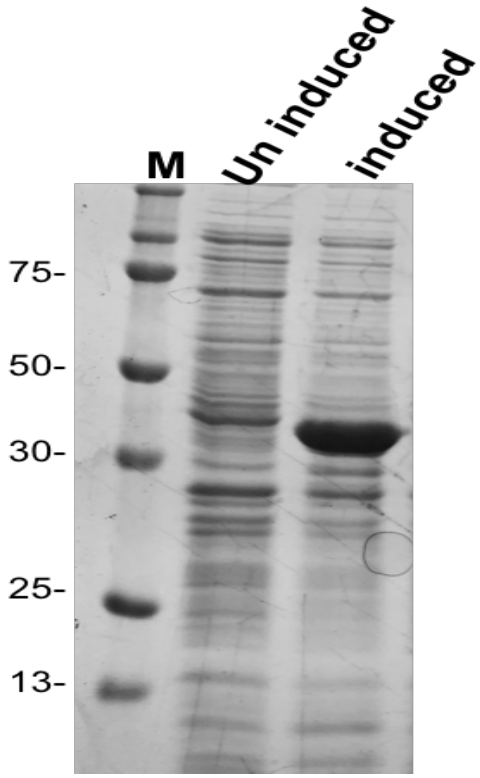

Figure: 2.1: SDS page of Test expression

The gel shows the protein marker and the un-induced lane which shows homogenate of the cells before adding IPTG. While the induced lane shows homogenate of cells after adding IPTG which shows the tropomyosin expression.

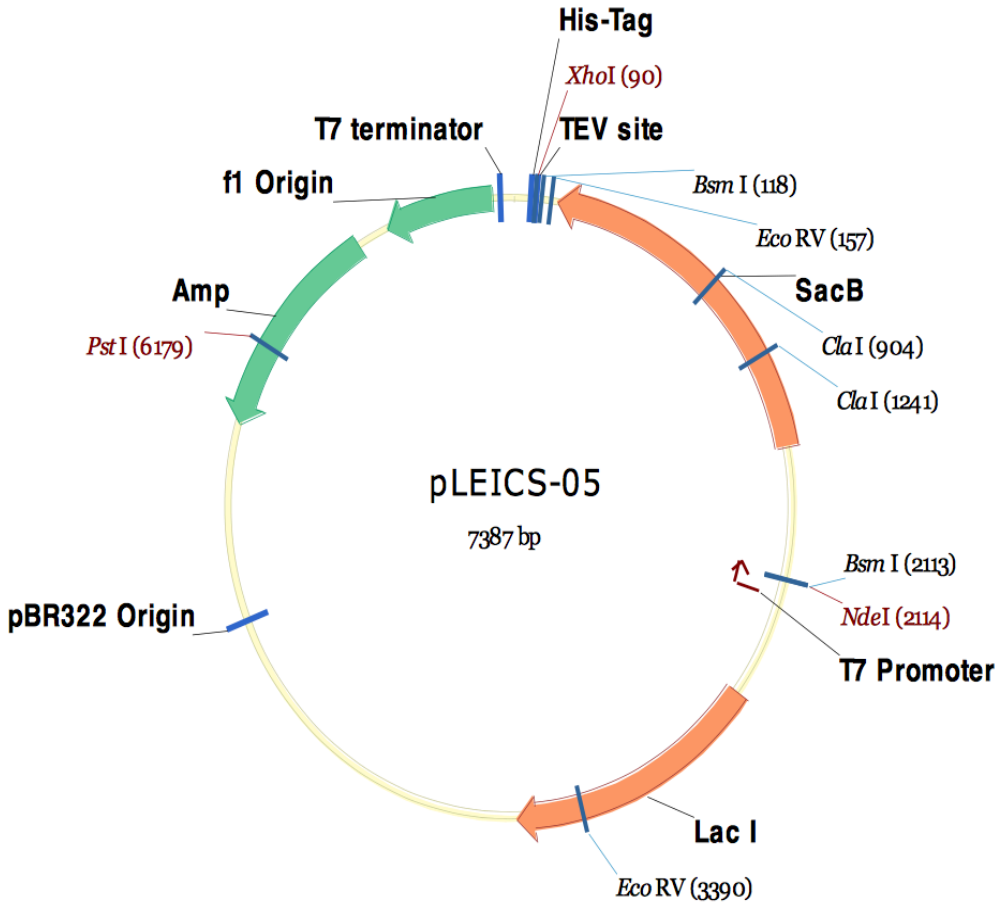

Figure 2.2: Expression vector of hsTpm (pLEICS-05)

2.1.2 Plasmids mini preps

The JM109 cells were used to purify the tropomyosin WT and mutations by following the protocol of Wizard® Plus Miniprep kit (Promega). The procedure was carried out after growing 5-10 ml cell culture overnight. Cells were spun down at 13,000 rpm for 5 minutes at room temperature and supernatant was discarded. Pellet was dissolved in various buffers as described in the protocol provided. At the end of the procedure the DNA product concentration was checked by Nano drop and stored in the -80°C.

2.1.3 Transformation

All tropomyosin cDNAs were grown in BL21 (DE3) Plys cells. The transformation was carried out using 10-20 µl of competent cells added to 1µl of DNA construct and the tube was gently flicked to mix the cells and incubated in ice for 30 minutes. The cells were heat shocked for 60 seconds at 42°C and directly the tube was placed back in ice for 2 minutes. The cells received 200 µl of fresh LB media and incubated at 37°C for 60 minutes with shacking at 220 rpm. The 200 µl cells then were spread on LB agar with the desired antibiotic and incubated overnight at 37°C.

2.2 Protein purification from tissue

Skeletal muscle contractile proteins: actin, troponin, tropomyosin, myosin, and myosin subfragmnet-1 (S1) were purified from rabbit skeletal muscle.

2.2.1 Skeletal muscle protein purification

2.2.1.1 Skeletal myosin preparation

The method of Margossian and Lowey was used to prepare muscle myosin (Margossian and Lowey, 1982). The rabbits were gift from Dr Kieran E Brack university of Leicester. The muscle of the back and legs of the rabbits were removed and placed in 4°C water then the muscles were minced and weighed. The muscles were stirred with three volumes of Guba-Straub buffer (0.3 M KCl, 1 mM EDTA, 0.1 M K_2HPO_4 , and 0.05 M KH_2PO_4) for 15 minutes at 4°C. The solution was centrifuged at 5,000 rpm, using SLC 6000 rotor for 20 minutes. The supernatant was used for myosin preparation while the pellet was containing the acetone powder for the actin preparation. The supernatant

filtered through nylon mesh then 14 volumes of cold water were added slowly with continuous stirring to precipitate the myosin. The mixture left overnight in the cold room without disturbance for myosin to sediment. Next day the top layer was siphoned and the sediment solution was spun down at 5,000 rpm, using SLC 6000 rotor for about 10 minutes. The myosin was in pellet so it was weighed and then dissolved in 0.25 volumes of (3 M KCl, 30 mM imidazole, pH 7.0) and left overnight. Adding an equal volume of cold water with stirring precipitated the actomyosin, then it was spun down at 5,000 rpm, using SLC 6000 rotor for about 10 minutes. However, if the size of the pellet was bigger than an extra cycle of precipitation is needed. The pellet was dissolved in 1.5 volumes of 30 mM imidazole, pH 7.0, 3 M KCl, 2.5 mM DTT then, dialyzed at 4°C overnight until it is completely dissolved. The Myosin concentration was determined by the standard coefficient and the myosin was diluted in an equal volume of glycerol and was stored at -20 °C.

2.2.1.2 Skeletal myosin sub-fragment-1 (S1) preparation

The myosin subfragment-1 purified from myosin based on the method described by Weeds and Taylor (Weeds and Taylor, 1975). By using cold water the myosin stock in glycerol was diluted in 20 volumes and was manually stirred till the solution became cloudy. The Myosin was spun down for 10 minutes at 13,000 rpm, using SLA 1500 rotor. The pellet was dissolved at about 10 mg/ml myosin concentration using 0.6 M NaCl and dialysed versus (120 mM NaCl, 20 mM NaH_2PO_4, and 1 mM EDTA, pH 7.0) overnight. The myosin digestion was carried out by incubating the myosin solution with 0.05 mg/ml chymotrypsin at 25°C for 10 minutes. The reaction was stopped by adding 0.1 mM PMSF (PMSF stock was in ethanol so it was diluted in 2 ml of water) with an addition of cocktail protease inhibitor tablets (1 tablet for 50 ml myosin solution). The myosin was dialysed versus (5 mM MOPS pH 7.0, 5 mM $MgCl_2$, 1 mM DTT, and 0.1 mM PMSF). To precipitate the light meromyosin the myosin was centrifuged at 20,000 rpm, using SS34 rotor for 20 minutes. The S1, which was in the supernatant, was filtered then loaded onto ion-exchange column (Q-Sepharose column), which had been equilibrated with dialysis buffer (5 mM MOPS pH 7.0, 5 mM $MgCl_2$, 1 mM DTT, and 0.1 mM PMSF). The column was washed with three column volumes and then using 0.5 L gradient of 0-

250 mM NaCl eluted the S1. The fractions were collected at 10 ml/tube and monitored the OD at 280 nm. The S1 purity was checked by 15% SDS-PAGE. The pure S1 fractions were pooled and brought to 65% ammonium sulphate which was added slowly over 60 minutes with continuous stirring at 4°C. Using SLA 1500 rotor the S1 solution was spun down at 13,000 rpm for 10 minutes. The pellets were dissolved and dialysed in ATPase high salt buffer (140 mM KCl, 10 mM MOPS pH 7.2, 3.5 mM $MgCl_2$, 1 mM DTT, and 1 mM NaN_3) overnight. The S1 concentration was determined by using extinction coefficient $A_{1\%}$ of 6.4 at OD 280 nm. The liquid nitrogen was used to instantly freeze S1 and then stored at -80 °C.

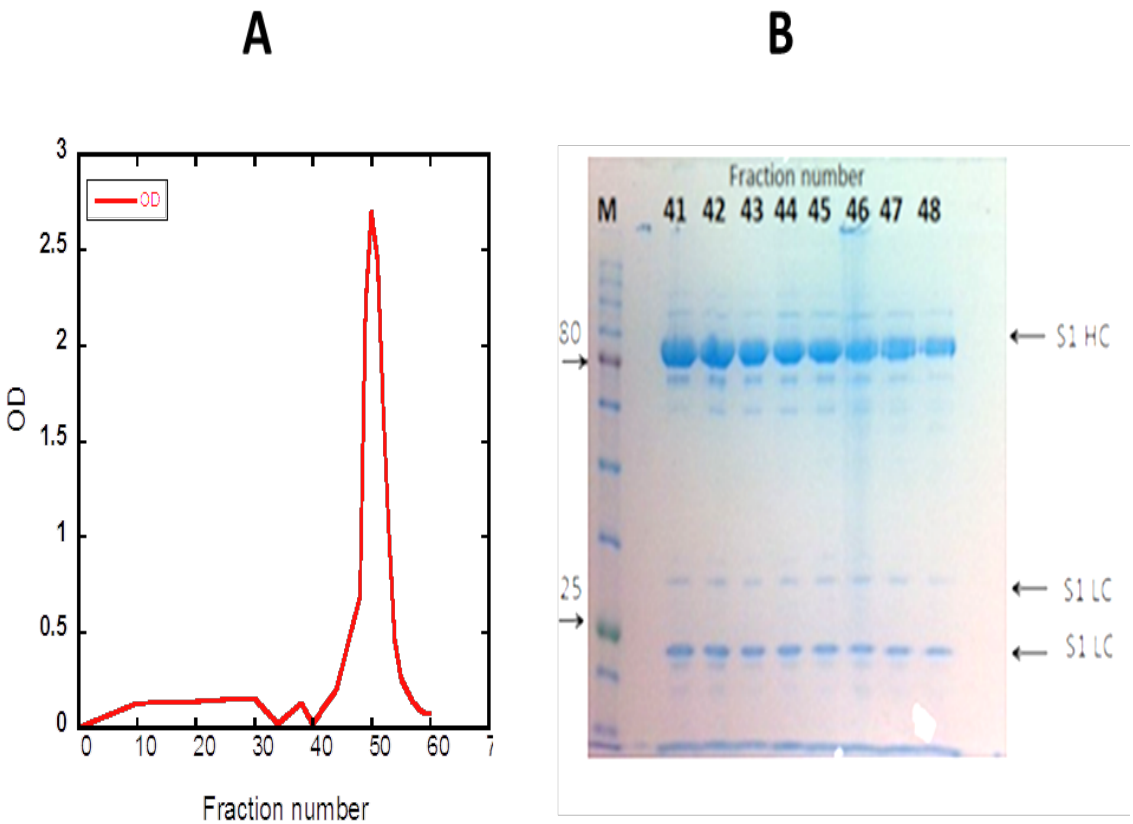

Figure 2.3: the purification of skeletal myosin subfragment-1(S1) by using Q-sepharose column.

(A) is the chart recorder of the absorbance at 280 nm. (B) Is the SDS-PAGE analysis of the fractions by using 15% SDS page. Numbers along the top correspond to the fraction numbers that related to A.

2.2.1.3 Preparation of skeletal acetone powder

The first pellet of (2.3.1.1 skeletal myosin preparation) was used to prepare the acetone powder (Pardee and Spaudich 1982). Different buffers were used to wash the pellet and stirred in each wash then filtered through a fine nylon mesh, and finally squeezed as dry as possible. The washes procedures were as following: ten volumes of cold water at 4 °C for two times, four volumes of 0.4 % $NaHCO_3$ at 4 °C only once, lastly four volumes of cold acetone for four times. The acetone powder was left in the fume hood to dry overnight at room temperature then the powder was weighed and stored at -20 °C.

2.2.1.4 Preparation of skeletal F-actin.

The skeletal F-actin was prepared from rabbit muscle acetone powder using the method of Spudich and Watt (Spudich and Watt, 1971). So, 100 ml of cold G-actin buffer (2 mM Tris-HCl pH 8.0, 0.2 mM ATP, 0.1 mM $CaCl_2$, 0.5 mM DTT, and 1 mM NaN_3) was added to 5 g of acetone powder and stirred for 20 minutes at 4 °C then it was spun down at 18,000 rpm, using SS34 rotor for 20 minutes. The supernatant was filtered through nylon mesh and the pellets were re-extracted by another 100 ml G-actin buffer. The two supernatants were collected and polymerized by using 0.1 volumes of 10x KME buffer (100 mM Tris- HCl pH 8.0, 500 mM KCl, 25 mM $MgCl_2$, 10 mM EGTA, and 10 mM NaN_3). Then, the polymerization method was done by incubating in water bath at 30°C for 1 hour. The F-actin solution was brought to 0.8 M KCl and kept manually stirred for about 10 minutes. The F-actin was spun down at 42,000 rpm, using T-1250 rotor for 2 hours. The F-actin pellets were washed and soaked in ATPase buffer. The concentration was determined and stored at 4°C.

2.2.1.5 Preparation of skeletal F-actin Pyrene

The method of Kouyama and Mihashi was used to label the Cys-374 of skeletal F-actin with N-(1-pyrenyl)-iodoacetamide PIA (Kouyama and Mihashi, 1981). The F-actin was prepared as described in section 2.3.2.1 to purify the F-actin, however; the pellets were soaked in labelling buffer (25 mM Tris-HCl pH 7.5, 100 mM KCl, 2 mM $MgCl_2$, 3 mM NaN_3, and 0.3 mM ATP). Next day the pellets were dissolved and dialysed at 1 mg/ml against same labelling buffer overnight. 7 moles of N-(1-pyrenyl) iodoacetamide were added per 1 mol of F-actin and gently mixed in dark at room temperature for 3 hours. The mixture was spun down using SS34 rotor at 10,000 rpm, for 10 minutes then supernatant was spun down at 42,000 rpm, using T-1250 rotor for two hours. The G-buffer was used to soak the pellets overnight; then next day the pellets were re-suspended and dialysed in G-buffer (at 5-5.5 mg/ml) for 48 hours. The N-(1-pyrenyl) iodoacetamide G-actin was spun down at 42,000 rpm, using T-1250 rotor for two hours and the supernatant was filtered and loaded onto gel filtration column (Sepharyl S200 or S300) that had been equilibrated with G-buffer. Fractions of 4 ml were collected and monitored at 290 nm. The purity of N-(1- pyrenyl) iodoacetamide G-actin was checked by 15% SDS gel and the pure fractions were pooled. The mixture was polymerised by 0.1 volume of 10x KME buffer, and incubated at 30 °C for 60 minutes.

The PIA F-actin was spun down at 42,000 rpm, using T-1250 rotor for two hours. The pellets soaked and re-suspended in ATPase buffer. The degree of pyrene labelling was determined by comparing the actin concentration at 290 ((A290- (A344*0.127)) * 38.5 µM/OD with the concentration of pyrene label at 344 (A344*45.5 µM/OD). The labelling ratio was between 85-95%. The N-(1-pyrenyl) iodoacetamide labelled skeletal F-actin was stored at 4°C.

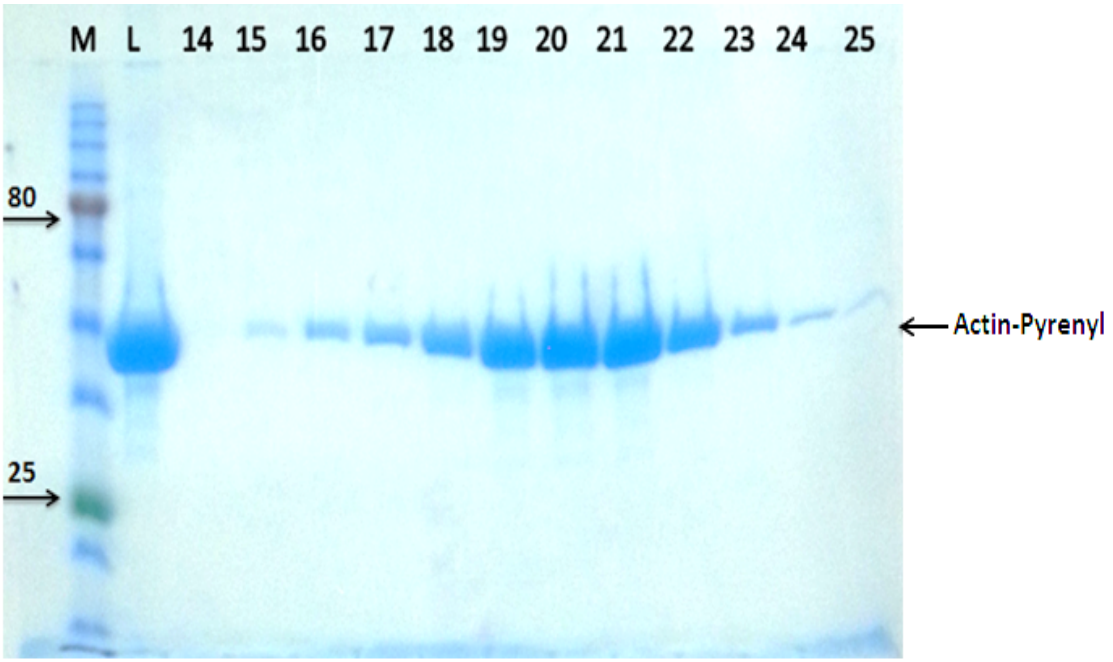

Figure 2.4: The SDS-PAGE analysis of N-(1-pyrenyl)-iodoacetamide-labelled skeletal F-actin by using 15% SDS gel.

The numbers along the top correspond to the fraction numbers that related to PIA-actin purified over gel filtration.

2.2.1.6 Skeletal troponin preparation

The method of Potter was used to extract the troponin complex from rabbit skeletal muscle acetone powder (Potter, 1982). 15 g of rabbit skeletal muscle acetone powder was extracted in 20 volumes of extraction buffer by continuous stirring overnight at 4 °C (1 M KCl, 20 mM TES pH 7 and 15 mM β– mercaptoethanol). The suspension was centrifuged at 14,000 rpm for 20 minutes at 4 °C using a SLA 3000 rotor. The supernatant was adjusted to pH 8.0 with 1 M potassium hydroxide and brought to 30% ammonium sulphate saturation (167 g/L) with slowly adding over 1 hour at 4 °C with a continuous gentle stirring. The pH was maintained between 7 and 8 during addition of ammonium sulphate. The mixture was spun down at 12,000 rpm for 20 minutes at 4 °C using a SLA 1500 rotor. The 30% supernatant was then brought to 50% ammonium sulphate saturation (73 g/L added) that was gently added over 1 hour to precipitate the troponin complex. The mixture was spun down at 12,000 rpm for 20 minutes at 4 °C using a SLA 1500 rotor. The 50% supernatant was kept for tropomyosin preparation and the pellet was dissolved in ATPase buffer (10 mM MOPS pH 7, 50 mM KCl, 3.5 mM

$MgCl_2$, 1 mM DTT, and 1 mM NaN_3) and dialysed extensively against two litres of the same ATPase buffer overnight. The troponin complex was spun down at 10,000 rpm for 10 minutes at 4°C, and then it was loaded onto a DEAE column, which had been equilibrated with the same dialysis buffer. The column was washed and applying a linear gradient of 50-600 mM KCl to elute the troponin. The troponin was collected in 6 ml fractions and monitored at 280 nm. 15 % SDS gel was run to check the purity and the fractions with pure skeletal Tn were pooled, concentrated and stored at -80 °C.

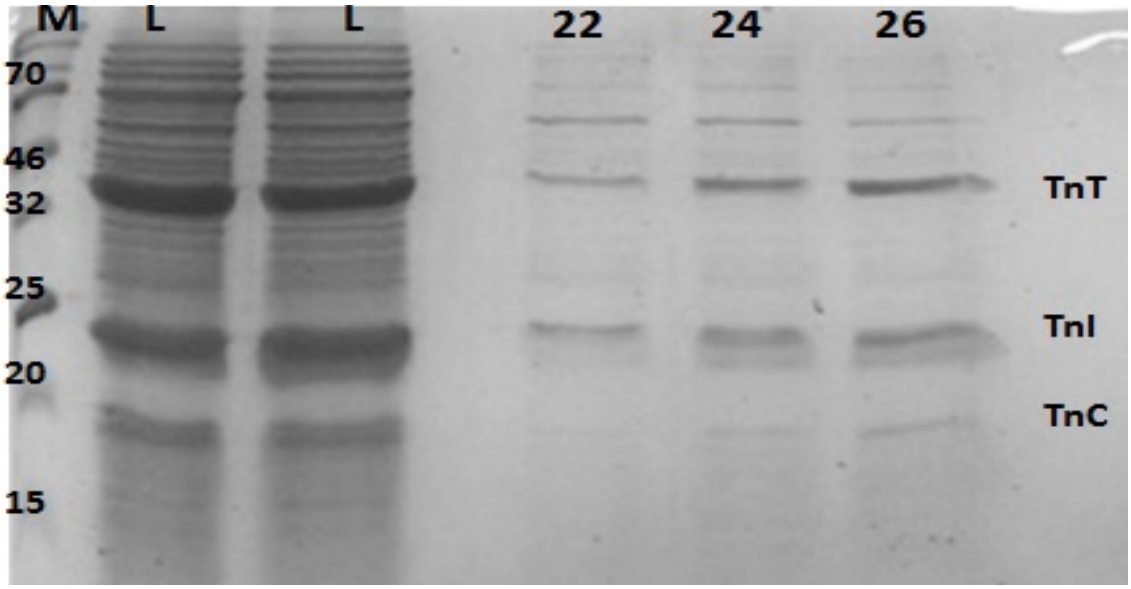

Figure 2.5: 15% SDS of skeletal troponin purification.

The 15 % SDS Gel shows the purification of skeletal troponin using the DEAE column. The numbers at the top represent the Load and fraction tubes.

2.2.1.7 Purification of skeletal tropomyosin

To extract the tropomyosin the 50% supernatant in (2.1.3.7 Skeletal Troponin Preparation) was brought up to 65% saturated ammonium sulphate. With a continuous gentle stirring the ammonium sulphate was added slowly over 1 hour at 4 °C. The new solution was spun down to precipitate the tropomyosin at 12,000 rpm for 20 minutes at 4 °C. The 65% pellet was dissolved and dialysed overnight in (10 mM MOPS pH 7.2, 50 mM KCl, 3.5 mM $MgCl_2$, 1 mM DTT, and 1 mM NaN_3). The tropomyosin crude was spun down at 18,000 rpm for 10 minutes at 4 °C, and then it was loaded onto a DEAE column, which had been equilibrated with the same dialysis buffer. The column was washed and the elution was by applying a linear gradient of 50-500 mM KCl and 5 ml fractions were collected and monitored at 280 nm. The purity of tropomyosin was checked by 12% SDS gel, figure 2.6. Using 65% ammonium sulphate, the pure tropomyosin fractions were pooled and concentrated and added stirred gently over 1 hour at 4 °C. The 65% pellet was dissolved and dialysed in minimum volume of high salt ATPase buffer overnight. The pure concentrated tropomyosin was spun down at 10,000 rpm for 10 minutes at 4 °C then the concentration was determined and the protein was stored at -80 °C.

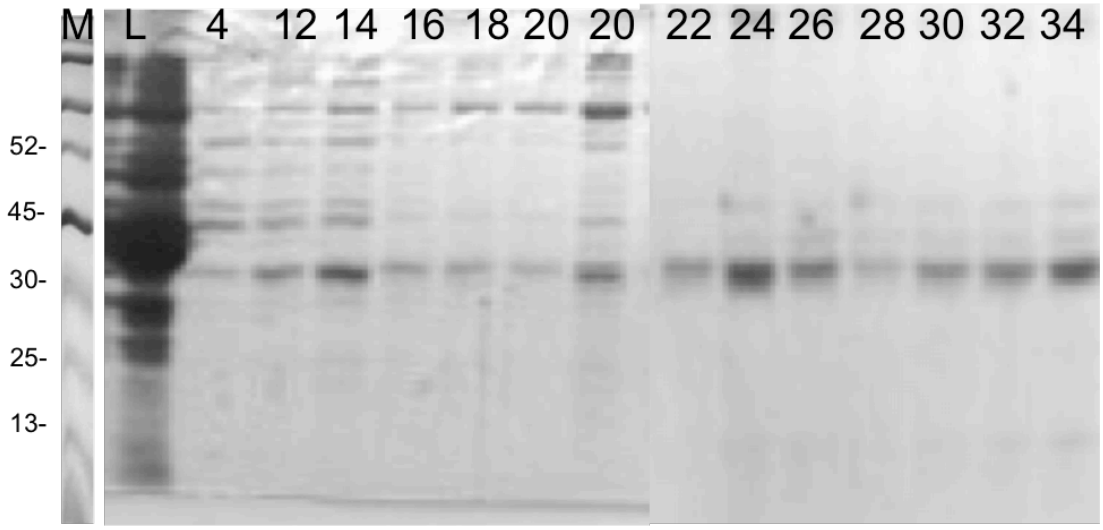

Figure 2.6: 12% SDS gel of skeletal tissue purified tropomyosin.

The 12% SDS Gel shows the purification of skeletal tropomyosin using the DEAE column. The numbers represent the fractions of tropomyosin.

2.2.1.8 Preparation of N-(1-pyrenyl) iodoacetamide-labelled tropomyosin

Based the method of Lehrer and Morris, the skeletal tropomyosin was labelled with N-(1-pyrenyl) iodoacetamide (PIA) (Geeves and Lehrer, 1994). Native skeletal tropomyosin was reduced at 40 °C for twenty minutes with DTT (50 mM) to denature the tropomyosin. The tropomyosin was dialysed at 3 mg/ml against 5 M GuHCl, 30 mM MES pH 7.5, 0.6 mM EDTA overnight. Next day seven folds' molar excess of PIA were added to the tropomyosin for 2-3 hours at room temperature and the reaction was stopped by adding 20 mM DTT. The labelled tropomyosin was spun down at 13,000 rpm in a bench centrifuge for 5 minutes at room temperature to remove the un-dissolved PIA. The PIA-tropomyosin was re-natured by dialysing against renaturing buffer (1 M NaCl, 5 mM MOPS pH 7.5, 1 mM EDTA). Then the tropomyosin was dialysed against ATPase buffer (10 mM MOPS pH 7, 50 mM KCl, 3.5 mM $MgCl_2$, 1 mM DTT, and 1 mM NaN_3). The solution was spun down at 12,000 rpm for 10 minutes at 4°C using a SS34 rotor. The concentration of Tm was determined by the Lowry method and pyrene was determined by using 45.5 µM /OD at 344 nm (Kouyama and Mihashi, 1981). The degree of labelling should typically be in the range 1.8-2.2 pyrene to Tpm.

2.3 General methods

2.3.1 Determination of protein concentration

The proteins concentrations were determined using spectrophotometer (Varian Cary 50 spectrophotometer). Absorption $A_{1\%}$ extinction coefficients were used for each protein after samples were scanned from 250 nm to 350 nm (Table 2.1).

Table 2.1: Extinction coefficients

Protein	A_1% Extinction coefficient at 280 nm
actin	11.5
Skeletal tropomyosin	3.3
Skeletal troponin	13.0
myosin	5.4
Skeletal Myosin subgragment-1	7.9

2.3.2 Polyacrylamide gel electrophoresis

The proteins were determined by using electrophoresis containing a 12% separating gel with a 4% stacking gel. The 2_X SDS sample buffer (20 mM Tris-HCl pH 8, 5% SDS, 10% mercaptoethanol, 20% ethanol, and 0.02% bromophenol blue) was used to dilute the protein sample by adding equal volumes then boiled for 3-5 minutes before loading. The Biorad minigel system was used to run the gels at 40-50 mA and 200 V until the dye reached the end of the gel. At the end of the run the gels were taken out and washed with water and stained with instant blue ready satin for about 10-20 minutes. The gels were then de-stained in several changes of fresh water until the background was clear.

2.3.3 Co-sedimentation assay

Co-sedimentation was carried out using F-actin (12 µM) with the skeletal tropomyosin mutations and wild type (2.5 µM). F-actin and the mutants were mixed and incubated for an hour with AMSB buffer (10 mM Mops, 0.5 mM DTT, 3.5 mM MgCl2, 0.5mM NaN_3 and 50 mM KCL at pH 7.2) to make the volume up to 200 µl. Following incubation, the samples were spun at 85000 rpm at 4°C using an ultra-centrifuge TLA100 for 40 minutes, leading to the formation of pellets. The supernatants were pipetted into Eppendorf tubes then sample buffer was added to the supernatants and pellets and left overnight in the 4 °C to allow denaturation. In the following day, the pellets were dissolved and pipetted into Eppendorf tubes to which sample buffer was added to make a final volume of 300 µl. All samples of tropomyosin mutations with or without F-actin, as well as F-actin alone were then heated at 95°C for 4 minutes. Samples of the Tpm mutants alone were also prepared in the same manner, for comparisons. After the separation, samples from the pellets and supernatants were then analysed on a 12% SDS-PAGE with P7702S protein marker.

2.3.4 Determination of Actomyosin Mg^{2+} ATPase Activity

The actomyosin ATPase was done by mixing and incubating actin, tropomyosin and troponin in a final volume 90 µl in ATPAse AOSB buffer (10 mM Mops, 0.5 mM DTT, 3.5 mM MgCl2 and 0.5mM NaN_3 at pH 7.2). The S1 only was used as blank. The reaction was initiated by adding 10 µl of 100 mM MgATP at time intervals of 7 minutes in total at 37 °C. After the 7 minutes, precisely, the reaction was stopped by adding 0.5 ml of 10% Trichloroacetic acid (TCA) to give a final volume of 600 µl. The reaction tube was spun down at 13,000 rpm for 5 minutes to remove un wanted binding then, 500 µl of the supernatant was taken and pipetted in a test tube. The method of Taussky and Schorr was used to determine the free inorganic phosphate (Pi) (Taussky and Schorr 1953). Each tube received 1 ml of 1% ammonium molybdate (in 0.5 M H_2So_4) and vortexed. Then, 0.5 ml of freshly prepared 10 g $FeSo_4$ dissolved in 25 ml 0.5 M H_2So_4 was added and vortexed. The mixture was incubated for 5 minutes to develop a blue colour. Alongside the experiment a set of standards containing 0, 65 nmole, 130 nmoles, 195 nmoles and 260 nmoles of inorganic phosphate were processed.

Using the spectrophotometer at 700 nm, the concentration of inorganic phosphate was determined for all samples and standard buffers. The blank buffer used contained zero nmoles of inorganic phosphate. The equation below was used to work out the optical density per nmole of Pi.

[(OD700 for 100 µl of Pi/65 nmoles of Pi) + (OD700 for 200 µl of Pi/130 nmoles of Pi) + (OD700 for 300 µl of Pi/195 nmoles of Pi) + (OD700 for 400 µl of Pi/260 nmoles of Pi)] / 4]

A control with S1 only in the absence of actin was carried out for every ATPase reaction. The OD that obtained from the control was subtracted from the acto-S1 OD. The amount of Pi produced from the acto-S1 ATPase was determined by the difference divided by the average OD per nmole of Pi. This measurement was done on 0.5 ml since the actual volume was 0.6 ml and a correction volume 6/5 must be taken. So, to calculate the amount of Pi produced from ATP hydrolysis the Pi nmoles was divided by the total reaction time. The ATPase rate (equation below) was expressed as nmoles of Pi per second.

ATPase rate = (nmoles of Pi produced)/ ((6/5) X reaction time).

2.3.5 Circular Dichroism

Circular Dichroism Spectrometer Chirascan was used with a cell path length of 0.1 cm at 25˚C in 10 mM sodium phosphate, pH 7.0 and 0.3 M NaF solution. The spectra recorded ranged between 190-250 nm in the far UV region with a bandwidth of 1 nm at a resolution of 1 nm and baseline corrected. Tropomyosin wild type and tropomyosin mutants' concentrations used were 5 µM. Thermal stability measurements forward were made by following the molar ellipticity of tropomyosin at 222 nm as a function of temperature in buffer containing 0.3 M NaF, 10 mM sodium phosphate, pH 7.0. Data were obtained at 1.0 °C intervals from 15 to 80 °C using a protein concentration of 5 µM.

2.3.6 Trypsin digestion

The trypsin digestion was performed on the WT Tpm and mutants based on method used by Ly and his colleagues (Ly and Lehrer, 2012). The experiment was performed in presence and absence of actin. In the presence of actin, the Tpm concentration used was 0.3 mg/ml mixed with 1.5 mg/ml actin (excess of actin) treated with 0.003 mg/mL trypsin (lot STBC8587V SIGMA) in a buffer contains (10 mM HEPES buffer (pH 7.5), 0.1 M NaCl, 5 mM $MgCl_2$, and 10 mM β-mercaptoethanol) at 26 °C. For Tpm alone, a 0.5 mg/mL Tpm treated with 0.001 mg/ mL trypsin. All experiments were performed on time course (0, 0.30, 1, 2, 3, 4, 5, 10, 30 and 60 minutes) and the reaction was stopped by pre-heated SDS sample buffer at 90 °C. The sample were analysed on 12% SDS gel and stained.

2.4 Enzymatic kinetics

2.4.1 Transient State Kinetic Measurements

For all transient kinetic measurements, we used the Hi-tech Scientific SF61 stopped flow apparatus equipped with a 100 watt Xe/Hg lamp. For the interpretation and analysis of the kinetic data we used KinetAsyst software package. To select the desired excitation wavelength the signal the manual set up was used and the photomultiplier voltage was used to maximize the signal. The Acquire Control Panel was used to adjust the running time and the channels.

2.4.1.1 Measurement of equilibrium constant between the blocked and closed states.

The transition between the blocked and close state was done by following the kinetic of binding (actin-PIA:Tpm:Tn) (in the ratio of 7:1:1) binding to S1 in the presence and absence of calcium. A large excess of actin-PIA was rapidly mixed with small amount of S1 (Head et al., 1995). The 364 nm wavelength was used for the excitation of the pyrene iodoacetamide fluorescence and the 400 nm cut-off filter (GG400 filter) was used to monitor the emission of fluorescence. The experiment was performed in ATPase buffer (10 mM Mops, pH 7.2, 140 mM KCl, 4 mM $MgCl_2$, 1 mM DTT, 1 mM NaN_3) at 25 °C and 6 to 8 transients were collected and averaged. The Fit Control Panel of the Fit asystant was used for the average of these transients which was then fitted to one exponential equation by a nonlinear least square curve fit. To determine the value of the equilibrium constant between blocked and closed states (K_B) the following equation linking the ratio of the observed rate constant for myosin head binding to thin filament (In the presence or absence of calcium) over the observed rate constant of myosin head binding to actin alone to K_B:

$$k_{obs} (+ \text{ or } - Ca^{2+}) / k_{obs} (\text{actin alone}) = K_B / (1+K_B)$$

2.4.1.2 Determination of the maximum rate constant of the transition between the ON and OFF states.

The kinetics of the ON/OFF state change of actin+Tpm-PIA* filaments was monitored by the excimer fluorescence of PIA-tropomyosin (Tpm*) (Lehrer and Geeves 1998). The excitation at 364 nm was used for the pyrene iodoacetamide fluorescence (labelled Tpm) and the 455 nm cut-off filter was used for the emission of excimer fluorescence. The UG5 filter (light over 400 nm to cut off) was used for Light scattering. The buffer used to carry out the measurements was (10 mM Mops, pH 7.2, 140 mM KCl, 5 mM $MgCl_2$, 1 mM DTT, 1 mM NaN_3) at 20°C. The actin-Tpm* were premixed and incubated for 60 minutes in a ratio of (6:1). The ATP concentration varied from 20 µM up to 2 mM. Then, an average of 6 to 10 transients were collected and fitted to one exponential equation by a non-linear least square curve fit using the Fit Control Panel of the Fit Asystant. The values were then calculated by hyperbolic formula as described in the figure legend.

2.4.2 Determination of the equilibrium binding constant of tropomyosin to troponin using steady state fluorescence.

The change in the excimer fluorescence was used to measure the binding of troponin to PIA-Tpm to calculate K_D. In this experiment, the Tpm concentration was 2 µM titrated with increasing troponin concentration from 0-7 µM in 2 ml of AMSB (10 mM MOPS pH 7, 50 mM KCl, 3.5 mM $MgCl_2$, 1 mM DTT, and 1 mM NaN_3) at 25° C. The correction volume was applied to adopt the change of volume due the adding of troponin. The curves were plotted as a function of the troponin concentration and hyperbola equation was applied to calculate the Tn bound to Tpm (K_D).

Chapter 3

Structural and functional characterization of tropomyosin3 mutations expressed in *Baculovirus*-Sf9 insect cells

3.1 Introduction

Mutations in genes that encode proteins in thin filaments of the muscle sarcomere were found to cause several congenital muscle diseases and disorders. A number of clinical features including hypotonia, non-or slowly progressive muscle weakness, slender build, predominant involvement of the proximal muscles, bulbar muscle weaknesses are shared by, nemaline myopathy, cap disease and congenital fiber type disproportion. Mutations in Tpm2 and Tpm3 were found in at least three different skeletal muscle diseases (Lehtokari et al., 2008; Nowak et al.,1999; Tajsharghi et al., 2007). Cap disease and distal arthrogryposis are caused by mutation in Tpm2 while CFTD is caused by mutation in Tpm3 and NM myopathy is caused by mutations in both Tpm2 and Tpm3. Since these myopathies are caused by mutations in a number of thin filament associated genes and in particular Tpn, they may eventually provide insight into the function of different Tpms and different regions of Tpm proteins (Kee and Hardeman, 2008).

An important structural property of tropomyosin is the end-to-end (Head to tail) interactions. This interaction between the N-terminal of one tropomyosin and the C-terminal of the adjacent tropomyosin plays a critical role in tropomyosin binding to actin and the cooperativity conferred by tropomyosin to thin filaments. Tropomyosin is subject to N-terminal acetylation and this acetylation is believed to be critical for the head to tail interactions. To obtain tropomyosin mutant proteins, an expression system that maintain acetylation is highly desirable. Many laboratories used *E.coli* expression systems to obtain tropomyosin. Proteins expressed in *E.coli* cannot be acetylated since *E.coli* does not possess the enzymes required for acetylation. However, it has been shown that the addition of an Ala-Ser- extension at the N-terminus mimics the acetylation and restores the end to end interactions (Monteiro et al., 1994). However, some reports have disputed this and suggested that this Ala-Ser-Tpm produces reduced cooperativity and perhaps other abnormalities (Coulton et al., 2006).

We have decided to use *baculovirus* SF-9 insect cells to express tropomyosin mutants for three main reasons: firstly the insect cells have an advantage in which the produced protein undergoes acetylation and other post-translational modification while the *E.coli* host expression systems does not. Secondly, *Baculovirus* can be grown in absence of serum and can be culture attached or in suspension in the host insect cells which gives a very efficient method for producing recombinant/mutated proteins. Thirdly, the host insect cells lack tropomyosin which diminishes the possibility of the contamination with the protein of interest. In this chapter, I will describe my attempt to set up a *baculovirus-SF-9* insect cell expression system in our laboratory and use it to express tropomyosin mutants in sufficient quantities. I will also present my data on the effect of several mutations in Tpm3 associated with congenital myopathies on its biochemical and structural properties. We selected the following mutations A4V, R90P, L100M, R167C, R167G, K169E, E240K, and R245G. Several of these mutations are at a site believed to interact with actin R90, R167, K169, E240 and R245. We hypothesised that these mutations will reduce tropomyosin binding to actin. Mutation A4V is at the N-terminal part of tropomyosin involved in the head to tail interactions and we hypothesised that this mutation will interfere with tropomyosin end to end interactions and consequently with actin binding. L100M is a mutation likely to disrupt the structure of tropomyosin because it is in position (a) of the heptad-peptide which is present in the core of the coiled coil and it is important for its stabilisation.

The effect of these mutations on the ability of Tn to activate and inhibit the actomyosin ATPase activity in the presence and absence of Ca^{2+} was assessed respectively. We have also analysed the effect of Tpm mutations on the cooperative activation of (actin-Tpm-Tn-myosin) ATPase by myosin heads. Co-sedimentation assays were used to test the binding of Tpm to actin. Additionally, we investigated the transition of thin filament from the blocked to the closed state by measuring the equilibrium constant K_B. To monitor the impact of these mutations on long range conformational effect we followed trypsin digestion at Arg133 in the presence and absence of actin respectively.

Although proteins were successfully produced and used in a variety of assays, it became clear that acetylation of Tpm was variable, resulting in unreliable data. Cosequently, this production method was not used in all future work. Nevertheless, the data are shown and conclusions are drawn where possible.

3.2 Results

3.2.1 Expression and purification

All tropomyosin's were expressed and purified from SF-9 (Clonal isolate of *Spodoptera Frugiperda* SF21 cells) insect cell cultures expressing Tpms (A4V, R90P, L100M, R167C, R167G, K169E, E240K, and R245G). All baculovirus constructs were a gift from Prof. Kristen Nowak (University of Western Australia).

The expression and purification was based on previous methods (Hitchcock-DeGregori and Heald, 1987; Urbancikova and Hitchcock-DeGregori, 1994; Akkari *et al.,* 2002). After cell lysis and removal of debris, crude extraction of Tpm was done by ammonium sulphate fractionation from 0-45% and then from 45-65%. The 65% pellet was dissolved and dialysed overnight in (10 mM MOPS pH 7.2, 50 mM KCl, 3.5 mM $MgCl_2$, 1 mM DTT, and 1 mM NaN_3). The crude tropomyosin was loaded onto a DEAE column, which had been equilibrated with the same dialysis buffer. Absorption measurement at 280 nm was used to monitor the various DEAE fractions (Figuer 3.1 Panel A). During the wash, a peak was eluted and analysed by gel electrophoresis which showed various bands that are insect cell proteins (Figuer 3.1 panel B). Once the flow through peak was back to zero, elution of the proteins bound to the column was achieved by a linear gradient of 50-500 mM KCl and 5 ml fractions. Absorption measurement was used to monitor the various eluted fractions (Figuer 3.1 Panel A). Analysis of these peak was carried out by gel electrophoresis which showed Tpm as the main band but also several other contaminant bands (Figuer 3.1 panel B).

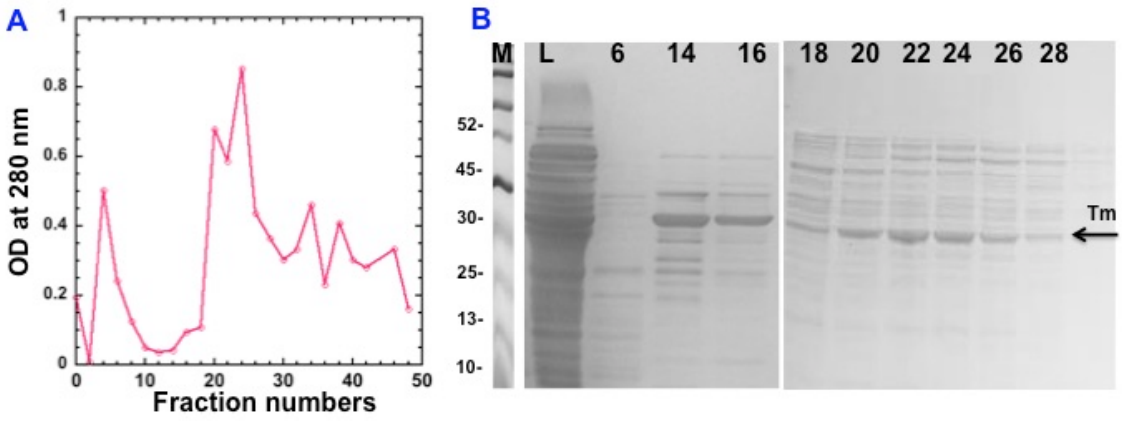

Figure 3.1: Tropomyosin purification OD spectra and 12% SDS gel

(A) DEAE elution profile using absorbance at 280 nm (y axis) of the various fractions (x axis) (B) SDS PAGE analysis of the various fractions (numbers given above the lanes) of the DEAE column.

3.2.2 Effect of increasing troponin concentration on maximal inhibition and activation of the actomyosin ATPase

The tropomyosin and troponin are actomyosin regulatory proteins in a calcium dependent manner. In the absence of Ca^{2+} the Tpm-Tn complex inhibits the actomyosin ATPase while in the presence of Ca^{2+}, the Tn-Tpm complex activates the actomyosin ATPase above the activity obtained for actin alone (Lehman and Craig, 2008). This assay was conducted to observe the effect of mutations on Tpm-Tn induced inhibition and activation of actomyosin ATPase in the absence and presence of calcium. Myosin heads hydrolyses ATP into ADP-Pi and thin filaments activate this substantially. The inorganic Pi production can be monitored by a colorimetric method.

Activation and inhibition of myosin ATPase activity rates were measured using actin 10 µM Tpm 2 µM, S1 2 uM, Tn 0-3 µM, 0.5 mM $CaCl_2$ or 1 mM EGTA in AOSB (10 mM Mops, 0.5 mM DTT, 3.5 mM $MgCl_2$ and 0.5mM NaN3 at pH 7.2) in 30 °C. For both activation and inhibition, the actomyosin ATPase activity in the absence of Tn is used as the reference level and is set at 100%.

This experiment was done for the WT and the mutants and the average of three experiments was plotted in (figure 3.2). Tissue purified skeletal muscle tropomyosin was used as a control in parallel with WT and mutants. Tissue purified skeletal muscle tropomyosin showed activation with increasing Tn concentration in presence of Ca^{2+} reaching a plateau of almost 100% activation (above the reference level of actin activation of myosin head ATPase) with about 1 µM Tn. In the absence of Ca^{2+}, troponin induced inhibition of the actomyosin ATPase and maximum inhibition was obtained at about 1 µM. Analysis of the baculovirus Sf9 insect cell tropomyosin wild type (No mutation) (WT) did show 50 % activation above the actin level. This is only half the activation observed for tissue purified tropomyosin. Surprisingly, the WT Tpm showed no inhibition of the actomyosin ATPase. The R245G showed good activation and inhibition compared to the tissue purified Tpm. For K169E and L100M Tpm mutants showed activation of the actomyosin ATPase similar to the WT and much less than the tissue purified tropomyosin. The inhibition of the actomyosin ATPase was similar to the tissue purified tropomyosin.

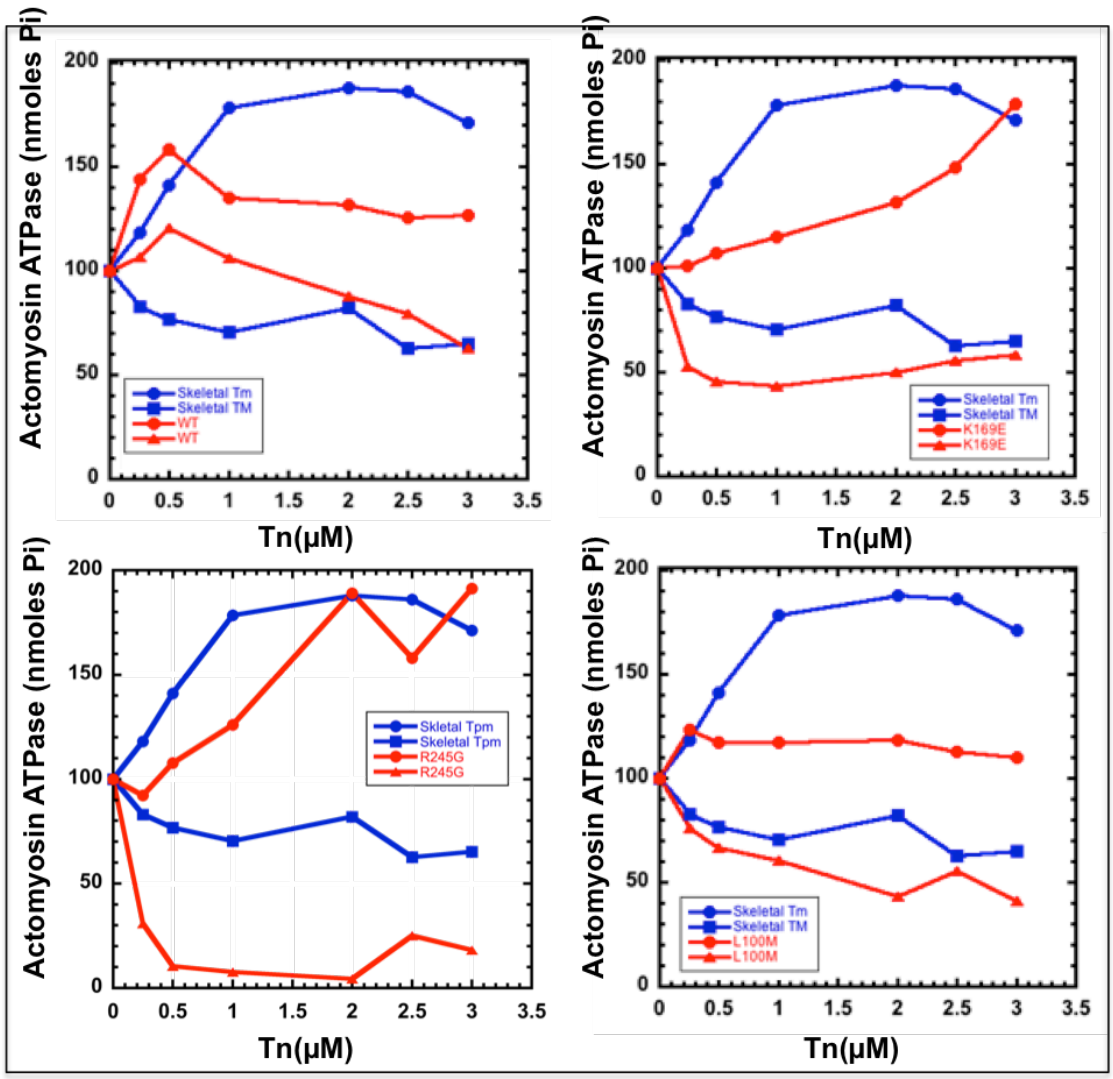

Figure 3.2: Activation and Inhibition of myosin ATPase activity

Effect of Tpm3 mutations on activation and inhibition of myosin S1 ATPase activity by interaction of Tn with actin-Tpm complexes in the presence and absence of Ca^{2+}. The blue curve represents the skeletal Tpm and the red curve represents the WT and mutants. Conditions are: actin 10 μM Tpm 2 μM S1 2 μM and Tn 0-3 μM 0.5 mM $CaCl_2$ and 1 mM EGTA in AOSB (10 mM Mops, 0.5 mM DTT, 3.5 mM $MgCl_2$ and 0.5mM NaN_3 at pH 7.2) in 30°C.

3.2.3 Effect of Tropomyosin mutations on the cooperative activation of actin-Tpm-Tn-myosin ATPase by myosin heads

Lehrer and Morris developed an actomyosin ATPase assay capable of visualising the cooperative behaviour of muscle thin filaments using the dependence of the actin activation of myosin ATPase by increasing S1 concentrations. The curve obtained for S1 alone represents the basal ATP hydrolysis by myosin heads. The curve obtained for S1+actin represents the actin activation of myosin heads ATPase. The ATPase obtained with S1 myosin head and actin filament alone follows a hyperbolic relationship as a function of myosin head concentration because they follow simple Michaelis menten enzyme kinetics. In the presence of tropomyosin, the curve become sigmoidal in both the absence and presence of troponin (with or without Ca^{2+}) (Lehrer and Morris, 1982). The experiment in (figure 3.3) showed a slightly sigmoidal curve for tissue purified skeletal muscle Tpm (red square) in the presence of Tn-Ca^{2+} and inhibition (red diamond) in the presence of Tn but without Ca^{2+}. Wild type Tpm alone was showing activation due to the S1 binding but not as much as in the presence of Tn-Ca^{2+} (red circle).

We analysed several tropomyosin mutants using this assay including Tpm A4V, Tpm R90P, Tpm R167G, Tpm R167C, Tpm K169E, Tpm E240K and Tpm R245G. The following results were obtained. 1) None of the mutants showed any sigmoidal behaviour for Tpm alone or Tpm with Tn (+/- Ca^{2+}). 2) All the Tpm mutants showed less activation in the presence of Tn-Ca^{2+} than for tropomyosin alone, unlike tissue purified Tpm. 3) All the mutants inhibited the actomyosin ATPase similarly to the tissue purified tropomyosin in the presence of Tn and absence of Ca^{2+}. 4) Tpm A4V and Tpm R90P showed slightly reduced activation of the actomyosin ATPase in the presence of Tn+Ca^{2+} in comparison to skeletal muscle Tpm. 5) Most significantly Tpm R167G, Tpm R167C and TpmE240K showed complete loss of the activation of the actomyosin ATPase in the presence of Tn-Ca^{2+} (The ATPase obtained was at the same level as inhibition).

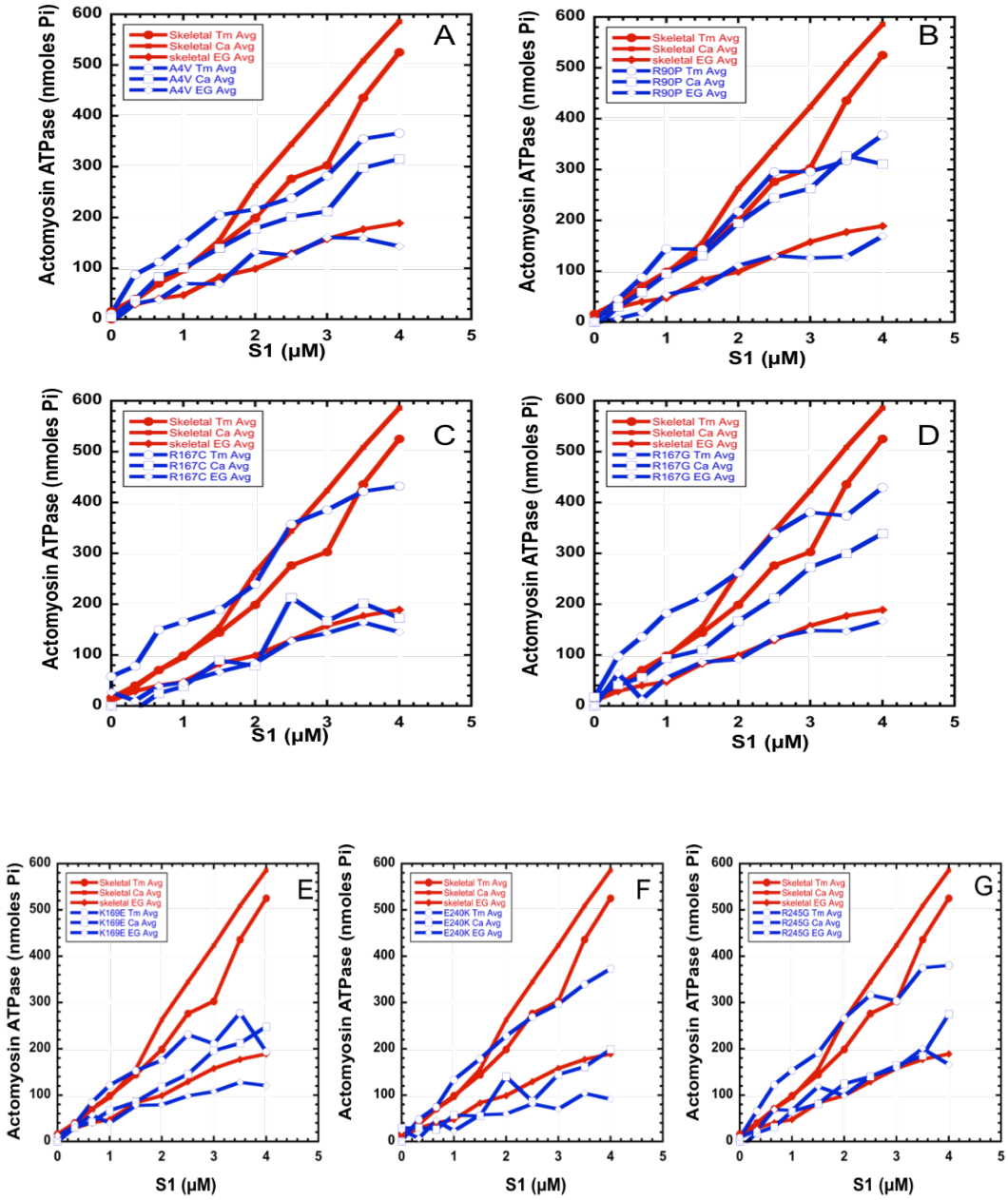

Figure 3.3: Effect of Tpm mutations on the S1 dependence of the actomyosin ATPase

Thin filament activation of S1 ATPase at increasing concentration of S1 in the presence and absence of calcium. The Red represents the Skeletal Tpm and the blue represents the mutations. Activity was measured in the presence of 8 μM skeletal actin, 2 μM Tpm, 2 μM Tn and 0-4 μM skeletal S1 at 30 °C in ATPase low salt buffer (10 mM KCl, 10 mM MOPS pH 7.2, 3.5 mM $MgCl_2$, 1 mM DTT, and 1 mM NaN_3). In the presence of Tn, the experiments were performed either in the presence of 0.5 mM $CaCl_2$ or 1 mM EGTA.

3.2.4 Effect of tropomyosin mutations on actin binding: Co-sedimentation

Tropomyosin binding to actin is the defining property of tropomyosin and is necessary for its ability to regulate muscle contraction together with troponin. In order to analyse the binding of tropomyosin to actin, single point co-sedimentation experiments were performed to determine simply if Tpm binds actinor not. At high speed centrifugation actin filaments form a pellet that will also contains any protein that has the ability to bind these filaments. If the protein does not bind actin it will stay in the supernatant. Analysis of the supernatant and pellet allows the determination of actin binding ability. Thin filament mixtures were premixed at a ratio of 14 Actin:2 Tpm then the co-sedimentation assay was done as described previously in methods section (2.4.3). The pellets and supernatants were analysed using 12% SDS-gel. Figure 3.4 shows the results. Actin filaments alone were used as a control and in which most actin was in the pellets. Tissu purified skeletal muscle Tpm spun alone and was predominantly in the supernatant. A small amount was observed in the pellet that may be due to aggregation. In the presence of actin, the majority was in the pellet with actin demonstrating an interaction between actin and tissue purified skeletal muscle tropomyosin. For the various Tpm mutants analysed the results were as follow: 1) Tpm WT and Tpm L100M showed no binding to actin. These two proteins were found in the supernatant and no proteins were found in the pellet with actin suggesting that these Tpm proteins did not bind actin filaments. 2). Both Tpm K169E and Tpm R245G were found in the pellets with actin but not when spun alone indicating that these two mutants showed binding to actin filaments. However, both mutants showed a reduction in the binding to actin since the size of the band in the supernatant of (Actin+Tpm) is more than what observed for skeletal muscle tropomyosin.

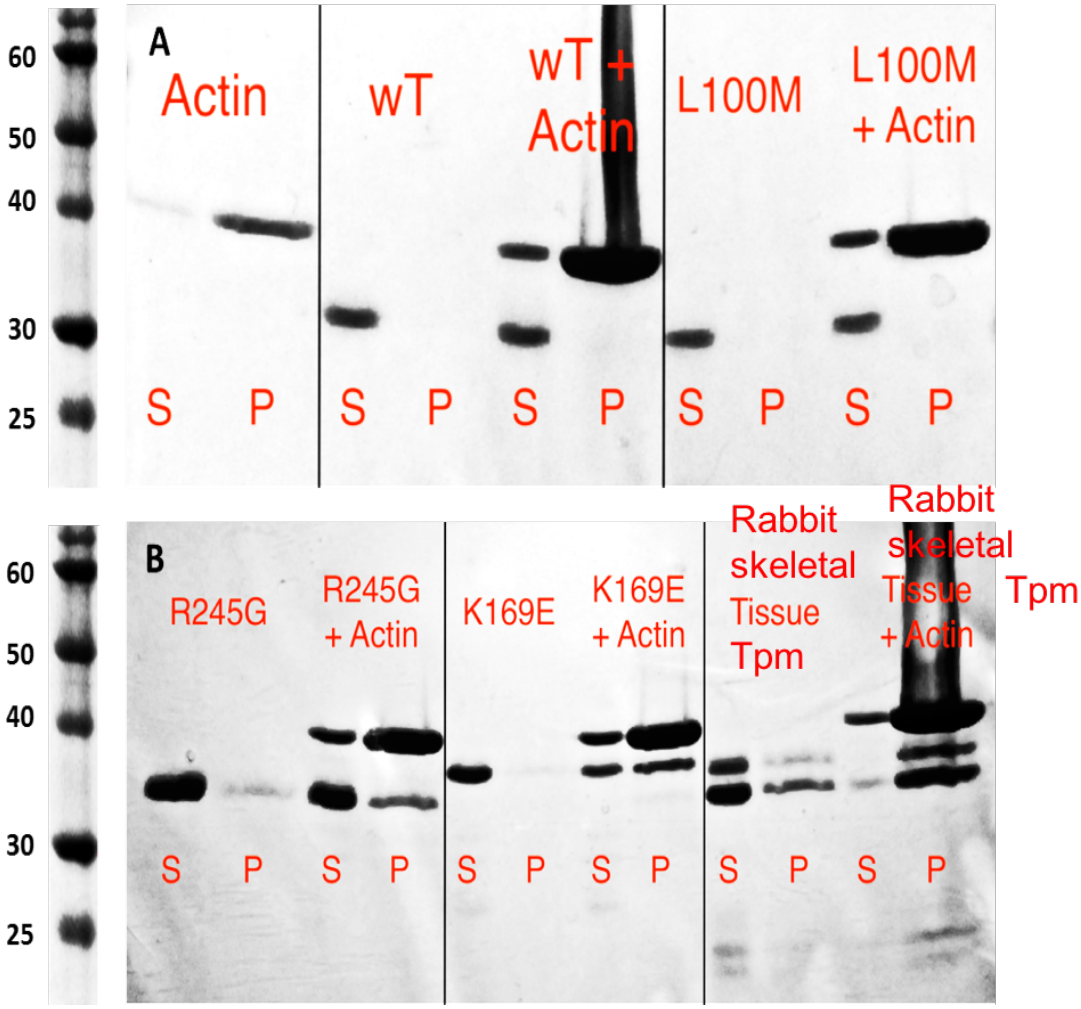

Figure 3.4: 12% SDS-PAGE for WT and Tpm mutations co-sedimentation with Actin

From left to right pellets (P) and supernatants (S) are shown: actin, WT, L100M, R245G, K169E and Skeletal Tpm. Thin filaments were reconstituted by incubating 12 µM actin, 2 µM Tpm in 10 mM MOPS, 50 mM KCl, 4 mM MgCl2, 0.1 mM CaCl2 and 1 mM DTT (pH 7.2) for 30 min and then spun down for 400 minutes at 85,000 rpm at 4 C.

3.2.5 The effect of mutations on the structure of tropomyosin using trypsin digestion essay

Sumida et al developed an assay to assess the impact of tropomyosin mutations on the structure and long range conformational change in tropomyosin using digestion of tropomyosin by trypsin at Arg133 (Sumida *et al*., 2008). We performed a time course of Tpm digestion by trypsin for all Tpm mutants in comparison to the WT as a control. The stability of Tpm will affects the time it takes for trypsin to digest the protein. In the absence of actin WT tropomyosin did not display any digestion after 1, 2 and 3 minutes of addition of trypsin. After 4 minutes a 15 kDa band appeared and after 30 minutes all Tpm was converted to two bands of small molecular weights 10 and 15 kDa. The three mutations L100M, K169E and R245G showed more resistance to trypsin digestion than the WT. The native Tpm band was still present after 30 min of digestion and an intermediate band of 24 kDa was observed much later in the digestion time course figure (3.5).

Since actin filaments bind tropomyosin and actin filaments are resistant to tryptic digestion (on a short timescale), we presumed that addition of actin filaments will protect tropomyosin from digestion by trypsin and will change the pattern of digestion. Figure (3.6) shows the digestion of Tpm in the presence of actin. Panel A and D showed that Tpm WT and Tpm L100M were completely digested at 30 min and no native Tpm band was visible at that time. Panels B and C showed that Tpm K169E and Tpm R245G showed a different pattern of tryptic digestion in the presence of actin filaments to the digestion pattern obtained in the absence of actin filaments. The native band was present even after 30 min of digestion suggesting the presence of actin filaments has protected these Tpm variants from digestion by trypsin.

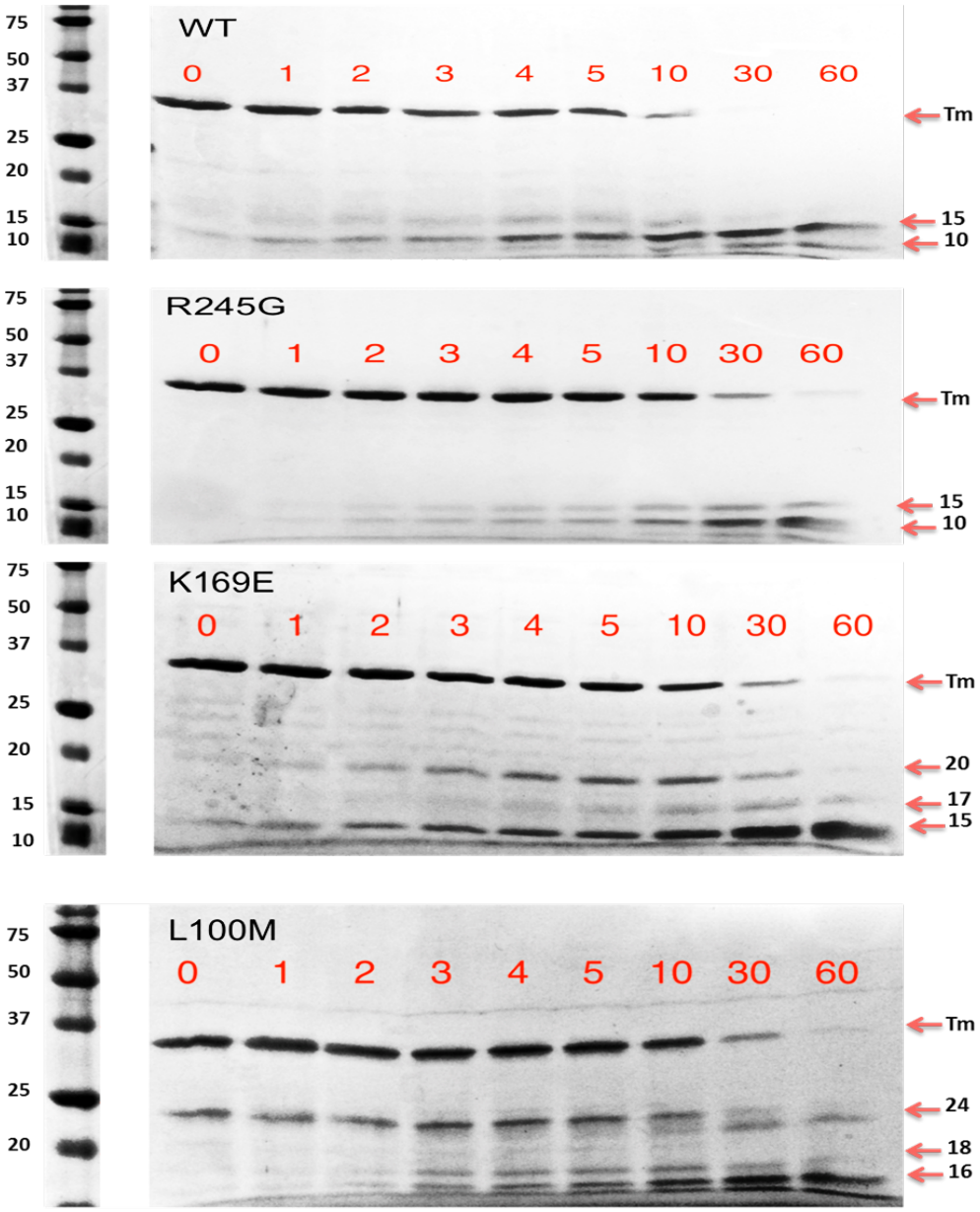

Figure 3.5: 12% SDS page results of chymotrypsin digestion of Tpm alone

The experiment performed for Tpm alone and concentration used was 0.6 mg/ml Tpm with 0.003 mg/mL trypsin (lot STBC8587V SIGMA) in a buffer contains (10 mM HEPES buffer (pH 7.5), 0.1 M NaCl, 5 mM MgCl2, and 10 mM β-mercaptoethanol) at 26 °C. Panel (A) shows the WT and numbers illustrates the time course. Panel (B) shows the R245G and the numbers illustrates the time course. Panel (C) shows the K169E and numbers illustrates the time course. Panel (D) shows the L100M and numbers illustrates the time course.

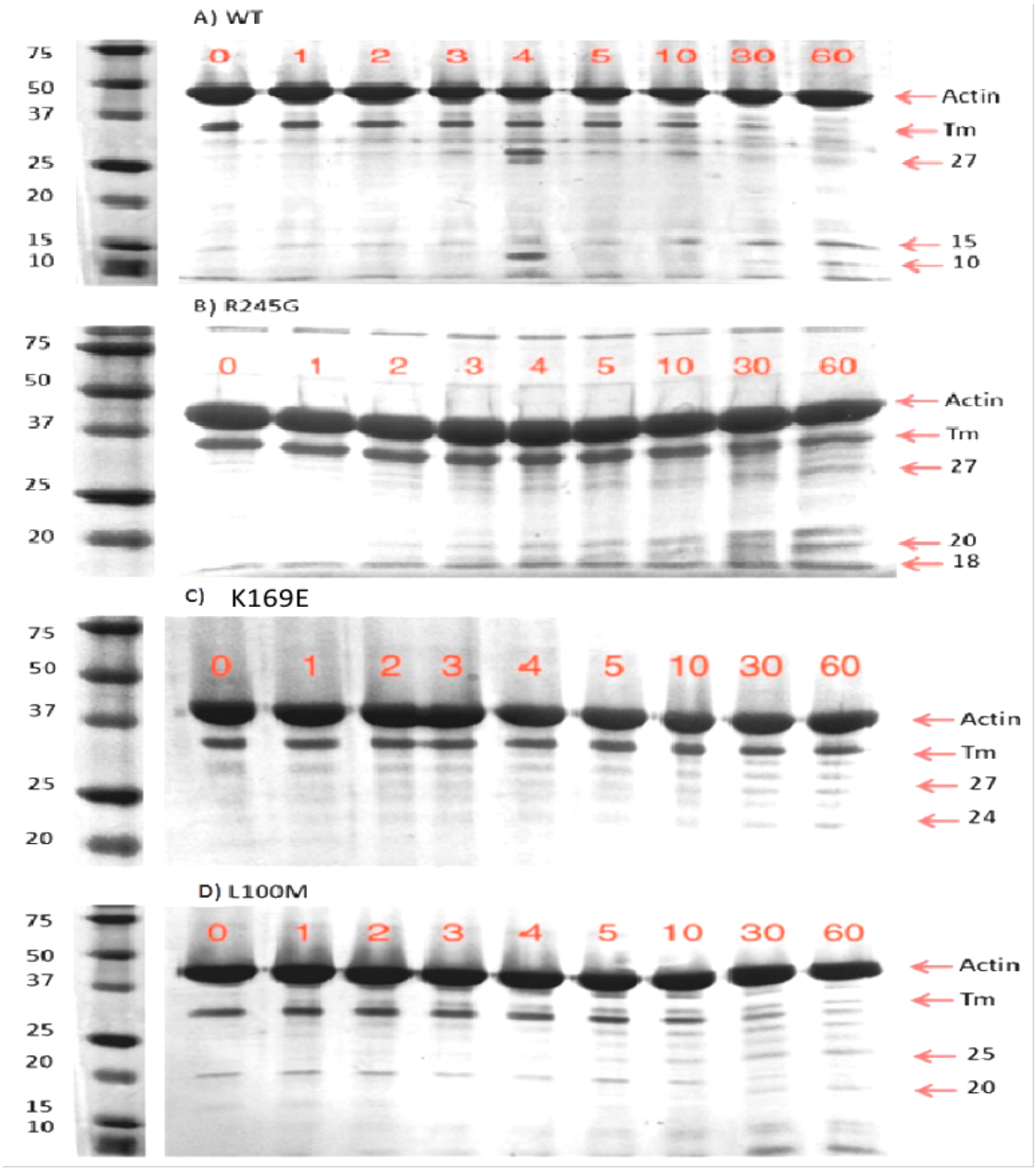

Figure 3.6: 12% SDS page results chymotrypsin digestion of Tpm in the presence of actin filaments

The experiment performed in the presence of actin and Tpm and concentration used was 0.3 mg/ml Tpm mixed with 1.5 mg/ml actin (excess of actin) treated with 0.003 mg/mL trypsin (lot STBC8587V SIGMA) in a buffer contains (10 mM HEPES buffer (pH 7.5), 0.1 M NaCl, 5 mM $MgCl_2$, and 10 mM β-mercaptoethanol) at 26 °C. Panel (A) shows the WT with actin and numbers illustrates the time course of digestion in minutes. Panel (B) shows the R245G and the numbers illustrates the time course of digestion in minutes. Panel (C) shows the K169E with actin and numbers illustrates the time course of digestion in minutes. Panel (D) shows the L100M with actin and numbers illustrates the time course of digestyion in minutes.

3.2.6 Effect of Tpm mutations on the transition between blocked and closed states (K_B)

The transition of thin filaments between the three states of thin filament, blocked, closed, and open state is controlled by Tn and Tpm proteins. The proportion of thin filament in the closed state over the proportion of thin filament in the blocked state defines K_B (Head et al., 1995). The kinetics of myosin head binding to thin filaments is different between the closed and blocked state. Consequently, to measure the effect of Tpm mutations on the equilibrium constant K_B, the kinetics of myosin head binding to thin filaments was followed at low Ca^{2+} (Blocked state) and high Ca^{2+} (closed state). To monitor the interaction of actin with myosin head, we used pyrene iodoacetamide labelled actin.

The changes in the emission spectra in (Figure 3.7) shows the pyrene labelled actin alone (green curve), in the presence of S1 (1/10 of actin) (blue curve) and after addition of ATP to dissociate S1 (red curve). The emission spectra of actin labelled with pyrene show clear peaks at 388 nm, 405 nm and 430 nm. In the presence of S1, the fluorescence is reduced and this reduction is abolished by addition of ATP. Thus, the monomer fluorescence at 380 nm can be used as a signal to monitor the kinetics of myosin head (S1) binding to actin.

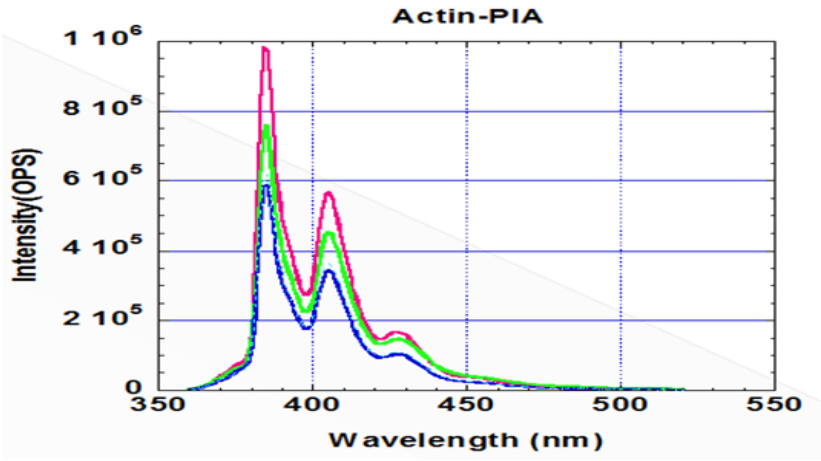

Figure 3.7: The fluorescence spectra of Acti-PIA

The figure shows the changes to the fluorescence emission spectra of PIA-actin after Tpm and S1 binding. actin-PIA alone (Red curve), with Tpm (Green curve) and S1 (Blue curve).

The dependence of the observed rate constant of S1 binding to actin (with various Tpm mutants and troponin +/- Ca^{2+}) was shown in (Figure 3.8). K_B is calculated from the slope of the lines describing S1 binding to thin filaments in comparison to actin alone (see Materials and Methods). Table 1 summarises the K_B values.

The observed rate constant obtained for actin alone and actin*.Tpm.Tn in the presence and absence of calcium was shown in (figure (3.8.A). In presence of Ca^{2+} tissue purified Tpm shows a linear increase in the observed rate constant (k_{obs}) which yields a K_B value 1.44. In absence of Ca^{2+} the K_B value for tissue purified Tpm is 0.165. The A4V mutation shows a linear increase in the observed rate constant (k_{obs}) which yields a K_B value of 7.036 in the presence of Ca2+ and 11562 in absence of Ca^{2+}. The results in the absence of Ca^{2+} are very surprising and suggest that this mutation may have abolished the ability of Tn in the absence of Ca^{2+} to induce the blocked state. For all mutants, the k_{obs} obtained in the presence and absence of calcium were linearly proportional to the actin concentration over the range 1-5 µM. Figure 3.8.B, 3.8.C and 3.8.D shows the dependence of the observed rate constant (k_{obs}) of S1 binding to actin on actin concentration for R90P, R167C and R167G. In the absence of Ca^{2+}, K_B values of 3.73 for Tpm R90P, 1359.5 for Tpm R167C and 2.73 for Tpm R167G were calculated. They are all much higher than the value obtained for skeletal TPM (0.165) indicating that these mutations reduced the proportion of thin filaments in the blocked state. In the presence of Ca^{2+}, K_B values of 3.49 for Tpm R90P, 6.312 for Tpm R167C and 1.13 for Tpm R167G were calculated. Figure 3.8.E, 3.9.F and 3.9.G shows the dependence of the observed rate constant (k_{obs}) of S1 binding to actin on actin concentration for K169E, E240K and R245G. For all curves k_{obs} was linearly dependent on actin concentration as for skeletal Tpm. In the absence of Ca^{2+}, K_B values of 0.47 for Tpm K169E, 1.73 for Tpm E240K and 4.82 for Tpm R245G were calculated. They are all much higher than the value obtained for skeletal Tpm (0.165) indicating that these mutations reduced the proportion of thin filaments in the blocked state. In the presence of Ca^{2+}, K_B values of 1.002 for Tpm K169E, 1.92 for Tpm E240K and 6.95 for Tpm R245G were calculated. All calculations of K_B are listed in the table 3.1

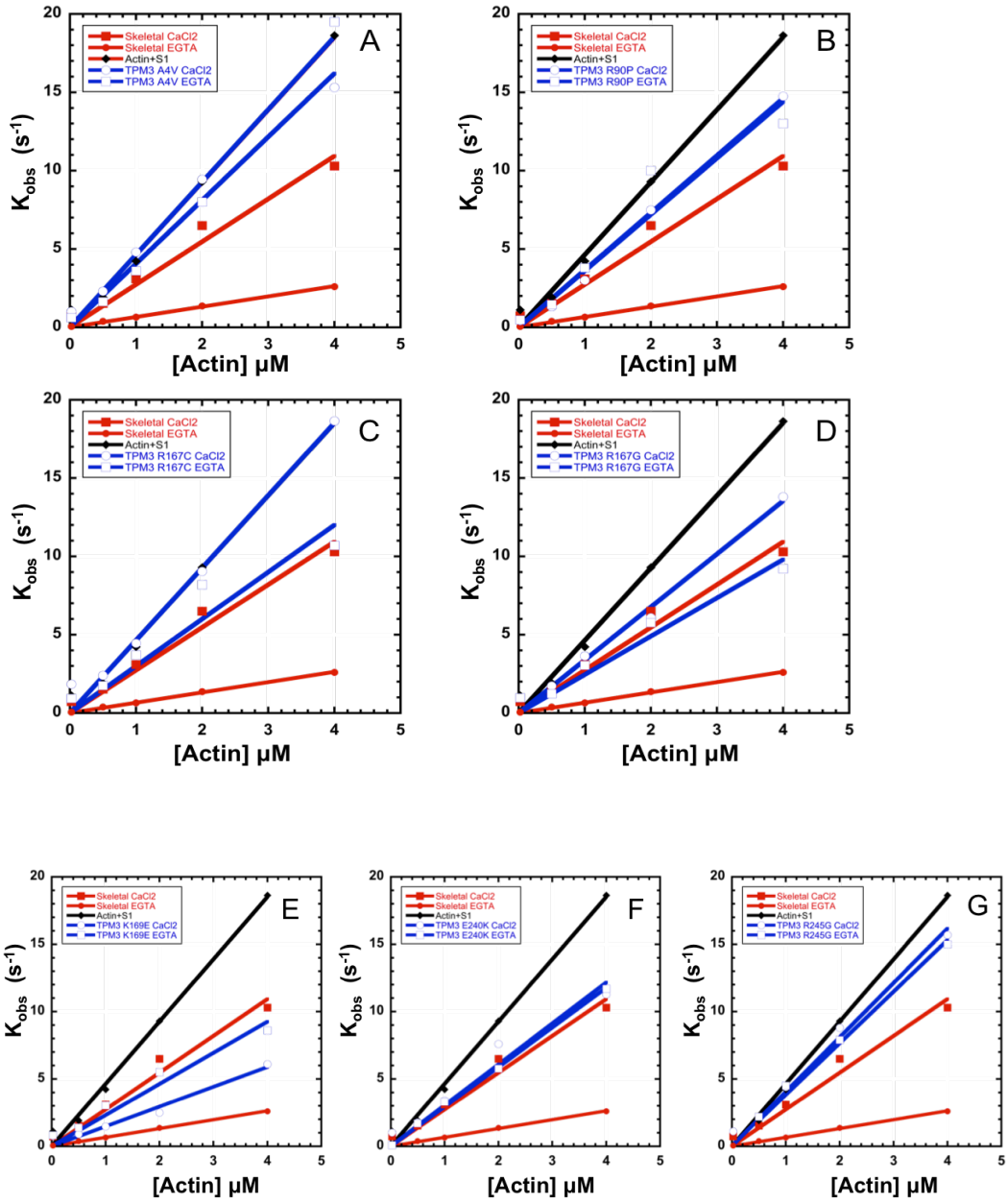

Figure 3.8: Binding kinetics of S1 to thin filaments reconstituted with pyrene labelled actin filaments, various Tpm mutants and Tn with and without calcium

The plots display the dependence of the observed rate of S1 binding on the concentration of PIA-labeled actin. The binding was done in 140 mM KCl, 10 mM Mops pH 7.2, 4 mM MgCl2, 1 mM DTT, 0.5 mM $CaCl_2$ or 1 mM EGTA, at 25 °C. (A) Shows the K_{obs} for actin-PIA alone (black) and actin-PIA with skeletal Tpm-Tn in presence of calcium (Red square) and absence of calcium (Red circle). The results for all Tpm mutants are shown in blue using square for the presence of calcium and circles for the absence of calcium. The thin filaments were reconstituted with actin-Tn and the following Tpm mutants: A4V (panel A), R90P (panel B), R167C (panel C), R167G (panel D), K169E (panel E), E240K (panel F), R245G (panel G).

Table 3.1: the calculated KB values of Tpm3 mutants in the absence of Ca^{2+} (EGTA K_B) and the presence of Ca^{2+} ($CaCl_2$ K_B).

Protein	K_B (EGTA)	K_B ($CaCl_2$)
A4V	11562.9	7.036
R90P	3.49	3.73
R167C	6.312	1359.5
R167G	1.13	2.73
K169E	1.002	0.47
E240K	1.73	1.92
R245G	4.82	6.95
Skeletal	0.165	1.44

3.3 Discussion

The aim of the work described in this chapter was to establish a *baculovirus* Sf9 insect cell expression system for tropomyosin 3. The system was used to obtain several tropomyosin mutants and investigate the effect of these mutations on the structure and biochemical properties of tropomyosin including Tpm stability and long range conformational change, binding to actin, cooperative activation and inhibition of the actomyosin ATPase and the transition between the blocked and closed states.

3.3.1 Expression and purification of Tpm3 using Sf-9 cells

To perform the experiments described in this chapter, a total of 12 proteins were prepared (Actin, S1 myosin head, skeletal Tpm, Skeletal Tn, WT and 7 Tpm mutants).
Tpm was successfully expressed and purified from a baculovirus Sf9 insect cell system. The yield was about 2 mg of Tpm variant per litre of culture. Tpm was purified although several contaminations persisted.

3.3.2 Effect of mutations on actomyosin ATPase steady state

The effect of Tpm 3 mutations on the actomyosin ATPase was investigated using two different experiments: 1) using varying Troponin in the presence and absence of calcium and 2) using varying S1 concentration.
In the ATPase experiments varying Troponin (+/- Ca^{2+}), the wild type did show reduced activation and no inhibition of the actomyosin ATPase in comparison to the tissue purified Tpm. This is unexpected and can only be explained by a lack or reduced level of acetylation. The R245G showed good activation and inhibition compared to the tissue purified Tpm and this suggests that this mutant had been acetylated and that the mutation did not affect the ability of tropomyosin to activate (In the presence of Tn-Ca^{2+}) or inhibit (In the presence of Tn but absence of $Ca^{2+)}$ the actomyosin ATPase. The K169E and L100M Tpm mutants showed an inhibition of the actomyosin ATPase similar to the tissue purified tropomyosin. This suggest that these two variants are acetylated fully or mostly. The two mutants showed reduced activation of the actomyosin ATPase in comparison to the tissue purified tropomyosin. These results suggest that these mutations may interfere with the switching to the ON state responsible for activation.

In the ATPase experiments with varying S1 the results showed that none of the mutants displayed the sigmoidal behaviour characteristic of Tpm. This point to abnormal cooperative behaviour of Tpm. All the Tpm mutants showed less activation in the presence of Tn-Ca^{2+} than for tropomyosin alone, unlike skeletal muscle Tpm and unlike the experiment done at low S1 (previous section, varying Tn). It is not clear if these effects are due to the mutations or to lack or incomplete acetylation.

3.3.3 Tropomyosin binding to actin

The results obtained in the ATPase experiments were somewhat surprising and suggested that the Tpm produced using *Baculovirus* Sf9 insect cells were not fully acetylated (and for WT may be not acetylated at all). We therefore performed actin binding since un-acetylated Tpm will not bind actin in the absence of troponin. Surprisingly two Tpm variants (Tpm WT and Tpm L100M) did not bind actin filaments. Both Tpm K169E and Tpm R245G bound to actin filaments although their binding to actin was reduced. It is possible that this reduction is due to the mutation since both K169E and R245G are believed to interact with actin. However, since the control wild type Tpm did not bind actin, we cannot conclude if the observed reduction in actin binding is due to the fact that these Tpm proteins may not have been fully acetylated and that the reduction in binding was simply due to a lack of acetylation or that the mutations of these Tpm residues affected the ability of Tpm to bind actin.

3.3.4 Long range effect of mutations on tropomyosin structure as assessed by tryptic digestion.

To investigate if the mutations affected the stability tropomyosin the trypsin digestions were performed. The wild type showed less resistant compared to the mutations except the R245G which showed more resistance to tryptic digestion. L100M is located at position (a) of the heptad repeat which is at the interface between the two tropomyosin monomers in the coiled coil. K169E is located at position (*g)* of the heptad which is involved in the stabilization of the coiled coil by electrostatic interaction. The assay used is aimed at analysing at the long-distance effect of Tpm mutations on the Tpm tryptic digestion at Arg-133 (Ly and Lehrer, 2012). The stability of Tpm will affects Tpm

digestion by trypsin. The three mutations L100M, K169E and R245G showed more resistance to trypsin digestion than the WT. These experiments suggest difference in the stability between WT and the 3 mutants. Tryptic digestion of Tpm in the presence of actin was used to assess Tpm binding to actin. Tpm WT and Tpm L100M pattern of tryptic digestion was similar to the one obtained in the absence of actin suggesting that both WT and L100M Tpm variants did not bind actin in agreement with co-sedimentation experiments. K169E and Tpm R245G showed a different pattern of tryptic digestion in the presence of actin filaments to the digestion pattern obtained in the absence of actin filaments suggesting that these Tpm variants did bind actin in agreement with co-sedimentation experiments.

3.3.5 Effect of Tpm variants on the closed to blocked transition

The transition between the blocked and closed state is an important step in muscle activation and relaxation. A mutant that reduces the proportion of the blocked state for thin filaments in the absence of Ca^{2+}, will affect muscle relaxation while a mutation that increases the proportion of the blocked state in the presence of Ca^{2+} will affect muscle switching to the active state, it is therefore important to investigate the impact of tropomyosin mutation on this transition. We used the assay developed by Geeves and Colleagues (Criddle and Geeves, 1985) in which the kinetics of myosin binding to pyrene labelled actin reconstituted with Tpm and Tn is compared between the absence and presence of Ca^{2+}. Most mutations increased K_B in the absence of Ca^{2+} suggesting that these mutations interfere with the blocked state.

In conclusion, we were able to express Tpm and various Tpm mutants using the Baculovirus Sf-9 insect cell system of expression. However, we decided to stop using this method for obtaining Tpm mutants and use the traditional method of *E.coli* expression (with the Ala-Ser extension) for several reasons: 1) we were not satisfied that the produced Tpm is fully acetylated. 2) The yield obtained of 2 mg/L will not be sufficient for transient kinetics investigations. 3) This system is time consuming since the time for this expression system takes (about 10 days) and the effort (price of the media, maintenance of cell culture and risk of contamination) is not suitable for biochemical and biophysical investigations that will require lots of proteins.

Chapter 4

Cloning, expression and purification of Tropomyosin 1 mutants using *E.coli*

4.1 Introduction

Tropomyosin is an important component of thin filaments. Its binding to actin is fundamental to its function. Although tropomyosin has been investigated for over 50 years, its mode of interaction with actin is not yet fully understood. In addition, a large number of mutations in tropomyosin has been associated with several muscle diseases. Hence establishing a robust expression and purification system is critical to perform tropomyosin structure-function studies. In the previous chapter, we demonstrated the challenge to use *Baculovirus* Sf-9 insect cell system of expression to express a large amount of large number of tropomyosin mutants. Consequently, we decided to use the traditional method of *E.coli* expression system. It has been shown that the addition of di or tri peptides at the N-terminal did mimic the acetylation of methionine and produces a protein able to bind actin and polymerises easily (Monteiro et al., 1994). We decided to use an Ala-Ser dipeptide extension to be in line with other labs who studied tropomyosin previously.

Mutagenesis studies done on skeletal muscle α-tropomyosin were performed to investigate the role of the internal periodic repeats. These studies showed a 10-30 folds decrease in the α-tropomyosin binding to actin when periods 2, 3, 4, 5 and 6 were deleted (Hitchcock-DeGregori and Varnell, 1990; Hitchcock-DeGregori and An, 1996; Hammell and Hitchcock-DeGregori, 1997; Hitchcock-DeGregori et al., 2002). These studies failed to identify single amino acids of tropomyosin that represent important determinants of actin binding. On the other hand, several genetic studies have identified several tropomyosin amino acids mutations associated with severe skeletal muscle diseases (Thierfelder at al., 1994, Wernicke at al., 1999).

The mutations used were found in Tpm3 and were introduced to Tpm1 for more understanding of the effect of these mutations on tropomyosin function and structure. The rational choice of these mutations was due to their conservative presence in tropomyosin sequence between different isoforms. The following mutations were investigated (R90G, E163K, R167G, E240K, R244G and M281I) as amino acids likely to affect tropomyosin binding to actin and switching between the three states. In addition, we hypothesised that for those mutations likely to make a contact with the same actin amino acid on the various actin monomers of a cooperative unit (R90, R167 and R244) double or triple mutations may give a clearer impact. The following double amino acid mutants were designed (R90GR167G, R90GR244G, R167GR244G and E163KE240K) and a triple amino acid mutant (R90GR167GR244G).

The aim of this chapter is to describe the cloning, expression and purification of tropomyosin using *E. coli* and shows that recombinant tropomyosin can be obtained in high purity and sufficient amount to characterise large number of mutations by number of biochemical and biophysical assays.

The mutations were analysed structurally and functionally using different techniques. Circular dichroism was used to analyse the secondary structure of the tropomyosin variants and their thermal stability. The effect of the mutations on the ability of Tn complex to activate and inhibit the actomyosin ATPase activity in the presence or absence of Ca^{2+} respectively was analysed. The tryptic assay was used to assess the effect of the mutations on rate of cleavage.

4.2 Results

4.2.1 Cloning and Expression of tropomyosin mutations

The DNA construct template of human Tpm1 was obtained as a gift from Dr C. Redwood (University of Oxford, UK). All WT and mutants were then cloned into pLEIC05 expression vector using the overlap extension PCR method. Two sets of primers were designed and ordered from Eurofins: 1) the WT 5' and 3' primers. 2) A set of 2 primers (one 5' and one 3') for each of the following single amino acid mutants (R90G, E163K, R167G, E240K, R244G and M281I). Then, the first product of the single mutation was used as a template to introduce the double amino acid mutants (R90GR167G, R90GR244G, R167GR244G and E163KE240K) and the double mutation (R90GR167G) was used as a template to produce the triple amino acid mutant (R90GR167GR244G). The results of the PCR are shown in figure 4.1 on an agarose gel with the predicted band around 892 bp. The sequence of the Tpm inserts into the final plasmids were then verified using DNA sequencing.

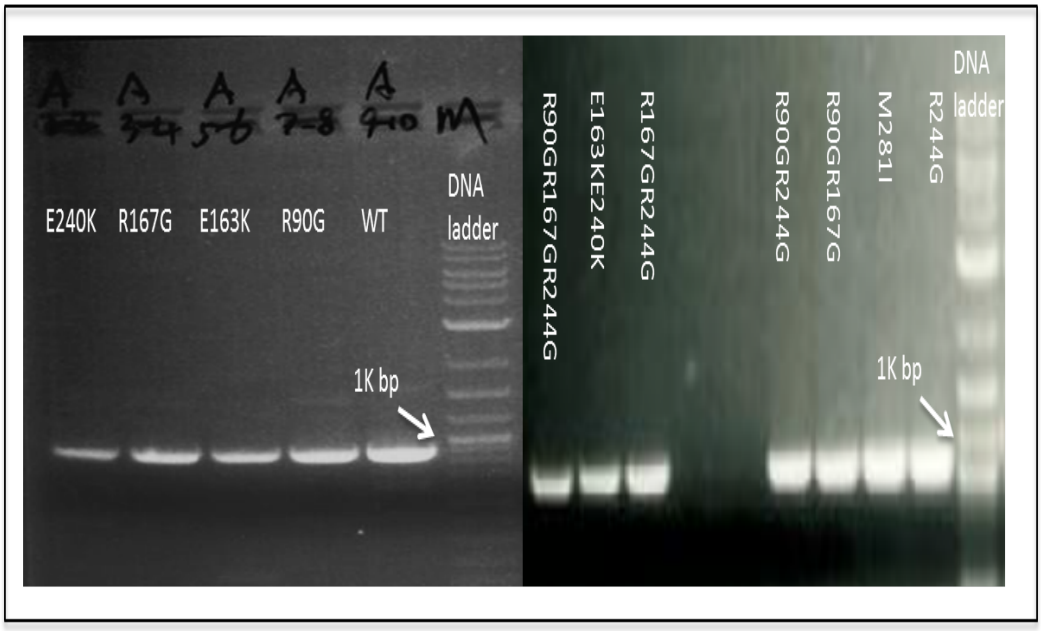

Figure 4.1: the PCR products on agarose gel for the various constructs of Tpm1 mutations

The DNA ladder shows the molecular weight of the bands and 1000bp as close band to the mutations band. The bands are labelled corresponding to the mutation. (Carried out by Dr. Xiaowen Yang at the University of Leicester).

Once the Tpm constructs were obtained and their sequence verified, they were expressed in *E.coli* cells and purified as mentioned in section (2.2.1.7). Since DEAE based chromatography did not give a good purity of the tropomyosin mutants (figure 4.2), I decided to try another type of column, a Hydroxyapatite CHT column. The column was washed by 5 mM PO_4 buffer overnight. Then, the crude sample was load onto the column and washed then eluted by increasing the concentration from 5-500 mM PO_4 buffer. Figure 4.3 shows an elution profile of Tpm from a CHT column and analysed by SDS page of various fractions. The gel shows that fractions 23-30 contains substantial amount of highly pure Tpm.

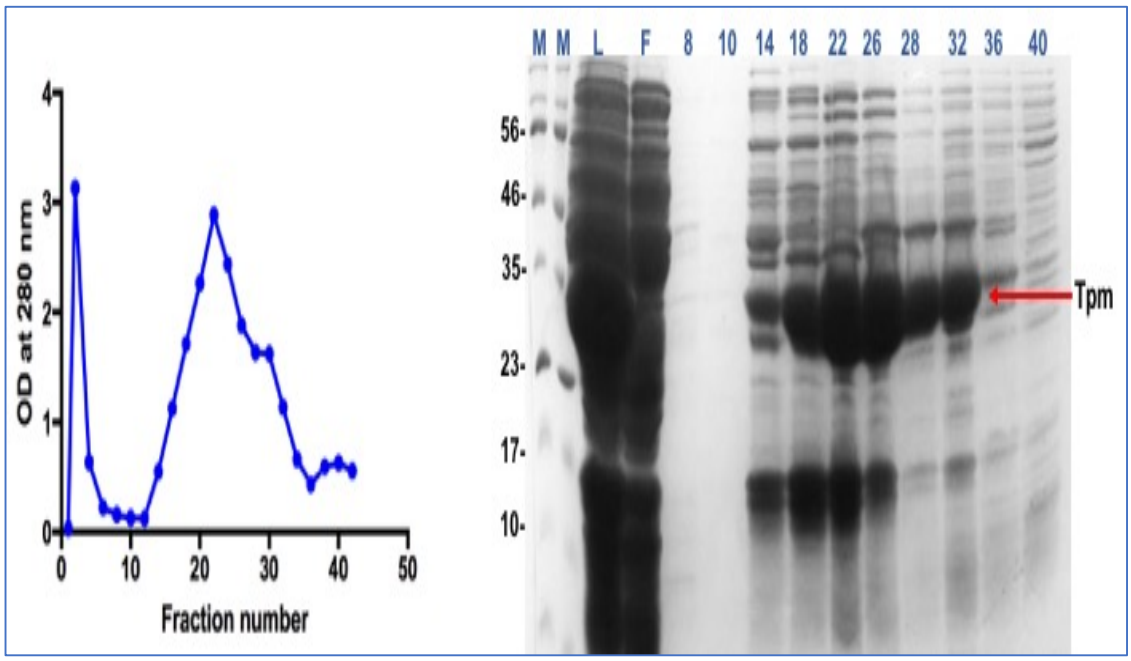

Figure 4.2 The OD spectra and the 12 % SDS page of Tpm using DEAE column

The first graph shows the spectra of the DEAE column of WT of Tpm1 after washing and applying a gradient from 50 - 500 mM KCL buffer. The samples were then loaded on 12 % SDS gel which shows the marker (M) and the sample before loading on column (L) and the (F) stands for flow through. The numbers are corresponding for the fractions of Tpm1.

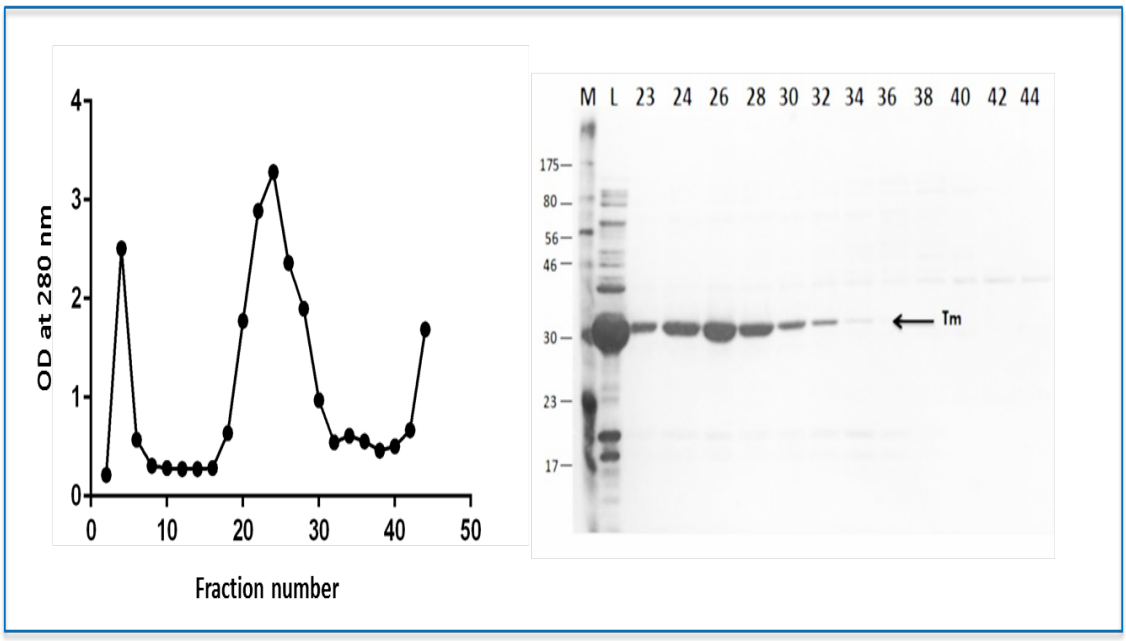

Figure 4.3: the OD spectra and the 12 % SDS page of Tpm using CHT column

The first graph shows the spectra of the CHT column of WT of Tpm1 after washing and applying a gradient from 5- 500 mM PO_4 buffer. The samples were then loaded on 12 % SDS gel which shows the marker and the sample before loading on column (L) and the numbers are corresponding for the fractions of pure Tpm1.

4.2.2 Investigation of the effect of tropomyosin mutations on actin binding by Co-sedimentation

Tropomyosin binding to actin plays a key role in the allosteric switching of thin filaments and modulation of actin-myosin interactions. It is important to check tropomyosin mutants ability to bind actin before performing investigations looking at the thin filament dynamics. (Geeves and Lehrer, 1994). A single point was used just for a qualitative investigation of the ability of Tpm to bind actin.

Co-sedimentation assay was done where 12 µM was incubated with 2 µM Tpm for 60 minutes then spun at high speed (85,000 rpm) for 1 hour. The supernatant and pellet were loaded on 12% SDS gel and analysed after staining. The excess of tropomyosin is to saturate the actin filament and enhance the binding. The binding to actin would confirm that the Ala-Ser extension is sufficient to maintain end to end interactions of Tpm and that the proteins are correctly expressed and purified Binding to actin is a prerequisite for subsequent experiments such as the actomyosin ATPase and transient kinetics measurements.

Figure 4.4 shows that all the Tpm mutations and WT proteins were soluble and when centrifuged alone they were present in the supernatant and the pellets had no tropomyosin. In contrast in the presence of actin, tropomyosin was found in the pellets suggesting that all Tpm mutants and the WT did bind to actin and No change was seen as a result of the mutation on actin binding.

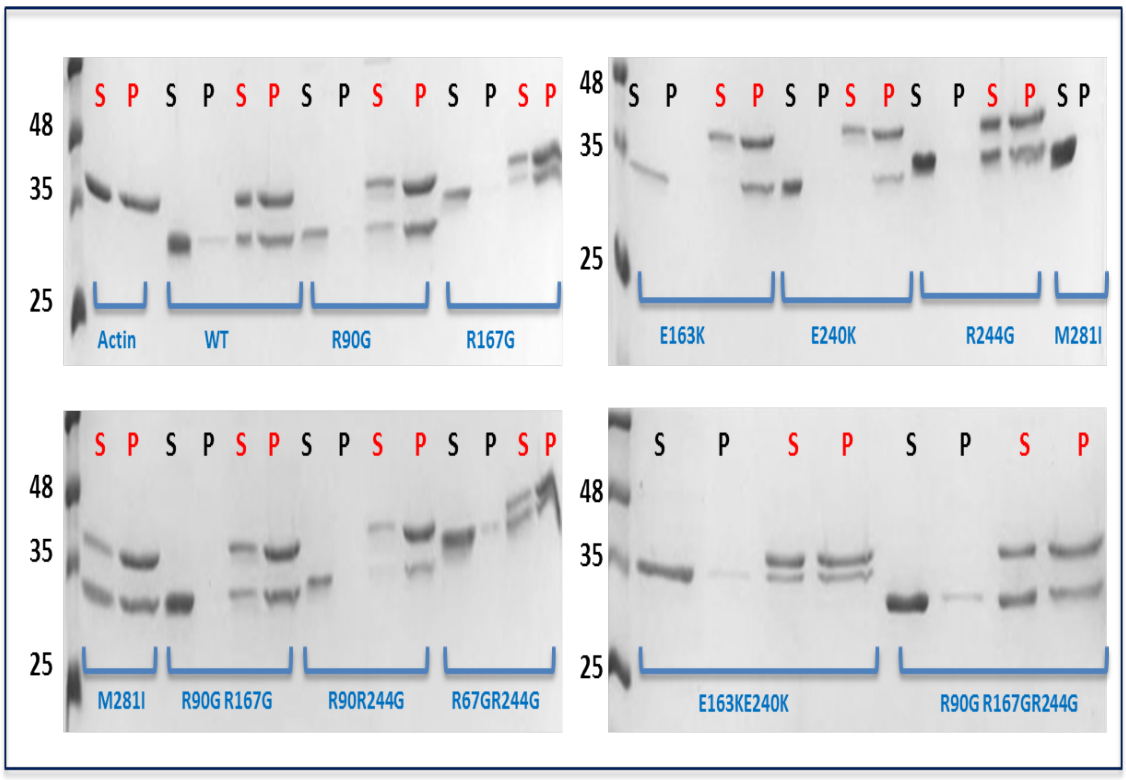

Figure 4.4: SDS-PAGE analysis of the results of the co-sedimentation with actin experiment.

From left to right Supernatant (S) pellets (P) the Red (actin+Tm) the Black (Tm alone) are shown: actin, wild type, R90G, R167G, E163K, E240K, R244G, M281I, R90G/R167G, R90G/R244G, R167G/R244G, E163K/E240K and R90GR167GR244G. The co-sedimentation assay was done by mixing 12 µM actin, 2 µM Tm in 10 mM MOPS, 50 mM KCl, 4 mM $MgCl_2$,0.1 mM $CaCl_2$ and 1 mM DTT (pH 7.2) for 60 min and then spun down for 40 minutes at 85,000 rpm at 4 °C.

4.2.3 Effect of tropomyosin mutations on tryptic digestion

Sumida group developed an assay to assess the impact of tropomyosin mutations on the structure and long range conformational change in tropomyosin using digestion of tropomyosin by trypsin at Arg133 (Sumida *et al*., 2008). We performed a time course of Tpm digestion by trypsin for all Tpm mutants in comparison to the WT as a control. The stability of Tpm will affects the time it takes for trypsin to digest the protein. The method was performed at 26°C with different time points in a buffer contains 10 mM HEPES buffer (pH 7.5), 0.1 M NaCl, 5 mM $MgCl_2$, and 10 mM β-mercaptoethanol. For Tpm alone the concentration of Tpm was 0.5 mg/ml treated with 0.001 mg/ml trypsin while in the presence of actin the 0.3 mg/ml Tpm was mixed with 1.5 mg/ml actin in excess in the same buffer. The sample then were loaded on 12% SDS-page gel and analysed.

The WT in (figure 4.5) was used as a control to compare the stability of Tm mutations using trypsin digestion. The WT exhibit two bands yielding 15 and 12 KDa starting from 30 seconds after trypsin addition and almost 90% of Tpm was digested by 10 minutes. The mutations R90G and E163K in figure 4.5 showed almost similar pattern to the WT. However, R167G exhibited three bands around 18 KDa, 15 KDa and 12 KDa which then were converted later to the 12 kDa as for the wild type. The E240K and R244G showed similar behaviour to the WT exhibiting two bands at 15 KDa and 12 KDa from about 5 minutes of tryptic digestion. Tpm mutations M281I, R90GR167G (figure 4.5) and R90GR244G, R167GR244G and R90GR167GR244G (figure 4.6) displayed the same digestion pattern to the WT. The E163KE240K digestion produced three bands of 18 KDa, 15 KDa and 12 KDa like the R167G Tpm mutant (4.6).

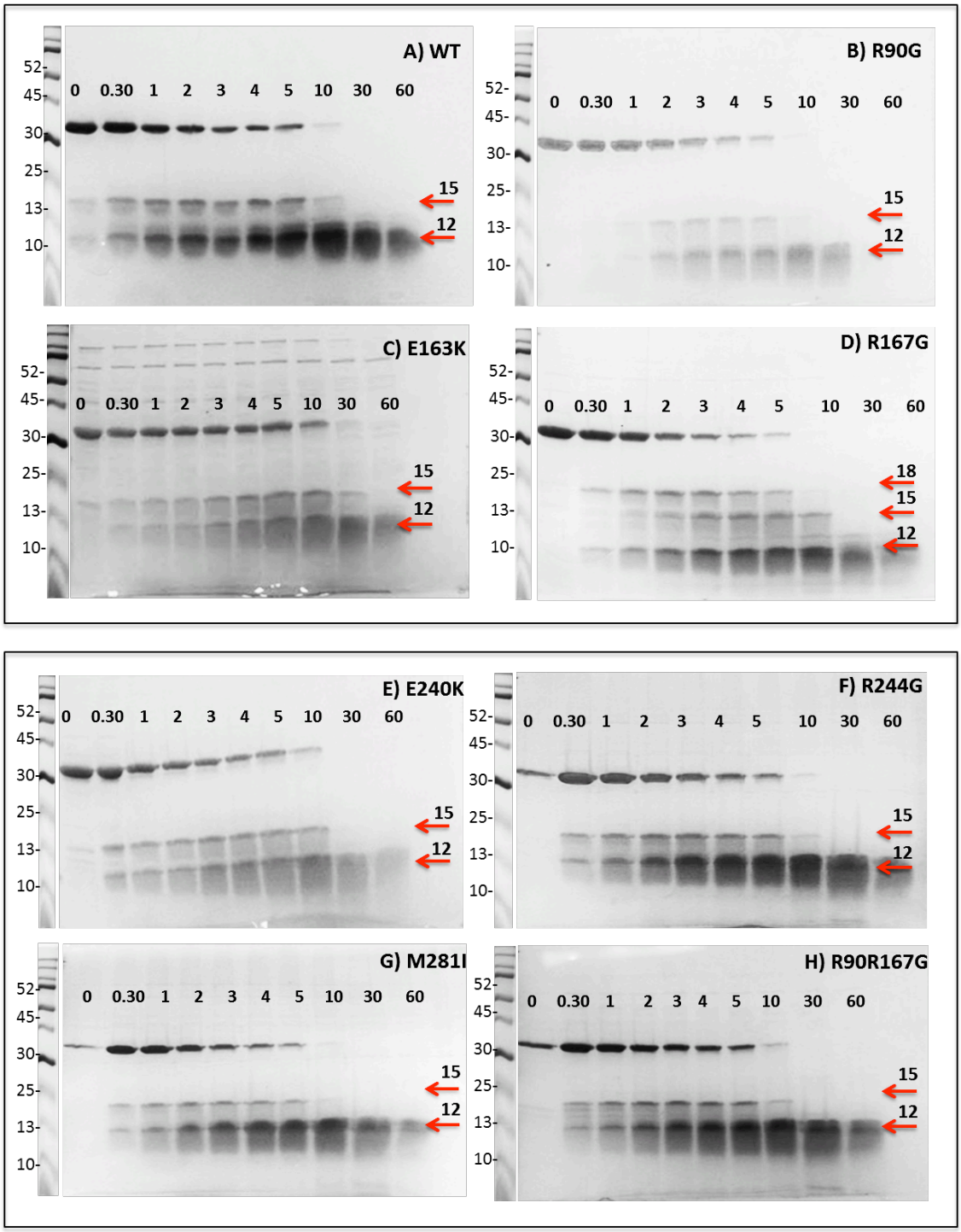

Figure 4.5: 12 % SDS gel for Tpm trypsin digestion result

The figure shows the 12% SDS page of tropomyosin 0.5 mg /ml was digested with 0.2 mg/ml trypsin in 10mM HEPES pH 7.5, 0.1 mM NaCl, 5mM MgCl2 and 10 mM β mercaptoethanol at 26C with time interval.

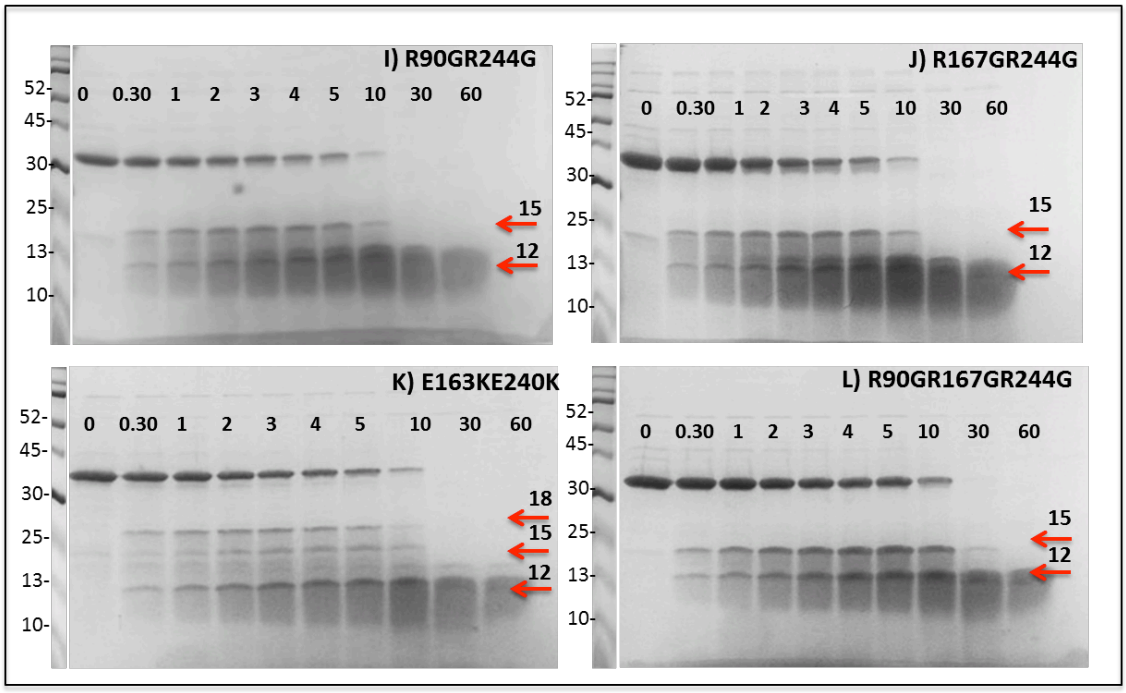

Figure 4.6: 12 % SDS gel for Tpm trypsin digestion result

The figure shows the 12% SDS page of tropomyosin 0.5 mg /ml was digested with 0.2 mg/ml trypsin in 10mM HEPES pH 7.5, 0.1 mM NaCl, 5mM $MgCl_2$ and 10 mM β mercaptoethanol at 26C with time interval.

The presence of actin in excess should protect the Tpm from being digested by trypsin. The aim of this experiment is to test the long-range effect of the mutations on Tpm digestion by trypsin in the presence of actin. The WT in figure 4.7 showed a clear resistance to tryptic digestion in the presence of actin as Tpm was not digested up to 30 minutes after addition of trypsin and only produced a faint band of 15 KDa later. However, TpmR90G, TpmR167G and TpmE163K showed different digestion pattern in which the Tpm was digested into three bands yielding around 27 KDa, 15 KDa and 12 KDa. The results obtained with mutations E240K, M281I and R90GR167G (figure 4.7) and R167GR244G, E163KE240K and R90GR167GR244G (figure 4.8) exhibited digestion product bands around 27 KDa, 15 KDa and 12 KDa in contrast to the results obtained in the absence of actin where Tpm was not digested. While digestion of Tpm R244G gave rise to bands around 27 KDa and 12 KDa (figure 4.7). The R90GR244G did show similar behaviour to the other mutations exhibiting bands yielding around 27 KDa, 15 KDa and 12 KDa.

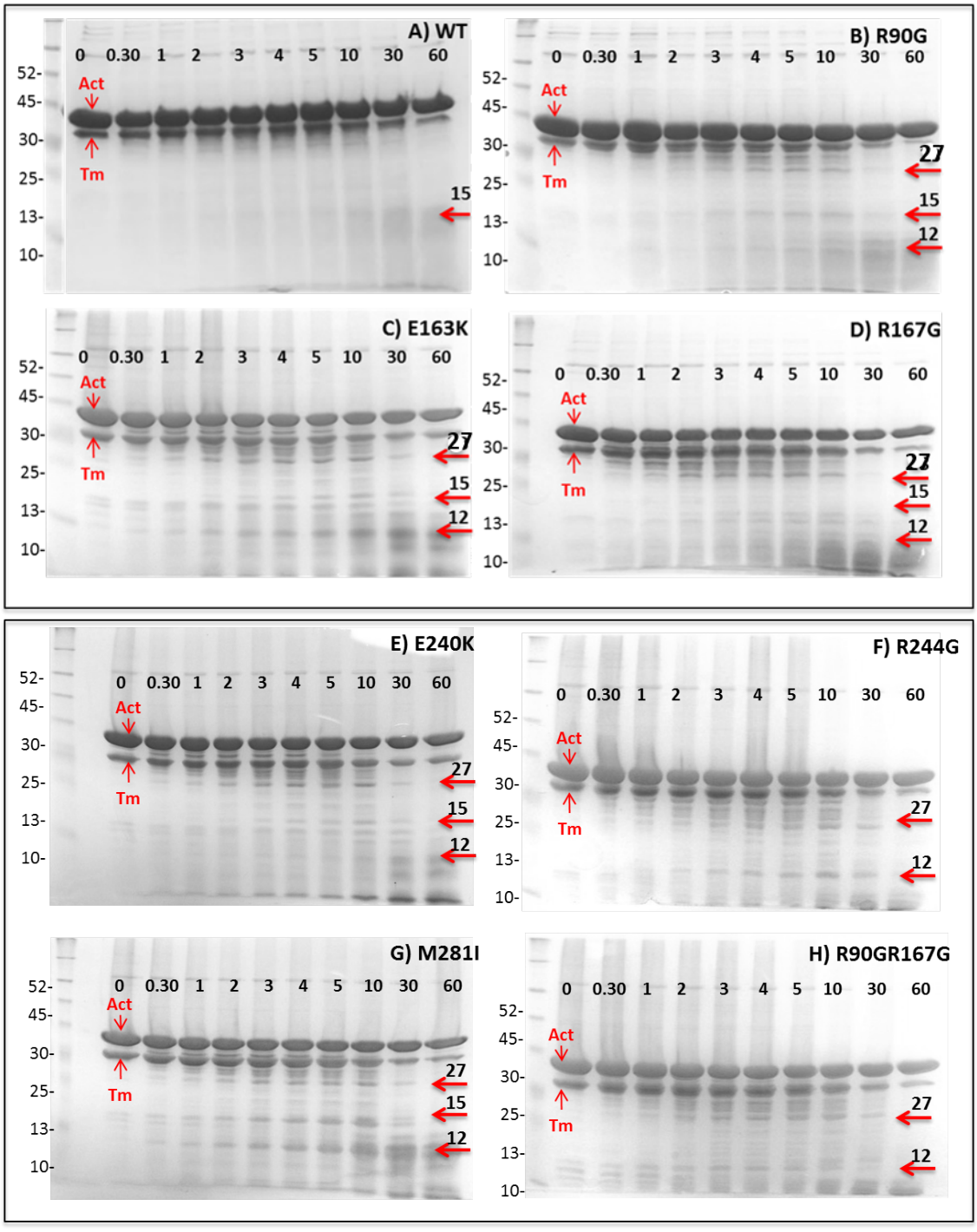

Figure 4.7: 12 % SDS Tpm-Actin trypsin digestion results

The figure shows the 12% SDS page of tropomyosin 0.3 mg /ml was mixed with 1.5 mg/ml actin and digested with 0.5 mg/ml trypsin in 10mM HEPES pH 7.5, 0.1 mM NaCl, 5mM $MgCl_2$ and 10 mM β mercaptoethanol at 26°C with time interval.

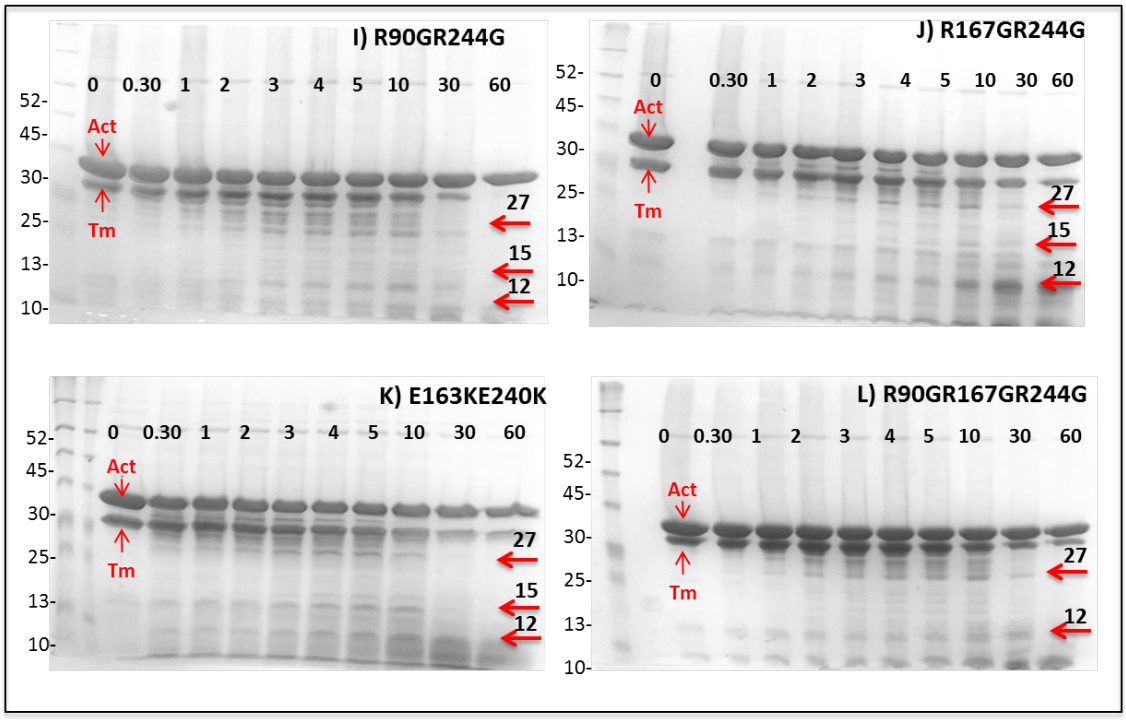

Figure 4.8: 12 % SDS Tpm-Actin trypsin digestion results

The figure shows the 12% SDS page of tropomyosin 0.3 mg /ml was mixed with 1.5 mg/ml actin and digested with 0.5 mg/ml trypsin in 10mM HEPES pH 7.5, 0.1 mM NaCl, 5mM $MgCl_2$ and 10 mM β mercaptoethanol at 26°C with time interval.

4.2.4 Functional investigations of the effect of tropomyosin mutations on the actomyosin ATPase

The tropomyosin and troponin are actomyosin regulatory proteins of the actomyosin ATPase in a calcium dependent manner. In the absence of Ca^{2+}, the Tpm-Tn complex inhibits the actomyosin ATPase while in the presence of Ca^{2+} the Tpm-Tn complex is able to activate the actomyosin ATPase.

The assays were conducted to observe the effect of mutations on Tpm induced inhibition and activation of actomyosin ATPase in the presecnce and absence of calcium.

Activation and inhibition of myosin ATPase activity rates were measured using 10 µM actin, 2 µM Tpm, 2 µM S1, Tn 0-3 µM, 0.5 mM $CaCl_2$ and 1 mM EGTA in AOSB (10 mM Mops, 0.5 mM DTT, 3.5 mM $MgCl_2$ and 0.5mM NaN_3 at pH 7.2) in 30 °C. For both activation and inhibition, the actomyosin ATPase activity in the absence of Tn was used as the reference level and is set at 100%.

This experiment was done for Tpm wild type and mutants and the average of three experiments was plotted (figure 4.9). Wild type tropomyosin was used as a control. The wild type tropomyosin showed an activation with increasing concentration of Tn in presence of Ca^{2+} and almost 50 % activation was achieved within 1.5 µM Tn (figure 4.9). On the other hand, in the absence of Ca2+, wild type Tpm showed clear inhibition with increasing Tn concentration (figure 4.9). R90G and R167G showed lower activation but similar inhibition to wild type Tpm (figure 4.9). E163K showed steady low activation and but no inhibition. E240K showed slightly lower activation than the wild type but showed less inhibition compared to the wild type. R244G and M281I displayed a defect in both activation and inhibition compared to the wild type (figure 4.10).

The R90GR167G are located within the same region in the repeated heptad (*f*) position and showed low activation in comparison to wild type (figure 4.11). The inhibition for R90GR167G seems to be faster at the initial concentration but remains steady afterword. The R90GR244G is showing a clear reduction in the activation and in the inhibition. The R167GR244G, E163KE240K and R90GR167GR244G are behaving almost similarly in which all reduced the activation compare to the wild type. In the inhibition, all three mutations showed similar behaviour to each other in which they all reduced the inhibition compared to the wild type.

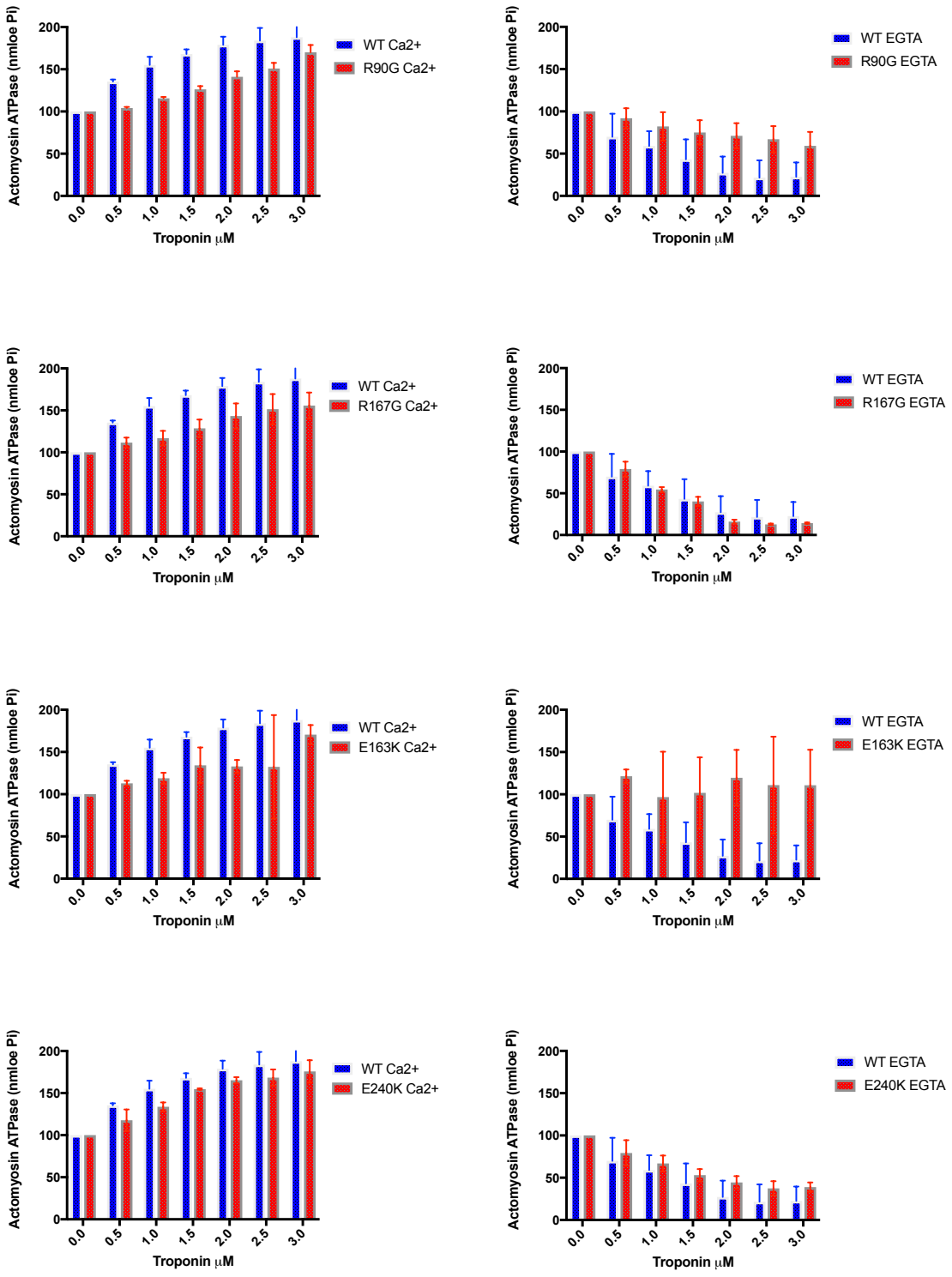

Figure 4.9: Activation and Inhibition of myosin ATPase activity by varying Tn

Effect of TPM1 mutations on activation and inhibition of myosin S1 ATPase activity by interaction of Tn with actin-Tpm complexes in the presence and absence of Ca^{2+}. The blue columns are WT while Red columns are mutations. Conditions actin 14 µM TPM 3 µM S1 2 µM and Tn 0-3 µM 0.5 mM $CaCl_2$ and 0.3 mM EGTA in AOSB (10 mM Mops, 0.5 mM DTT, 3.5 mM $MgCl_2$ and 0.5mM NaN_3 at pH 7.2) in 30°C.

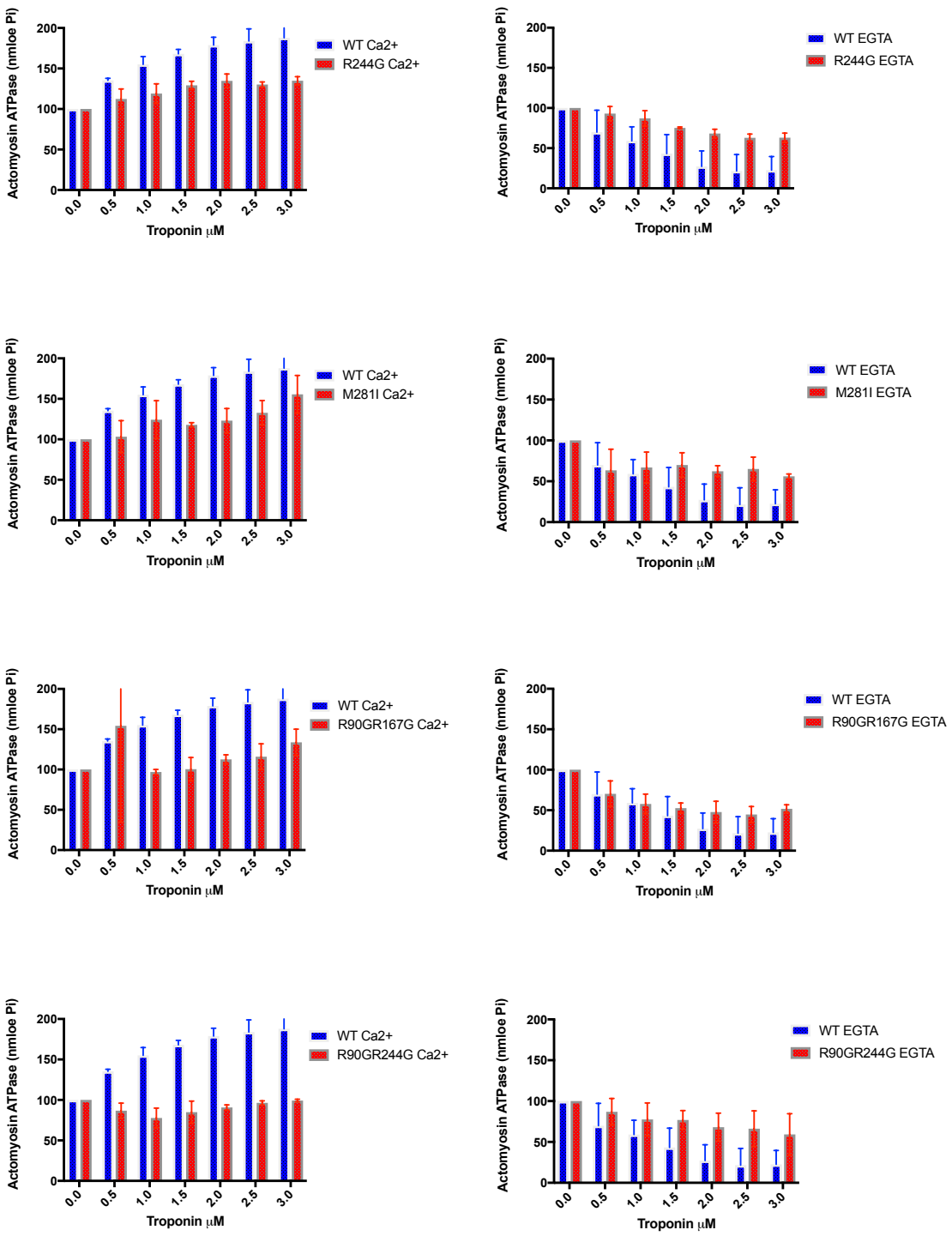

Figure 4.10: Activation and Inhibition of actomyosin ATPase activity by varying Tn for the different Tpm variants.

Effect of TPM1 mutations on activation and inhibition of myosin S1 ATPase activity by interaction of Tn with actin-Tpm complexes in the presence and absence of Ca^{2+}. Conditions actin 14 μM TPM 3 μM S1 2 μM and Tn 0-3 μM 0.5 mM $CaCl_2$ and 0.3 mM EGTA in AOSB (10 mM Mops, 0.5 mM DTT, 3.5 mM $MgCl_2$ and 0.5mM NaN_3 at pH 7.2) in 30°C.

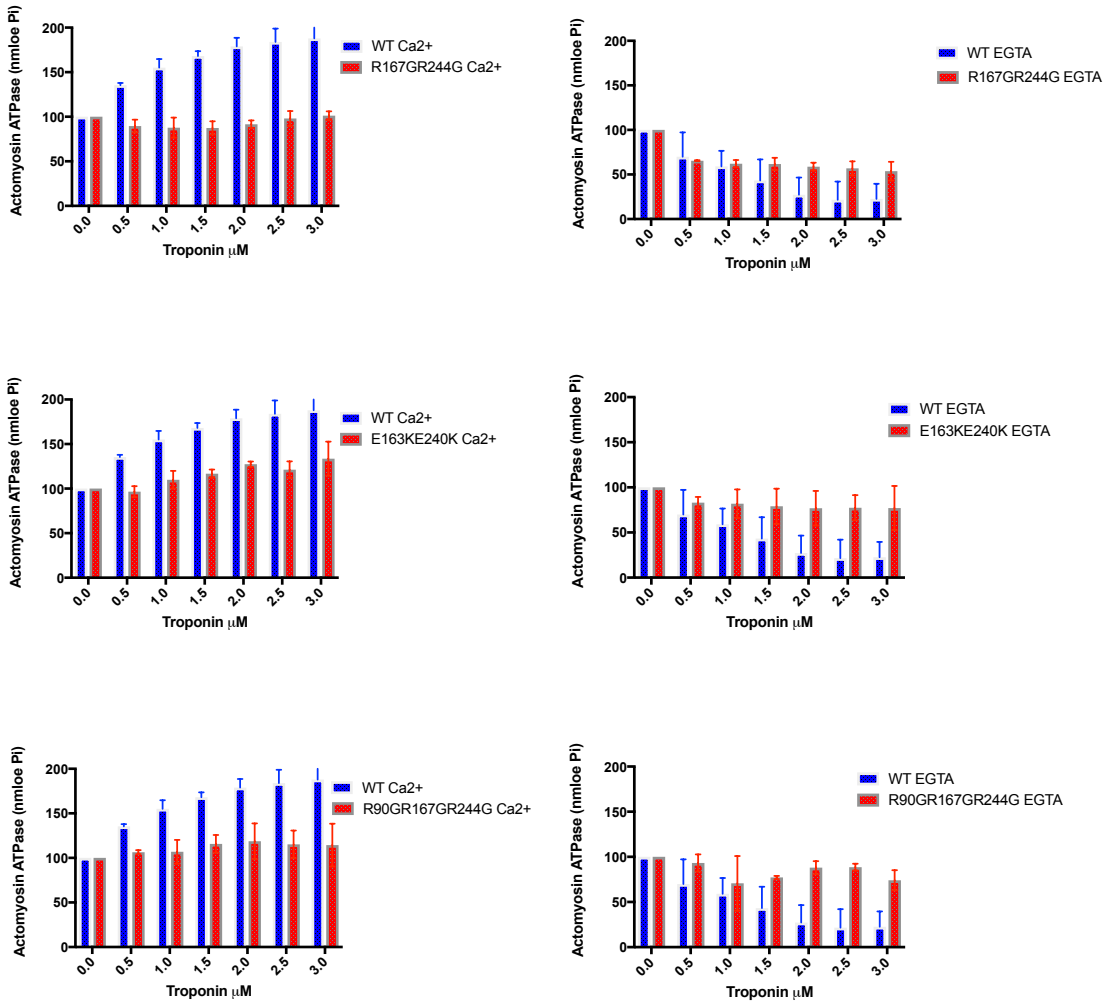

Figure 4.11: Activation and Inhibition of myosin ATPase activity by varying Tn

Effect of Tpm1 mutations on activation and inhibition of myosin S1 ATPase activity by interaction of Tn with actin-TPM complexes in the presence and absence of Ca^{2+}. Conditions actin 14 μM TPM 3 μM S1 2 μM and Tn 0-3 μM 0.5 mM $CaCl_2$ and 0.3 mM EGTA in AOSB (10 mM Mops, 0.5 mM DTT, 3.5 mM $MgCl_2$ and 0.5mM NaN_3 at pH 7.2) in 30°C.

To summarise, all Tpm mutations except (R90G, E163K and E240K) showed a clear reduction in the activation of the actomyosin ATPase in the presence of Ca^{2+} compared to the wild type Tpm (figure 4.12, top panel). On the other hand, all mutations except (R167G and E240K) display reduced ability to inhibit the actin activation of myosin ATPase in the absence of Ca^{2+} compared to the wild type Tpm (figure 4.12, bottom panel).

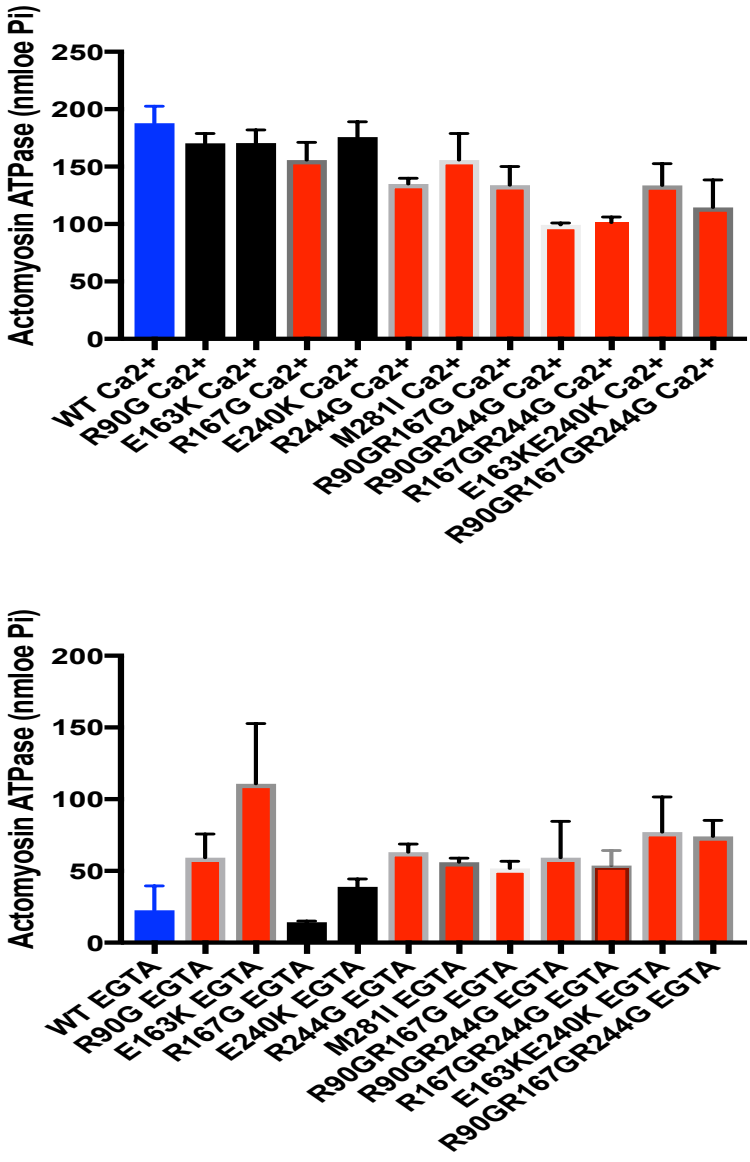

Figure 4.12: summary of Tpm mutations on ATPase

The figure shows the summary of the effect of Tropomyosin mutations on the activation of ATPase in presence of Ca^{2+} top. While the inhibition of ATPase in presence of EGTA showed in the bottom.

4.2.5 Investigation of the effect of the effect of Tpm mutations on its secondary structure using Circular dichroism

The secondary structure of a protein can be evaluated using a fast and accurate spectroscopic method: Circular dichroism (CD). The CD measures the difference of absorption of right and left handed circularly polarized light (Greenfield, 2006). The CD method allows an estimation of the secondary structure of proteins and establish the proportion of α–helices, β-sheet or random coil. We aimed to measure the effect of Tpm mutations overall Tpm secondary structure. The WT was used as a reference for comparison with the mutants that may induce a change in protein structure.

The CD experiments were performed using Circular Dichroism Spectrometer Chirascan with a cell path length of 0.1 cm at 25°C in 10 mM sodium phosphate, pH 7.0 and 0.3 M NaF solution. The experiment was done using a range of wavelengths between 190-260 nm in the far UV region at a resolution of 1 nm and speed 50 nm/minute and a bandwidth 1 nm. Three scans were averaged for the all Tpms (wild type and mutants) concentration used was 5 µM.

Tropomyosin is a coiled coil composed of two alpha helices and its CD spectra is shown in figure (4.7). The WT spectrum is a replicate of the typical CD spectra for a typical 100% alpha helical protein with 2 minima at 208 nm and 222 nm. Therefore, the WT was used as a reference to compare the effect of Tpm mutations on its secondary structure. All mutations showed similar spectra compared to the WT spectrum. However, there were differences in the amplitude of the CD signal most likely due to the variation in protein concentrations. The spectra were then analysed by a CD data analysis software to estimate the percentage of secondary structure elements which are shown in table (4.2). The outcomes of the CD spectra confirmed that the structure of Tpm was not substantially affected by the mutations.

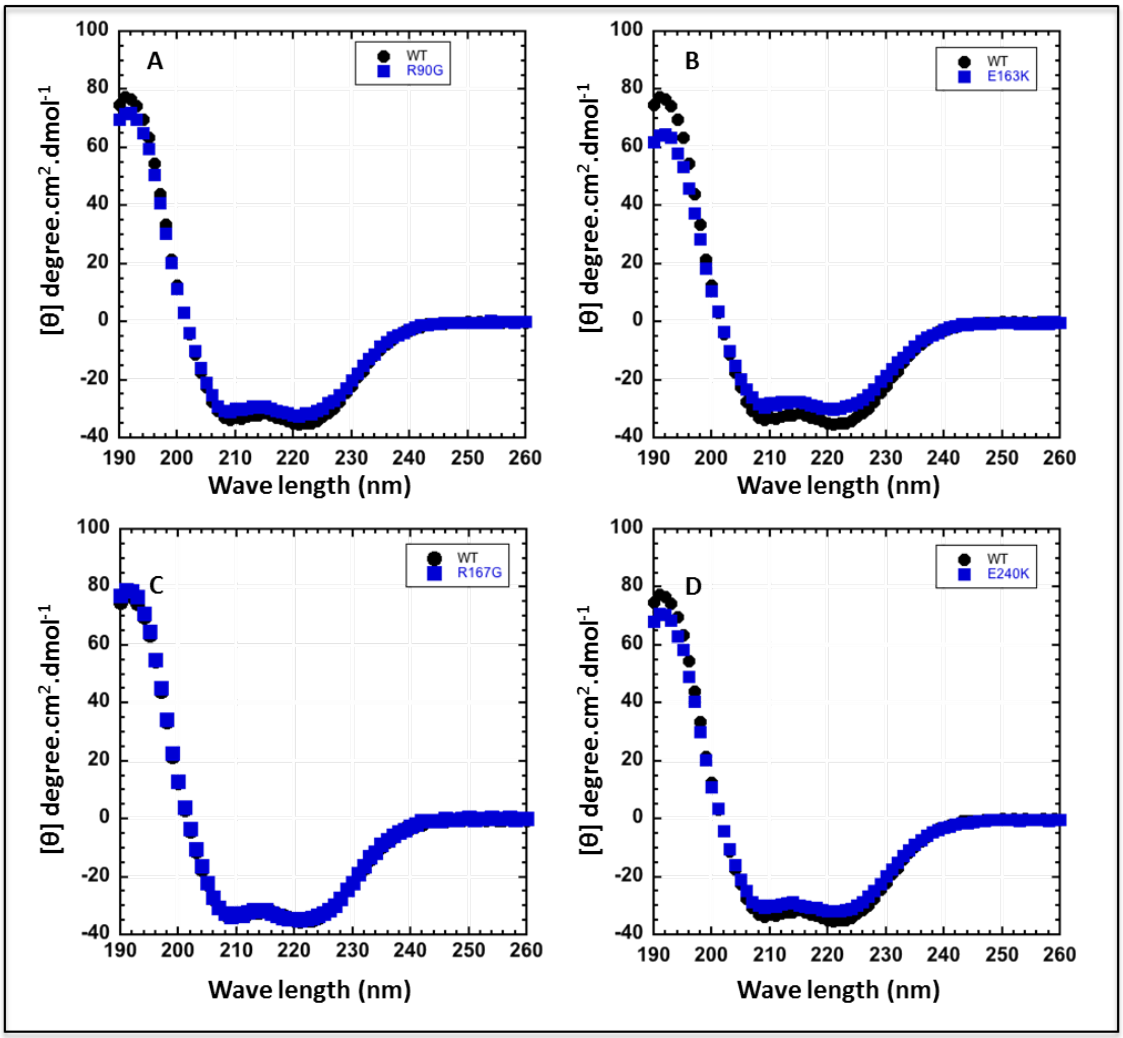

Figure 4.13: Circular Dichroism spectra of Tpm WT and mutants

CD spectra of the Tpm using the different Tpm mutants (Panel AWT and R90G; Panel B WT E163K; Panel C WT R167G, and Panel D WT and E240K) were measured in the presence of 10 mM NaH2PO4, pH 7.0 and 0.3 M NaF. All samples were used at a concentration of 5µM.

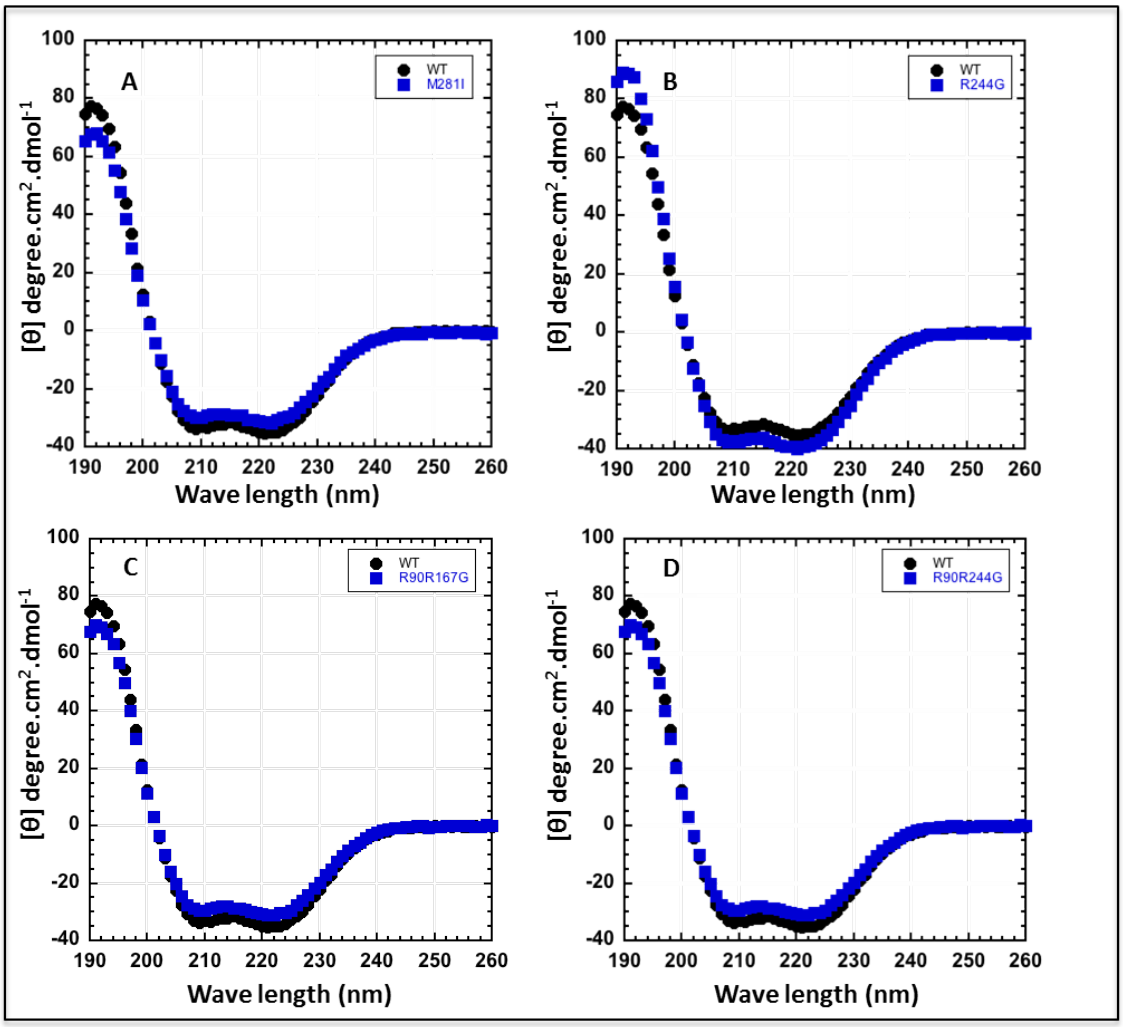

Figure 4.14: Circular Dichroism spectra of Tpm WT and mutants

CD spectra of the Tpm using the different Tpm mutants (Panel: WT and M281I,; Panel B WT and R244G ,; Panel C: Wt and R90GR167G, and Panel D: WT and R90GR244G) were measured in the presence of 10 mM NaH2PO4, pH 7.0 and 0.3 M NaF. All samples were used at a concentration of 5 µM.

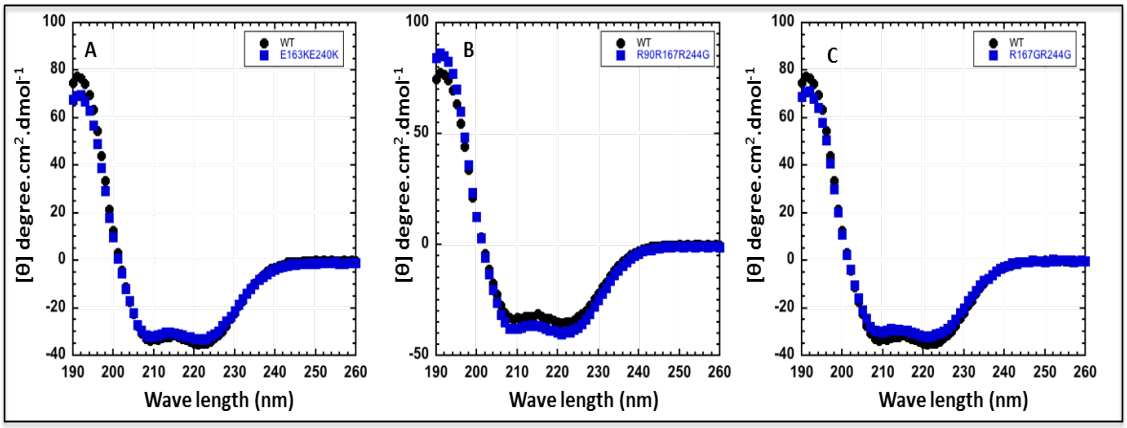

Figure 4.15: Circular Dichroism spectra of Tpm WT and mutants

CD spectra of the Tpm using the different Tpm mutants (Panel A: WT and R167GR244G , Panel B: WT and E163KE240K and Panel C: WT and R90GR167GR244G) were measured in the presence of 10 mM NaH2PO4, pH 7.0 and 0.3 M NaF. All samples were used at a concentration of 5 µM.

Table 4.1: Estimation of alpha helical and beta strands in the tropomyosin secondary structure

Protein	α helix 190-260	β sheet 190-260
WT	99.6%	3.1
R90G	99.6%	3.1
R167G	99.6%	3.1
E163K	99.6%	3.2
E240K	99.6%	3.2
R244G	99.6%	3.0
M281I	99.6%	3.2
R90GR167G	99.6%	3.1
R90GR244G	99.6%	3.2
R167GR244G	99.6%	3.1
E163KE240K	99.6%	3.2
R90GR167GR244G	99.6%	3.1

The change in molar ellipticity at 222 nm induced by increasing temperature was used to measure the thermal stability of tropomyosin using a buffer contains 0.3 M NaF, 10 mM sodium phosphate, pH 7.0. The measurements were collected at 1.0 °C intervals between 15-80 °C.

The normalised plots of ellipticity versus temperature were used to evaluate Tpm mutations effect on the temperature induced denaturation and the denaturation mid-point temperatures were calculated in table 4.2. The unfolding curve midpoint for the WT was 47.0 +- 0.2. The mutations R90G and R167G in figure 4.7 showed a reduction in the unfolding curve midpoint to 45.3 +- 0.2 and 45.0 +- 0.2 respectively while the E163K showed an increase in the unfolding curve midpoint to 48.4 +- .02. On the other hand, TpmE240K, R244G, M281I and R90GR167G mutants showed almost similar values 47.3 +- 0.02, 46.8 +- 0.2, 46.9 +-0.2 and 47.2 +- 0.2 respectively to the WT. Mutations R90GR244G and R167GR244G showed clear shift in the curves and a decrease in the unfolding curve midpoint with values of 43.3 +- 0.2 and 44.5 +- 0.2. The last two mutations E163K and R90GR167GR244G showed also a reduction in the the unfolding curve midpoint with values of 46.0 +- 0.2 and 46.5 +-0.2 respectively. Overall, some of the mutations did show an impact on the secondary structure thermal stability compared to the WT.

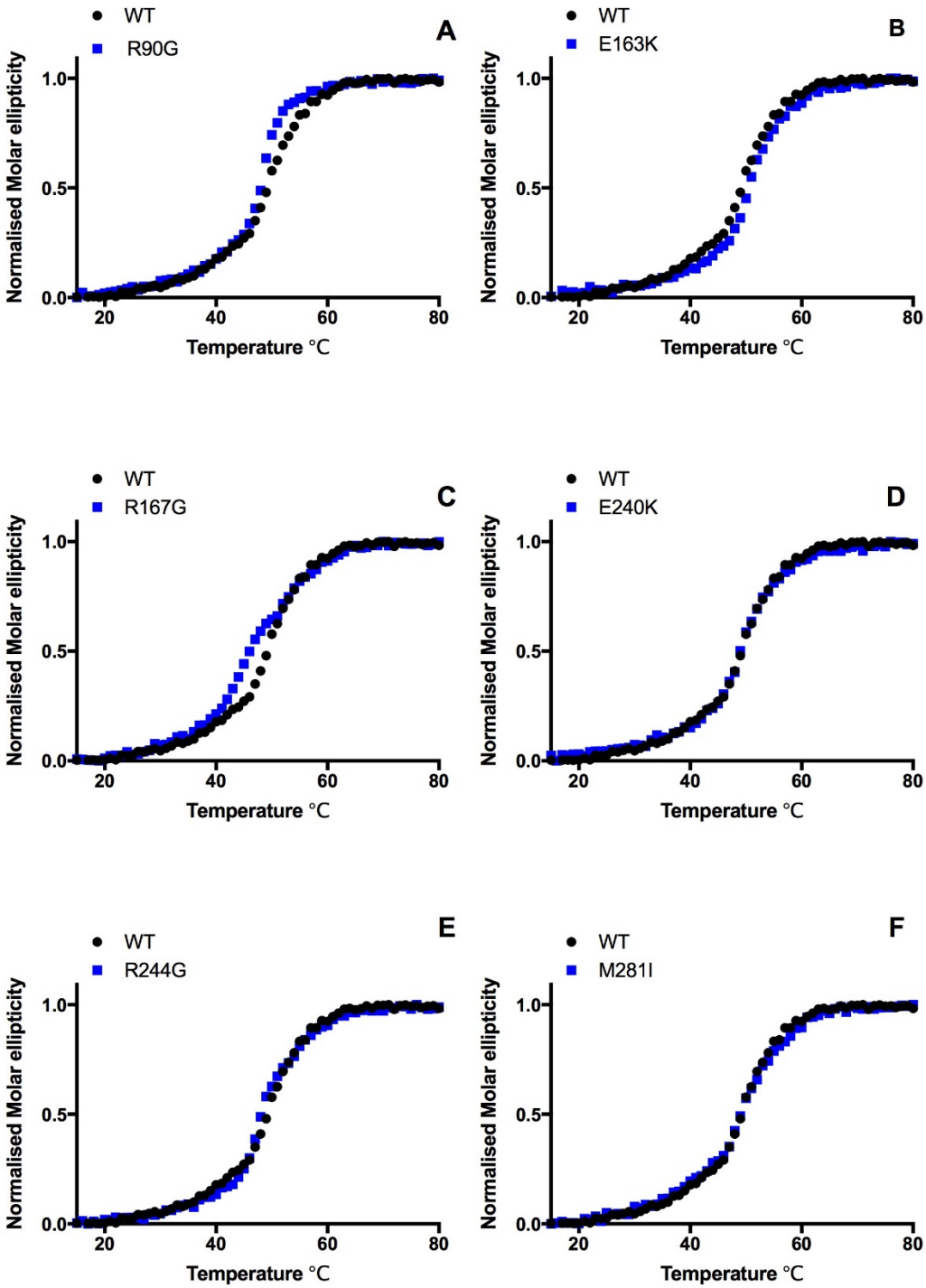

Figure 4.16: Thermal denaturation of Tpm WT and mutants

The graph illustrates Thermal denaturation spectra of (A) WT and R90G (B) WT and E163K (C) WT and R167G (D) WT and E240K (E) WT and R244G (F) WT and M281I. All samples were in 10 mM NaH2PO4, pH 7.0 and 0.3 M NaF. It was monitored at 222 nm between 15-80 °C at a rate of 1 °C/min.

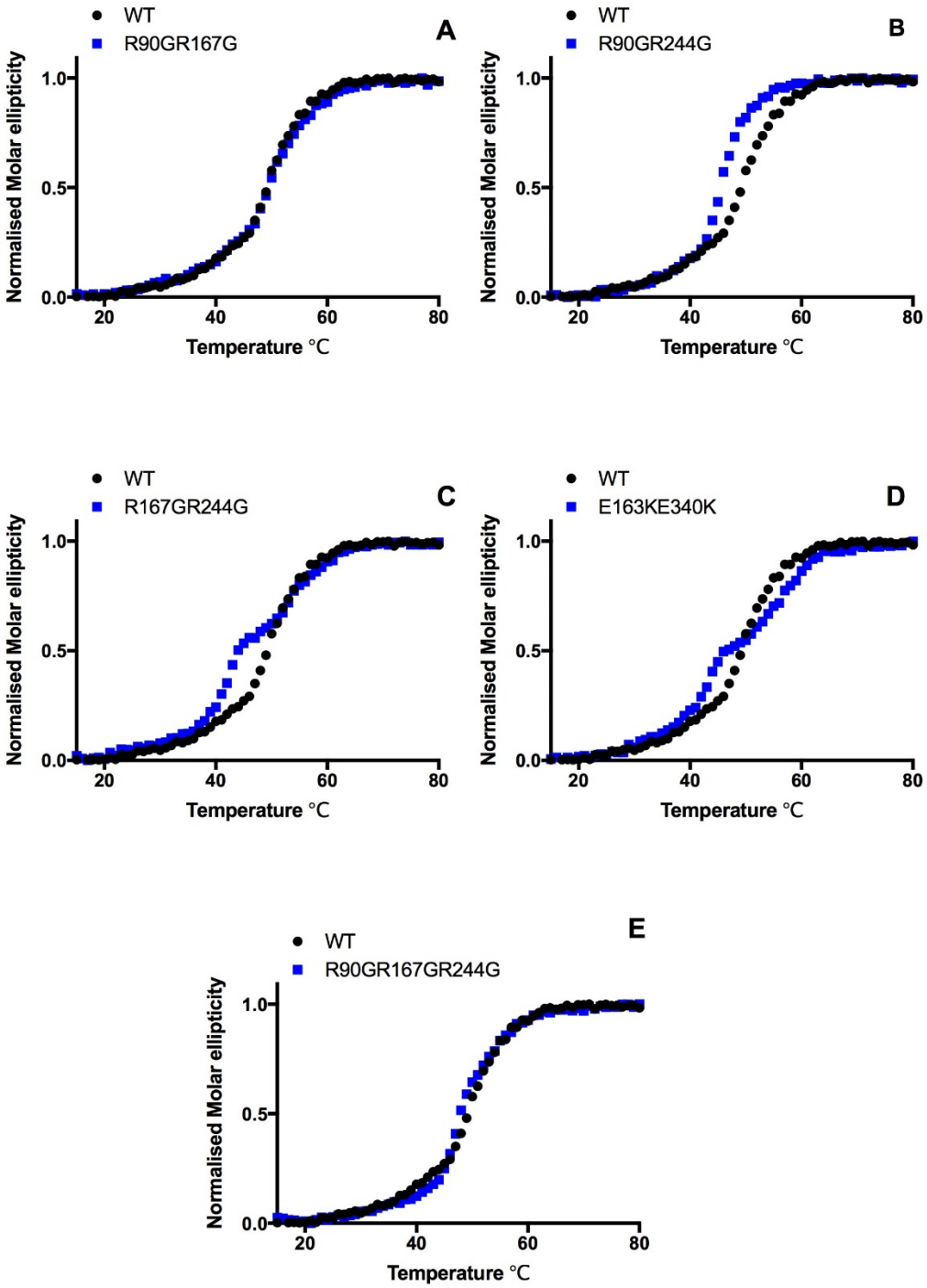

Figure 4.17: Thermal denaturation of Tpm WT and mutants

The graph illustrates Thermal denaturation spectra of (A) WT and R90GR167G (B) WT and R90GR244G (C) WT and R167GR244G (D) WT and E163KE240K (E) WT and R90GR167GR244G. All samples were in 10 mM NaH2PO4, pH 7.0 and 0.3 M NaF. It was monitored at 222 nm between 15-80 °C at a rate of 1 °C/min.

Table 4.2: Mid-point melting temperatures of tropomyosin mutations

Protein	Melting point
WT	47.0 +- 0.2
R90G	45.3 +- 0.2
R167G	45.0 +- 0.2
E163k	48.4 +- 0.2
E240K	47.3 +- 0.2
R244G	46.8 +- 0.2
M281I	46.9 +- 0.2
R90G/R167G	47.2 +- 0.2
R90G/R244G	43.3 +- 0.2
R167G/R244G	44.5 +- 0.3
E163K/E240K	46.0 +- 0.3
R90G/R167G/R244G	46.5 +- 0.2

For a better visualisation of the impact of mutations in Tpm on the thermal unfolding, First-derivative graphs were generated from the data obtained in the temperature dependence experiments (figure 4.18-20). It can be seen that the mutations R90G, E163K, E240K, M281I and R90GR167G are not different compared to the wild type. However, R167G, R244G, R90GR244G and R90GR167GR244G did show a clear difference in the melting point which shifted the curve to lower temperature. Interestingly, the R167GR244G and E163KE240K did show two peaks, the first one at around 40 °C and the second one at around 54-56 °C. Each peak corresponds to a transition. Wild type Tpm and Tpm mutants R90G, E163K, E240K, M281I, R167G, R244G, R90GR244G and R90GR167GR244G showed a single unfolding transition while R167GR244G and E163KE240K showed two unfolding transitions. This show that the stability of Tpm is different for different mutations.

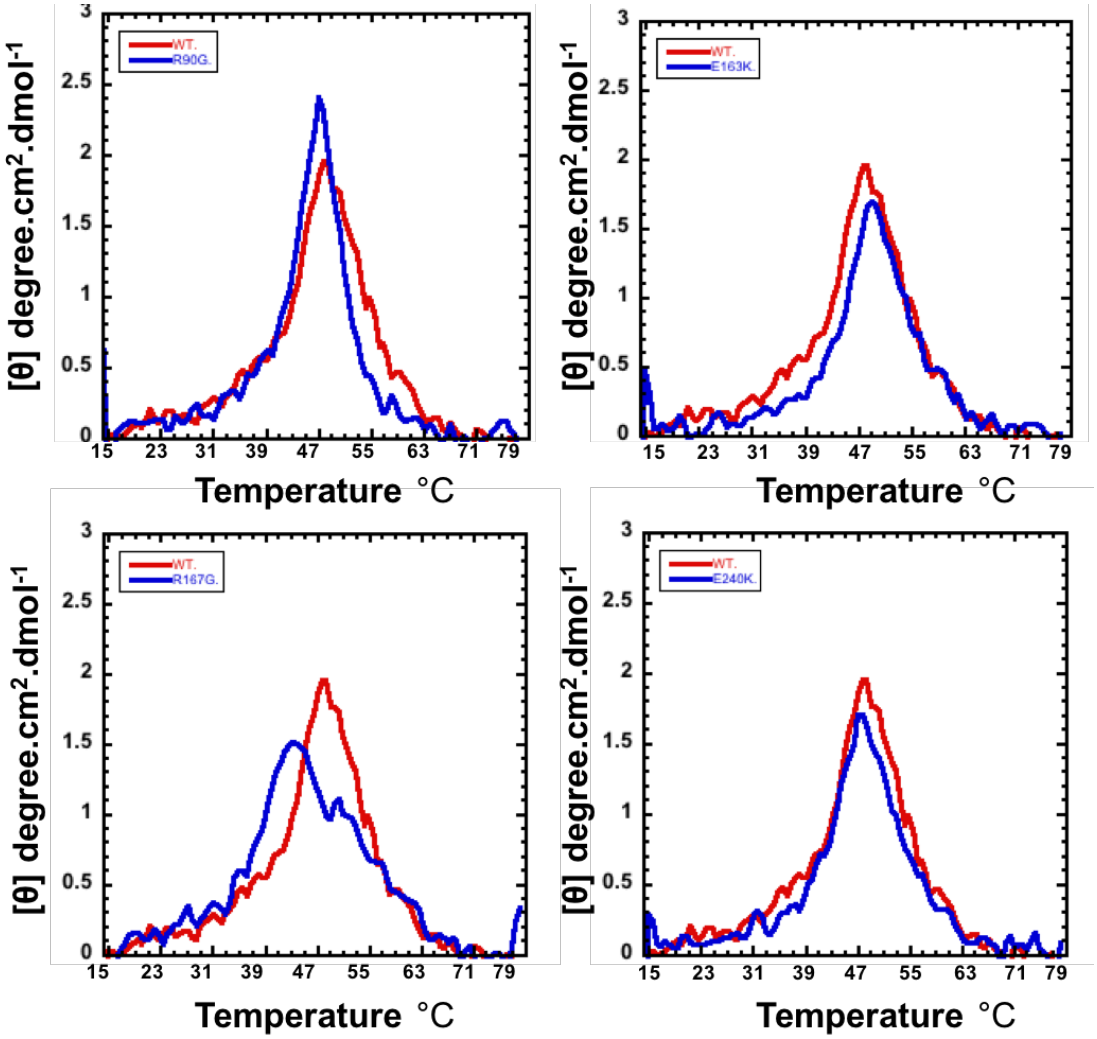

Figure 4.18: First- derivative graphs of temperature dependence experiment

The figure shows the First-derivative graphs of the WT and the mutations using the data obtained from temperature dependence.

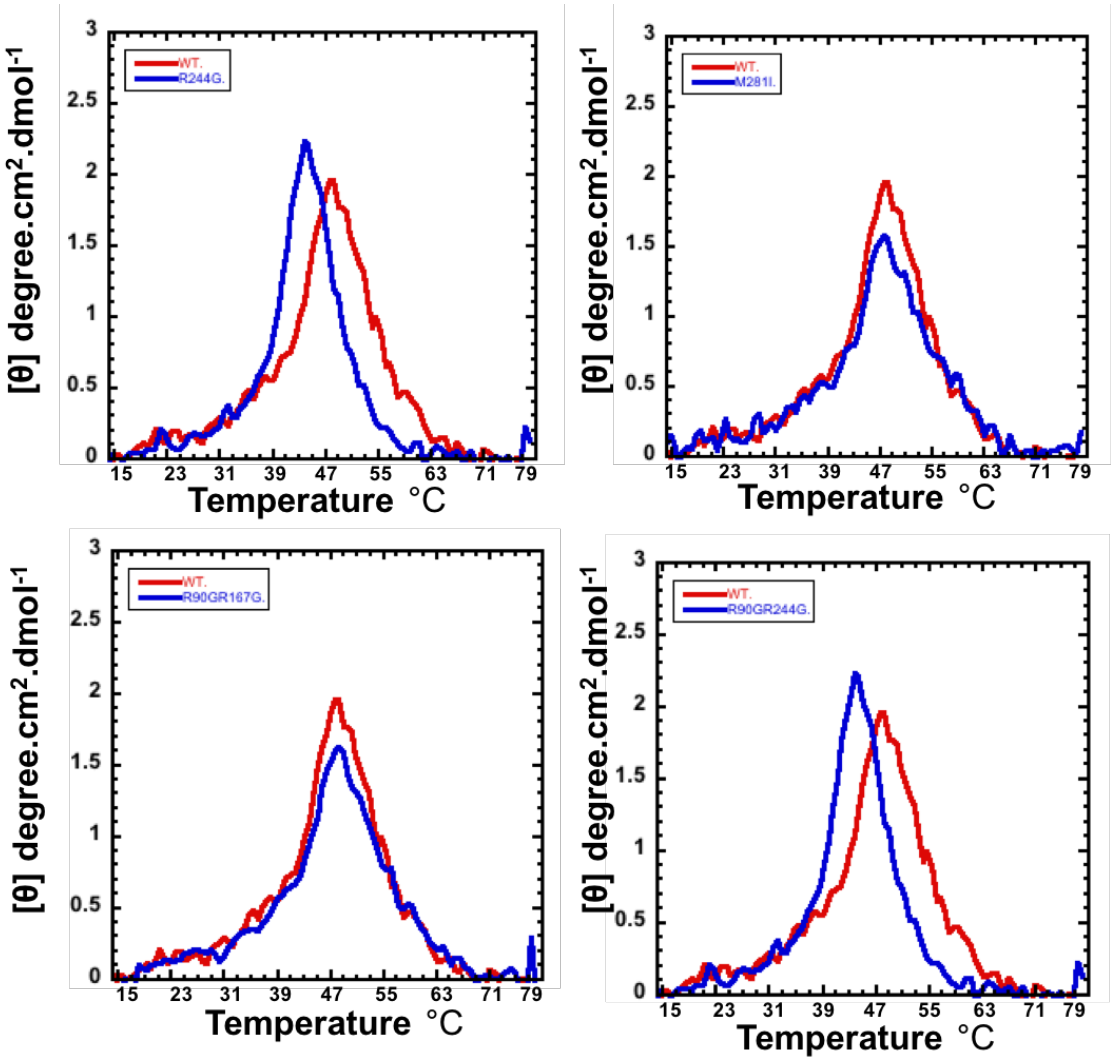

Figure 4.19: First- derivative graphs of temperature dependence experiment.

The figure shows the First-derivative graphs of the WT and the mutations using the data obtained from temperature dependence.

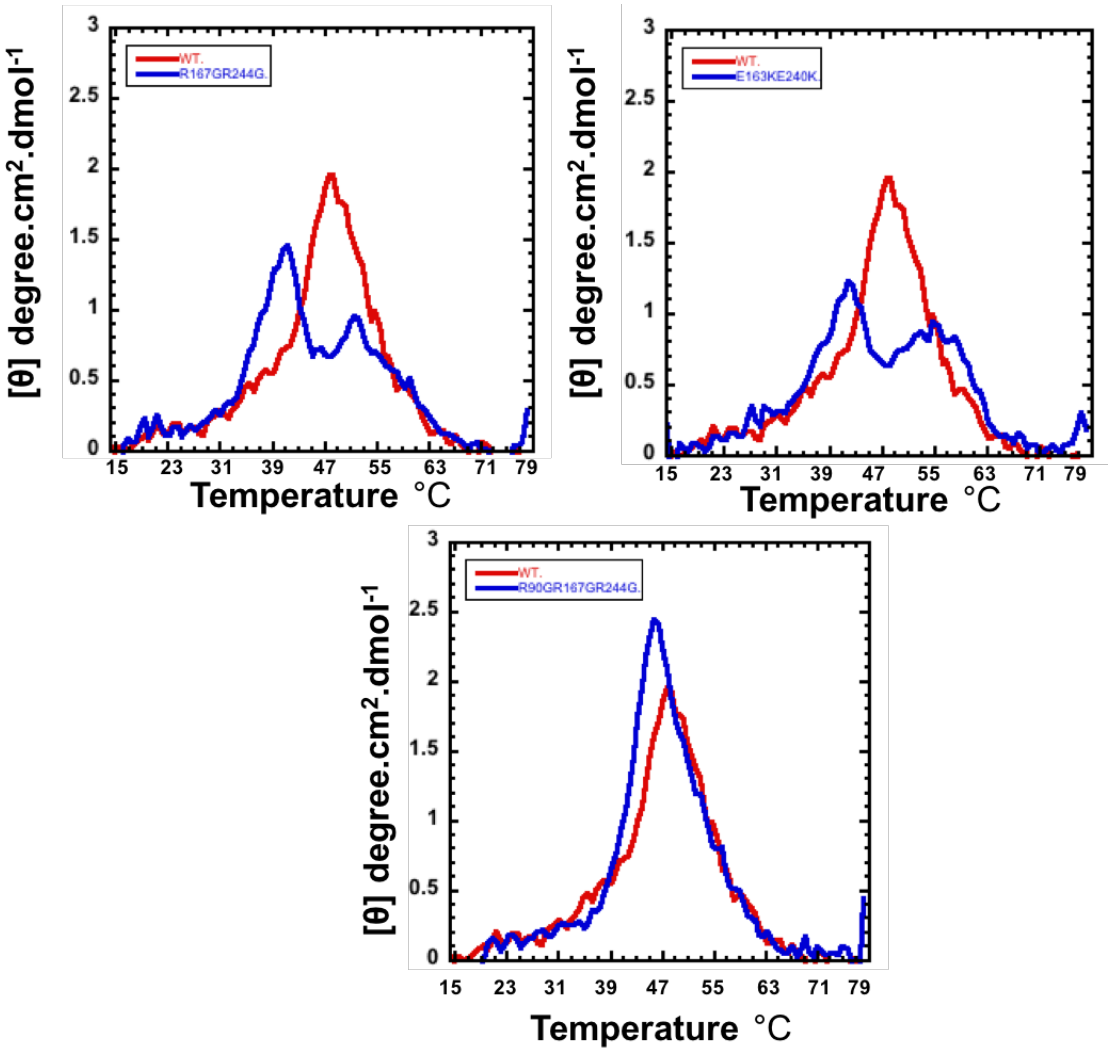

Figure 4.20: First- derivative graphs of temperature dependence experiment.

The figure shows the First-derivative graphs of the WT and the mutations using the data obtained from temperature dependence.

4.3 Discussion

The aim of this chapter was to establish a reliable method for the expression and purification of tropomyosin mutants capable of delivering reasonable amounts of highly pure tropomyosin mutants. Another aim was to assess their secondary structure by circular dichroism and their function by an actomyosin ATPase assay. The tropomyosin cDNA was cloned into the pLEICS-05 vector (a vector designed for high yield protein expression) with addition of Ala–Ser at the N-terminus to mimic the acetylation. We cloned and expressed Tpm wild type and 11 mutants. The tropomyosin mutants were purified using fractionation by ammonium sulphate and two different chromatography steps (DEAE and hydroxylapatite CHT) to get pure protein as seen in figure (4.3). It was possible to obtain around 16-20 mg of highly purified tropomyosin from 2 litres of *E.coli* culture for each of the Tpm variants. These quantities are sufficient for biochemical and biophysical characterisation. The following tropomyosin single amino acid mutants were produced (R90G, E163K, R167G, E240K, R244G and M281I). We have also introduced double and triple mutations to the Tpm sequence at the same position of heptad repeat (*f*) (R90GR167G, R90GR244G, R167GR344G and R90GR167GR244G) and at (*b*) (E163KE240K). The rationale for the double and triple mutants is to disrupt as many individual sites as possible in the one Tpm- seven actin monomers binding sites unites. Also, their position was found to be conservative among different isoforms.
the actomyosin ATPase (although with some differences that may be due to the mutations). Thus, we can characterise fully their impact on the biochemical, kinetic and functional properties of tropomyosin.

4.3.1 Effect of Tpm1 mutations on the structure of tropomyosin

Circular dichroism was used to determine the effect of the mutation on tropomyosin secondary structure. The spectra of all proteins showed that WT and all other mutants were 100% α-helical suggesting that the introduced mutation do not cause any gross change to the helical coiled coil structure of tropomyosin. A small variation in the amplitude of the spectra is likely due to inaccuracy of measurements of protein concentrations. The CD experiments showed that several Tom mutants changed the

thermal unfolding mid point as shown clearly in the first derivative graphs. The mutations which were substituted from Arginine, a polar amino acid, to glycine, a nonpolar (uncharged) amino acid may have slightly disturbed the stability of the coiled coil as seen by the small decrease in the mid curve melting point. A decrease in the thermal unfolding mid point mutations for (R90G, R167G, R244G R90GR244G and R90GR167GR244G) have decreased the tropomyosin stability.

4.3.2 Trypsin digestion

In tropomyosin heptad repeat, position (*a)* and (*d)* drive inter-helical hydrophobic interactions that provide stability to the coiled coil. The positions are primarily occupied by Leu, Ala, Leu, Val, Tyr, and Met. However, in both α - and β –Tm At position 137 in *d* position an alternative Asp is present. The instability of Tpm increased because of the presence of Asp-137 during tryptic cleavage at Arg-133 (Sumida et al., 2008). A slight increase in local flexibility was seen in a molecular dynamics simulation where Asp-137 mutated to a canonical Leu (Nirody et al., 2010).

The trypsin digestions occur at Arg-133 (Ly and Lehrer, 2012). The experiment was performed in presence and absence of Actin. The Tpm mutants showed variations in the rate and pattern of cleavage in the absence of actin filaments when compared to the wild type. The wild type showed similar pattern of cleavage as obtained by (Ly and Lehrer, 2012) (Conbversion of Tpm to ~ 12-15 kDa). However, some of the mutation have increased the rate of cleavage like (R90G and R167G) and the latter has yielded a band ~ 18 kDa. The distance between the R167G and R133 is about 34 residues and it consequently the observed change is likely due to long range change in conformation. It is possible that the substituted residue from a large positively charged aminoacid to a smaller glycine aminoacid has disturbed the stability of the coiled coil and affected the local structure around Arg 133. This change is not always the same since substitution of other residues at other locations from Glutamic acid to Lysine (acidic to basic amino acid) produced a different effect (a decreased rate of cleavage which suggest an increased stability).

The presence of actin was to protect Tpm from cleavage and the wild type showed a much stronger resistance to cleavage due to the binding to actin. However, the mutation R90G and R167G were the least protected by actin and that led to fast rate of cleavage compared to the wild type. The reason could be a reduction in interaction with actin.

4.3.3 Effect of Tpm1 mutations on the steady state actomyosin ATPase

To determine the mutations' effect on thin filaments functioning, the ATPase assays were carried out in the presence of troponin. The wild type has showed a clear activation and inhibition of ATPase. The troponin complex mainly binds tropomyosin by its TnT subunit. All tropomyosin mutations except (R90G, E163K and E240K) affected the activation of actomyosin ATPase and reduced it to the level of actin. Single mutations (R167G and E240K) did not affect the ability of Tpm-Tn to inhibit the actomyosin ATPase in the absence of Ca^{2+}. Double mutation E163KE240K and triple mutation R90GR167GR244G reduced the ability of the tropomyosin-troponin complex to inhibit the actomyosin ATPase in the absence of Ca^{2+}. The mutations likely affected the ATPase due to their location which may have interfered with TnT binding site. These changes in activation and/or inhibition of the actomyosin ATPase suggest a change in the allosteric transitions in thin filaments. The next chapter describes the effect of these mutations on thin filament dynamics.

Chapter 5

Effects of Tropomyosin mutations on thin filament dynamics

5.1 Introduction

The majority of studies on tropomyosin mutants investigating tropomyosin structure-function relationship or investigating the mechanism of disease causing mutations had focused on steady state analysis of actin binding and actomyosin ATPase. Our approach is to investigate the impact of these mutations on tropomyosin stability and long range communication between different parts of tropomyosin, the transition between the different thin filament states, the kinetics of switching, the size of the cooperative unit and interaction with actin and troponin. The structure, interaction and conformational changes of tropomyosin are essential in the regulation of muscle contraction (Perry, 2003). The Ca^{2+} induced tropomyosin dependent transitions in muscle thin filament are very fine examples of cooperative allosteric transitions that control physiological processes. It is well established that muscle thin filaments exist in three states and that tropomyosin plays a fundamental role in the switching between these states (El-Mezgueldi, 2014). Thin filament dynamics has been intensively studied using various equilibrium and kinetic approaches (Alahyan *et al*., 2006; McKillop and Geeves 1993, Maytum *et al*., 2003). Consequently, several methods to study thin filament dynamics have been developed and their application to tropomyosin mutations will be very informative.

The cooperative allosteric transitions in thin filaments can be characterised by several parameters including the size of the cooperative unit (n) and the equilibrium constant of transition between the blocked and closed state. Thin filament cooperativity is primarily ruled by Tpm molecules covering seven actin monomers and interacting head to tail along the actin filaments (Lehrer, 1994). The size of cooperative unit is the number of actin monomers activated or inhibited simultaneously by tropomyosin movement following Ca2+ binding to TnC or myosin head binding to thin filaments (Lehrer *et al*., 1997). K_B reflects the distribution of the thin filament between the closed state and the blocked state which plays a vital role in activation and relaxation of muscle. The maximum rate of switching, the interaction of tropomyosin with troponin and long range conformational communication are likely to play an important role in

thin filament regulation. The aim of this chapter is to investigate the impact of different Tpm mutations on the equilibrium constant between the blocked and closed state K_B, the size of the cooperative unit *n*, the maximum rate of the the transition to the Off state and troponin binding affinity.

5.2 Results

5.2.1 Effect of Tpm mutations on the transition between blocked and closed states (K_B)

The switch to the blocked state in the absence of calcium is fundamental for muscle relaxation while the switch from the blocked to the closed states is important during activation by calcium. Therefore, characterising the proportion of the blocked state (measured by the equilibrium constant K_B) in different physiological condition is essential. K_B is measured from the ratio of thin filaments in the closed state over thin filaments in the blocked state. K_B is predicted to be less than 1 when the thin filaments are predominantly in the blocked state (for example in the presence of Tn and absence of Ca^{2+}). While the K_B is expected to be more than 1 when thin filaments are predominantly in the closed state (for example in the presence of Tn and Ca^{2+}). The K_B was calculated separately for both in presence and absence of calcium using the following formula for slope obtained.

$$\frac{kobs(EGTA\ or\ Calcium)}{kobs(Actin\ alone)} = \frac{KB}{1 + KB}$$

Re-arranging this equation gives

$$KB = \frac{kobs(EGTA\ or\ Calcium)}{(kobs(actin\ alone) - kobs(EGTA\ or\ calcium)}$$

The transition between blocked and closed states can be monitored by the large fluorescence change of pyrene iodoacetamide labelled actin induced by myosin head strong binding (Head et al., 1995).

The transients of myosin heads binding to thin filament reconstituted with pyrene iodoacetamida labelled actin filaments and various Tpm mutants are plotted in figure 5.1. Each graph shows the transient obtained with one Tpm mutant (red curve) compared to the transient obtained with WT Tpm (blue curve). R90G, R90R167G,

R90GR244G R167GR244G and E163KE240K shows a faster transient compared to the WT while R167G showed slower transient. The E163K, E240K, R244G R90GR167GR244G, and M281I showed almost comparable transient to the WT.

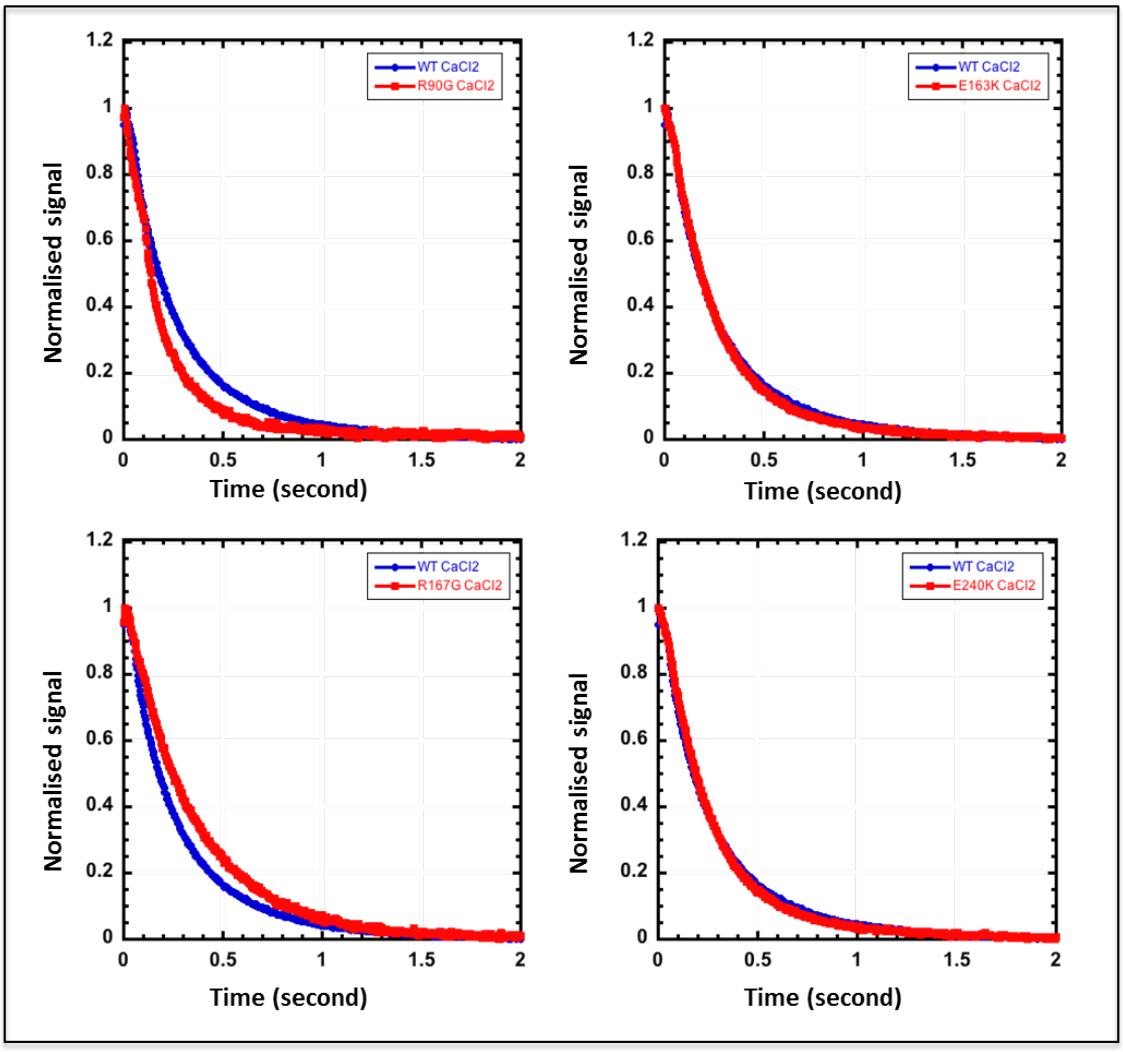

Figure 5.1: Transient of Binding of S1 to PIA-actin-Tpm-Tn in the presence of calcium for Tpm mutations

The kinetic spectra trace of act-PIA binding to S1 in the presence of calcium at 4 µM actin-PIA. Conditions: 140 mM KCl, 10 mM Mops pH 7.2, 4 mM MgCl2, 1 mM DTT, 0.2 mM CaCl2 or 1 mM EGTA, at 25 °C.

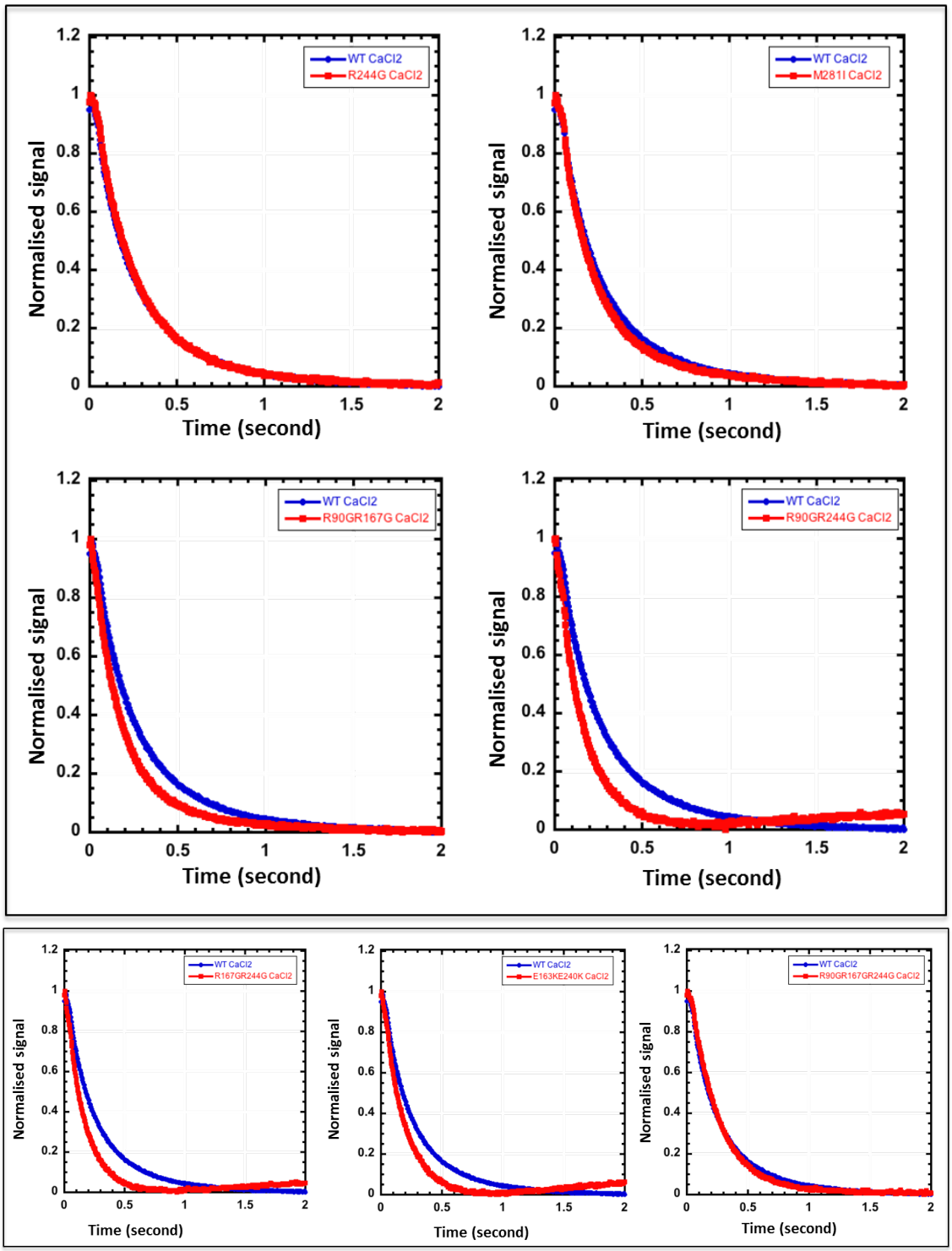

Figure 5.2: Transient of Binding of S1 to PIA-actin-Tpm-Tn in the presence of calcium for Tpm mutations

The kinetic spectra trace of act-PIA binding to S1 in the presence of calcium at 4 µM actin-PIA. Conditions: 140 mM KCl, 10 mM Mops pH 7.2, 4 mM MgCl2, 1 mM DTT, 0.2 mM CaCl2 or 1 mM EGTA, at 25 °C.

On the other hand, the mutations in the absence of calcium showed different behaviour compared to the WT. in figure 5.3 the mutations R90G, E163K, R167G, R244G, M281I, R90GR244G, R167GR244G and E240K shows faster transients compared to the WT. In contrast R90GR167G and E163KE240K showed similar traces compared to the WT.

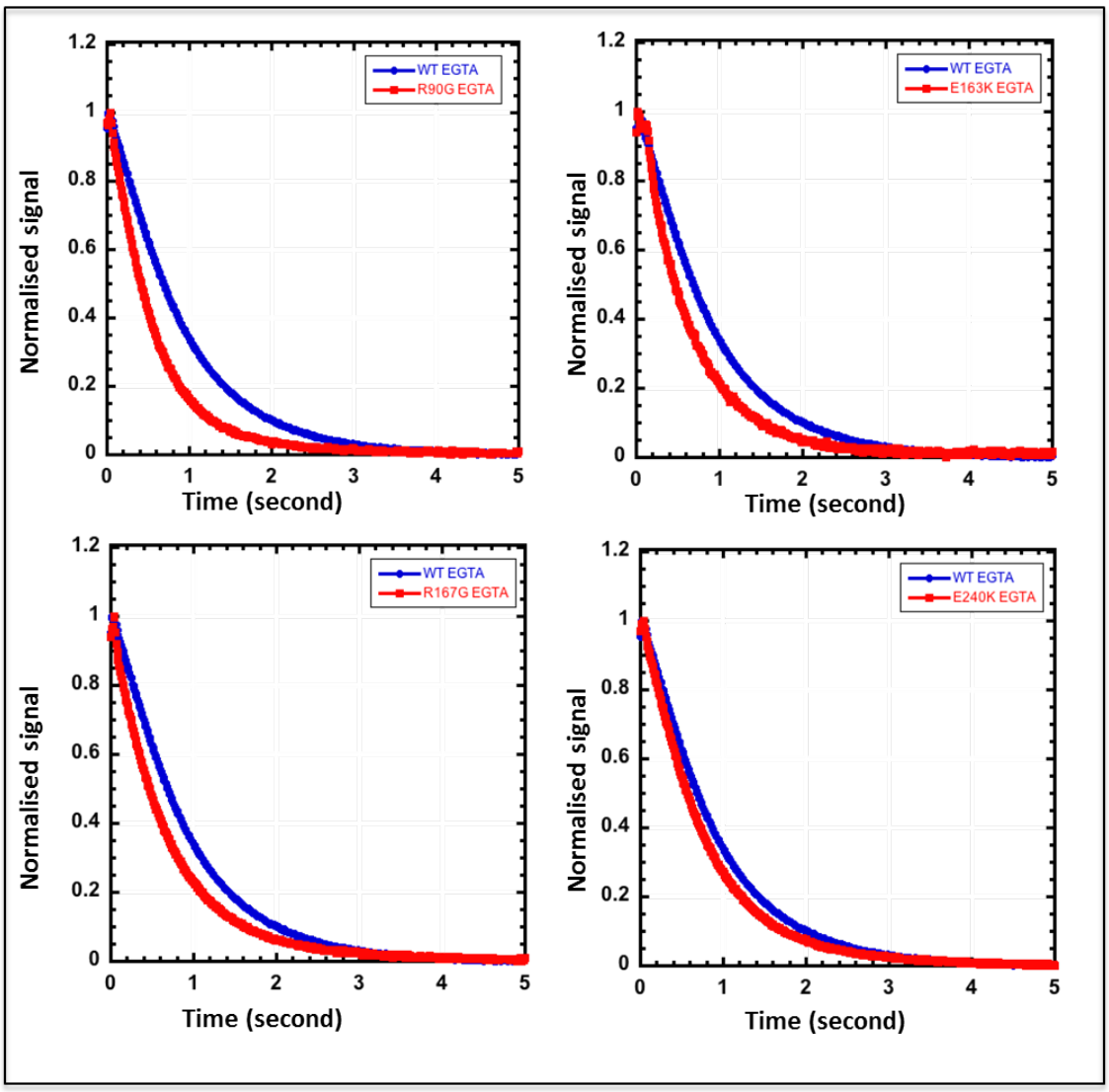

Figure 5.3: Transient of Binding of S1 to PIA-actin-Tpm-Tn in the absence of calcium for Tpm mutations

The kinetic spectra trace of act-PIA binding to S1 in the absence of calcium at 4 µM actin-PIA. Conditions: 140 mM KCl, 10 mM Mops pH 7.2, 4 mM MgCl2, 1 mM DTT, 0.2 mM CaCl2 or 1 mM EGTA, at 25 °C.

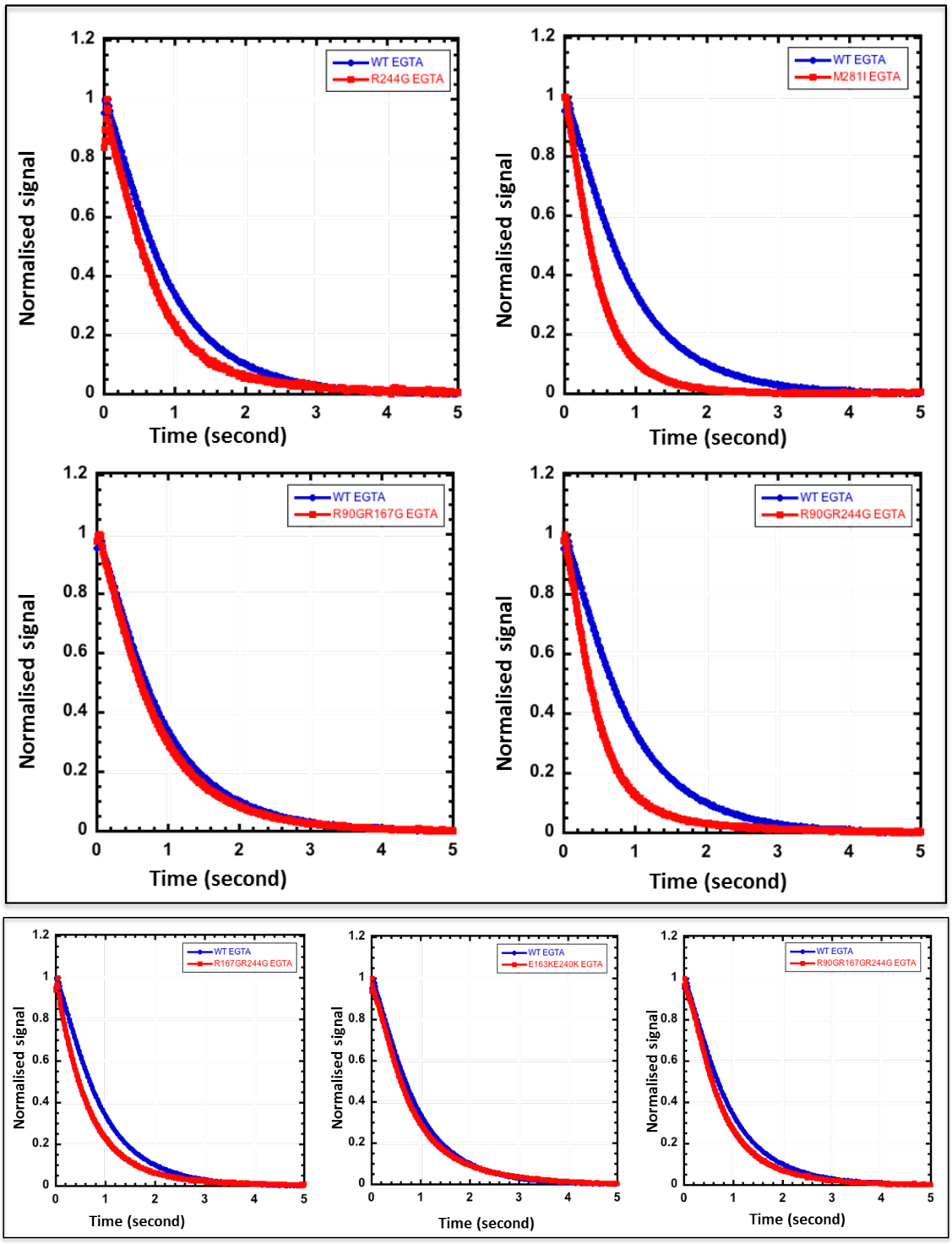

Figure 5.4: Transient of Binding of S1 to PIA-actin-Tpm-Tn in the absence of calcium for Tpm mutations

The kinetic spectra trace of act-PIA binding to S1 in the absence of calcium at 4 µM actin-PIA. Conditions: 140 mM KCl, 10 mM Mops pH 7.2, 4 mM MgCl2, 1 mM DTT, 0.2 mM CaCl2 or 1 mM EGTA, at 25 °C.

The tropomyosin plays a vital role on the transition over actin monomers. Therefore, the mutations may affect the tropomyosin transition and increase or decrease K_B value. Figure (5.5) shows the dependence of the observed rate constant of S1 binding to actin (with various Tpm mutants and troponin and/or Ca^{2+}, obtained from the transients in figure 4). K_B was calculated from the slope of the lines describing S1 binding to thin filaments in comparison to actin alone of three times replicate (see Materials and Methods). Table 5.1 summarise the K_B values. The figure (5.5 A) shows the observed rate constant obtained for actin alone and (actin+Tpm+Tn) in the presence and absence of calcium. In presence of Ca^{2+} the WT Tpm shows a linear increase in the observed rate constant (k_{obs}) which yields a K_B value >1.0. In absence of Ca^{2+} the skeletal Tpm calculated K_B value is 0.2. For all mutants, the k_{obs} obtained for actin alone as well as in the presence and absence of calcium were linearly proportional to the actin concentration over the range 1-10 μM. Figure 5.5.B and 5.5.C showed the dependence of the observed rate constant (k_{obs}) of S1 binding to actin on actin concentration for R90G and R167G. For all curves k_{obs} was linearly dependent on actin concentration as for WT Tpm. In the absence of Ca^{2+}, K_B values of 0.3 for Tpm R90G and 0.2 for Tpm R167G were calculated. They are all almost similar to the value obtained for WT Tpm (0.2). In the presence of Ca^{2+}, a K_B value of >1 was obtained for R90G and R167G. Figure 5.5.D shows the dependence of the observed rate constant (k_{obs}) of S1 binding to actin on actin concentration for E163K. In the absence of Ca^{2+}, K_B values of 0.9 slightly lower than WT. In the presence of Ca^{2+}, a KB value of >1.0 was calculated. Figure 5.5.E, 5.5.F, 5.5.G and 5.5.H shows the dependence of the observed rate constant (k_{obs}) of S1 binding to actin on actin concentration for E240K, R244G, M281I and R90G/R167G. In the absence of Ca^{2+}, K_B values of 0.2 for E240K, 0.1 for R244G, 0.2 for M281I and 0.2 R90G/R244G were calculated. In the presence of Ca^{2+}, K_B value of >1.0 for E240K, R244G, M281I and R90G/R244G was calculated. Figure 5.6.I and 5.6.L shows the dependence of the observed rate constant (k_{obs}) of S1 binding to actin on actin concentration for R90G/R244G and R90G/R167G/R244G. In the absence of Ca^{2+}, K_B values of 0.2 for R90G/R244G and 0.1 for Tpm R90G/R167G/R244G were calculated. In the presence of Ca^{2+}, K_B value of >1.0 for R90G/R244G and R90G/R244G was calculated.

However, figure 5.6.J and 5.6.K shows the dependence of the observed rate constant (k_{obs}) of S1 binding to actin on actin concentration for R167G/R244G and E163K/E240K respectively. In the absence of Ca^{2+}, K_B values of 0.07 for R167G/R244G and 0.03 for E163K/E240K showed very low value compared to the WT. In the presence of Ca^{2+}, the K_B value of >1.0 for R167G/R244G and E163K/E240K was calculated.

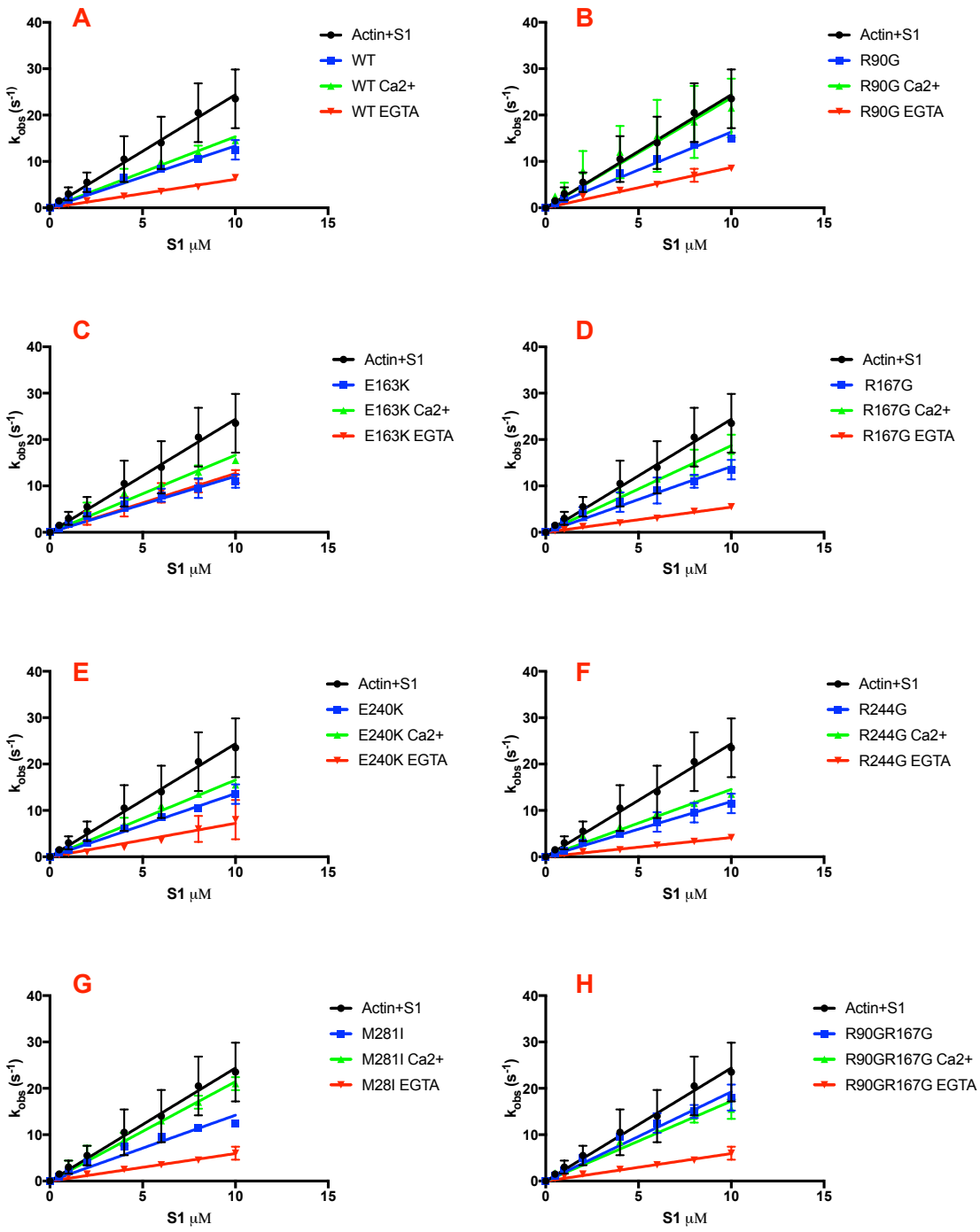

Figure 5.5: The binding of S1 to PIA-actin in the presence and absence of calcium for Tpm mutations

The figure shows the observed rate of S1 binding as a function of PIA-labelled actin concentration in the presence and absence of calcium. It illustrates actin alone (Black) the Tm alone (Blue) in the presence of Ca^{2+} (Green) and the absence of Ca^{2+} (Red). Conditions: 140 mM KCl, 10 mM Mops pH 7.2, 4 mM $MgCl_2$, 1 mM DTT, 0.2 mM $CaCl_2$ or 1 mM EGTA, at 25 °C.

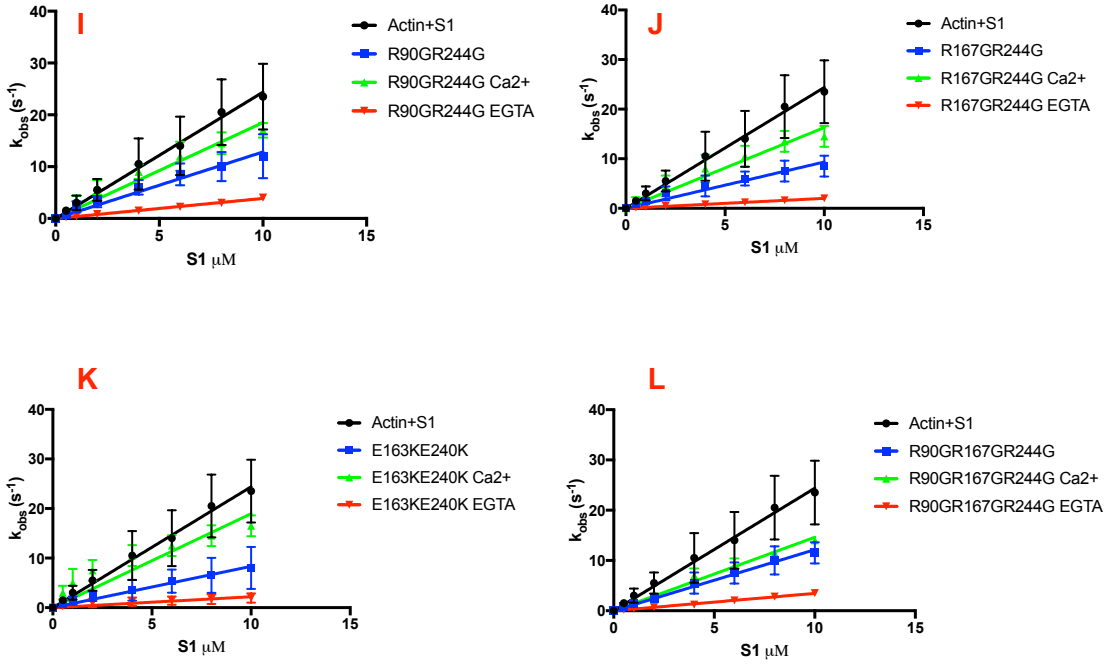

Figure 5.6: The binding of S1 to PIA-actin in the presence and absence of calcium for Tpm mutations

The figure shows the observed rate of S1 binding as a function of PIA-labelled actin concentration in the presence and absence of calcium. It illustrates actin alone (Black) the Tm alone (Blue) in the presence of Ca^{2+} (Green) and the absence of Ca^{2+} (Red). Conditions: 140 mM KCl, 10 mM Mops pH 7.2, 4 mM $MgCl_2$, 1 mM DTT, 0.2 mM $CaCl_2$ or 1 mM EGTA, at 25 °C.

Table 5.1: Summary of the effect of Tpm mutations on the thin filament switching parameter KB (n2)

Protein	K_B ($CaCl_2$)	K_B (EGTA)
WT	> 1.0	0.3 ± 0.01
R90G	> 1.0	0.5 ± 0.02
E163K	> 1.0	1.0 ± 0.03
R167G	> 1.0	0.2 ± 0.01
E240K	> 1.0	0.4 ± 0.03
R244G	> 1.0	0.1 ± 0.009
M281I	> 1.0	0.2 ± 0.01
R90GR167G	> 1.0	0.2 ± 0.01
R90GR244G	> 1.0	0.1 ± 0.005
R167GR244G	> 1.0	0.09 ± 0.003
E163KE240K	> 1.0	0.09 ± 0.01
R90GR167GR244G	> 1.0	0.1 ± 0.005

5.2.2 Effect of Tpm mutations on the size of cooperative unit *n*

The role of Tpm is based on introducing cooperativity to muscle contraction and relaxation during the contractile cycle. This is derived from the capability of the Ca^{2+} binding and dissociation in a single site to make changes to many actin monomers. The number of actin monomers that can simultaneously switch between the three states defines the cooperative unit. The cooperativity is due to the ability of Tpm to cover many actin monomers and is modulated by Tpm flexibility and head to tail interactions; both of which are affected by Tm mutations isoforms and TnT interaction (Geeves and Lehrer, 1994).

Lehrer and Geeves have developed a method to measure the size of the cooperative unit for studying striated muscle Tpm using pyrene labelled tropomyosin. Tpm is labelled with N-(1-pyrenyl)-iodoacetamide at Cys-190 of Tpm. The Pyrene labelled Tpm dimer can exhibit an excimer fluorescence that increases when S1 binds thin filaments and switch them to the ON state (Geeves and Lehrer, 1994). Measuring myosin-S1 association/dissociation in parallel with thin filaments ON-OFF transition allow the determination of the size of cooperative unit n. Mirza and his collaborators has identified the size of cooperativity for both skeletal and cardiac Tpm with 7.0 ± 0.1 and 10.7 ± 0.4 respectively (Mirza *et al*., 2007).

The aim of this experiment was to assess the effect of the Tpm mutation on the size of cooperativity unit. The conformational changes associated with the ON-OFF transition can be monitored by the excimer fluorescence of pyrene iodoacetamide labelled Tpm while the binding of S1 to actin can be followed by light scattering. The experiment was performed two times by premixing actin+Tpm* in a molar ratio of 6:1 and titrated by step wise of high concentration of S1 (100 µM). The change in the excimer fluorescence and light scattering were followed and the slope of both was used to calculate the size of *n* (table 5.2).

A spectrum of the PIA-labelled Tpm (cys-190) is shown in (Fig 5.7). PIA-labelled Tpm exhibits a combination of monomer peaks at 385 nm and 410 nm and excimer peak at 480 nm. Addition of myosin S1 to actin-PIA-Tpm had only a minor effect on monomer fluorescence but increases the excimer substantially. This is reversed by the addition of Mg^{2+}ATP (figure 5.7).

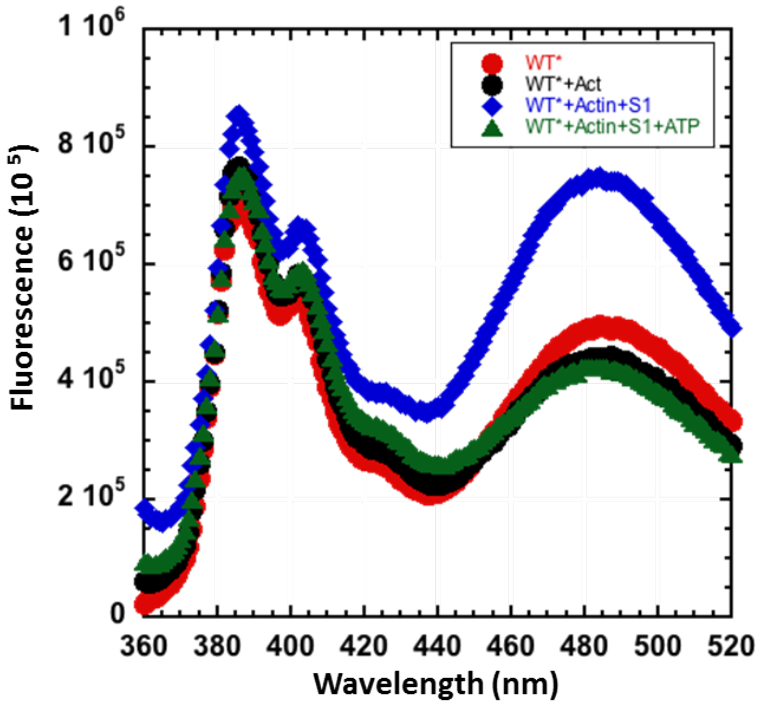

Figure 5.7: Excimer fluorescence spectra of PIA-labelled Tpm (Tpm*)

The Red spectrum is (Tpm*) alone and the Black (Tpm*+actin) and the Blue (Tpm*+Actin+S1) the Green is (Tpm*+Actin+S1+ATP). the experiment performed in presence of 3µM actin, 0.5 µM Tpm*, 3 µM S1, 1 mM Mg^{2+}ATP in buffer containing 10 mM Mops pH 7.2, 50 mM KCl, 4 mM $MgCl_2$, and 1 mM DTT, at 25°C.

In S1 binding kinetics, the excimer fluorescence signal consists of two components: a fast and slow and the data are fit to the sum of two exponentials. The observed rate of the fast signal was linearly dependent on S1 concentration. The light scattering showed a single exponential increase when S1 was rapidly mixed with (Tpm*+actin). In figure 5.8 the WT light scattering slope yielded (1.0821) and the excimer fluorescence slope yielded (8.7978) and the ratio of the excimer slope over the light scattering slope give a value of 8.05 ± 0.05 for the size of cooperative unit. The obtained value is in agreement with the value obtained by Lehrer and his group (n values 8-10) (Geeves *et al*., 1997). Tpm mutants R167G and R90GR167G showed almost similar n value of 4.9 ± 0.1 and 4.2 ± 0.2 respectively. These mutations have a reduction in the size of cooperativity value compared to the WT. The lowest value of n was observed with the mutations E163K, R244G, R90GR244G and R167GR244G with 3.6 ± 0.2, 3.3 ± 0.1, 3.3 ± 0.2, and 2.8 ± 1.15. A value of 6.4 ± 0.4 was obtained for Tpm R90G. The size of cooperative unit seems to be affected by the mutations in Tpm and reduced the value obtained compared to the WT value.

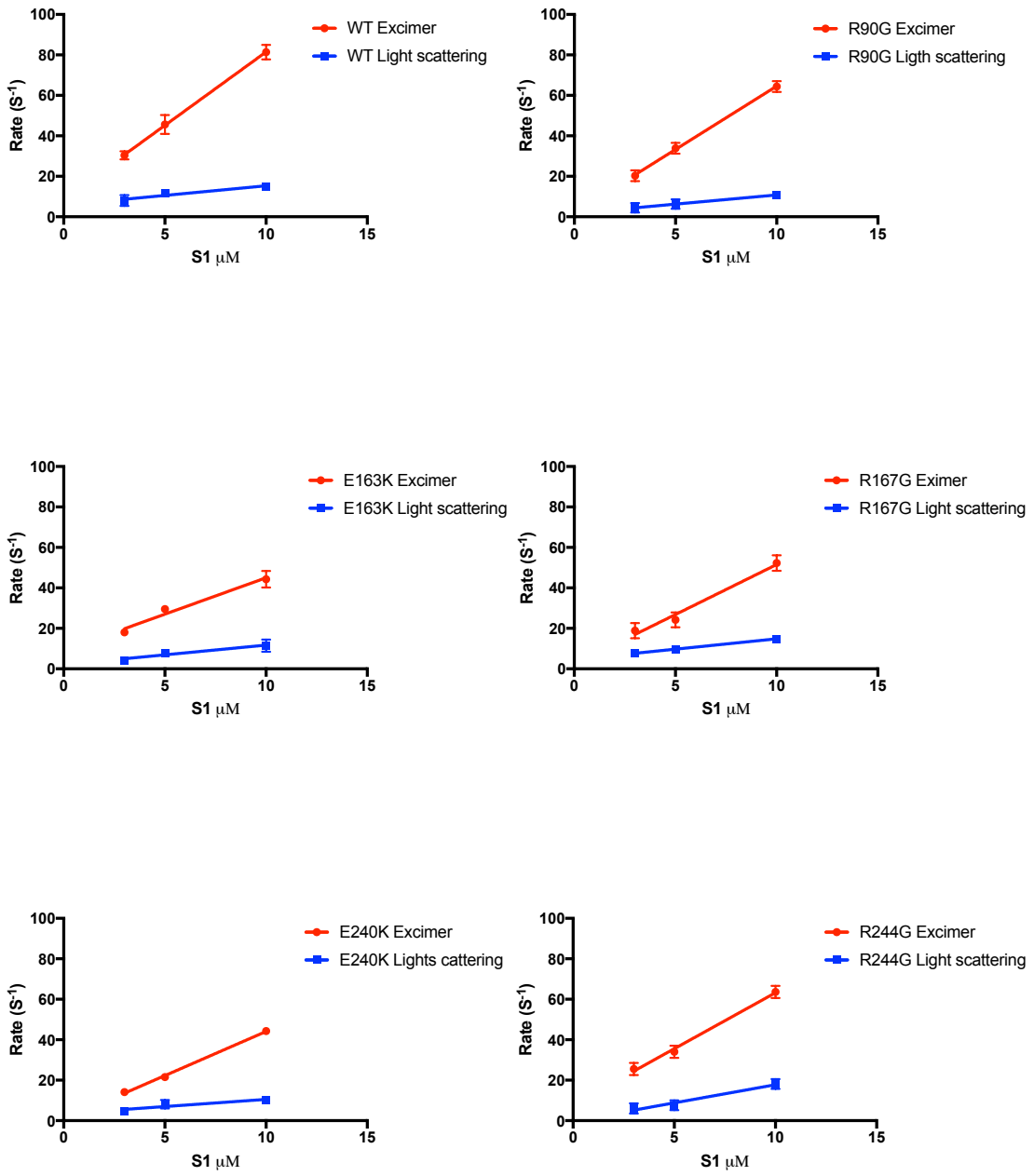

Figure 5.8: Determination of cooperative unit size from kinetics of binding of actin-tropomyosin with S-1

The Red line represents the excimer fluorescence and the Blue line represents the light scattering and the ratio of slope of both give the n value. Pyrene-tropomyosin- actin complex was performed by mixing stock solutions to final concentrations of 6 µM actin, 1 µM Tropomyosin. This pyrene-tropomyosin-actin complex was mixed with 2.5-10 µM S1 (final concentration) in the stopped-flow apparatus in 140 mM KCl, 20 mM Mops pH 7.2, 4 mM $MgCl_2$, 0.2 mM $CaCl_2$, and 1 mM DTT, at 20°C.

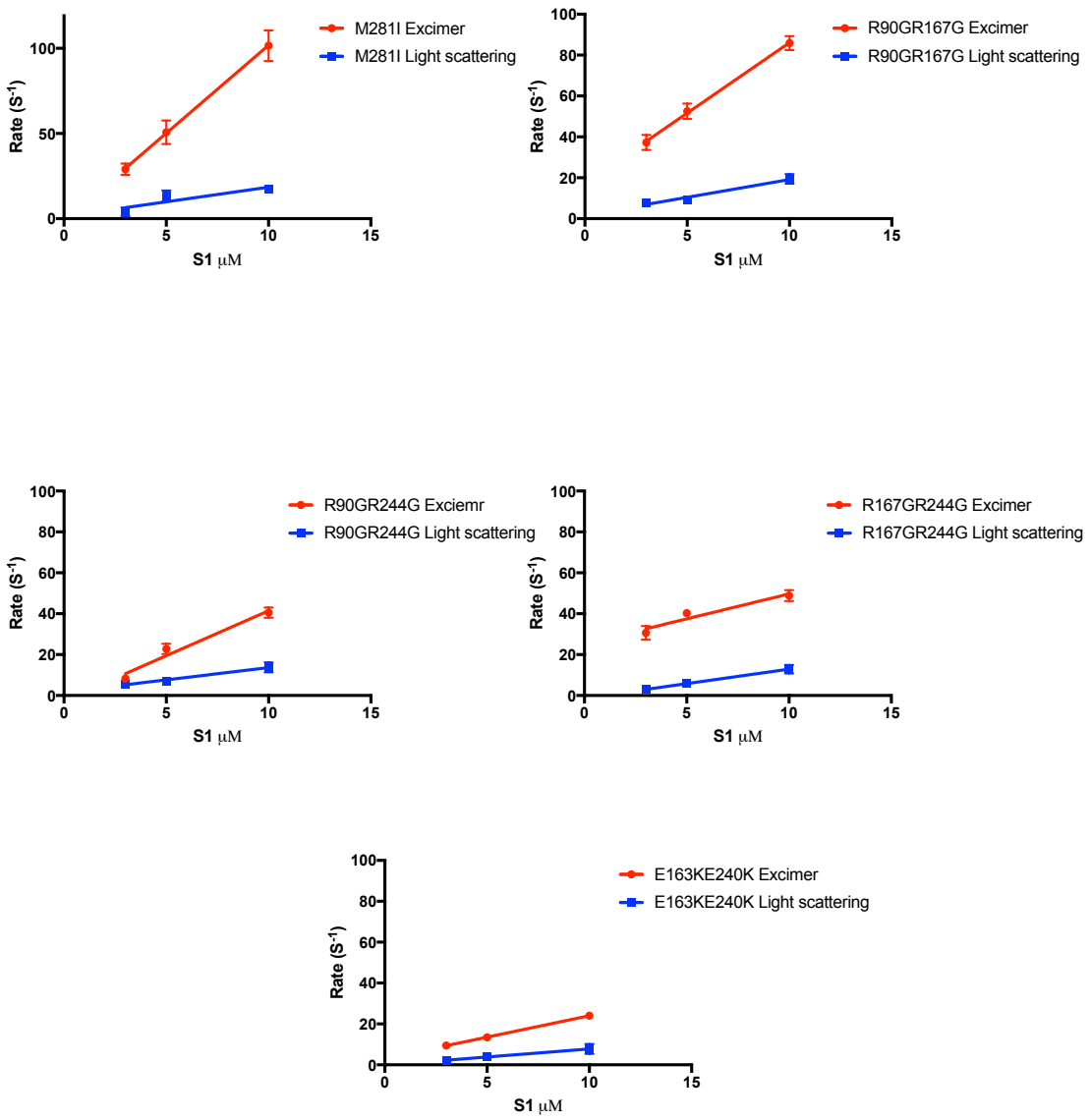

Figure 5.9: Determination of cooperative unit size from kinetics of binding of actin-tropomyosin with S-1

The Red line represents the excimer fluorescence and the Blue line represents the light scattering and the ratio of slope of both give the *n* value. Pyrene-tropomyosin- actin complex was performed by mixing stock solutions to final concentrations of 6 µM actin, 1 µM Tropomyosin. This pyrene-tropomyosin-actin complex was mixed with 2.5-10 µM S1 (final concentration) in the stopped-flow apparatus in 140 mM KCl, 20 mM Mops pH 7.2, 4 mM $MgCl_2$, 0.2 mM $CaCl_2$, and 1 mM DTT, at 20°C.

Table 5.2: Summary of the effect of Tpm mutations on the size of cooperative unit *n*

Protein	Size of *n*
WT	8.05 ± 0.05
R90G	6.4 ± 0.4
E163K	3.6 ± 0.2
R167G	4.9 ± 0.1
E240K	5.8 ± 0.2
R244G	3.3 ± 0.1
M281I	5.7 ± 0.1
R90GR167G	4.2 ± 0.2
R90GR244G	3.3 ± 0.2
R167GR244G	2.8 ± 1.15
E163KE240K	4.2 ± 1.45

5.2.3 Effect of Tpm mutations on ATP induced acto-S1 dissociation from thin filament (Maximum OFF rate)

In the cross-bridge cycle the standard step of muscle contraction is controlled by the ATP induced dissociation of actomyosin-S1. The observed rate is linearly dependent upon the concentration of ATP over the measurable range as described in different studies (Lyme and Taylor, 1971).

If ATP is used to induce acto-S1 dissociation, the light scattering will fall as ATP binds and dissociate the bound S1 but the excimer fluorescence will remain in the ON state as long there are myosin heads bound to a cooperative unit. Once the last myosin head dissociates from the cooperative unit, the fluorescence falls rapidly as the filament switches to the OFF state. (Geeves and Lehre, 1994).

The fall in fluorescence of pyrene labelled Tpm (PIA Tpm) can be conveniently used to follow the transition to the closed state. A single exponential is observed for this transition. The observed rate of ON-OFF transition increases as the concentration of ATP increases and the relationship between the maximum rate constant for ON-OFF transition and ATP concentration can be fit to a hyperbolic equation:

$$(kobs = \frac{kobsmax * [ATP]}{\frac{Kobsmax}{2} + [ATP]}).$$

Figures 5.10 and 5.11 show the concentration dependence of the rate of ON-OFF transition observed at 25˚C when actin: S1: PIA-Tpm (6:6:1). The hyperbolic curves plateau and the maximum obtained from these curves correspond to the maximum rate constant for the ON-OFF transition. These values are displayed in table 5.3. The WT gave a maximum rate constant of 475.1 S^{-1} while the R90G, E240K, R244G R90GR167G and M281I showed lower maximum ON-OFF rate constant in the range 170-200 S^{-1}. Other mutations showed almost similar rate compared to the WT (range 350-450 S^{-1}).

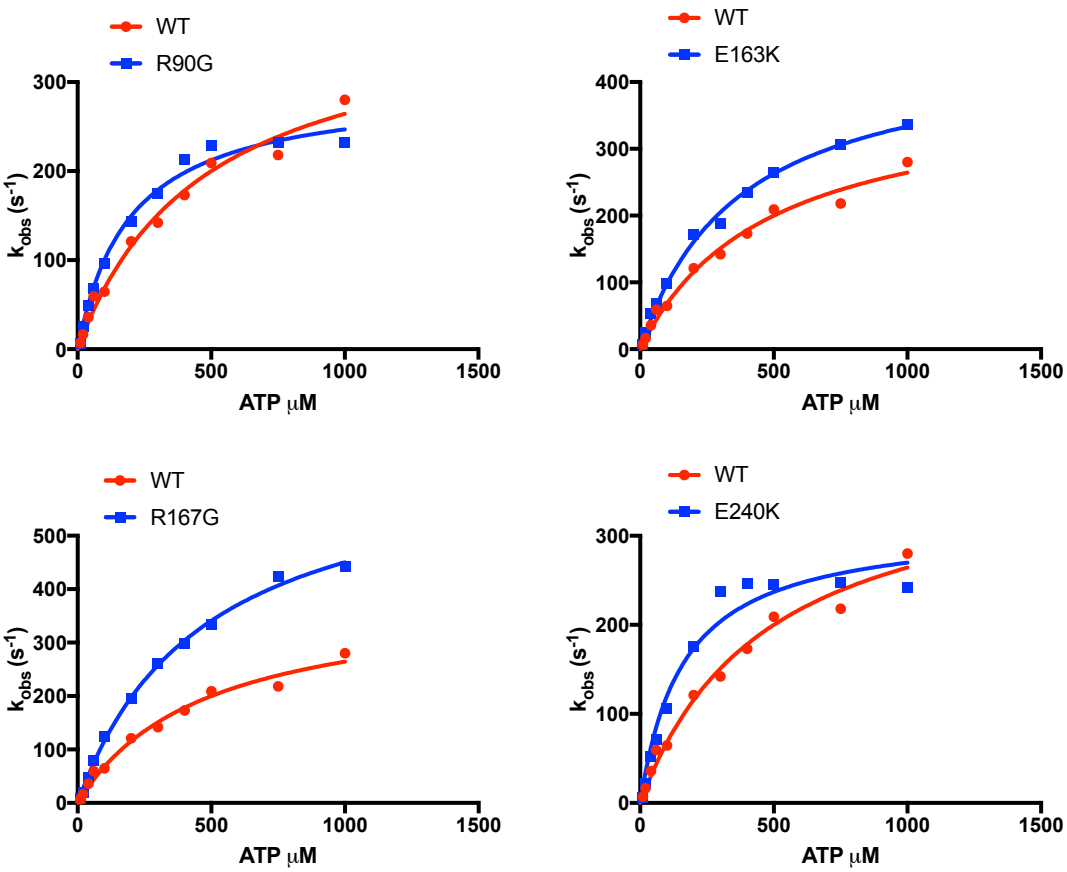

Figure 5.10: maximum OFF rate of ATP induced acto-S1 dissociation

The Red curve shows the WT and the Blue curve represents the mutations. The rate obtained for both WT and mutation was calculated by hyperbolic formula. The buffer used to carry out the measurements was (10 mM Mops, pH7.2, 140mMKCl, 5mMMgCl_2, 1mM DTT, 1 mM NaN_3) at 20˚C. the tables are the values obtained by hyperbolic equation.

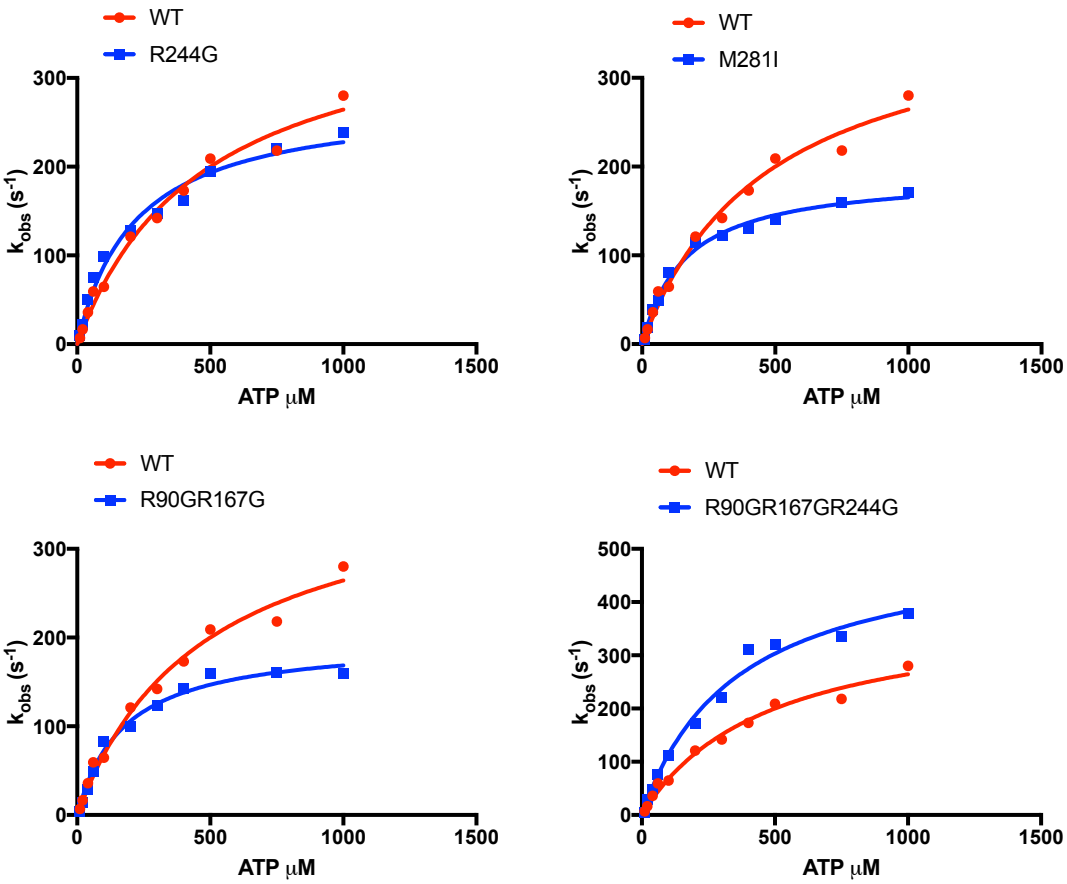

Figure 5.11: maximum OFF rate of ATP induced acto-S1 dissociation

The red curve shows the WT and the blue curve represents the mutations. The rate obtained for both WT and mutation was calculated by hyperbolic formul. The buffer used to carry out the measurements was (10 mM Mops, pH7.2, 140mMKCl, 5mMMgCl_2, 1mM DTT, 1 mM NaN_3) at 20˚C. the tables are the values obtained by hyperbolic equation.

Table 5.3: summary of maximum OFF rate ATP induced acto-S1 dissociation

Protein	Maximum OFF rate of ATP induced acto-S1 dissociation (S^{-1})
WT	475.1
R90G	195.4
R167G	472.8
E163K	368
E240K	161.4
R244G	217.3
M281I	160.6
R90GR167G	173.7
R90GR167GR244G	356.6

5.2.4 Effect of Tpm mutations on Tropomyosin-Troponin affinity.

The fundamental function of striated muscle is through contraction and force generation which are tightly regulated by Tropomyosin and Troponin. The contraction and force generation are based on the ability of myosin heads sites on actin to be exposed by Tropomyosin and Troponin (Gordon *et al*; 2000).

The troponin binding to tropomyosin alone was analysed to assess the impact of tropomyosin mutations on interactions with troponin. That was achieved using a titration of PIA-Tpm (2 µM) with increasing concentration of Troponin (0-7 µM) in a fluorimeter. All binding curves were hyperbolic and were fit to a hyperbola to extract the K_d. The data were obtained by using hyperbolic equation:

$$(bound = \frac{Boundmax * [Tn]}{Kd + [Tn]}).$$

Tpm WT binding to troponin is characterised by a dissociation constant $K_d = 0.11x10^{-5}$ M (table 5.4). Remarkably all mutations have increased the affinity of tropomyosin for troponin by 2 folds.

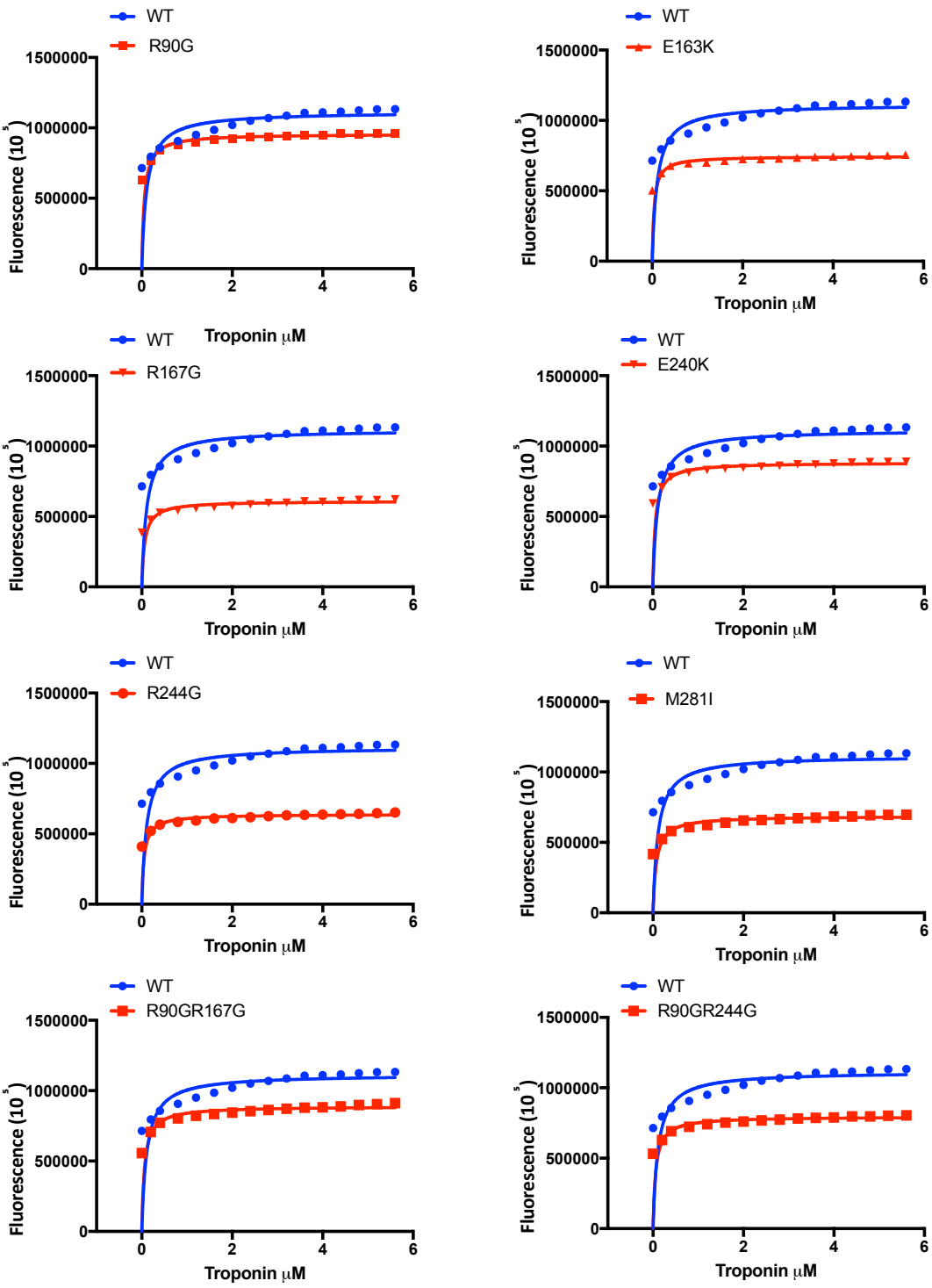

Figure 5.12: Tropomyosin-Troponin binding curves

The Red curve shows the data before volume correction and the Blue shows the best fitting curve after volume correction. The Tm concentration was 2 µM titrated with increasing troponin concentration from 0-7 µM in 2 ml of AMSB (10 mM MOPS pH 7, 50 mM KCl, 3.5 mM $MgCl_2$, 1 mM DTT, and 1 mM NaN_3) at 25°C. The curves were plotted as a function of the troponin concentration and hyperbola equation was applied to calculate the Tn bound to Tm (Kd).

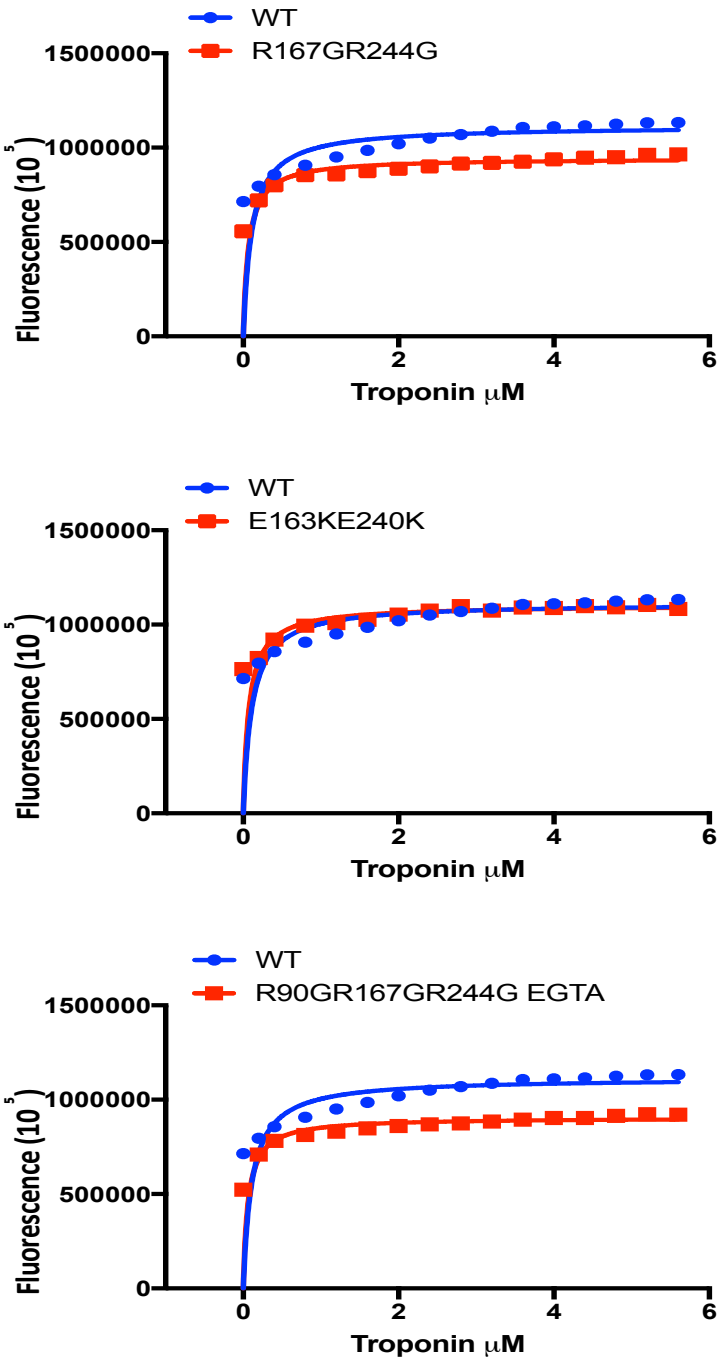

Figure 5.13: Tropomyosin-Troponin binding curves

The Red curve shows the data before volume correction and the Blue shows the best fitting curve after volume correction. The Tm concentration was 2 µM titrated with increasing troponin concentration from 0-7 µM in 2 ml of AMSB (10 mM MOPS pH 7, 50 mM KCl, 3.5 mM $MgCl_2$, 1 mM DTT, and 1 mM NaN_3) at 25°C. The curves were plotted as a function of the troponin concentration and hyperbola equation was applied to calculate the Tn bound to Tm (Kd).

Table 5.4: Summary of the tropomyosin troponin binding constant

Protein	K_d 10^{-5} M
WT	0.11
R90G	0.05429
E163K	0.04191
R167G	0.06432
E240K	0.05317
R244G	0.05145
M281I	0.07198
R90GR167G	0.05924
R90GR244G	0.05896
R167GR244G	0.07024
E163E240K	0.07488
R90GR167GR244G	0.06302

5.3 Discussion

Tropomyosin plays a fundamental role in the regulation of muscle contraction. Calcium binding to troponin induces a conformational change in troponin which lead to tropomyosin movement on the surface of actin and this uncover several actin monomers for myosin binding. The allosteric transition in thin filaments play a major role in thin filament regulation and tropomyosin is a key player in these transitions.

The aim of this chapter is to characterise the effect of tropomyosin mutations on the transition between these states by assessing their impact on several parameters: K_B, size of n, co-sedimentation, Maximum Off rate constant, trypsin digestion and tropomyosin troponin interaction.

5.3.1 Effect of tropomyosin mutations on K_B

The transition between blocked and closed states was monitored by the large fluorescence change of PIA-labelled actin upon S1 myosin heads binding (Head et al., 1995; Alahyan et al., 2006). The kinetics of S1 binding to PIA-actin was followed in the presence and absence of calcium and the ratio between the two defines the K_B. The wild type did show similar value to the value obtained by (Boussouf and Gevees 2007). However, the mutation did not show substantial difference in the value obtained except for two mutations that showed lower value of 0.07 and 0.03 for R167GR244G and E163KE240K respectively.

The tropomyosin binds actin in electrostatic way at two positions on every actin aspartic acid at residue 25 and a cluster of basic residues (lysine at residues 326 and 237 and arginine at reside 147) respectively (Li *et al*., 2011; Barua *et al*., 2011). It has been suggested that R244 binds Asp25 while E240 binds K326 on actin (Marston *et al*., 2013; Barua *et al*., 2012). Therefore, these two mutation may have altered the binding to actin and consequently altered the K_B.

5.3.2 The mutations have reduced the size of cooperative unit

The average number of actin monomers that can be switched ON or OFF is the cooperative unit size, *n*, and that is induced by the binding or dissociation of a single strong-binding myosin head. The wild type size of n value is similar to the value obtained in the literature (Mahmooda *et al*., 2007; Bing et al., 2000). All the mutations showed a reduction in the value obtained of *n*. At the moment, it is not clear why all mutations affected cooperativity.

5.3.3 The maximum OFF rate constant.

The ATP induced S1 dissociation measures the rate of last S1 dissociate from thin filament and cause rapid fall of the signal. Different factors can affect the rate of S1 dissociation. These factors include temperature and ionic strength as (Geeves et al., 1986) has reported. Based on their condition it was reported that at 20 ºC the rate of ATP was 480 S^{-1}.

In our experiment, the test was done in a temperature 25 ºC and the rate for the S1 dissociation with wild type Tpm was 475 S^{-1}. All the mutations except R167G have increased the rate of S1 dissociation substantially. This increase of rate might be due to the alteration of the actin binding sites with tropomyosin and lead to rapid dissociation of S1.

5.3.4 Tropomyosin troponin binding

All mutations increased tropomyosin affinity for troponin although by a modest 2 folds. The measurement done here are in the absence of actin and this change in affinity is unlikely to affect thin filament assembly but may affect some of the regulatory steps.

Chapter 6

General discussion

6.1 Introduction

Tropomyosin plays a fundamental role in the Ca^{2+} dependent regulation of striated muscle contraction. These functions are mediated by its interaction with actin and troponin. Although, tropomyosin has been intensively studied for 50 years, the molecular basis of its interaction with actin remains unexplained. Several, structural and biochemical studies have revealed important features in the tropomyosin-actin interaction namely: 1) Individual tropomyosin molecules bind weakly to actin. 2) On the surface of actin, the tropomyosin forms a continuous strand that binds tightly to actin. 3) The continuous strand of tropomyosin is curved and forms an arc whose curvature matches the actin filament helical shape. 4) The continuity of the tropomyosin cable is due to the end-to-end interactions between adjacent molecules of tropomyosin. 5) Tropomyosin N-terminal acetylation plays a critical role in the end-to-end interactions and hence in the formation of the continuous strand and interaction with actin. 6) Tropomyosin occupies three different positions on the surface of actin that have specific biochemical properties. 7) The movement between these states is cooperative-allosteric and is regulated by the troponin complex interactions with both actin and tropomyosin. However, a detailed mechanism of tropomyosin interaction with actin and switching between the various biochemical states is not yet available and is awaiting the precise determination of tropomyosin amino acids involved in binding actin thin filaments, in the different biochemical states.

Tropomyosin has been linked to several cardiac and skeletal muscle diseases. Tropomyosin mutations have been identified in patients with hypertrophic cardiomyopathies, dilated cardiomyopathies, skeletal muscle nemaline myopathies, congenital fibre-type disproportion (CFTD), distal arthrogryposis and cap myopathies. The molecular mechanism by which these mutations lead to these pathologies is not understood.

Consequently, understanding the nature of tropomyosin interaction with actin and troponin and the impact of various disease associated mutations on these interactions and on tropomyosin movement between the various regulatory steps is of great importance.

The aim of this project was to characterise the impact of several mutations (found in various skeletal muscle diseases) on tropomyosin secondary structure, actin and troponin binding properties and actin-tropomyosin-troponin switching between different regulatory states. We also used double and triple mutations in order to disrupt tropomyosin interactions more severely.

6.2 Expression and purification of tropomyosin mutants.

The ideal way to investigate the mutations is a tissue sample from normal humans and from affected patients since it preserves the acetylation status *in vivo* isoforms distribution and dimerization patterns. However, tissue biopsies are no more than 50 mg (total tissue) and can only be obtained in exceptional circumstances. In addition, biophysical methods such as stopped flow based transient kinetics, fluorimetry, isothermal calorimetry require a substantial amount of protein (total amount of protein needed is several mg). Therefore, for a comprehensive investigation we need to express a recombinant protein. The importance of end-to-end interactions involved in cooperativity depends on N-terminal acetylation. Many laboratories have used an N-terminal addition of di-peptide Ala-Ser to the tropomyosin protein to mimic the N-terminal acetylation produced in *E.coli* expression system and to obtain recombinant proteins. However, others have suggested that the N-terminal extension may not reproduce the acetylation modification fully and may produce tropomyosin with reduced cooperativity and perhaps other abnormalities. Therefore, we planned to express tropomyosin using the baculovirus-SF9 system that can produce acetylated proteins. We established a successful expression system using baculovirus-SF9 cells. During the expression and purification of Tpm3 in the *baculovirus* system I have faced two major problems. Firstly, after purification I obtained around 2 mg of recombinant tropomyosin per litre of insect cell culture. This is a low amount for transient kinetics investigation, however since tropomyosin is used at stoichiometry of a tropomyosin per 7 actins; enough tropomyosin to perform several experiments could be obtained from 2-3 litres of insect cells culture. Nevertheless, it was time consuming to carry 3 litres expression for several mutants and we had to use incubators which were not dedicated for insect cells which increased the risk of contamination of our cultures. Secondly, the Wild type was not fully acetylated and consequently did not bind to actin in the co-

sedimentation assay. We do not understand why the Wild type tropomyosin was not acetylated but is possible that the insect cells acetylation was inappropriate or not sufficient. Therefore, it was essential to change the host cell system to obtain more reliable and functional Tpm protein. We have decided to switch to the expression of tropomyosin mutants with an Ala-Ser extension.

6.3 Effect of tropomyosin mutations on its interaction with actin and troponin.

In muscle, the thin filaments are made of actin, tropomyosin and troponin. Activation/inhibition of thin filament following Ca^{2+} binding/dissociation is mediated by a set of elegant allosteric transitions that starts at the Ca^{2+} binding site in TnC and travels via TnI, TnT and Tpm to the actin filament inducing a conformation which is either active (in presence of Ca^{2+}) or inactive (in absence of Ca^{2+}). Tropomyosin interactions with both actin and troponin are key to these allosteric transitions. Therefore, it is important to measure the impact of tropomyosin mutations on these interactions. Co-sedimentation experiments showed that all the mutations investigated in this work did not have major impact on tropomyosin interaction with actin. However, this method is only qualitative testing the ability of the Tpm to bind actin (or not) and does not measure how much tropomyosin is bound to actin and consequently these mutations may have weakened the affinity of actin for tropomyosin but we could not see this in our qualitative essay. Hence it will be desirable to perform quantitative binding analysis to assess the impact of these tropomyosin mutations on the affinity of actin for tropomyosin. Furthermore, it appears to be that the nature of interaction between actin and tropomyosin is more complex involving both discrete binding sites between individual actin binding sites on tropomyosin and corresponding actin subunits and the continuous nature of the tropomyosin strand and its curved shape. Thus, single amino acid mutations are unlikely to affect tropomyosin binding to actin even if they contribute to the overall affinity of tropomyosin binding to actin.

In contrast, our troponin binding measurements using pyrene labelled tropomyosin revealed that all mutations increased the affinity of tropomyosin for troponin. The dissociation constant was increased between 2-4 folds. It is not apparent how these tropomyosin mutations improved the tropomyosin affinity for the troponin complex by 2-4 folds. It is also important to note that although Tpm R90 is outside troponin binding site on tropomyosin, it still increased troponin affinity. This could be explained by a long-range effect of R90G mutation on the Tpm structure. In fact, all mutations may simply increase tropomyosin flexibility and allow for a better fit of the sites of interaction.

6.4 Effect of tropomyosin mutations on thin filament dynamics

The previous section showed that all the tropomyosin mutants we expressed did not abolish or drastically reduce actin or troponin binding and this paved the way for investigating the impact of these mutations on the Ca^{2+} dependent activation and inhibition of the actomyosin ATPase and thin filament dynamics. The ATPase experiments revealed that all the mutations investigated have reduced the Ca^{2+} dependent activation of the actomyosin ATPases Except (R90G, E163K and E20K). This is in agreement with several studies that showed a reduction in calcium sensitivity at R167 and R244 also in the Ca^{2+} dependent activation of the actomyosin ATPase (Robaszkiewicz *et al*., 2012; Marston *et al*., 2013; Robaszkiewicz *et al*., 2015). In contrast, the actomyosin ATPase inhibition induced by troponin-tropomyosin in the absence of Ca^{2+} was not affected by R167 and E240K while all the others mutations were not inhibited. The findings are in agreement with the suggestion that tropomyosin E163 may form an electrostatic bond with Arg28 on actin. It has also been suggested that tropomyosin E240 may interact with actin K326; however, it is not known what role does this interaction is playing in the regulation of the actomyosin ATPase (Li et al., 2010; Barua et al., 2012).

Tropomyosin and troponin represent the protein complex responsible for the cooperative-allosteric transitions in thin filaments which are at the heart of the activation and inhibition of muscle contraction. Consequently, characterising tropomyosin residues responsible for all allostery and cooperativity displayed by thin filaments is critical for understanding the molecular basis of the regulation of muscle contraction. We have assessed the impact of all 10 mutants on the equilibrium constant for the transition between the blocked and closed states (K_B), on the maximum rate constant for the ON-OFF transition and the size of cooperative unit n. One important finding is that all our mutants decreased the size of the cooperative unit from a value of 8 for the WT to a value between 3-6. That means that these mutations interfere with the propagation of the allosteric signal (from 8 actin monomers to as little as 3-4 actin monomers). The structural basis of this decrease is not clear but it may be possible that for mutations R90G, R167G and R244G and the corresponding double and triple mutants a change from an Arginine to a small and flexible Glycine may reduce the rigidity of the tropomyosin molecule. In contrast, apart from E163K no mutation affected the equilibrium constant between the blocked and closed states (K_B). This support the finding in the actomyosin ATPase in which these mutations did not alter the ability of these mutants to inhibit the actomyosin ATPase. For E163K, the K_B value in the absence of calcium was increasing from 0.2 for the WT (80% of thin filament is in the blocked state) to 1.0 (45% of thin filament is in the blocked state). This suggests that E163K may be involved in stabilization of the blocked state. This is in agreement with the location of E163 in the beta-band which thought to represent binding site in the OFF state. On the other hand, R90, R167 and R244 are not involved in the formation of the blocked state which is in agreement with their location in the alpha-band thought to be involved in binding in the ON state (Holthauzen et al. 2004; McLachlan and Stewart 1976).

6.5 Implications in disease mechanism

Genetic studies have shown that several types of cardiomyopathies and congenital skeletal muscle myopathies (nemaline myopathy, cap myopathy, distal arthrogryposis and congenital fibre-type disproportion) are caused by mutations in the various tropomyosin gene (Tpm1, Tpm2 and Tpm3) (Thierfelder *et al*., 1994; Yun *et al*., 2015). There is a huge interest in the field in unravelling the molecular dysfunction induced by these mutations and how they contribute to the disease onset and progression. Up to today the functional investigations carried out have yet to establish specific functional changes that correlate and can explain the various disease phenotypes. For instance, nemaline myopathy gives both loss of function and gain of function.

Our investigations have identified several structural features in the various Tpm mutations associated with diseases (R90G, E163K, R167G, E240K, R244G) including: i) No change in the secondary structure by CD. ii) A change in tropomyosin thermal stability. iii) A change in the pattern of tryptic digestion at R133. These observations suggest that tropomyosin helical coiled coil structure is maintained overall but the flexibility of this chain have changed. Furthermore, our functional studies revealed that Tpm mutations did not induce a change in actin binding but all increased the affinity of tropomyosin to troponin. In addition, cooperativity in the absence of Tn has decreased for all Tpm mutants. These findings suggest that Tpm mutants do not decrease the incorporation of Tpm in thin filaments (since actin binding is not affected noticeably and troponin binding is strengthened) and consequently the mutants on Tpm act as a poison peptide whichy is incorporated in thin filaments and affect their function. All mutants except E163K had little effect on K_B which suggest that these mutations do not seem to affect the switching of the thin filament to the blocked state in the absence of Ca^{2+}. E163K did however affect K_B in the absence of Ca^{2+} and this mutant may affect muscle relaxation. In addition, all mutants led to a decrease in cooperatrivity. Cooperativity is an important determinant of both muscle activation and relaxation and so a decrease in cooperativity could compromise both muscle activation and relaxation in these patients.

In agreement with these findings, another laboratory found that fibers extracted from patient with R167C mutation produced reduced force (by about 37%) and actomyosin ATPase at saturating calcium (Yun *et al*., 2015). In addition, an animal model of TpmM9R showed muscle weakness (Corbett *et al*., 2001).

6.6 Conclusion

In conclusion our studies showed that obtaining a functional fully acetylated tropomyosin using eukaryotic expression system remains a challenging task and the expression of tropomyosin with an Ala-Ser extension in E.coli remains the most viable way to obtain a sufficient amount of pure protein for biochemical and biophysical investigations. Our studies of the 6 single amino acids substitution have confirmed the complex nature of actin-tropomyosin-troponin interactions. My data suggests that the flexibility of the tropomyosin chain in very important for its function and is affected by tropomyosin primary sequence. Crucially, we have demonstrated that tropomyosin cooperative behaviour is very sensitive to the nature of amino acid at position 90, 163, 167, 240, 244 and 281. We have also demonstrated that E163 has involved in the tropomyosin interaction with actin in the blocked state. These findings further advance our understanding of tropomyosin structure-function relationship.

References

Akkari, P. A., Song, Y., Hitchcock-DeGregori, S., Blechynden, L. and Laing, N. (2002) 'Expression and biological activity of Baculovirus generated wild-type human slow alpha tropomyosin and the Met9Arg mutant responsible for a dominant form of nemaline myopathy', Biochemical and Biophysical Research Communications, 296(2), 300-304.

Alahyan, M., Webb, M. R., Marston, S. B. and El-Mezgueldi, M. (2006) 'The mechanism of smooth muscle caldesmon-tropomyosin inhibition of the elementary steps of the actomyosin ATPase', Journal of Biological Chemistry, 281(28), 19433-19448.

Alberts, B. (2015) Molecular biology of the cell, Sixth edition. ed., New York, NY: Garland Science, Taylor and Francis Group.

Anderson, P. A., Greig, A., Mark, T. M., Malouf, N. N., Oakeley, A. E., Ungerleider, R. M., Allen, P. D. and Kay, B. K. (1995) 'Molecular basis of human cardiac troponin T isoforms expressed in the developing, adult, and failing heart', Circulation research, 76(4), 681-686.

Arndt, K. M., Pelletier, J. N., Muller, K. M., Pluckthun, A. and Alber, T. (2002) 'Comparison of in vivo selection and rational design of heterodimeric coiled coils', Structure, 10(9), 1235-1248.

Astbury, W., Reed, R. and Spark, L. (1948) 'An X-ray and electron microscope study of tropomyosin', Biochemical Journal, 43(2), 282.

Bacchiocchi, C., Graceffa, P. and Lehrer, S. S. (2004) 'Myosin-induced movement of alpha alpha, alpha beta, and beta beta smooth muscle tropomyosin on actin observed by multisite FRET', Biophysical Journal, 86(4), 2295-2307.

Bacchiocchi, C. and Lehrer, S. S. (2002) 'Ca2+-induced movement of tropomyosin in skeletal muscle thin filaments observed by multi-site FRET', Biophysical Journal, 82(3), 1524-1536.

Bagshaw, C. R. (1982) Muscle contraction, London; New York: Chapman and Hall.

Bagshaw, C. R. and Trentham, D. R. (1974) 'The characterization of myosin–product complexes and of product-release steps during the magnesium ion-dependent adenosine triphosphatase reaction', Biochemical Journal, 141(2), 331-349.

Barua, B., Fagnant, P. M., Winkelmann, D. A., Trybus, K. M. and Hitchcock-DeGregori, S. E. (2013) 'A Periodic Pattern of Evolutionarily Conserved Basic and Acidic Residues Constitutes the Binding Interface of Actin-Tropomyosin', Journal of Biological Chemistry, 288(14), 9602-9609.

Barua, B., Pamula, M. C. and Hitchcock-DeGregori, S. E. (2011) 'Evolutionarily conserved surface residues constitute actin binding sites of tropomyosin', Proceedings of the National Academy of Sciences of the United States of America, 108(25), 10150-10155.

Barua, B., Winkelmann, D. A., White, H. D. and Hitchcock-DeGregori, S. E. (2012) 'Regulation of actin-myosin interaction by conserved periodic sites of tropomyosin', Proceedings of the National Academy of Sciences of the United States of America, 109(45), 18425-18430.

Behrmann, E., Mueller, M., Penczek, P. A., Mannherz, H. G., Manstein, D. J. and Raunser, S. (2012) 'Structure of the Rigor Actin-Tropomyosin-Myosin Complex', Cell, 150(2), 327-338.

Berg, J. M., Tymoczko, J. L. and Stryer, L. (2007) Biochemistry, 6th ed., New York: W.H. Freeman.

Bing, W., Knott, A., Redwood, C., Esposito, G., Purcell, I., Watkins, H. and Marston, S. (2000) 'Effect of hypertrophic cardiomyopathy mutations in human cardiac muscle alpha-tropomyosin (Asp175Asn and Glu180Gly) on the regulatory properties of human

cardiac troponin determined by in vitro motility assay', Journal of Molecular and Cellular Cardiology, 32(8), 1489-1498.

Bivin, D. B., Stone, D. B., Schneider, D. K. and Mendelson, R. A. (1991) 'Cross-Helix Separation of Tropomyosin Molecules in acto-Tropomyosin as Determined by Neutron-Scattering', Biophysical Journal, 59(4), 880-888.

Bloemink, M. J., Melkani, G. C., Bernstein, S. I. and Geeves, M. A. (2016) 'The Relay/Converter Interface Influences Hydrolysis of ATP by Skeletal Muscle Myosin II', Journal of Biological Chemistry, 291(4), 1763-1773.

Blumenschein, T. M. A., Stone, D. B., Fletterick, R. J., Mendelson, R. A. and Sykes, B. D. (2006) 'Dynamics of the C-terminal region of TnI in the troponin complex in solution', Biophysical Journal, 90(7), 2436-2444.

Borovikov, Y. S., Rysev, N. A., Avrova, S. V., Karpicheva, O. E., Borys, D. and Moraczewska, J. (2017) 'Molecular mechanisms of deregulation of the thin filament associated with the R167H and K168E substitutions in tropomyosin Tpm1.1', Archives of Biochemistry and Biophysics, 614, 28-40.

Borovikov, Y. S., Rysev, N. A., Chernev, A. A., Avrova, S. V., Karpicheva, O. E., Borys, D., Sliwinska, M. and Moraczewska, J. (2016) 'Abnormal movement of tropomyosin and response of myosin heads and actin during the ATPase cycle caused by the Arg167His, Arg167Gly and Lys168Glu mutations in TPM1 gene', Archives of Biochemistry and Biophysics, 606, 157-166.

Boussouf, S. E. and Geeves, M. A. (2007) 'Tropomyosin and troponin cooperativity on the thin filament', Regulatory Mechanisms of Striated Muscle Contraction, 592, 99-109.

Brown, J. H., Kim, K. H., Jun, G., Greenfield, N. J., Dominguez, R., Volkmann, N., Hitchcock-DeGregori, S. E. and Cohen, C. (2001) 'Deciphering the design of the

tropomyosin molecule', Proceedings of the National Academy of Sciences of the United States of America, 98(15), 8496-8501.

Brown, J. H., Zhou, Z. C., Reshetnikova, L., Robinson, H., Yammani, R. D., Tobacman, L. S. and Cohen, C. (2005) 'Structure of the mid-region of tropomyosin: Bending and binding sites for actin', Proceedings of the National Academy of Sciences of the United States of America, 102(52), 18878-18883.

Brown, L. J., Sale, K. L., Hills, R., Rouviere, C., Song, L. K., Zhang, X. J. and Fajer, P. G. (2002) 'Structure of the inhibitory region of troponin by site directed spin labeling electron paramagnetic resonance', Proceedings of the National Academy of Sciences of the United States of America, 99(20), 12765-12770.

Chang, A. N., Greenfield, N. J., Singh, A., Potter, J. D. and Pinto, J. R. (2014) 'Structural and protein interaction effects of hypertrophic and dilated cardiomyopathic mutations in alpha-tropomyosin', Frontiers in Physiology, 5.

Chang, B., Nishizawa, T., Furutani, M., Fujiki, A., Tani, M., Kawaguchi, M., Ibuki, K., Hirono, K., Taneichi, H., Uese, K., Onuma, Y., Bowles, N. E., Ichida, F., Inoue, H., Matsuoka, R., Miyawaki, T. & Noncompaction Study, C. (2011) Identification of a novel TPM1 mutation in a family with left ventricular noncompaction and sudden death. *Molecular Genetics and Metabolism*, 102(2), 200-206.

Chen, Y. D., Yan, B., Chalovich, J. M. and Brenner, B. (2001) 'Theoretical kinetic studies of models for binding myosin subfragment-1 to regulated actin: Hill model versus Geeves model', Biophysical Journal, 80(5), 2338-2349.

Cho, Y.-J., Liu, J. and Hitchcock-DeGregori, S. E. (1990) 'The amino terminus of muscle tropomyosin is a major determinant for function', Journal of Biological Chemistry, 265(1), 538-545.

Cho, Y. J., Liu, J. and Hitchcockdegregori, S. E. (1990) 'THE AMINO TERMINUS OF MUSCLE TROPOMYOSIN IS A MAJOR DETERMINANT FOR FUNCTION', Journal of Biological Chemistry, 265(1), 538-545.

Chong, P. and Hodges, R. S. (1982) 'Proximity of sulfhydryl groups to the sites of interaction between components of the troponin complex from rabbit skeletal muscle', J Biol Chem, 257(5), 2549-2555.

Clark, K. A., McElhinny, A. S., Beckerle, M. C. and Gregorio, C. C. (2002) 'Striated muscle cytoarchitecture: An intricate web of form and function', Annual Review of Cell and Developmental Biology, 18, 637-706.

Clarke, N. F., Kolski, H., Dye, D. E., Lim, E., Smith, R. L. L., Patel, R., Fahey, M. C., Bellance, R., Romero, N. B., Johnson, E. S., Labarre-Vila, A., Monnier, N., Laing, N. G. & North, K. N. (2008) Mutations in TPM3 are a common cause of congenital fiber type disproportion. *Annals of Neurology*, 63(3), 329-337.

Clayton, L., Reinach, F., Chumbley, G. and MacLeod, A. (1988) 'Organization of the hTM nm gene: Implications for the evolution of muscle and non-muscle tropomyosins', Journal of molecular biology, 201(3), 507-515.

Clayton, L., Reinach, F. C., Chumbley, G. M. and Macleod, A. R. (1988) 'Organization of The Htmnm Gene - Implications for The Evolution of Muscle And Non-Muscle Tropomyosins', Journal of Molecular Biology, 201(3), 507-515.

Colpan, M., Moroz, N. A. and Kostyukova, A. S. (2013) 'Tropomodulins and tropomyosins: working as a team', Journal of Muscle Research and Cell Motility, 34(3-4), 247-260.

Conen, P. E., Murphy, E. G. and Donohue, W. L. (1963) 'Light and Electron Microscopic Studies Of "Myogranules" in a Child with Hypotonia and Muscle Weakness', Canadian Medical Association journal, 89, 983-6.

Cooke, R., Crowder, M. S., Wendt, C. H., Barnett, V. A. and Thomas, D. D. (1984) 'Muscle Cross-Bridges - Do They Rotate', Advances in Experimental Medicine and Biology, 170, 413-427.

Cooper, G. M. and Hausman, R. E. (2013) The cell: a molecular approach, 6th ed., Sunderland, MA: Sinauer Associates.

Corbett, M. A., Robinson, C. S., Dunglison, G. F., Yang, N., Joya, J. E., Stewart, A. W., Schnell, C., Gunning, P. W., North, K. N. and Hardeman, E. C. (2001) 'A mutation in alpha-tropomyosin(slow) affects muscle strength, maturation and hypertrophy in a mouse model for nemaline myopathy', Human Molecular Genetics, 10(4), 317-328.

Corsi, A. and Perry, S. V. (1958) 'Some observations on the localization of myosin, actin and tropomyosin in the rabbit myofibril', The Biochemical journal, 68(1), 12-7.

Coulton, A., Lehrer, S. S. and Geeves, M. A. (2006) 'Functional homodimers and heterodimers of recombinant smooth muscle tropomyosin', Biochemistry, 45(42), 12853-12858.

Craig, R. and Padrón, R. (2004) 'Molecular structure of the sarcomere', Myology. 3rd ed. Myology. 3rd ed. New York: McGrawHill.

Craig, R. and Woodhead, J. L. (2006) 'Structure and function of myosin filaments', Current Opinion in Structural Biology, 16(2), 204-212.

Crick, F. H. (1953) 'The packing of α-helices: simple coiled-coils', Acta crystallographica, 6(8-9), 689-697.

Criddle, A. H., Geeves, M. A. and Jeffries, T. (1985) 'The Use of Actin Labeled with N-(1-Pyrenyl)Iodoacetamide to Study the Interaction of Actin with Myosin Subfragments and Troponin Tropomyosin', Biochemical Journal, 232(2), 343-349.

Daniel, R. M., Dunn, R. V., Finney, J. L. and Smith, J. C. (2003) 'The role of dynamics in enzyme activity', Annual Review of Biophysics and Biomolecular Structure, 32, 69-92.

Devine, C. E. and Somlyo, A. P. (1971) 'Thick filaments in vascular smooth muscle', The Journal of cell biology, 49(3), 636-649.

Dominguez, R. (2004) 'Actin-binding proteins - a unifying hypothesis', Trends in Biochemical Sciences, 29(11), 572-578.

Dominguez, R. (2011) 'Tropomyosin: The Gatekeeper's View of the Actin Filament Revealed', Biophysical Journal, 100(4), 797-798.

Dominguez, R., Freyzon, Y., Trybus, K. M. and Cohen, C. (1998) 'Crystal structure of a vertebrate smooth muscle myosin motor domain and its complex with the essential light chain: Visualization of the pre-power stroke state', Cell, 94(5), 559-571.

Donkervoort, S., Papadaki, M., de Winter, J. M., Neu, M. B., Kirschner, J., Bolduc, V., Yang, M. L., Gibbons, M. A., Hu, Y., Dastgir, J., Leach, M. E., Rutkowski, A., Foley, A. R., Kruger, M., Wartchow, E. P., McNamara, E., Ong, R., Nowak, K. J., Laing, N. G., Clarke, N. F., Ottenheijm, C. A. C., Marston, S. B. and Bonnemann, C. G. (2015) 'TPM3 Deletions Cause a Hypercontractile Congenital Muscle Stiffness Phenotype', Annals of Neurology, 78(6), 982-994.

Dufour, C., Weinberger, R. P. and Gunning, P. (1998) 'Tropomyosin isoform diversity and neuronal morphogenesis', Immunology and cell biology, 76(5), 424-429.

Eaton, B. L., Kominz, D. R. and Eisenberg, E. (1975) 'Correlation between the inhibition of the acto-heavy meromyosin ATPase and the binding of tropomyosin to F-actin. Effects of Mg2+ ion, potassium chloride troponin I, and troponin C', Biochemistry, 14(12), 2718-2725.

Ebashi, S. and Endo, M. (1968) 'Calcium ion and muscle contraction', Progress in biophysics and molecular biology, 18, 123-83.

Eisenberg, E. and Hill, T. L. (1985) 'Muscle-Contraction and Free-Energy Transduction in Biological-Systems', Science, 227(4690), 999-1006.

El-Mezgueldi, M. (2014) 'Tropomyosin dynamics', Journal of Muscle Research and Cell Motility, 35(3-4), 203-210.

Engel, A. and Franzini-Armstrong, C. (2004) Myology: basic and clinical, 3rd ed., New York: McGraw-Hill, Medical Pub. Division.

Farah, C. and Reinach, F. (1995) 'The troponin complex and regulation of muscle contraction', The FASEB Journal, 9(9), 755-767.

Farah, C. S. and Reinach, F. C. (1995) 'The Troponin Complex and Regulation of Muscle-Contraction', Faseb Journal, 9(9), 755-767.

Fatkin, D. and Graham, R. M. (2002) 'Molecular mechanisms of inherited cardiomyopathies', Physiological Reviews, 82(4), 945-980.

Filatov, V. L., Katrukha, A. G., Bulargina, T. V. and Gusev, N. B. (1999) 'Troponin: Structure, properties, and mechanism of functioning', Biochemistry-Moscow, 64(9), 969-985.

Fisher, D., Wang, G. and Tobacman, L. S. (1995) 'NH2-terminal truncation of skeletal muscle troponin T does not alter the Ca2+ sensitivity of thin filament assembly', Journal of Biological Chemistry, 270(43), 25455-25460.

Fowler, V. M. (1986) 'New Views of the Red-Cell Network', Nature, 322(6082), 777-778.

Fowler, V. M., Greenfield, N. J. and Moyer, J. (2003) 'Tropomodulin contains two actin filament pointed end-capping domains', Journal of Biological Chemistry, 278(41), 40000-40009.

Fraser, I. D. C. and Marston, S. B. (1995) 'In-Vitro Motility Analysis of Actin-Tropomyosin Regulation by Troponin and Calcium - The Thin Filament Is Switched as a Single Cooperative Unit', Journal of Biological Chemistry, 270(14), 7836-7841.

Frauenfelder, H., Sligar, S. G. and Wolynes, P. G. (1991) 'The Energy Landscapes and Motions of Proteins', Science, 254(5038), 1598-1603.

Fujii, T., Iwane, A. H., Yanagida, T. and Namba, K. (2010) 'Direct visualization of secondary structures of F-actin by electron cryomicroscopy', Nature, 467(7316), 724-U117.

Fujisawa, T., Kostyukova, A. and Maeda, Y. (2001) 'The shapes and sizes of two domains of tropomodulin, the P-end-capping protein of actin-tropomyosin', Febs Letters, 498(1), 67-71.

Fokstuen, S., Munoz, A., Melacini, P., Iliceto, S., Perrot, A., Ozcelik, C., Jeanrenaud, X., Rieubland, C., Farr, M., Faber, L., Sigwart, U., Mach, F. O., Lerch, R., Antonarakis, S. E. & Blouin, J. L. (2011) Rapid detection of genetic variants in hypertrophic cardiomyopathy by custom DNA resequencing array in clinical practice. *Journal of Medical Genetics*, 48(8), 572-576.

Frisso, G., Limongelli, G., Pacileo, G., Del Giudice, A., Forgione, L., Calabro, P., Iacomino, M., Detta, N., Di Fonzo, L. M., Maddaloni, V., Calabro, R. & Salvatore, F. (2009) A child cohort study from southern Italy enlarges the genetic spectrum of hypertrophic cardiomyopathy. *Clinical Genetics*, 76(1), 91-101.

Gagne, S. M., Tsuda, S., Li, M. X., Smillie, L. B. and Sykes, B. D. (1995) 'Structures of the Troponin-C Regulatory Domains in the Apo and Calcium-Saturated States', Nature Structural Biology, 2(9), 784-789.

Gasmi-Seabrook, G. M. C., Howarth, J. W., Finley, N., Abusamhadneh, E., Gaponenko, V., Brito, R. M. M., Solaro, R. J. and Rosevear, P. R. (1999) 'Solution structures of the C-terminal domain of cardiac troponin C free and bound to the N-terminal domain of cardiac troponin I', Biochemistry, 38(26), 8313-8322.

Geeves, M. A. (2016) 'The ATPase Mechanism of Myosin and Actomyosin', Biopolymers, 105(8), 483-491.

Geeves, M. A. and Holmes, K. C. (1999) 'Structural mechanism of muscle contraction', Annual Review of Biochemistry, 68, 687-728.

Geeves, M. A. and Holmes, K. C. (2005) 'The molecular mechanism of muscle contraction', Fibrous Proteins: Muscle and Molecular Motors, 71, 161-+.

Geeves, M. A., Jeffries, T. E. and Millar, N. C. (1986) 'ATP-Induced Dissociation of Rabbit Skeletal Actomyosin Subfragment-1 - Characterization of an Isomerization of The Ternary Acto-S1-ATP Complex', Biochemistry, 25(26), 8454-8458.

Geeves, M. A. and Lehrer, S. S. (1994) 'Dynamics of the Muscle Thin Filament Regulatory Switch - The Size of The Cooperative Unit', Biophysical Journal, 67(1), 273-282.

Geeves, M. A., Perreault-Micale, C. and Coluccio, L. M. (2000) 'Kinetic analyses of a truncated mammalian myosin I suggest a novel isomerization event preceding nucleotide binding', Journal of Biological Chemistry, 275(28), 21624-21630.

Genchev, G. Z., Kobayashi, T. and Lu, H. (2013) 'Calcium Induced Regulation of Skeletal Troponin - Computational Insights from Molecular Dynamics Simulations', Plos One, 8(3).

Gimona, M., Watakabe, A. and Helfman, D. M. (1995) 'Specificity of Dimer Formation in Tropomyosins - Influence of Alternatively Spliced Exons on Homodimer and Heterodimer Assembly', Proceedings of the National Academy of Sciences of the United States of America, 92(21), 9776-9780.

Goll, D. E., Temple, J., Suzuki, A. and Holmes, G. R. (1972) 'Studies on Purified Alpha-Actinin .1. Effect of Temperature and Tropomyosin on Alpha-Actinin -Actin Interaction', Journal of Molecular Biology, 67(3), 469-&.

Gomes, A. V., Liang, J. S. and Potter, J. D. (2005) 'Mutations in human cardiac Troponin I that are associated with restrictive cardiomyopathy affect basal ATPase activity and the calcium sensitivity of force development', Journal of Biological Chemistry, 280(35), 30909-30915.

Goodwin, L. O., Leesmiller, J. P., Leonard, M. A., Cheley, S. B. and Helfman, D. M. (1991) '4 Fibroblast Tropomyosin Isoforms are Expressed from the Rat Alpha-Tropomyosin Gene Via Alternative RNA Splicing and the Use Of 2 Promoters', Journal of Biological Chemistry, 266(13), 8408-8415.

Gordon, A. M., Homsher, E. and Regnier, M. (2000) 'Regulation of contraction in striated muscle', Physiological Reviews, 80(2), 853-924.

Graceffa, P. and Lehrer, S. S. (1980) 'The Excimer Fluorescence of Pyrene-Labeled Tropomyosin - a Probe of Conformational Dynamics', Journal of Biological Chemistry, 255(23), 1296-1300.

Greenfield, N. J., Huang, Y. J., Palm, T., Swapna, G. V. T., Monleon, D., Montelione, G. T. and Hitchcock-DeGregori, S. E. (2001) 'Solution NMR structure and folding dynamics of the N terminus of a rat non-muscle alpha-tropomyosin in an engineered chimeric protein', Journal of Molecular Biology, 312(4), 833-847.

Greenfield, N. J., Huang, Y. J., Swapna, G. V. T., Bhattacharya, A., Rapp, B., Singh, A., Montelione, G. T. and Hitchcock-DeGregori, S. E. (2006) 'Solution NMR structure of the junction between tropomyosin molecules: Implications for actin binding and regulation', Journal of Molecular Biology, 364(1), 80-96.

Greenfield, N. J., Kostyukova, A. S. and Hitchcock-DeGregori, S. E. (2005) 'Structure and tropomyosin binding properties of the N-terminal capping domain of tropomodulin 1', Biophysical Journal, 88(1), 372-383.

Greenfield, N. J., Montelione, G. T., Farid, R. S. and Hitchcock-DeGregori, S. E. (1998) 'The structure of the N-terminus of striated muscle alpha-tropomyosin in a chimeric peptide: Nuclear magnetic resonance structure and circular dichroism studies', Biochemistry, 37(21), 7834-7843.

Greenfield, N. J., Palm, T. and Hitchcock-DeGregori, S. E. (2002) 'Structure and interactions of the carboxyl terminus of striated muscle alpha-tropomyosin: It is important to be flexible', Biophysical Journal, 83(5), 2754-2766.

Gunning, P., Hardeman, E., Jeffrey, P. and Weinberger, R. (1998a) 'Creating intracellular structural domains: spatial segregation of actin and tropomyosin isoforms in neurons', Bioessays, 20(11), 892-900.

Gunning, P., O'neill, G. and Hardeman, E. (2008) 'Tropomyosin-based regulation of the actin cytoskeleton in time and space', Physiological Reviews, 88(1), 1-35.

Gunning, P., Weinberger, R., Jeffrey, P. and Hardeman, E. (1998b) 'Isoform sorting and the creation of intracellular compartments', Annual Review of Cell and Developmental Biology, 14, 339-372.

Gunning, P. W., Schevzov, G., Kee, A. J. and Hardeman, E. C. (2005) 'Tropomyosin isoforms: divining rods for actin cytoskeleton function', Trends in Cell Biology, 15(6), 333-341.

Hammell, R. L. and HitchcockDeGregori, S. E. (1997) 'The sequence of the alternatively spliced sixth exon of alpha-tropomyosin is critical for cooperative actin binding but not for interaction with troponin', Journal of Biological Chemistry, 272(36), 22409-22416.

Head, J. G., Ritchie, M. D. and Geeves, M. A. (1995) 'Characterization of the Equilibrium Between Blocked and Closed States of Muscle Thin-Filaments', European Journal of Biochemistry, 227(3), 694-699.

Heald, R. W. and Hitchcockdegregori, S. E. (1988) 'The Structure of the Amino Terminus of Tropomyosin is Critical for Binding to Actin in the Absence and Presence of Troponin', Journal of Biological Chemistry, 263(11), 5254-5259.

Helfman, D. M., Cheley, S., Kuismanen, E., Finn, L. A. and Yamawakikataoka, Y. (1986) 'Nonmuscle and Muscle Tropomyosin Isoforms are Expressed from a Single Gene by Alternative RNA Splicing and Polyadenylation', Molecular and Cellular Biology, 6(11), 3582-3595.

Herzberg, O. and James, M. N. G. (1985) 'Structure of the Calcium Regulatory Muscle Protein Troponin-C At 2.8-A Resolution', Nature, 313(6004), 653-659.

Herzberg, O., Moult, J. and James, M. (1986a) 'A model for the Ca2+-induced conformational transition of troponin C. A trigger for muscle contraction', Journal of Biological Chemistry, 261(6), 2638-2644.

Herzberg, O., Moult, J. and James, M. (1986b) 'A model for the Ca2+-induced conformational transition of troponin C. A trigger for muscle contraction', Journal of Biological Chemistry, 261(6), 2638-2644.

Hershberger, R. E., Norton, N., Morales, A., Li, D. X., Siegfried, J. D. & Gonzalez-Quintana, J. (2010) Coding Sequence Rare Variants Identified in MYBPC3, MYH6, TPM1, TNNC1, and TNNI3 from 312 Patients with Familial or Idiopathic Dilated Cardiomyopathy. *Circulation-Cardiovascular Genetics*, 3(2), 155-161.

Hill, L. E., Mehegan, J. P., Butters, C. A. and Tobacman, L. S. (1992) 'ANALYSIS OF TROPONIN-TROPOMYOSIN BINDING TO ACTIN - Troponin Does Not Promote Interactions Between Tropomyosin Molecules', Journal of Biological Chemistry, 267(23), 16106-16113.

Hill, T. L., Eisenberg, E. and Chalovich, J. M. (1981) 'Theoretical-Models for Cooperative Steady-State ATPase Activity of Myosin Subfragment-1 On Regulated Actin', Biophysical Journal, 35(1), 99-112.

Hill, T. L., Eisenberg, E. and Greene, L. (1980) 'Theoretical-Model for The Cooperative Equilibrium Binding of Myosin Subfragment-1 To the Actin-Troponin-Tropomyosin Complex', Proceedings of the National Academy of Sciences of the United States of America-Biological Sciences, 77(6), 3186-3190.

Hitchcock-DeGregori, S. E. (2008) 'Tropomyosin: Function Follows Structure', Tropomyosin, 644.

Hitchcock-DeGregori, S. E., Song, Y. H. and Greenfield, N. J. (2002) 'Functions of tropomyosin's periodic repeats', Biochemistry, 41(50), 15036-15044.

HitchcockDeGregori, S. E. and An, Y. M. (1996) 'Integral repeats and a continuous coiled coil are required for binding of striated muscle tropomyosin to the regulated actin filament', Journal of Biological Chemistry, 271(7), 3600-3603.

Hitchcockdegregori, S. E. and Heald, R. W. (1987a) 'Altered Actin and Troponin Binding of Amino-Terminal Variants of Chicken Striated-Muscle Alpha-Tropomyosin Expressed in *Escherichia-Coli'*, Journal of Biological Chemistry, 262(20), 9730-9735.

Hitchcockdegregori, S. E. and Varnell, T. A. (1990) 'Tropomyosin has Discrete Actin-Binding Sites With 7-Fold and 14-Fold Periodicities', Journal of Molecular Biology, 214(4), 885-896.

Hoedemaekers, Y. M., Caliskan, K., Michels, M., Frohn-Mulder, I., van der Smagt, J. J., Phefferkorn, J. E., Wessels, M. W., ten Cate, F. J., Sijbrands, E. J. G., Dooijes, D. & Majoor-Krakauer, D. F. (2010) The Importance of Genetic Counseling, DNA Diagnostics, and Cardiologic Family Screening in Left Ventricular Noncompaction Cardiomyopathy. *Circulation-Cardiovascular Genetics*, 3(3), 232-U43.

Holmes, K. C. and Lehman, W. (2008) 'Gestalt-binding of tropomyosin to actin filaments', Journal of Muscle Research and Cell Motility, 29(6-8), 213-219.

Holmes, K. C., Popp, D., Gebhard, W. and Kabsch, W. (1990) 'Atomic Model of the Actin Filament', Nature, 347(6288), 44-49.

Holthauzen, L. M. F., Correa, F. and Farah, C. S. (2004) 'Ca2+-induced rolling of tropomyosin in muscle thin filaments - The alpha- and beta-band hypothesis revisited', Journal of Biological Chemistry, 279(15), 15204-15213.

Homsher, E., Kim, B., Bobkova, A. and Tobacman, L. S. (1996) 'Calcium regulation of thin filament movement in an in vitro motility assay', Biophysical Journal, 70(4), 1881-1892.

Hooper, S. L., Hobbs, K. H. and Thuma, J. B. (2008) 'Invertebrate muscles: Thin and thick filament structure; molecular basis of contraction and its regulation, catch and asynchronous muscle', Progress in Neurobiology, 86(2), 72-127.

Houdusse, A., Love, M. L., Dominguez, R., Grabarek, Z. and Cohen, C. (1997) 'Structures of four Ca 2+-bound troponin C at 2.0 Å resolution: further insights into the Ca 2+-switch in the calmodulin superfamily', Structure, 5(12), 1695-1711.

Houdusse, A., Szent-Gyorgyi, A. G. and Cohen, C. (2000a) 'Three conformational states of scallop myosin S1', Proceedings of the National Academy of Sciences of the United States of America, 97(21), 11238-11243.

Houdusse, A., Szent-Gyorgyi, A. G. and Cohen, C. (2000b) 'Three conformational states of scallop myosin S1', Proceedings of the National Academy of Sciences of the United States of America, 97(21), 11238-11243.

Huxley, H. (1953) 'Electron microscope studies of the organisation of the filaments in striated muscle', Biochimica et biophysica acta, 12(1), 387-394.

Huxley, H. E. (1963) 'Electron microscope studies on the structure of natural and synthetic protein filaments from striated muscle', Journal of molecular biology, 7(3), 281-IN30.

Ishii, Y., Hitchcockdegregori, S., Mabuchi, K. and Lehrer, S. S. (1992) 'Unfolding Domains of Recombinant Fusion Alpha-Alpha-Tropomyosin', Protein Science, 1(10), 1319-1325.

Ishii, Y. and Lehrer, S. S. (1990) 'Excimer Fluorescence of Pyrenyliodoacetamide-Labeled Tropomyosin - A Probe of the State of Tropomyosin in Reconstituted Muscle Thin-Filaments', Biochemistry, 29(5), 1160-1166.

Ishii, Y. and Lehrer, S. S. (1991) '2-Site Attachment of Troponin to Pyrene-Labeled Tropomyosin', Journal of Biological Chemistry, 266(11), 6894-6903.

Janco, M., Suphamungmee, W., Li, X., Lehman, W., Lehrer, S. S. and Geeves, M. A. (2013) 'Polymorphism in tropomyosin structure and function', Journal of Muscle Research and Cell Motility, 34(3-4), 177-187.

Jayasinghe, I. D. and Launikonis, B. S. (2013) 'Three-dimensional reconstruction and analysis of the tubular system of vertebrate skeletal muscle', Journal of Cell Science, 126(17), 4048-4058.

Jha, P. K., Leavis, P. C. and Sarkar, S. (1996) 'Interaction of deletion mutants of troponins I and T: COOH-terminal truncation of troponin T abolishes troponin I binding and reduces Ca2+ sensitivity of the reconstituted regulatory system', Biochemistry, 35(51), 16573-16580.

Johnson, M., Coulton, A. T., Geeves, M. A. and Mulvihill, D. P. (2010) 'Targeted Amino-Terminal Acetylation of Recombinant Proteins in E. coli', Plos One, 5(12).

Johnson, P. and Smillie, L. (1975) 'Rabbit skeletal α-tropomyosin chains are in register', Biochemical and biophysical research communications, 64(4), 1316-1322.

Jongbloed, R. J., Marcelis, C. L., Doevendans, P. A., Schmeitz-Mulkens, J. M., Van Dockum, W. G., Geraedts, J. P. and Smeets, H. J. (2003) 'Variable clinical manifestation of a novel missense mutation in the alpha-tropomyosin (TPM1) gene in familial hypertrophic cardiomyopathy', Journal of the American College of Cardiology, 41(6), 981-986.

Kabsch, W., Mannherz, H. G., Suck, D., Pai, E. F. and Holmes, K. C. (1990) 'Atomic-Structure of the Actin - Dnase-I Complex', Nature, 347(6288), 37-44.

Kabsch, W. and Vandekerckhove, J. (1992) 'Structure and Function of Actin', Annual Review of Biophysics and Biomolecular Structure, 21, 49-76.

Katrukha, A. G., Bereznikova, A. V., Esakova, T. V., Pettersson, K., Lövgren, T., Severina, M. E., Pulkki, K., Vuopio-Pulkki, L.-M. and Gusev, N. B. (1997) 'Troponin I is released in bloodstream of patients with acute myocardial infarction not in free form but as complex', Clinical chemistry, 43(8), 1379-1385.

Karibe, A., Tobacman, L. S., Strand, J., Butters, C., Back, N., Bachinski, L. L., Arai, A. E., Ortiz, A., Roberts, R., Homsher, E. & Fananapazir, L. (2001) Hypertrophic cardiomyopathy caused by a novel alpha-tropomyosin mutation (V95A) is associated with mild cardiac phenotype, abnormal calcium binding to troponin, abnormal myosin cycling, and poor prognosis. *Circulation*, 103(1), 65-71.

Kazmierczak, K., Xu, Y. Y., Jones, M., Guzman, G., Hernandez, O. M., Kerrick, W. G. L. and Szczesna-Cordary, D. (2009) 'The Role of the N-Terminus of the Myosin Essential Light Chain in Cardiac Muscle Contraction', Journal of Molecular Biology, 387(3), 706-725.

Kee, A. J. and Hardeman, E. C. (2008) 'Tropomyosins in Skeletal Muscle Diseases', Tropomyosin, 644, 143-157.

Kirwan, J. P. and Hodges, R. S. (2010) 'Critical interactions in the stability control region of tropomyosin', Journal of Structural Biology, 170(2), 294-306.

Kopylova, G. V., Shchepkin, D. V., Borovkov, D. I. and Matyushenko, A. M. (2016) 'Effect of Cardiomyopathic Mutations in Tropomyosin on Calcium Regulation of the Actin-

Myosin Interaction in Skeletal Muscle', Bulletin of Experimental Biology and Medicine, 162(1), 42-44.

Kostyukova, A., Maeda, K., Yamauchi, E., Krieger, I. and Maeda, Y. (2000) 'Domain structure of tropomodulin - Distinct properties of the N-terminal and C-terminal halves', European Journal of Biochemistry, 267(21), 6470-6475.

Kostyukova, A. S., Choy, A. and Rapp, B. A. (2006) 'Tropomodulin binds two tropomyosins: A novel model for actin filament capping', Biochemistry, 45(39), 12068-12075.

Kostyukova, A. S., Hitchcock-DeGregori, S. E. and Greenfield, N. J. (2007) 'Molecular basis of tropomyosin binding to tropomodulin, an actin-capping protein', Journal of Molecular Biology, 372(3), 608-618.

Kostyukova, A. S., Rapp, B. A., Choy, A., Greenfield, N. J. and Hitchcock-DeGregori, S. E. (2005) 'Structural requirements of tropomodulin for tropomyosin binding and actin filament capping', Biochemistry, 44(12), 4905-4910.

Kostyukova, A. S., Tiktopulo, E. I. and Maeda, Y. (2001) 'Folding properties of functional domains of tropomodulin', Biophysical Journal, 81(1), 345-351.

Kraft, T., Xu, S., Brenner, B. and Yu, L. C. (1999) 'The effect of thin filament activation on the attachment of weak binding cross-bridges: A two-dimensional X-ray diffraction study on single muscle fibers', Biophysical Journal, 76(3), 1494-1513.

Kremneva, E., Boussouf, S., Nikolaeva, O., Maytum, R., Geeves, M. A. and Levitsky, D. I. (2004a) 'Effects of two familial hypertrophic cardiomyopathy mutations in alpha-tropomyosin, Asp175Asn and Glu180Gly, on the thermal unfolding of actin-bound tropomyosin', Biophysical Journal, 87(6), 3922-3933.

Kremneva, E., Boussouf, S., Nikolaeva, O., Maytum, R., Geeves, M. A. and Levitsky, D. I. (2004b) 'Effects of two familial hypertrophic cardiomyopathy mutations in alpha-tropomyosin, Asp175Asn and Glu180Gly, on the thermal unfolding of actin-bound tropomyosin', Biophysical Journal, 87(6), 3922-3933.

Krieger, I., Kostyukova, A., Yamashita, A., Nitanai, Y. and Maeda, Y. (2002) 'Crystal structure of the C-terminal half of tropomodulin and structural basis of actin filament pointed-end capping', Biophysical Journal, 83(5), 2716-2725.

Kwok, S. C. and Hodges, R. S. (2004) 'Stabilizing and destabilizing clusters in the hydrophobic core of long two-stranded alpha-helical coiled-coils', Journal of Biological Chemistry, 279(20), 21576-21588.

Lakdawala, N. K., Dellefave, L., Redwood, C. S., Sparks, E., Cirino, A. L., Depalma, S., Colan, S. D., Funke, B., Zimmerman, R. S., Robinson, P., Watkins, H., Seidman, C. E., Seidman, J. G., McNally, E. M. & Ho, C. Y. (2010) Familial Dilated Cardiomyopathy Caused by an Alpha-Tropomyosin Mutation the Distinctive Natural History of Sarcomeric Dilated Cardiomyopathy. *Journal of the American College of Cardiology*, 55(4), 320-329.

Lakdawala, N. K., Funke, B. H., Baxter, S., Cirino, A. L., Roberts, A. E., Judge, D. P., Johnson, N., Mendelsohn, N. J., Morel, C., Care, M., Chung, W. K., Jones, C., Psychogios, A., Duffy, E., Rehm, H. L., White, E., Seidman, J. G., Seidman, C. E. & Ho, C. Y. (2012) Genetic Testing for Dilated Cardiomyopathy in Clinical Practice. *Journal of Cardiac Failure*, 18(4), 296-303.

Lamboley, C. R., Murphy, R. M., McKenna, M. J. and Lamb, G. D. (2014) 'Sarcoplasmic reticulum Ca2+ uptake and leak properties, and SERCA isoform expression, in type I and type II fibres of human skeletal muscle', Journal of Physiology-London, 592(6), 1381-1395.

Landis, C., Back, N., Homsher, E. and Tobacman, L. S. (1999) 'Effects of tropomyosin internal deletions on thin filament function', Journal of Biological Chemistry, 274(44), 31279-31285.

Landis, C. A., Bobkova, A., Homsher, E. and Tobacman, L. S. (1997) 'The active state of the thin filament is destabilized by an internal deletion in tropomyosin', Journal of Biological Chemistry, 272(22), 14051-14056.

Lange, S., Ehler, E. and Gautel, M. (2006) 'From A to Z and back? Multicompartment proteins in the sarcomere', Trends in Cell Biology, 16(1), 11-18.

Leavis, P. C., Gergely, J. and Szent-Gyorgyi, A. G. (1984) 'Thin Filament Proteins and Thin Filament-Linked Regulation of Vertebrate Muscle Contractio', CRC critical reviews in biochemistry, 16(3), 235-305.

Lees-Miller, J., Goodwin, L. and Helfman, D. (1990) 'Three novel brain tropomyosin isoforms are expressed from the rat alpha-tropomyosin gene through the use of alternative promoters and alternative RNA processing', Molecular and cellular biology, 10(4), 1729-1742.

Leesmiller, J. P., Yan, A. and Helfman, D. M. (1990) 'Structure and Complete Nucleotide-Sequence of the Gene Encoding Rat Fibroblast Tropomyosin-4', Journal of Molecular Biology, 213(3), 399-405.

Lehman, W. and Craig, R. (2008) 'Tropomyosin and the Steric Mechanism of Muscle Regulation', Tropomyosin, 644, 95-109.

Lehman, W., Craig, R., Uman, P. and Vibert, P. (1995) 'Tropomyosin Movement in Thin-Filaments Following Ca^{2+}-Activation', Molecular Biology of the Cell, 6, 133-133.

Lehman, W., Craig, R. and Vibert, P. (1994) 'Ca^{2+}-Induced Tropomyosin Movement in Limulus Thin-Filaments Revealed By 3-Dimensional Reconstruction', Nature, 368(6466), 65-67.

Lehman, W., Galinska-Rakoczy, A., Hatch, V., Tobacman, L. S. and Craig, R. (2009) 'Structural Basis for the Activation of Muscle Contraction by Troponin and Tropomyosin', Journal of Molecular Biology, 388(4), 673-681.

Lehman, W., Hatch, V., Korman, V., Rosol, M., Thomas, L., Maytum, R., Geeves, M. A., Van Eyk, J. E., Tobacman, L. S. and Craig, R. (2000) 'Tropomyosin and actin isoforms modulate the localization of tropomyosin strands on actin filaments', Journal of Molecular Biology, 302(3), 593-606.

Lehman, W., Orzechowski, M., Li, X. E., Fischer, S. and Raunser, S. (2013) 'Gestalt-Binding of tropomyosin on actin during thin filament activation', Journal of Muscle Research and Cell Motility, 34(3-4), 155-163.

Lehrer, S. S. (1975) 'Intramolecular crosslinking of tropomyosin via disulfide bond formation: evidence for chain register', Proceedings of the National Academy of Sciences, 72(9), 3377-3381.

Lehrer, S. S. (2011) 'The 3-state model of muscle regulation revisited: is a fourth state involved?', Journal of Muscle Research and Cell Motility, 32(3), 203-208.

Lehrer, S. S. and Geeves, M. A. (1998) 'The muscle thin filament as a classical cooperative/allosteric regulatory system', Journal of Molecular Biology, 277(5), 1081-1089.

Lehrer, S. S., Golitsina, N. L. and Geeves, M. A. (1997) 'Actin-tropomyosin activation of myosin subfragment 1 ATPase and thin filament cooperativity. The role of tropomyosin flexibility and end-to-end interactions', Biochemistry, 36(44), 13449-13454.

Lehrer, S. S. and Morris, E. P. (1982) 'Dual Effects of Tropomyosin and Troponin-Tropomyosin on Actomyosin Subfragment-1 ATPase', Journal of Biological Chemistry, 257(14), 8073-8080.

Lehrer, S. S. and Qian, Y. (1990) 'Unfolding Refolding Studies of Smooth-Muscle Tropomyosin - Evidence for A Chain Exchange Mechanism in The Preferential Assembly of The Native Heterodimer', Journal of Biological Chemistry, 265(2), 1134-1138.

Lehtokari, V.-L., Pelin, K., Donner, K., Voit, T., Rudnik-Schoeneborn, S., Stoetter, M., Talim, B., Topaloglu, H., Laing, N. G. and Wallgren-Pettersson, C. (2008) 'Identification of a founder mutation in TPM3 in nemaline myopathy patients of Turkish origin', European Journal of Human Genetics, 16(9), 1055-1061.

Lehtokari, V. L., Pelin, K., Donner, K., Voit, T., Rudnik-Schoneborn, S., Stoetter, M., Talim, B., Topaloglu, H., Laing, N. G. and Wallgren-Pettersson, C. (2008) 'Identification of a founder mutation in TPM3 in nemaline myopathy patients of Turkish origin', European Journal of Human Genetics, 16(9), 1055-1061.

Leszyk, J., Collins, J. H., Leavis, P. C. and Tao, T. (1988) 'Cross-linking of rabbit skeletal muscle troponin subunits: labeling of cysteine-98 of troponin C with 4-maleimidobenzophenone and analysis of products formed in the binary complex with troponin T and the ternary complex with troponins I and T', Biochemistry, 27(18), 6983-6987.

Lewis, W. G. and Smillie, L. B. (1980) 'The amino acid sequence of rabbit cardiac tropomyosin', Journal of Biological Chemistry, 255(14), 6854-6859.

Li, M. X., Gagne, S. M., Tsuda, S., Kay, C. M., Smillie, L. B. and Sykes, B. D. (1995) 'Calcium-Binding to The Regulatory N-Domain of Skeletal-Muscle Troponin-C Occurs in A Stepwise Manner', Biochemistry, 34(26), 8330-8340.

Li, X., Holmes, K. C., Lehman, W., Jung, H. and Fischer, S. (2010a) 'The Shape and Flexibility of Tropomyosin Coiled Coils: Implications for Actin Filament Assembly and Regulation', Journal of Molecular Biology, 395(2), 327-339.

Li, X., Lehman, W., Fischer, S. and Holmes, K. C. (2010b) 'Curvature variation along the tropomyosin molecule', Journal of Structural Biology, 170(2), 307-312.

Li, X., Tobacman, L. S., Mun, J. Y., Craig, R., Fischer, S. and Lehman, W. (2011) 'Tropomyosin Position on F-Actin Revealed by EM Reconstruction and Computational Chemistry', Biophysical Journal, 100(4), 1005-1013.

Li, Y., Mui, S., Brown, J. H., Strand, J., Reshetnikova, L., Tobacman, L. S. and Cohen, C. (2002) 'The crystal structure of the C-terminal fragment of striated-muscle alpha-tropomyosin reveals a key troponin T recognition site', Proceedings of the National Academy of Sciences of the United States of America, 99(11), 7378-7383.

Lieber, R. L. (2002a) Skeletal muscle structure, function & plasticity: the physiological basis of rehabilitation, 2nd ed., Philadelphia: Lippincott Williams & Wilkins.

Lieber, R. L. (2002b) Skeletal muscle structure, function & plasticity: the physiological basis of rehabilitation, 2nd ed., Philadelphia: Lippincott Williams & Wilkins.

Lin, J. J.-C., Eppinga, R. D., Warren, K. S. and McCrae, K. R. (2008) 'Human tropomyosin isoforms in the regulation of cytoskeleton functions' in TropomyosinSpringer, 201-222.

Linari, M., Brunello, E., Reconditi, M., Fusi, L., Caremani, M., Narayanan, T., Piazzesi, G., Lombardi, V. and Irving, M. (2015) 'Force generation by skeletal muscle is controlled by mechanosensing in myosin filaments', Nature, 528(7581), 276-+.

Lodish, H. F. (2003) Molecular cell biology, 5th ed., New York: W.H. Freeman and Company.

Lorenz, M., Popp, D. and Holmes, K. C. (1993) 'Refinement of the F-Actin Model Against X-Ray Fiber Diffraction Data by the Use of a Directed Mutation Algorithm', Journal of Molecular Biology, 234(3), 826-836.

Lowey, S., Waller, G. S. and Trybus, K. M. (1993) 'Function of Skeletal-Muscle Myosin Heavy and Light-Chain Isoforms by an In-Vitro Motility Assay', Journal of Biological Chemistry, 268(27), 20414-20418.

Ly, S. and Lehrer, S. S. (2012) 'Long-Range Effects of Familial Hypertrophic Cardiomyopathy Mutations E180G and D175N on the Properties of Tropomyosin', Biochemistry, 51(32), 6413-6420.

Lymn, R. W. and Taylor, E. W. (1971) 'Mechanism of Adenosine Triphosphate Hydrolysis by Actomyosin', Biochemistry, 10(25), 4617-&.

MacIntosh, B. R. (2003) 'Role of calcium sensitivity modulation in skeletal muscle performance', News in Physiological Sciences, 18, 222-225.

Macleod, A. R., Houlker, C., Reinach, F. C., Smillie, L. B., Talbot, K., Modi, G. and Walsh, F. S. (1985) 'A Muscle-Type Tropomyosin in Human-Fibroblasts - Evidence for Expression by an Alternative RNA Splicing Mechanism', Proceedings of the National Academy of Sciences of the United States of America, 82(23), 7835-7839.

Mak, A. S. and Smillie, L. B. (1981) 'Structural interpretation of the two-site binding of troponin on the muscle thin filament', Journal of molecular biology, 149(3), 541-550.

Malnic, B., Farah, C. S. and Reinach, F. C. (1998) 'Regulatory properties of the NH2- and COOH-terminal domains of troponin T - ATPase activation and binding to troponin I and troponin C', Journal of Biological Chemistry, 273(17), 10594-10601.

Margossian, S. S. and Lowey, S. (1982) 'Preparation of Myosin and Its Subfragments From Rabbit Skeletal-Muscle', Methods in Enzymology, 85, 55-71.

Marston, S., Memo, M., Messer, A., Papadaki, M., Nowak, K., McNamara, E., Ong, R., El-Mezgueldi, M., Li, X. C. and Lehman, W. (2013) 'Mutations in repeating structural motifs of tropomyosin cause gain of function in skeletal muscle myopathy patients', Human Molecular Genetics, 22(24), 4978-4987.

Mason, J. M. and Arndt, K. M. (2004) 'Coiled coil domains: Stability, specificity, and biological implications', Chembiochem, 5(2), 170-176.

Matyushenko, A. M., Shchepkin, D. V., Kopylova, G. V., Popruga, K. E., Artemova, N. V., Pivovarova, A. V., Bershitsky, S. Y. and Levitsky, D. I. (2017) 'Structural and Functional Effects of Cardiomyopathy-Causing Mutations in the Troponin T-Binding Region of Cardiac Tropomyosin', Biochemistry, 56(1), 250-259.

Maytum, R., Westerdorf, B., Jaquet, K. and Geeves, M. A. (2003) 'Differential regulation of the actomyosin interaction by skeletal and cardiac troponin isoforms', Journal of Biological Chemistry, 278(9), 6696-6701.

McKillop, D. F. A. and Geeves, M. A. (1993) 'Regulation of The Interaction Between Actin and Myosin Subfragment-1 - Evidence For 3 States of The Thin Filament', Biophysical Journal, 65(2), 693-701.

McLachlan, A. and Stewart, M. (1975) 'Tropomyosin coiled-coil interactions: evidence for an unstaggered structure', Journal of molecular biology, 98(2), 293-304.

McLaughlin, P. J., Gooch, J. T., Mannherz, H. G. and Weeds, A. G. (1993) 'Structure of Gelsolin Segment-1-Actin Complex and The Mechanism of Filament Severing', Nature, 364(6439), 685-692.

Memo, M. and Marston, S. (2013) 'Skeletal muscle myopathy mutations at the actin tropomyosin interface that cause gain- or loss-of-function', Journal of Muscle Research and Cell Motility, 34(3-4), 165-169.

Miki, M., Hai, H., Saeki, K., Shitaka, Y., Sano, K. I., Maeda, Y. and Wakabayashi, T. (2004) 'Fluorescence resonance energy transfer between points on actin and the C-terminal region of tropomyosin in skeletal muscle thin filaments', Journal of Biochemistry, 136(1), 39-47.

Miki, M., Makimura, S., Saitoh, T., Bunya, M., Sugahara, Y., Ueno, Y., Kimura-Sakiyama, C. and Tobita, H. (2011) 'A Three-Dimensional FRET Analysis to Construct an Atomic Model of the Actin-Tropomyosin Complex on a Reconstituted Thin Filament', Journal of Molecular Biology, 414(5), 765-782.

Miki, M., Makimura, S., Sugahara, Y., Yamada, R., Bunya, M., Saitoh, T. and Tobita, H. (2012) 'A Three-Dimensional FRET Analysis to Construct an Atomic Model of the Actin-Tropomyosin-Troponin Core Domain Complex on a Muscle Thin Filament', Journal of Molecular Biology, 420(1-2), 40-55.

Minakata, S., Maeda, K., Oda, N., Wakabayashi, K., Nitanai, Y. and Maeda, Y. (2008) 'Two-crystal structures of tropomyosin C-terminal fragment 176-273: Exposure of the hydrophobic core to the solvent destabilizes the tropomyosin molecule', Biophysical Journal, 95(2), 710-719.

Mirza, M., Robinson, P., Kremneva, E., Copeland, O. n., Nikolaeva, O., Watkins, H., Levitsky, D., Redwood, C., El-Mezgueldi, M. and Marston, S. (2007) 'The effect of mutations in alpha-tropomyosin (E40K and E54K) that cause familial dilated

cardiomyopathy on the regulatory mechanism of cardiac muscle thin filaments', Journal of Biological Chemistry, 282(18), 13487-13497.

Moore, J. R., Li, X., Nirody, J., Fischer, S. and Lehman, W. (2011) 'Structural implications of conserved aspartate residues located in tropomyosin's coiled-coil core', Bioarchitecture, 1(5), 250-255.

Morita, H., Rehm, H. L., Menesses, A., McDonough, B., Roberts, A. E., Kucherlapati, R., Towbin, J. A., Seidman, J. G. & Seidman, C. E. (2008) Shared genetic causes of cardiac hypertrophy in children and adults. *New England Journal of Medicine*, 358(18), 1899-1908.

Mudry, R. E., Perry, C. N., Richards, M., Fowler, V. M. and Gregorio, C. C. (2003) 'The interaction of tropomodulin with tropomyosin stabilizes thin filaments in cardiac myocytes', Journal of Cell Biology, 162(6), 1057-1068.

Murakami, K., Stewart, M., Nozawa, K., Tomii, K., Kudou, N., Igarashi, N., Shirakihara, Y., Wakatsuki, S., Yasunaga, T. and Wakabayashi, T. (2008) 'Structural basis for tropomyosin overlap in thin (actin) filaments and the generation of a molecular swivel by troponin-T', Proceedings of the National Academy of Sciences of the United States of America, 105(20), 7200-7205.

Murakami, K., Yumoto, F., Ohki, S., Yasunaga, T., Tanokura, M. and Wakabayashi, T. (2005) 'Structural basis for Ca2+-regulated muscle relaxation at interaction sites of troponin with actin and tropomyosin', Journal of Molecular Biology, 352(1), 178-201.

Muthuchamy, M., Pieples, K., Rethinasamy, P., Hoit, B., Grupp, I. L., Boivin, G. P., Wolska, B., Evans, C., Solaro, R. J. and Wieczorek, D. F. (1999) 'Mouse model of a familial hypertrophic cardiomyopathy mutation in alpha-tropomyosin manifests cardiac dysfunction', Circulation Research, 85(1), 47-56.

Nakajimataniguchi, C., Matsui, H., Nagata, S., Kishimoto, T. & Yamauchitakihara, K. (1995) Novel Missense Mutation in Alpha-Tropomyosin Gene Found in Japanese Patients with Hypertrophic Cardiomyopathy. *Journal of Molecular and Cellular Cardiology*, 27(9), 2053-2058.

Narita, A., Yasunaga, T., Ishikawa, T., Mayanagi, K. and Wakabayashi, T. (2001) 'Ca2+-induced switching of troponin and tropomyosin on actin filaments as revealed by electron cryo-microscopy', Journal of Molecular Biology, 308(2), 241-261.

Nevzorov, I. A., Nikolaeva, O. P., Kainov, Y. A., Redwood, C. S. and Levitsky, D. I. (2011) 'Conserved Noncanonical Residue Gly-126 Confers Instability to the Middle Part of the Tropomyosin Molecule', Journal of Biological Chemistry, 286(18).

Nevzorov, I. A., Redwood, C. S. and Levitskii, D. I. (2008) 'Effect of mutation Arg9lGly on the thermal stability of beta-tropomyosin', Biofizika, 53(6), 917-21.

Nirody, J., Li, X., Sousa, D., Sumida, J., Fischer, S., Lehrer, S. S. and Lehman, W. (2010) 'Electron Microscopy and Molecular Dynamics on a D137L Mutant of Tropomyosin', Biophysical Journal, 98(3), 414A-414A.

Nitanai, Y., Minakata, S., Maeda, K., Oda, N. and Maeda, Y. (2007) 'Crystal structures of tropomyosin: Flexible coiled-coil', Regulatory Mechanisms of Striated Muscle Contraction, 592, 137-151.

Nowak, K. J., Wattanasirichaigoon, D., Goebel, H. H., Wilce, M., Pelin, K., Donner, K., Jacob, R. L., Hubner, C., Oexle, K., Anderson, J. R., Verity, C. M., North, K. N., Iannaccone, S. T., Muller, C. R., Nurnberg, P., Muntoni, F., Sewry, C., Hughes, I., Sutphen, R., Lacson, A. G., Swoboda, K. J., Vigneron, J., Wallgren-Pettersson, C., Beggs, A. H. and Laing, N. G.

(1999) 'Mutations in the skeletal muscle alpha-actin gene in patients with actin myopathy and nemaline myopathy', Nature Genetics, 23(2), 208-212.

O'Shea, E. K., Klemm, J. D., Kim, P. S. and Alber, T. (1991) 'X-ray structure of the GCN4 leucine zipper, a two-stranded, parallel coiled coil', Science, 254(5031), 539-544.

Ochala, J. (2008) 'Thin filament proteins mutations associated with skeletal myopathies: Defective regulation of muscle contraction', Journal of Molecular Medicine-Jmm, 86(11), 1197-1204.

Oda, T., Iwasa, M., Aihara, T., Maeda, Y. and Narita, A. (2009) 'The nature of the globular-to fibrous-actin transition', Nature, 457(7228), 441-445.

Ohtsuki, I. and Nagano, K. (1982) 'Molecular arrangement of troponin-tropomyosin in the thin filament', Advances in biophysics, 15, 93-130.

Olive, M., Goldfarb, L. G., Lee, H. S., Odgerel, Z., Blokhin, A., Gonzalez-Mera, L., Moreno, D., Laing, N. G. and Sambuughin, N. (2010) 'Nemaline Myopathy Type 6: Clinical and Myopathological Features', Muscle & Nerve, 42(6), 901-907.

Olivotto, I., Girolami, F., Ackerman, M. J., Nistri, S., Bos, J. M., Zachara, E., Ommen, S. R., Theis, J. L., Vaubel, R. A., Re, F., Armentano, C., Poggesi, C., Torricelli, F. & Cecchi, F. (2008) Myofilament protein gene mutation screening and outcome of patients with hypertrophic cardiomyopathy. *Mayo Clinic Proceedings*, 83(6), 630-638.

Olson, T. M., Kishimoto, N. Y., Whitby, F. G. and Michels, V. V. (2001) 'Mutations that alter the surface charge of alpha-tropomyosin are associated with dilated cardiomyopathy', Journal of Molecular and Cellular Cardiology, 33(4), 723-732.

Orzechowski, M., Li, X. C., Fischer, S. and Lehman, W. (2014) 'An Atomic Model of the Tropomyosin Cable on F-actin', Biophysical Journal, 107(3), 694-699.

Oshea, E. K., Lumb, K. J. and Kim, P. S. (1993) 'Peptide Velcro - Design of A Heterodimeric Coiled-Coil', Current Biology, 3(10), 658-667.

Otsuka, H., Arimura, T., Abe, T., Kawai, H., Aizawa, Y., Kubo, T., Kitaoka, H., Nakamura, H., Nakamura, K., Okamoto, H., Ichida, F., Ayusawa, M., Nunoda, S., Isobe, M., Matsuzaki, M., Doi, Y. L., Fukuda, K., Sasaoka, T., Izumi, T., Ashizawa, N. & Kimura, A. (2012) Prevalence and Distribution of Sarcomeric Gene Mutations in Japanese Patients with Familial Hypertrophic Cardiomyopathy. *Circulation Journal*, 76(2), 453-461.

Otterbein, L. R., Graceffa, P. and Dominguez, R. (2001) 'The crystal structure of uncomplexed actin in the ADP state', Science, 293(5530), 708-711.

Palm, T., Greenfield, N. J. and Hitchcock-DeGregori, S. E. (2003) 'Tropomyosin ends determine the stability and functionality of overlap and troponin T complexes', Biophysical Journal, 84(5), 3181-3189.

Pardee, J. D. and Spudich, J. A. (1982) 'Purification of Muscle Actin', Methods in Enzymology, 85, 164-181.

Parry, D. (1975) 'Analysis of the primary sequence of α-tropomyosin from rabbit skeletal muscle', Journal of molecular biology, 98(3), 519-535.

Paul, D. M., Morris, E. P., Kensler, R. W. and Squire, J. M. (2009) 'Structure and Orientation of Troponin in the Thin Filament', Journal of Biological Chemistry, 284(22), 15007-15015.

Pearlstone, J. R. and Smillie, L. B. (1983) 'Effects of troponin-I plus-C on the binding of troponin-T and its fragments to alpha-tropomyosin. Ca2+ sensitivity and cooperativity', Journal of Biological Chemistry, 258(4), 2534-2542.

Perrin, B. J. and Ervasti, J. M. (2010) 'The Actin Gene Family: Function Follows Isoform', Cytoskeleton, 67(10), 630-634.

Perry, S. (1998) 'Troponin T: genetics, properties and function', Journal of Muscle Research & Cell Motility, 19(6), 575-602.

Perry, S. V. (2001) 'Vertebrate tropomyosin: distribution, properties and function', Journal of Muscle Research and Cell Motility, 22(1).

Perry, S. V. (2003) 'When was actin first extracted from muscle?', Journal of Muscle Research and Cell Motility, 24(8), 597-599.

Poole, K. J. V., Lorenz, M., Evans, G., Rosenbaum, G., Pirani, A., Craig, R., Tobacman, L. S., Lehman, W. and Holmes, K. C. (2006) 'A comparison of muscle thin filament models obtained from electron microscopy reconstructions and low-angle X-ray fibre diagrams from non-overlap muscle', Journal of Structural Biology, 155(2), 273-284.

Potter, J. D. (1982) 'Preparation of Troponin and its Sub-Units', Methods in Enzymology, 85, 241-263.

Probst, S., Oechslin, E., Schuler, P., Greutmann, M., Boye, P., Knirsch, W., Berger, F., Thierfelder, L., Jenni, R. & Klaassen, S. (2011) Sarcomere Gene Mutations in Isolated Left Ventricular Noncompaction Cardiomyopathy Do Not Predict Clinical Phenotype. *Circulation-Cardiovascular Genetics*, 4(4), 367-374.

Putkey, J. A., Sweeney, H. L. and Campbell, S. T. (1989) 'Site-Directed Mutation of The Trigger Calcium-Binding Sites in Cardiac Troponin-C', Journal of Biological Chemistry, 264(21), 12370-12378.

Rajan, S., Ahmed, R. P. H., Jagatheesan, G., Petrashevskaya, N., Boivin, G. P., Urboniene, D., Arteaga, G. M., Wolska, B. M., Solaro, R. J., Liggett, S. B. and Wieczorek, D. F. (2007) 'Dilated cardiomyopathy mutant tropomyosin mice develop cardiac dysfunction with significantly decreased fractional shortening and myofilament calcium sensitivity', Circulation Research, 101(2), 205-214.

Raven, P. B. (2013) Exercise physiology: an integrated approach, Australia; Belmont, CA: Wadsworth Cengage Learning.

Rayment, I. and Holden, H. M. (1993) 'Myosin Subfragment-1 - Structure and Function of a Molecular Motor', Current Opinion in Structural Biology, 3(6), 944-952.

Rayment, I., Holden, H. M., Whittaker, M., Yohn, C. B., Lorenz, M., Holmes, K. C. and Milligan, R. A. (1993a) 'Structure of The Actin-Myosin Complex and its Implications for Muscle-Contraction', Science, 261(5117), 58-65.

Rayment, I., Rypniewski, W. R., Schmidtbase, K., Smith, R., Tomchick, D. R., Benning, M. M., Winkelmann, D. A., Wesenberg, G. and Holden, H. M. (1993b) '3-Dimensional Structure of Myosin Subfragment-1 - A Molecular Motor', Science, 261(5117), 50-58.

Rebbeck, R. T., Karunasekara, Y., Board, P. G., Beard, N. A., Casarotto, M. G. and Dulhunty, A. F. (2014) 'Skeletal muscle excitation-contraction coupling: Who are the dancing partners?', International Journal of Biochemistry & Cell Biology, 48, 28-38.

Redwood, C. and Robinson, P. (2013) 'Alpha-tropomyosin mutations in inherited cardiomyopathies', Journal of Muscle Research and Cell Motility, 34(3-4), 285-294.

Regitz-Zagrosek, V., Erdmann, J., Wellnhofer, E., Raible, J. & Fleck, E. (2000) Novel mutation in the alpha-tropomyosin gene and transition from hypertrophic to hypocontractile dilated cardiomyopathy. *Circulation*, 102(17), E112-E116.

Resetar, A. M., Stephens, J. M. and Chalovich, J. M. (2002) 'Troponin-tropomyosin: An allosteric switch or a steric blocker?', Biophysical Journal, 83(2), 1039-1049.

Robaszkiewicz, K., Dudek, E., Kasprzak, A. A. and Moraczewska, J. (2012) 'Functional effects of congenital myopathy-related mutations in gamma-tropomyosin gene', Biochimica Et Biophysica Acta-Molecular Basis of Disease, 1822(10), 1562-1569.

Robaszkiewicz, K., Ostrowska, Z., Cyranka-Czaja, A. and Moraczewska, J. (2015) 'Impaired tropomyosin-troponin interactions reduce activation of the actin thin filament', Biochimica Et Biophysica Acta-Proteins and Proteomics, 1854(5), 381-390.

Ruizopazo, N. and Nadalginard, B. (1987) 'Alpha-Tropomyosin Gene Organization - Alternative Splicing of Duplicated Isotype-Specific Exons Accounts for The Production of Smooth and Striated-Muscle Isoforms', Journal of Biological Chemistry, 262(10), 4755-4765.

Ruizopazo, N., Weinberger, J. and Nadalginard, B. (1985) 'Comparison of Alpha-Tropomyosin Sequences from Smooth and Striated-Muscle', Nature, 315(6014), 67-70.

Rynkiewicz, M. J., Schott, V., Orzechowski, M., Lehman, W. and Fischer, S. (2015) 'Electrostatic interaction map reveals a new binding position for tropomyosin on F-actin', Journal of Muscle Research and Cell Motility, 36(6), 525-533.

Sadayappan, S., Finley, N., Howarth, J. W., Osinska, H., Klevitsky, R., Lorenz, J. N., Rosevear, P. R. and Robbins, J. (2008) 'Role of the acidic N ' region of cardiac troponin I in regulating myocardial function', Faseb Journal, 22(4), 1246-1257.

Sanders, C., Sykes, B. D. and Smillie, L. B. (1988) 'Comparison of The Structure and Dynamics of Chicken Gizzard and Rabbit Cardiac Tropomyosins - H-1-NMR Spectroscopy and Measurement of Amide Hydrogen-Exchange Rates', Biochemistry, 27(18), 7000-7008.

Schutt, C. E., Myslik, J. C., Rozycki, M. D., Goonesekere, N. C. W. and Lindberg, U. (1993) 'The Structure of Crystalline Profilin Beta-Actin', Nature, 365(6449), 810-816.

Seidman, J. G. and Seidman, C. (2001a) 'The genetic basis for cardiomyopathy: from mutation identification to mechanistic paradigms', Cell, 104(4), 557-567.

Seidman, J. G. and Seidman, C. (2001b) 'The genetic basis for cardiomyopathy: from mutation identification to mechanistic paradigms', Cell, 104(4), 557-567.

Sellers, J. R. and Knight, P. J. (2007) 'Folding and regulation in myosins II and V', Journal of Muscle Research and Cell Motility, 28(7-8), 363-370.

Shy, G. M., Engel, W. K., Somers, J. E. and Wanko, T. (1963) 'Nemaline Myopathy. A New Congenital Myopathy', Brain: a journal of neurology, 86, 793-810.

Singh, A. and Hitchcock-DeGregori, S. E. (2003) 'Local destabilization of the tropomyosin coiled coil gives the molecular flexibility required for actin binding', Biochemistry, 42(48), 14114-14121.

Singh, A. and Hitchcock-DeGregori, S. E. (2006) 'Dual requirement for flexibility and specificity for binding of the coiled-coil tropomyosin to its target, actin', Structure, 14(1), 43-50.

Singh, A. and Hitchcock-DeGregori, S. E. (2009) 'A Peek into Tropomyosin Binding and Unfolding on the Actin Filament', Plos One, 4(7).

Slupsky, C. M. and Sykes, B. D. (1995) 'NMR solution structure of calcium-saturated skeletal muscle troponin C', Biochemistry, 34(49), 15953-15964.

Smith, C. A. and Rayment, I. (1996) 'X-ray structure of the magnesium(II)center dot ADP center dot vanadate complex of the Dictyostelium discoideum myosin motor domain to 1.9 angstrom resolution', Biochemistry, 35(17), 5404-5417.

Sousa, D., Cammarato, A., Jang, K., Graceffa, P., Tobacman, L. S., Li, X. and Lehman, W. (2010) 'Electron Microscopy and Persistence Length Analysis of Semi-Rigid Smooth Muscle Tropomyosin Strands', Biophysical Journal, 99(3), 862-868.

Sousa, D. R., Stagg, S. M. and Stroupe, M. E. (2013) 'Cryo-EM Structures of the Actin:Tropomyosin Filament Reveal the Mechanism for the Transition from C- to M-State', Journal of Molecular Biology, 425(22), 4544-4555.

Spudich, J. A., Huxley, H. E. and Finch, J. T. (1972) 'Regulation of Skeletal-Muscle Contraction .2. Structural Studies of Interaction of Tropomyosin-Troponin Complex with Actin', Journal of Molecular Biology, 72(3), 619-&.

Spyracopoulos, L., Li, M. X., Sia, S. K., Gagne, S. M., Chandra, M., Solaro, R. J. and Sykes, B. D. (1997) 'Calcium-induced structural transition in the regulatory domain of human cardiac troponin C', Biochemistry, 36(40), 12138-12146.

Stefancsik, R., Jha, P. K. and Sarkar, S. (1998) 'Identification and mutagenesis of a highly conserved domain in troponin T responsible for troponin I binding: Potential role for coiled coil interaction', Proceedings of the National Academy of Sciences, 95(3), 957-962.

Stone, D. and Smillie, L. B. (1978) 'Amino-Acid Sequence of Rabbit Skeletal Alpha-Tropomyosin - NH2-Terminal Half and Complete Sequence', Journal of Biological Chemistry, 253(4), 1137-1148.

Sumida, J. P., Wu, E. and Lehrer, S. S. (2008) 'Conserved Asp-137 imparts flexibility to tropomyosin and affects function', Journal of Biological Chemistry, 283(11), 6728-6734.

Sun, Y. J. and Goldman, Y. E. (2011) 'Lever-Arm Mechanics of Processive Myosins', Biophysical Journal, 101(1), 1-11.

Sung, L. A., Fowler, V. M., Lambert, K., Sussman, M. A., Karr, D. and Chien, S. (1992) 'Molecular-Cloning and Characterization of Human Fetal Liver Tropomodulin - A Tropomyosin-Binding Protein', Journal of Biological Chemistry, 267(4), 2616-2621.

Syska, H., Wilkinson, J. M., Grand, R. J. and Perry, S. (1976) 'The relationship between biological activity and primary structure of troponin I from white skeletal muscle of the rabbit', Biochemical Journal, 153(2), 375-387.

Szczesna, D. and Fajer, P. G. (1995) 'The Tropomyosin Domain is Flexible and Disordered in Reconstituted Thin-Filaments', Biochemistry, 34(11), 3614-3620.

Szczesna-Cordary, D. (2003) 'Regulatory light chains of striated muscle myosin. Structure, function and malfunction', Current Drug Targets-Cardiovascular & Hematological Disorders, 3(2), 187-197.

Tajsharghi, H., Kimber, E., Holmgren, D., Tulinius, M. and Oldfors, A. (2007) 'Distal arthrogryposis and muscle weakness associated with a beta-tropomyosin mutation', Neurology, 68(10), 772-775.

Takeda, S., Yamashita, A., Maeda, K. and Maeda, Y. (2003) 'Structure of the core domain of human cardiac troponin in the Ca2+-saturated form', Nature, 424(6944), 35-41.

Taussky, H. H. and Shorr, E. (1953) 'A microcolorimetric method for the determination of inorganic phosphorus', The Journal of biological chemistry, 202(2), 675-85.

Tesi, C., Piroddi, N., Colomo, F. and Poggesi, C. (2002) 'Kinetics of force relaxation following sudden Ca2+ removal in single myofibrils from skeletal muscle', Biophysical Journal, 82(1), 394A-394A.

Thierfelder, L., Watkins, H., Macrae, C., Lamas, R., McKenna, W., Vosberg, H. P., Seidman, J. G. and Seidman, C. E. (1994) 'Alpha-Tropomyosin and Cardiac Troponin-T Mutations Cause Familial Hypertrophic Cardiomyopathy - A Disease of The Sarcomere', Cell, 77(5), 701-712.

Tobacman, L. S. and Butters, C. A. (2000) 'A new model of cooperative myosin-thin filament binding', Journal of Biological Chemistry, 275(36), 27587-27593.

Trentham, D. R., Eccleston, J. F. and Bagshaw, C. R. (1976) 'kinetic-Analysis Of ATPase Mechanisms', Quarterly Reviews of Biophysics, 9(2), 217-281.

Tripet, B., VanEyk, J. E. and Hodges, R. S. (1997) 'Mapping of a second actin tropomyosin and a second troponin C binding site within the C terminus of troponin I, and their importance in the Ca2+-dependent regulation of muscle contraction', Journal of Molecular Biology, 271(5), 728-750.

Trybus, K. M. (1994) 'Role of Myosin Light-Chains', Journal of Muscle Research and Cell Motility, 15(6), 587-594.

Tyska, M. J. and Warshaw, D. M. (2002) 'The myosin power stroke', Cell Motility and the Cytoskeleton, 51(1), 1-15.

Urbancikova, M. and Hitchcockdegregori, S. E. (1994) 'Requirement of Amino-Terminal Modification for Striated-Muscle Alpha-Tropomyosin Function', Journal of Biological Chemistry, 269(39), 24310-24315.

Van de Meerakker, J. B. A., Christiaans, I., Barnett, P., Deprez, R. H. L., Ilgun, A., Mook, O. R. F., Mannens, M., Lam, J., Wilde, A. A. M., Moorman, A. F. M. & Postma, A. V. (2013) A novel alpha-tropomyosin mutation associates with dilated and non-compaction cardiomyopathy and diminishes actin binding. *Biochimica Et Biophysica Acta-Molecular Cell Research*, 1833(4), 833-839.

Van Driest, S. L., Will, M. L., Atkins, D. L. and Ackerman, M. J. (2002) 'A novel TPM1 mutation in a family with hypertrophic cardiomyopathy and sudden cardiac death in childhood', American Journal of Cardiology, 90(10), 1123-1127.

Van Driest, S. L., Ellsworth, E. G., Ommen, S. R., Tajik, A. J., Gersh, B. J. & Ackerman, M. J. (2003) Prevalence and spectrum of thin filament mutations in an outpatient referral population with hypertrophic cardiomyopathy. *Circulation*, 108(4), 445-451.

Van Eerd, J.-P. and Takahashi, K. (1975) 'The amino acid sequence of bovine cardiac troponin-C. Comparison with rabbit skeletal troponin-C', Biochemical and biophysical research communications, 64(1), 122-127.

Vassylyev, D. G., Takeda, S., Wakatsuki, S., Maeda, K. and Maéda, Y. (1998) 'Crystal structure of troponin C in complex with troponin I fragment at 2.3-Å resolution', Proceedings of the National Academy of Sciences, 95(9), 4847-4852.

Van Spaendonck-Zwarts, K. Y., van Rijsingen, I. A. W., van den Berg, M. P., Deprez, R. H. L., Post, J. G., van Mil, A. M., Asselbergs, F. W., Christiaans, I., van Langen, I. M., Wilde, A. A. M., de Boer, R. A., Jongbloed, J. D. H., Pinto, Y. M. & van Tintelen, J. P. (2013) Genetic analysis in 418 index patients with idiopathic dilated cardiomyopathy: overview of 10 years' experience. *European Journal of Heart Failure*, 15(6), 628-636.

Vinogradova, M. V., Stone, D. B., Malanina, G. G., Karatzaferi, C., Cooke, R., Mendelson, R. A. and Fletterick, R. J. (2005) 'Ca2+-regulated structural changes in troponin', Proceedings of the National Academy of Sciences of the United States of America, 102(14), 5038-5043.

Von der Ecken, J., Muller, M., Lehman, W., Manstein, D. J., Penczek, P. A. and Raunser, S. (2015) 'Structure of the F-actin-tropomyosin complex', Nature, 519(7541), 114-U272.

Vrhovski, B., Thézé, N. and Thiébaud, P. (2008) 'Structure and evolution of tropomyosin genes' in TropomyosinSpringer, 6-26.

Wahl, P., Tawada, K. and Auchet, J. C. (1978) 'Study of Tropomyosin Labeled with A Fluorescent-Probe by Pulse Fluorimetry In Polarized-Light - INTERACTION OF THAT PROTEIN WITH TROPONIN AND ACTIN', European Journal of Biochemistry, 88(2), 421-424.

Wang, K., Knipfer, M., Huang, Q. Q., VanHeerden, A., Gutierrez, G., Quian, X. and Stedman, H. (1996) 'Human foetal skeletal muscle nebulin sequence encodes a blueprint for thin filament architecture: Sequence motifs and affinity profiles of tandem repeats and terminal SH3', Journal of Muscle Research and Cell Motility, 17(1), 114-114.

Wang, K. and Wright, J. (1988) 'Architecture of The Sarcomere Matrix of Skeletal-Muscle - Immunoelectron Microscopic Evidence That Suggests a Set of Parallel Inextensible Nebulin Filaments Anchored at the Z-Line', Journal of Cell Biology, 107(6), 2199-2212.

Wegner, A. (1979) 'Equilibrium of The Actin-Tropomyosin Interaction', Journal of Molecular Biology, 131(4), 839-853.

Wegner, A. (1980) 'The Interaction of Alpha-Alpha-Tropomyosin and Alpha-Beta-Tropomyosin with Actin-Filaments', Febs Letters, 119(2), 245-248.

Wernicke, D., Thiel, C., Plehm, R., Hammes, A., Ganten, U., Morano, I., Davies, M. J. and Thierfelder, L. (1999) 'Characterization of a transgenic rat model of familial hypertrophic cardiomyopathy with missense mutations Asp175Asn or Glu180Gly in alpha-tropomyosin', Circulation, 100(18), 268-268.

Whitby, F. G. and Phillips, G. N. (2000) 'Crystal structure of tropomyosin at 7 Angstroms resolution', Proteins-Structure Function and Genetics, 38(1), 49-59.

Whittaker, M., Wilsonkubalek, E. M., Smith, J. E., Faust, L., Milligan, R. A. and Sweeney, H. L. (1995) 'A 35-Angstrom Movement of Smooth-Muscle Myosin on ADP Release', Nature, 378(6558), 748-751.

Xu, C., Craig, R., Tobacman, L., Horowitz, R. and Lehman, W. (1999) 'Tropomyosin positions in regulated thin filaments revealed by cryoelectron microscopy', Biophysical Journal, 77(2), 985-992.

YamauchiTakihara, K., NakajimaTaniguchi, C., Matsui, H., Fujio, Y., Kunisada, K., Nagata, S. & Kishimoto, T. (1996) Clinical implications of hypertrophic cardiomyopathy associated with mutations in the alpha-tropomyosin gene. *Heart*, 76(1), 63-65.

Yuen, M., Cooper, S. T., Marston, S. B., Nowak, K. J., McNamara, E., Mokbel, N., Ilkovski, B., Ravenscroft, G., Rendu, J., de Winter, J. M., Klinge, L., Beggs, A. H., North, K. N., Ottenheijm, C. A. C. and Clarke, N. F. (2015) 'Muscle weakness in TPM3-myopathy is due to reduced Ca2+-sensitivity and impaired acto-myosin cross-bridge cycling in slow fibres', Human Molecular Genetics, 24(22), 6278-6292.

Zhou, X., Morris, E. P. and Lehrer, S. S. (2000) 'Binding of troponin I and the troponin I-troponin C complex to actin-tropomyosin. Dissociation by myosin subfragment 1', Biochemistry, 39(5), 1128-1132.